BEFORE YOU READ THIS ISSUE...
Renew your 1976 Subscription
Turn to card inside front cover

laser technology

MICROWAVES

ANUARY
76

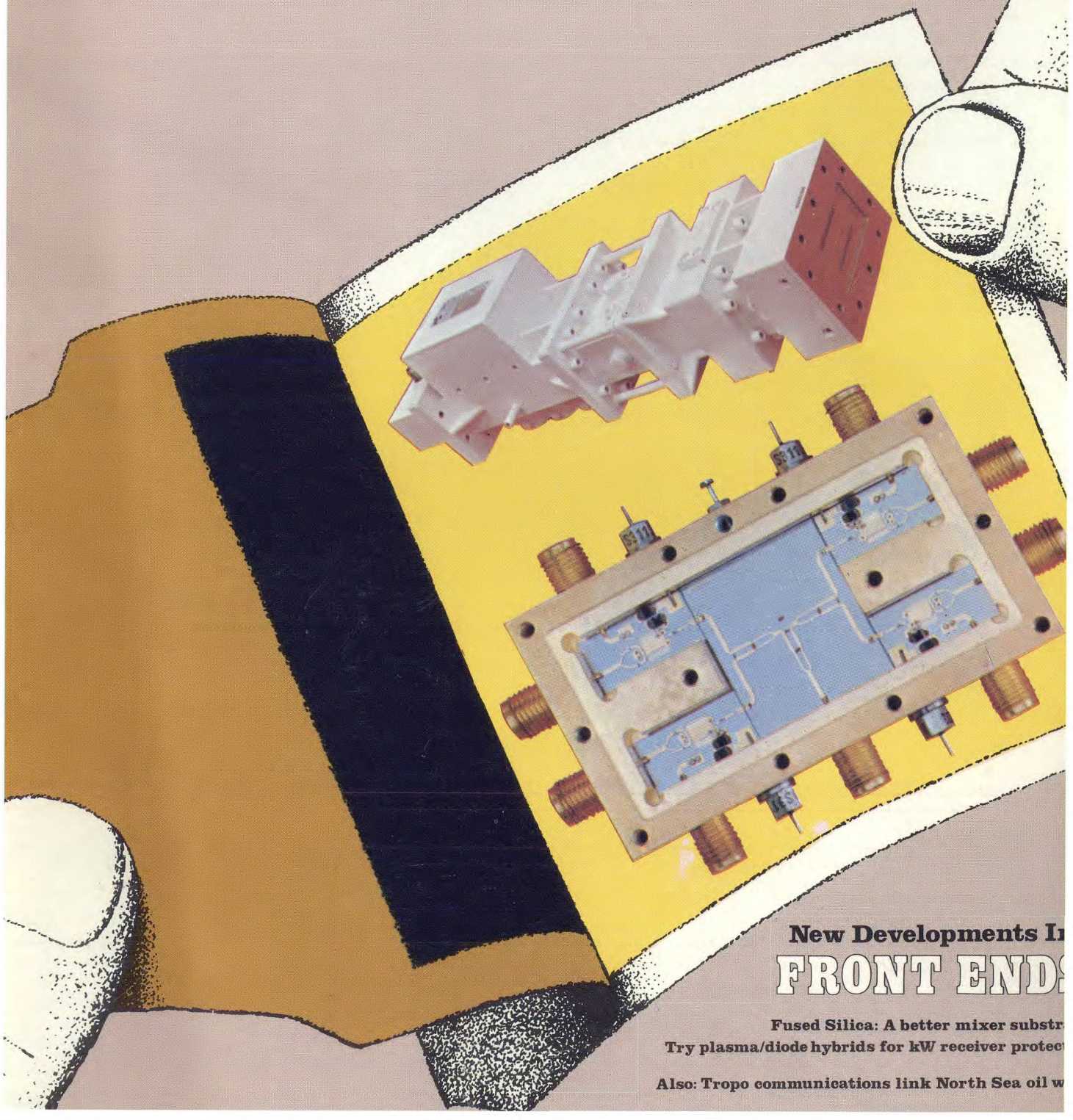

New Developments I

FRONT END

Fused Silica: A better mixer substr

Try plasma/diode hybrids for kW receiver protec

Also: Tropo communications link North Sea oil w

MICROWAVES

January 1976
Vol. 15, No. 1

news

9 British P.O. Adds Some Bounce To The Oil Business
13 Improved Semiconductor Laser Developed For IOCs
14 Computer-Controlled IR Scanner Quickly Pinpoints Thermal Problems
16 SOS Switch Could Reduce Phased Array Prime Power Needs
19 Washington
22 International
24 R & D
32 Industry
28 Meetings
30 For Your Personal Interest . . .

editorial

26 ABM—An Expensive Lesson

technical section

Front-Ends

34 **Fused Silica: A Better Substrate For Mixers?** Dr. E. James Crescenzi, Ferenc A. Marki and Dr. W. Keith Kennedy of Watkins-Johnson examine the advantages of using fused silica substrates for J-band mixers.

44 **What's New With Receiver Protectors?** Harry Goldie of Westinghouse Defense and Electronic Systems Center describes plasma/diode receiver protectors consisting of tritium ignitors for handling the high peak input powers and PIN diode limiters for minimizing residual spike and flat leakage.

54 **How Noisy Is That Load?** Dr. Mats E. Viggh of Transmission Lines, Inc. states that the output power of a noise standard is usually considered proportional to temperature and independent of frequency. At millimeter wavelengths, this assumption leads to error.

58 1975 Annual Index

products and departments

62 **Product Features:** Flatpack, TO-8 Modules Offer High-Rel Hybrid Construction
63 Hybrid Paramp Downconverters Cover 2.2 to 35 GHz
64 Program Updates Test System For Swept Non-Linear Measurements
65 New Products
76 New Literature
78 Application Notes
79 Advertisers' Index
80 Product Index

About the cover: New developments in front-end components are represented by a multi-stage plasma/diode receiver protecter, developed at Westinghouse, Baltimore. Some new mixer designs by Watkins-Johnson use fused silica as a substrate. Cover composition by Robert Meehan.

coming next month: Semiconductors

Staff Report On Gallium Arsenide Field-Effect Transistors. This in-depth report examines current research efforts aimed at improving the stability, reliability and performance of this much-publicized device. Included is a preview of some radically new FETs which should debut in 1976.

How Much Pulsed Power Can a PIN Diode Handle? Fred Doninick of GHz Devices, develops a thermal analysis of PIN diode performance. Once physical and pulse parameters are known, peak pulsed power ratings can be easily predicted.

Power Amp Design For 900 MHz Mobile Radio. Junius Taylor and Gordon McIntosh of Motorola Semiconductor provide a look inside the new power semiconductors emerging for this important radio band, concluding with a discussion of design techniques for broadband, 12.5 V amplifiers. Detailed instructions for building a 15 W design are included.

Publisher/Editor
Howard Bierman

Managing Editor
Richard T. Davis

Associate Editor
Stacy V. Bearse

Contributing Editor
Harvey J. Hindin

Washington Editor
Paul Harris
Snyder Associates
1050 Potomac St., NW
Washington, DC 20007
(202) 965-3700

Editorial Assistant
Gail Murphy

Production Editor
Sherry Lynne Karpen

Art
Robert Meehan, Dir.

Production
Dollie S. Viebig, Mgr.
Dan Coakley

Circulation
Trish Edelmann, Mgr.
Sherry Karpen,
Reader Service

Promotion Manager
Albert B. Stempel

Directory Coordinator
Janice Tapp

Editorial Office
50 Essex St.,
Rochelle Park, N.J. 07662
Phone (201) 843-0550
TWX 710-990-5071

A Hayden Publication
James S. Mulholland, Jr.,
President

MICROWAVES is sent free to individuals actively engaged in microwave work at companies located in the U.S., Canada and Western Europe. Subscription price for non-qualified copies is $10.00 for U.S., $15.00 a year elsewhere. Additional single copies $1.50 ea. (U.S.); $2.00 ea. (foreign); except additional Product Data Directory reference issue, $10.00 ea. (U.S.); $18.00 (foreign). POSTMASTER, please send Form 3579 to Fulfillment Manager, MICROWAVES, P.O. Box 13801, Philadelphia, PA 19101.

Back Issues of MicroWaves are available on microfilm, microfiche, 16mm or 35mm roll film. They can be ordered from Xerox University Microfilms, 300 North Zeeb Road, Ann Arbor, MI 48106. For immediate information, call (313) 761-4700.

Hayden Publishing Co., Inc., James S. Mulholland, President, printed at Brown Printing Co., Inc., Waseca, MN
Copyright © 1976 Hayden Publishing Co., Inc., all rights reserved.

news/industry

RCA's Government Communications Systems Division, Camden, NJ, a $189,000 contract from the **Federal Aviation Administration** to test and evaluate new tracking radars.

American Electronic Labs, Colmar, PA, a $355,766 contract from the **Navy's Special Products Division** for spares for the ALQ/99 countermeasures system.

Hazeltine Corp., Greenlawn, NY, a $550,000 contract from the **Federal Aviation Administration** to produce 10 "open planar array" antennas for use with existing Air Traffic Control Radar Beacon systems.

Westinghouse's Defense and Space Center, Aerospace & Electric Systems Division, Baltimore, MD, a $4,278,000 contract from the **Warner Robins Air Logistics Center,** Robins AFB, GA for electronic countermeasure pod power modification kits.

Zeta Labs, Mountain View, CA, a $345,000 contract from **Salenia S. p. A.,** for the Siro satellite transponder local oscillator subsystem.

Watkins-Johnson Co., Palo Alto, CA, a $96,925 contract from **Intelsat** for a 6-GHz, solid-state, low-noise amplifier.

Radiation Systems, Inc., McLean, VA, announced that in the first quarter ended Sept. 30, 1975, earnings were $65,000 on sales of $738,000. In the comparable three months last year, earnings of $53,000 were reported on sales of $723,000.

Scientific-Atlanta, Atlanta, GA, reported first quarter sales and earnings in the quarter ended September 30, 1975 were $9,192,000 or 30% above the first quarter last year. Net earnings for the same quarter were $353,000 or $.35 per share as compared to $239,000 and $.25 per share for the same period last year.

Varian, Palo Alto, CA, reports record sales of $310.4 million for the fiscal year ended Sept. 30, 1975, up 6% from $293.0 million reported last year. Net earnings were $7.7 million, an increase of 6% and earnings per average share were $1.11 compared to $1.08 in 1974.

Alpha Industries, Inc., Woburn, MA, reported that for the 6 months ended September 30, 1975, net income was $37,358 on a sales volume of $3,578,-720. This contrasts with a loss of $52,074 on sales of $4,061,936 in the same period one year ago.

Polarad Electronics Corp., Lake Success, NY, announced that sales totaled $8,971,138, an increase of 34% over last year's $6,689,496 and net earnings were $1,241,722 as compared with $748,382 reported for last year.

People on the Move

Philip B. Cox has been elected a vice president of **Omni Spectra, Inc.,** Tempe, AZ and has also been promoted to assistant general manager of the mw subsystems division.

Bill K. Bryant has been appointed vice president, manufacturing of **Amphenol RF Division,** Bunker **Ramo Corp.,** Danbury, CT and **Darrell E. Rutter** has been appointed controller of **Amphenol's RF Division.**

Campbell Kennedy has been named assistant sales manager (mw) for **The M-O Valve Company, Ltd,** Chelmsford, England. He will be based at **The English Electric Valve Co.,** Chelmsford.

Gus Bidwell has been named marketing manager at **Tropel** (a division of **Coherent Radiation**) Fairport, NY. —*S.L.K.*

Fused Silica: A Better Substrate For Mixers?

Fused silica, a material commonly used in optics, has just recently been exploited for J-band mixer applications. It allows thin-film circuits to be built on relatively low dielectric substrates.

CONSIDERING all the superlatives applied to microwave integrated circuit technology over the past ten years, one would expect all microwave mixers operating in the 10 to 20 GHz range to now be constructed using thin-film techniques. To the contrary, however, a survey of commercially-available mixers reveals that soft, teflon-type circuit board construction is still most frequently employed. This approach is obviously favored for the advantages of using a low diectric constant material to realize a broadband component, and has persisted in spite of the severe parasitic problems of packaged devices, and the dimensional non-reproducibility inherent to soft, printed-circuit techniques.

A well-established optical material, fused silica (vitreous quartz), has just recently been applied to thin-film MIC design to circumvent the problems of soft circuit-board. The material blends several of the previously exclusive features of high-dielectric alumina with those of low-dielectric, teflon-type, copper-clad circuit-board; it permits the fabrication of a thin-film circuit on a low-dielectric ($\epsilon_r = 3.8$) substrate.

The properties of microstrip lines on fused silica have been thoroughly studied and documented by Schneider[1]. Further work by Snell[2] demonstrates that low-frequency filter protoypes can be scaled, by a factor of 10, to X-band, with high accuracy. Van Heuven and Van Nie[3] report low dispersion (below 3 percent measurement resolution) for microstrip on fused silica at 12 GHz.

Fused silica is routinely prepared to optical flatness and surface finish (<0.25 microinch). Its mechanical precision, chemical purity and ability to withstand high temperatures make it a natural candidate for MIC construction using thin-film deposition processes and photolithographic techniques. The surface finish of polished and fused silica is free from inclusions or pits, which are commonly found in polished alumina. It is actually comparable to single crystal sapphire in surface finish. Other physical comparisons with alumina and sapphire include a much lower coefficient of thermal expansion, along with the disadvantage of very poor thermal conductivity. The low thermal conductivity of fused silica makes it inappropriate for direct attachment of active semiconductor devices, even with moderate power dissipation.

Low dielectric constant key

The electrical characteristics of fused silica are compared with those of alumina in Table 1, which is tailored to mixer applications by considering only thin (0.010 inch) substrates. The focus on thin substrates is motivated by the desire to employ double-sided circuit topologies for broadband single and double-balanced mixers. Double-sided topology requires such MIC techniques as broadside-coupled balanced lines, microwave vias (interconnections between the two sides of a substrate), suspended substrate coplanar lines and microwave shorts (direct vias through the substrate to a ground plane), as illustrated in Fig. 1.

Comparing thin substrates, the lower dielectric constant of fused silica allows the deposition of higher impedance lines, as are fre-

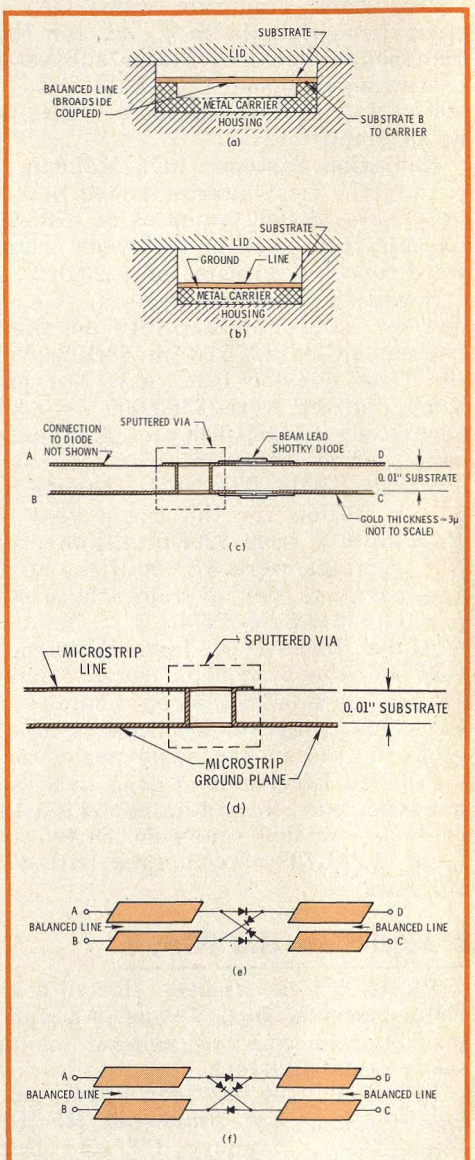

1. Fused silica substrate eases the application of suspended substrate (a) and microstrip (b) design techniques involving microwave vias (c) and shorts (d). Diode-quad mixer applications which take advantage of vias are shown in (e) and (f).

Dr. E. James Crescenzi, Jr., Manager, Solid State R&D Department, **Ferenc A. Marki**, Member of the Technical Staff and **Dr. W. Keith Kennedy**, Manager, Solid State Division, Watkins-Johnson Company, 3333 Hillview Avenue, Palo Alto, CA 94304.

quently required for mixer applications. One practical limitation on line width is often the width of commercially-available beam lead diodes and capacitors. These commonly call for a 0.010 inch wide conductor for attachment, which results in a restrictively low, 50-ohm microstrip impedance on 0.01 inch thick alumina, and a much more tolerable 75-ohm impedance on fused silica.

In many cases, as will be illustrated by a series of examples, the higher impedance of fused silica allows the diode and capacitor leads to be blended into a matching structure, limiting the component discontinuity to the dimension of the body of the device alone. This technique, combined with the effect of a lower propagation constant, can reduce the electrical length of the apparent discontinuity from 40 degrees on alumina, to only 9 degrees on fused silica, at 18 GHz. In effect, the parasitics of beam-lead devices are substantially less when mounted on fused silica. But it must be recognized that the electrical length of a beam-lead diode measuring 0.030 inch long is nontrivial even on fused silica, where $\lambda/4$ is about a tenth of an inch at 18 GHz.

An example of beam lead components mounted in a mixer circuit is shown in Fig. 2. Key to these device interconnections is a microwave via formed by metalizing the internal surface of a 0.015 inch diameter hole in the 0.010 inch thick fused silica (see SEM photo, Fig. 3). The excellent step coverage of the hole edges and walls is accomplished by an rf bias sputtering process that involves metal deposition in a plasma in which atoms impinge on the substrate at various angles and with high energy. Shadowing problems inherent in evaporation processes are thus largely eliminated.

If fused silica has one major disadvantage for thin-film MIC fabrication, it is the potential metallurgical problems which accompany high-stress gold deposition. One of these complications is illustrated in Fig. 4, which shows the etched microstrip line pulled away from the substrate for examination. The photograph reveals that what had first been assumed to be poor adhesion (lifting along line edges), is actually a fracture of the fused silica substrate, several microns deep, caused by excessively high stress in the gold film.

This problem led to rather extensive process development at the Watkins-Johnson Company, resulting in a low-stress, gold film deposition process for fused silica. Etched circuits fabricated with the low-stress process, mounted on metal carriers by high-temperature braze techniques, have survived exhaustive temperature cycling tests without deterioration.

Table 1: Thin (0.01-inch) Substrate Comparison

	Alumina	Fused Silica
Bulk dielectric constant	9.8	3.8
Microstrip effective dielectric constant (50 Ω line)	6.5	3.0
Phase-length of 0.002 inch length difference (at 18 GHz)	2.8°	1.9°
Maximum achievable impedance (0.002-inch min line width)	90 Ω	135 Ω
Impedance of line 0.010" wide (common width of beam lead components)	50 Ω	75 Ω
Beam lead component electrical length of uncontrolled or undesired impedance	42° (component body and leads)	9.5° (component body only)
Substrate thermal conductivity (cal./sec. cm°C)	0.09	0.003
Coefficient of expansion (cm/cm°C)	6.6×10^{-6}	0.55×10^{-6}
Mechanical fabrication		
a) surface finish	excellent, but problem with inclusions.	optical finish available
b) hole fabrication	laser drilling (mechanical drilling very costly)	low cost mechanical drilling (laser drilling not available)
c) tightly coupled lines	more difficult on fused silica (0.0010" gap required for baluns on fused silica)	
Circuit resolution (thin-film photolithographic)	excellent	slightly superior due to surface finish
Ease of metallization (sputter deposition)	routine	special process required to minimize surface stress

Vias simplify circuit design

The composite technology of double-sided circuits, sputtered microwave via holes and beam-lead component attachment, made possible by a substrate such as fused silica, is demonstrated by the single-balanced bridge mixer illustrated in Fig. 5. Broadband baluns transform microstrip inputs to balanced lines driving a diode bridge. Two beam lead diodes are mounted on each side of the substrate, and quad electrical connections are accomplished with

(continued on p. 39)

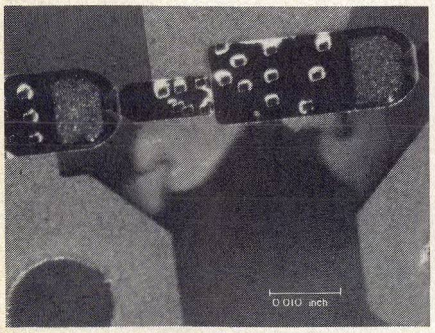

2. Beam lead diodes are thermocompressively bonded to microstrip on this fused silica substrate. Alpha Industries' Type D 5600 Schottky barrier diodes are shown.

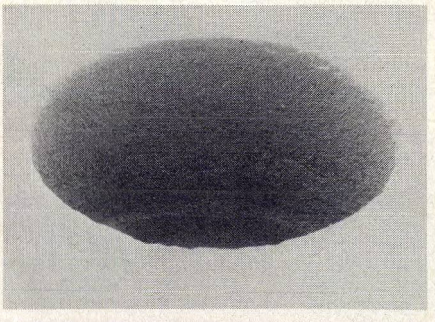

3. This SEM photo of a metallized, 0.015 inch diameter hole illustrates excellent step coverage. The result: a 0.010 inch, low inductance connection between substrate surfaces.

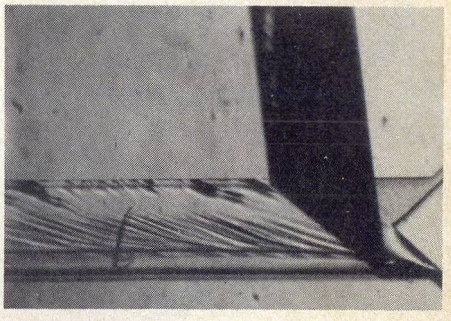

4. Surface fractures show failure of fused silica under high-stress gold film. This problem can be avoided by employing a low stress deposition process.

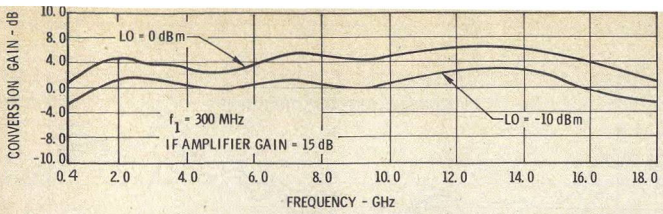

5. This single-balanced, four-diode bridge operates with reduced (−10 dBm) LO power. Beam-lead capacitors are mounted on the LO and rf baluns with minimal discontinuity due to larger transmission line dimensions on fused silica.

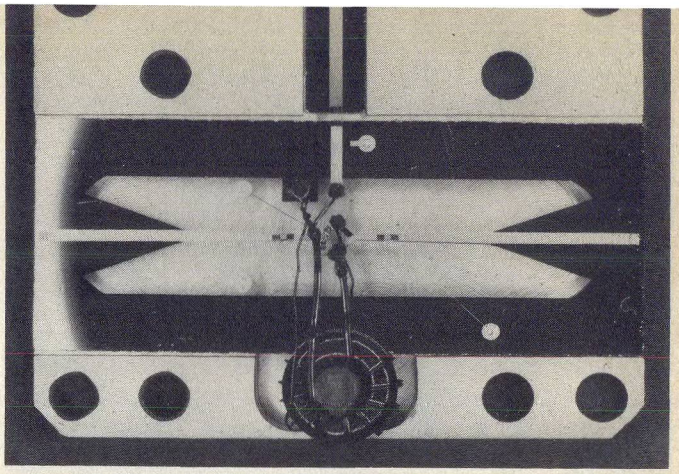

sputtered hole microwave vias. As mentioned, the thin-film transmission line dimensions on fused silica are quite compatible with the imbedding of beam-lead blocking capacitors thus allowing dc bias to be introduced through very high impedance etched lines for starved local oscillator operation. An i-f balun is comprised of a torroid and paired wires. Note that the conversion gain of this mixer, integrated with a thin-film TO-8 i-f amplifier (WJ A-1), is flat within ±3 dB over a 0.5 to 18 GHz range. Local oscillator power in this case is −10 dBm, typical of starved LO requirements encountered in synthesizer phase-locked loop applications.

For many applications, it is advantageous to build a single-balanced mixer using some sort of microwave hybrid that decouples or isolates the rf signal from the local oscillator or pump. This can be conveniently accomplished by use of balanced and unbalanced transmission lines to simultaneously apply LO and rf signals to a pair of diodes.

The balanced line requires a balun to transform an unbalanced transmission line input (i.e., coax or microstrip) to a balanced output. A planar balun capable of thin-film realization, similar to that described by DeBrecht[4], is shown in Fig. 6a. The three tightly coupled lines are etched on a dielectric with the ground plane removed, thus forming a suspended substrate. The line, which is grounded at the input and connected to the center line at the output, forces balanced currents to flow in the desired path, and presents a high impedance to the unbalanced mode. The equivalent circuit of the balun is a quarter wavelength section with quarter wave short-circuited shunt stubs at both ends. Characteristics of coplanar lines of this type have been analyzed by Wen[5], and recently, by Hatsuda[6]. Impedances appropriate for the mixer application are reliazable on both fused silica and alumina.

The balun depicted in Fig. 6a can be integrated with a power divider-transformer section, as shown in Fig. 6b, to form a single-balanced mixer. The rf divider applies equal unbalanced signals to each diode, with one diode effectively terminating each branch of the power divided (diodes appear in opposite polarity). The LO balun drives the diodes in series, and is loaded by the rf power divider, which appears as a short-circuited stub to the balanced mode of the balun. The rf ground return is achieved through a bypass capacitor at the node connection of the diodes, which also serves as the point of rf to i-f diplexing.

Central to the physical realization of the mixer of Fig. 6b is an obviously non-planar requirement —that of a low impedance ground return. The choice of thin (0.010 inch thick) fused silica and the use of the sputter deposition process to coat the inner walls of 0.015 inch diameter holes to form ground returns was thus an essential element of the design approach for this mixer. Note that this tech-

(continued on p. 40)

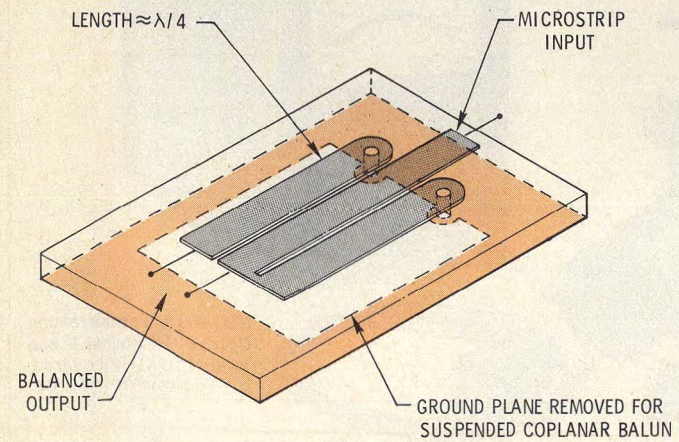

6. Metallized shorts and vias simplify the design of planar topologies. The planar balun (a) and biased single-balanced mixer (b) use metallized holes to ground upper and lower resonators to a ground plane deposited on opposite side of substrate (as indicated by color tint). The inverted single balanced mixer (c) uses metallized vias to connect microstrip inputs sputtered on opposite side of substrate. Grey areas indicate metallization on top substrate surface while colored areas depict ground plane on bottom surface.

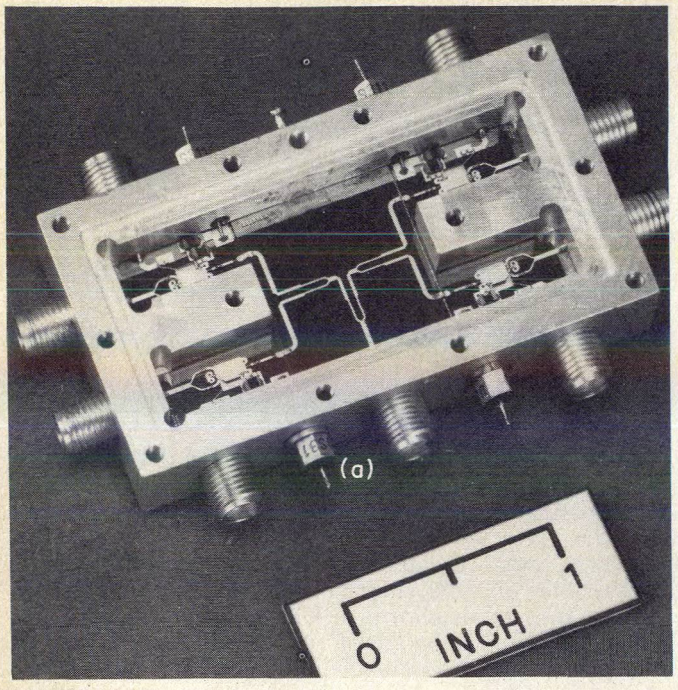

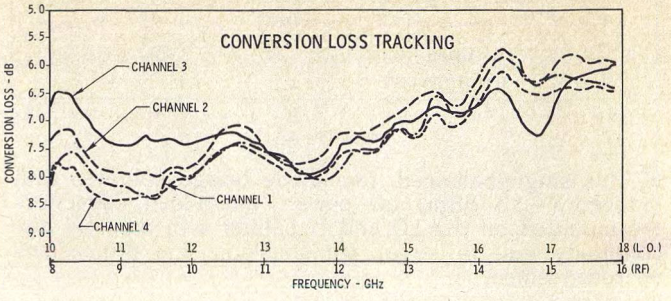

(b)

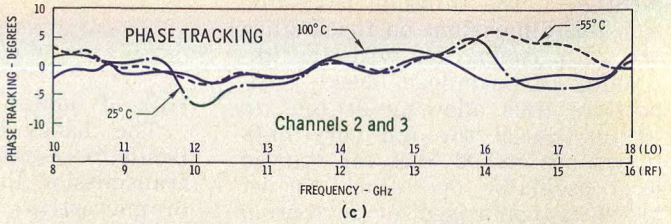

(c)

7. Four mixers of the type shown in Fig. 6b are driven by a common LO through a power dividing network. Note close conversion loss (b) and phase (c) tracking. HP 5082-2767 beam lead diodes are used in the design.

nique, applied to alumina substrate, involves low-cost laser drilling, and has proven to be an excellent design approach at lower frequencies.

Since the resultant mixer is principally located on the top surface of the substrate, it is a relatively simple matter to incorporate beam lead capacitors as dc blocks such that the mixer can be dc biased for starved LO operation.

A mixer circuit realization of more elegant simplicity is shown in Fig. 6c. Note that the mixer elements are realized by etching a pattern in a ground plane and are thus located on the reverse side of the substrate, which is the tinted portion of Fig. 6c. The balun is similar to that of Fig. 6a, but the rf diode drive is realized with an unbalanced single coplanar line. This results in a structure with superior L to R isolation, and one which is relatively simple to manufacture. Transitions from coplanar to microstrip lines are achieved with 0.015 inch diameter sputtered through holes in the

(continued on p. 43)

Wide application range (18-170 GHz) and high measuring accuracy... typical merits of Hitachi Millimeter Wave Test Equipment

1513/1514 Attenuator
50dB maximum
0.1dB or ±1% accuracy

2210 Frequency Meter
Pure 'dip' over waveguide band

MT-469A Temperature Controlled Power Meter
18 to 110 GHz covered by Thermistor mounts

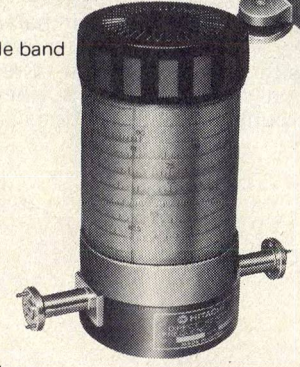

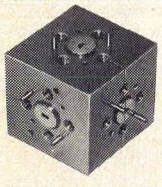

3703 Matched Hybrid Tee
Covers 80 to 90 percent of waveguide band

Hitachi Electronics, Ltd.
1-23-2, Kanda Suda-cho, Chiyoda-ku, Tokyo 101, Japan Tel: (255)8411 TELEX: J24178

OVERSEAS AFFILIATED COMPANIES

- **HITACHI SHIBADEN CORPORATION OF AMERICA**
  Head Office : 58-25 Brooklyn-Queens Expressway, Woodside, N.Y. 11377, U.S.A. Tel: (212) 898-1261 TELEX: 7105822495
  Western Office : 21015-21023 So. Figueroa Street, Carson, Calif. 90745, U.S.A. Tel: (213) 328-2110
  Midwest Office : 1725 North 33rd Ave., Melrose Park, Illinois 60160, U.S.A. Tel: (312) 344-4020
  Southwest Office : 14169 Proton Road, Dallas, Texas 75240, U.S.A. Tel: (214) 233-7623
  Southeast Office : 3610 Clearview Parkway, Doraville, Georgia 30340, U.S.A. Tel: (404) 451-9453
- **HITACHI DENSHI LTD.(CANADA)**
  922 Dillingham Road, Pickering, Ontario, L1W 1Z6 Canada Tel: (416) 839-5134, 839-5173 TELEX: 623574
- **HITACHI SHIBADEN EUROPA GMBH**
  6 Frankfurt Am Main, Kennedy Allee 109, F.R. Germany Tel: (0611) 639063-4 TELEX: 414509
- **HITACHI SHIBADEN (U.K.) LTD.**
  Head Office : Lodge House, Lodge Road, Hendon, London NW4 4DQ, England Tel: (01) 203-4242 TELEX: 27449
  Leeds Office : Video House, 55 Manor Road, Leeds, LS11, 5PZ, England Tel: 0532-30294

READER SERVICE NUMBER 40

FUSED SILICA

0.010 inch thick fused silica. Rf to i-f diplexing is achieved with a single beam lead capacitor and simple microstrip low-pass filter on top (grey) microstrip circuit side. It should be noted that a disadvantage of this structure is that it is relatively difficult to incorporate dc bias for starved LO operation.

Unbiased, the inverted mixer shown in Fig. 6c functions as an excellent J-band biphase modulator, due to the inherent isolation of the balun. In this application low frequency (up to 2 GHz) modulation is applied to I port to drive the transfer function between two equal amplitude states with a relative phase delay difference of 180 degrees. DC tests show phase error less than three degrees and amplitude of 0.25 dB from 14-16 GHz. Carrier suppression of over 30 dB was also achieved. This performance is thought to be a unique new result for single balanced biphase modulators. An important advantage of this design is the small size and planar nature of the circuit topology, which is expected to simplify the integration of such devices in quadraphase modulator assemblies.

It was mentioned previously that the reduced effective dielectric constant of fused silica relative to alumina causes the discontinuities created by beam-lead devices to be of lesser electrical length, thus reducing the level of parasitics. This advantage is exploited in the phase-matched four-mixer assembly shown in Fig. 7, which is based on the topology introduced in Fig. 6b. In this circuit, a common LO signal is fed to a four-way power divider.[7]

Of particular interest in this design are the temperature properties of fused silica. Phase tracking of the two mixer pairs remained within ±7 degrees over a temperature range of −55 to +100°C. This phase error is too small to isolate the specific sources of phase temperature dependence, other than just to state that the fused silica approach is successful for matched mixers.

Performance includes 22 dB LO to rf isolation, 32 dB LO to i-f isolation and 25 dB rf to i-f isolation. Interchannel isolation (rf input to i-f output) is 45 dB. With a +8 dBm LO drive level, the $2F_L \pm 2F_R = F_{IF}$ intercept point is +19 dBm.

Acknowledgement

The authors wish to acknowledge the contributions of Richard Oglesbee, David Stauffer and Ramon Pereira toward the fabrication and electrical evaluation of the quartz-based mixers. Also, the efforts of Joseph Gibes and Dr. Walter Wilser in developing the fused silica metallization process were essential to the work reported here. ●●

References

1. M. V. Schneider, "Microstrip Lines for Microwave Integrated Circuits," BSTJ, pp. 1421-1444, (May, June, 1969).

2. W. W. Snell, Jr., "Low-Loss Microstrip Filters Developed By Frequency Scaling," BSTJ, pp. 1919-1931, (July-August, 1971).

3. J. H. C. van Heuven & A. G. van Nie, "Properties of Microstrip Lines on Fused Quartz," *IEEE Trans. Microwave Theory & Tech.*, pp. 113-114, (February, 1970).

4. Robert E. DeBrecht, "Coplanar Balun Circuits for GaAs FET High-Power Push-Pull Amplifiers," 1973 IEEE-MTT, International Microwave Symposium, pp. 309-311.

5. C. P. Wen, "Coplanar Waveguide: A surface strip transmission line suitable for nonreciprocal gyromagnetic device applications," *IEEE Trans. Microwave Theory Tech*, Vol. MTT-17, pp. 1007-1090, (December, 1969).

6. T. Hatsuda, "Computation of Coplanar—Type Strip-Line Characteristics by Relaxation Method and its Application to Microwave Circuits," *IEEE Trans. on Microwave Theory & Tech.*, Vol. MTT-23, No. 10, pp. 795-802, (October, 1975).

7. S. B. Cohn, "A Class of Broadband Three-Port TEM-Mode Hybrids," *IEEE Trans. on Microwave Theory and Techniques*, Vol. MTT-16, No. 2, pp. 110-116, (February, 1968).

Test your retention

1. What is the dielectric constant of fused silica? Why is this an asset?
2. How do the thermal properties of fused silica compare with those of alumina?
3. What is a common surface finish for fused silica?
4. What substrate thickness is practical for double-sided circuit topologies at J-band?

PYROFILM MAKES IT!

- Ground Plane Spacing available in .125, .250 and .062
- Guaranteed VSWR
- DC to 8 GHz VSWR 1.2
  8 - 12.4 GHz VSWR 1.35
  12.4 - 18 GHz VSWR 1.35 available
- Up to 3 Watts

For a complete descriptive literature, write to: **PYROFILM**, 60 South Jefferson Road, Whippany, N.J. 07981 or discuss your design with one of our application engineers by calling (201) 887-8100.

PILLSHAPE TERMINATIONS, ATTENUATORS, RESISTORS & CAPACITORS...WITH Ku BAND SPECS.

Setting New Standards in Reliability

PYROFILM

READER SERVICE NUMBER 43

What's New With Receiver Protectors?

Don't count the TR tube out yet! By combining a gas plasma front stage with diode limiters, kW of power can be stopped with minimal output spike and flat leakage.

RECEIVER protectors act as fast-acting sophisticated fuses to prevent damage to sensitive radar receivers. This damage can result from power reflected from the antenna during the transmit period or from nonsynchronous pulses due to high-power EMI or high-power jamming. There are four competing technologies used in the design of receiver protectors:

- gas plasma
- ferrite
- semiconductor diode
- multipactor

Hybrid combinations of these technologies are also quite common and all are commercially available.

The decision as to which system is most useful depends on the specific application. Each should provide certain common characteristics such as low-insertion loss, fast recovery period and low-leakage power under a wide spectrum of environmental conditions and over a wide range of power level and ambient temperatures. They also should have an operating life of at least several thousand hours with a high degree of reliability. Reliability is not only important from the radar MTBF point of view, but is economically important because of the shift in the last decade from point contact mixers as low-noise front ends to expensive pre-amplifiers such as paramps, TDAs, FETs and expensive Schottky barrier mixers.

Passive protectors eliminate power supply

A recent and most useful trend in receiver protection has been the elimination of the power supply. This allows protection even when the radar is off and eliminates the need for a mechanical shutter. Passive receiver protectors (RPs) will also protect a radar against nonsynchronous pulses such as nuclear blasts.

In certain applications, the recovery period must be brief (about 50 nsec) so that a vacuum multipactor type is mandatory.[1] This relatively expensive device requires voltage supplies to power an ion source, an electron gun and an oxygen source. Passive protection, therefore, is not attainable for the multipactor RP. Because leakage power is relatively high, a multistage diode limiter is required to follow the mutipactor if one is protecting a mixer, TDA, paramp or FET.

If recovery time is not a critical factor, however, a selection may be made from ferri-diode, plasma-diode or straight diode receiver protectors. Pure ferrite devices have a slow response, resulting in a spike leakage almost equal to the peak incident rf power. Pure plasma devices with the nuclear ignitor are still not reliable[2]. If rf power is above a few tens of watts, the pure diode RP is rarely used because the diode must be externally driven and the passive protection capability is lost. Passive, all-diode RPs that can handle relatively high rf power levels are still in the developmental stage. The choice thus narrows to the ferri-diode and plasma-diode for a wide variety of radar (waveguide) applications.

The ferri-diode has one serious drawback compared to the plasma-diode; it cannot handle full transmitter power during an antenna arc, whereas a gas plasma is well suited for short-term overloads. This advantage is due to the increased percentage ionization which enhances rf conductivity in the gas plasma as the rf incident power increases. Rather than absorb rf power as the ferrite device does, the plasma reflects the rf power through a circulator to a dummy load Fig. 1.

This high reflectance prevents heating of the pre-TR plasma stage and explains why gas plasmas can handle larger average power levels than ferrite devices at equivalent frequencies and for similar conditions of volume and cooling. The important difference is that, above a certain optimum level, that occurs at low to moderate power, absorbed rf power decreases with increasing rf incident power. In ferrites, the device is matched to the line over a wide range of rf power up to relatively high levels and temperature, therefore, increases monotonically with increasing incident power.

Plasma-diode RPs

Many systems, therefore, use passive plasma-diode receiver protectors because of their high rf power capability. They also offer relatively fast recovery periods using halogen gases (200 nsec at 200 watts of average power at X-band) and can protect all types of low-noise amplifiers. Insertion loss is conveniently

(continued on p. 48)

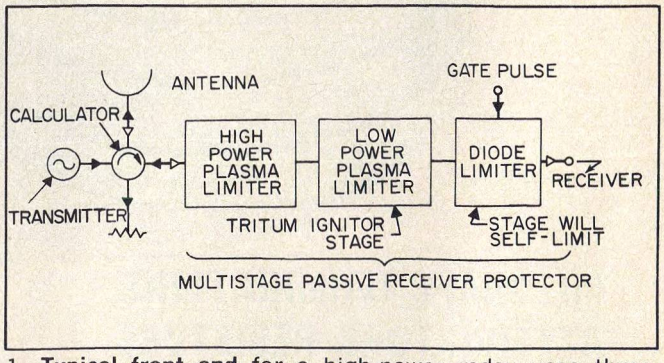

1. **Typical front end** for a high-power radar uses three stages of passive receiver protection.

Harry Goldie, Supervisory Engineer, Westinghouse Defense and Electronic Systems Center, Systems Development Division, Advanced Technology Laboratory, Baltimore, MD 21203.

HOW TO MEASURE NOISE FIGURE – Accurately, Easily & Automatically

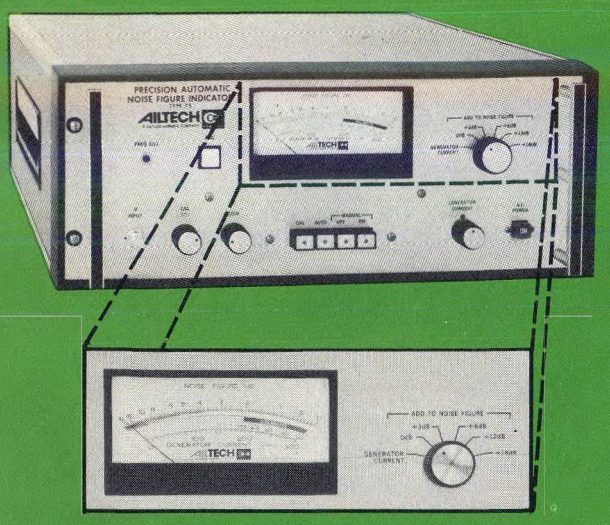

AILTECH'S 75

The *Precision* Automatic Noise Figure Indicator (PANFI)

The AILTECH 75 PANFI has become the noise figure measurement standard in many laboratories around the world. Why? Because its operational features simplify what used to be a difficult, cumbersome measurement.

Its basic ±0.15 dB tracking accuracy almost eliminates the need for manual Y-factor measurements and tedious calculations. Features such as front panel signal level monitoring, high-resolution readout—with an offset range switch that lets you take full advantage of it, and calibration for the noise generator you are using, eases the measurement and provides full confidence in its validity.

When you have a noise figure measurement problem, the AILTECH 75 PANFI could be the solution. In addition, we back our instruments with many years of experience and proven, recognized expertise in receiver noise measurements.

Call or write us for free consultation and your AILTECH Noise Figure Slide Rule.

AILTECH A CUTLER-HAMMER COMPANY CONTROL

EAST COAST • 815 BROADHOLLOW ROAD • FARMINGDALE, NEW YORK 11735
TELEPHONE: (516) 595-6471 • TELEX: 510-224-6558
WEST COAST • 19535 EAST WALNUT DRIVE • CITY OF INDUSTRY, CA. 91748
TELEPHONE: (213) 965-4911 • TELEX: 910-584-1811
INTERNATIONAL OFFICE
FRANCE — La Garenne-Colombes, Telephone 7885100, Telex 842-62821
GERMANY — Munich, Telephone (0811) 5233023, Telex 841-529420
UNITED KINGDOM — Crowthorne, Telephone 5777, Telex 851-847238
JAPAN — Tokyo, Telephone (404) 8701, Telex 781-02423320 (Nippon Automatic)

READER SERVICE NUMBER 33

low—0.6 dB at X-band for 8% bandwidths.

A decade ago for many years up until the early 1970's, the gas-type TR tube was the prime target for a host of improvement programs. The main objective was to eliminate the gas-type TR in favor of the more reliable solid-state technologies that were then emerging into maturity. Over the years, ample evidence had accumulated of the poor reliability and short operating life of gas-type TR tubes.

In spite of this reputation, over the last six years, a series of developments has occurred in the gas plasma field that have renewed interest in the gas-type TR. It has reemerged to become an important element in modern radar systems. These developments include the pioneering work of Maddix[3] and others in analyzing the gas cleanup problem (so that plasma stage operating life became predictable) eliminating the old dc keepalive[2], integrating plasma stages with variable basewidth PIN diodes[4,5] and the development of pre-TR windowless discharge.[6] There have also been improvements in processing techniques and discrete element design. In the latter case, each stage is separately optimized over the anticipated rf power level for optimal electrical characteristics.

All of these recent developments radically altered the electrical characteristics of the once lowly gas-type TR. Operating life, now predictable hence designable, is made to be over 10,000 hours at relatively high mean power levels. Leakage power is not a problem because cascaded diode limiters reduce it to tens of milliwatts at the expense of a few tenths of a dB insertion loss. For example, 0.1 dB power limiter stages at X-band over an 8% bandwidth and 0.03 dB per limiter stages at L-band over a 10% bandwidth

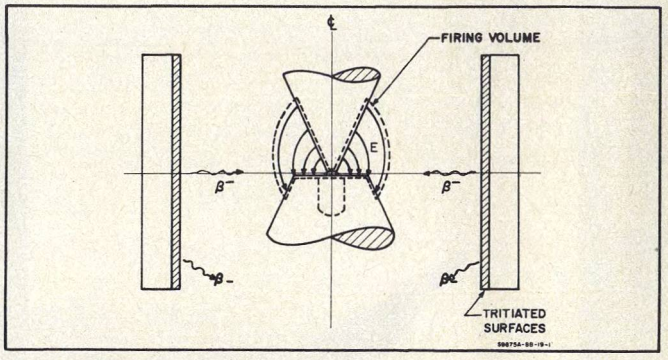

2. **The tritiated titanium ignitor** has tritiated inner surfaces to supply free electrons to the cone gap which eliminates the need for a dc power supply or keepalive.

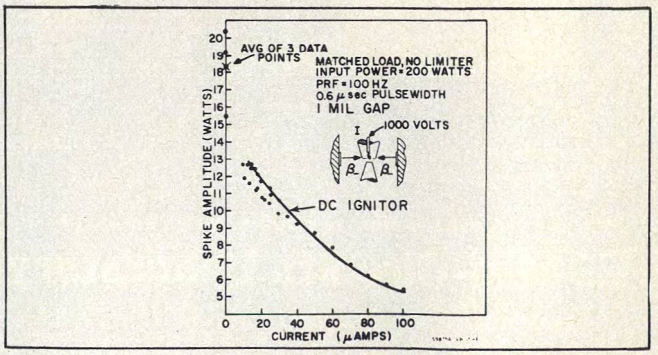

3. **Spike power is higher for a tritiated ignitor** because the electron density provided by a tritium primer is less than that provided by a dc keepalive. This means higher firing thresholds and necessitates using diode limiter stages to reduce spike and flat leakage. The dc ignitor curve is shown for comparison.

are now commercially available from such firms as Westinghouse, Varian, Microwave Associates and Micro-Dynamics. Recovery period is now typically in the one to two hundreds of nanoseconds range due to the use of halogen gases in the high-power stages.

As a result, the tendency to replace gas TRs with ferrite and semiconductor diodes has been considerably slowed. The tritiated titanium ignitor (Fig. 2) eliminates the keepalive dc discharge as the electron primer, thus removing the two main factors that shorten TR life and reliability: gas dissociation and sputtering due to ion bombardment. As shown by the spike amplitude data of a single stage, Fig. 3, the free-electron density provided by a tritium primer is significantly smaller than that provided by the dc keepalive, resulting in higher spike leakage and higher firing thresholds. It then becomes necessary to use one or two cascaded diode limiter stages to reduce spike and flat leakage amplitudes to levels compatible with receiver protection.

Figure 4 shows the statistical distribution of spike amplitudes for the case of dc and tritium ignitors with and without a limiter stage. This data reveals that a dc ignitor TR without a limiter has the same spike leakage as a tritium ignitor with a single limiter. The distribution of electron currents in front of a tritium primer is shown in Figs. 5 and 6. This data was taken at characteristic TR gas pressures in an ion chamber using a movable probe with no bias voltage applied.

Optimize each limiting stage

Tests show that receiver protectors with tritium ignitors and diode limiters and without a dc keepalive discharge are most likely to fail due to gas cleanup at the input window. This cleanup is due to sorbed gas molecules in the discharge areas. Lifetimes have been found proportional to the square of the gas volume-to-discharge area of ratio[3] and could, in principle, be increased indefinitely by adding sufficient gas volume. The lifetimes of a TR are predictable, provided a short-term initial measurement of pressure decrease can be determined experimentally.

In the past, TRs and receiver protectors frequently used a glass window discharge. The window is soft soldered with quartz wool against the glass to shorten the discharge recovery time; however, the wool greatly increases the discharge area. This design has a short operating life because of the high molecular sorption rates during discharge. Figure 7 depicts a discrete-stage design that eliminates the window discharge in

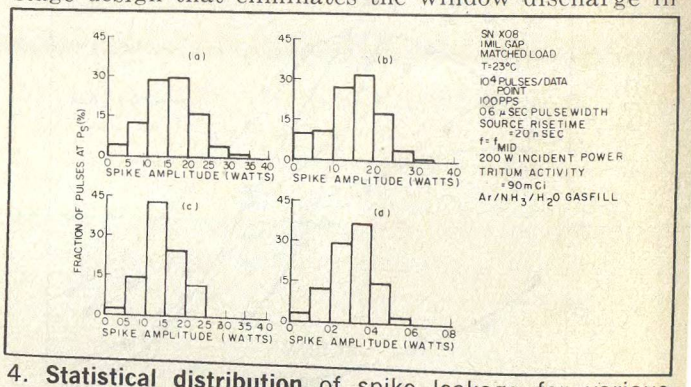

4. **Statistical distribution** of spike leakage for various operating modes using 90 milli-Curie ignitor: (a) no limiter in circuit, dc keepalive quiescent; (b) one diode limiter used but dc keepalive quiescent; (c) no limiter in circuit; dc keepalive on; (d) one diode limiter used with dc keepalive on. Note that spike leakage of (b) and (c) are equivalent indicating keepalive can be replaced by nuclear ignitor.

(continued on p. 50)

NEW! Digitally Programmable Phase-Locked "Mini-Synthesizers"

In any band from 0.5-18GHz, these completely self-contained Series DSR/DSM miniature synthesizers will provide fast-switching digital frequency programming in 250kHz steps, with very low phase noise. Shown above: All-solid-state source, BCD-programmable in 250kHz steps from 4.8-5.33GHz; switching time less than 10msec; FM noise, 40Hz in a 3kHz bandwidth, 10kHz-10MHz; phase-locked to ultra-stable internal crystal; only 27 cubic inches! (Higher speeds and resolutions available.) **Send for the complete CTI signal-source engineering file.**

CTI

COMMUNICATION TECHNIQUES INC.

1279 Route 46, Parsippany, N.J. 07054, CALL: (201) 263-7200, TWX: 710-987-8341

READER SERVICE NUMBER 50

the ignitor stage by transferring it to a gas-filled quartz vial. The use of quartz as the surface adjacent to the discharge, as opposed to the soft-soldered window with its residue of flux, significantly suppresses gas cleanup and allows the use of halogen gases having fast recovery periods. It also means that the pre-TR being a separate stage with its own characteristics, could be optimized for its primary function—that of a very high-power limiter, with a fast plasma extinguishing period, having a large gas receiver volume for long life. This is accomplished by the use of large multiple vials located in the same plane.

Reliability is further increased by internally pressurizing the waveguide surrounding the quartz vials. A mica window is placed in front of the pre-TR to form a hermetic envelope for the N_2 cell. This keeps the high-Q slot area where the intense E-fields exist, free of water vapor, dust and other contaminants. The pressurized nitrogen also fills the circular gap formed by the quartz envelope and surrounding metal, thus preventing arcing, corrosion and pitting.

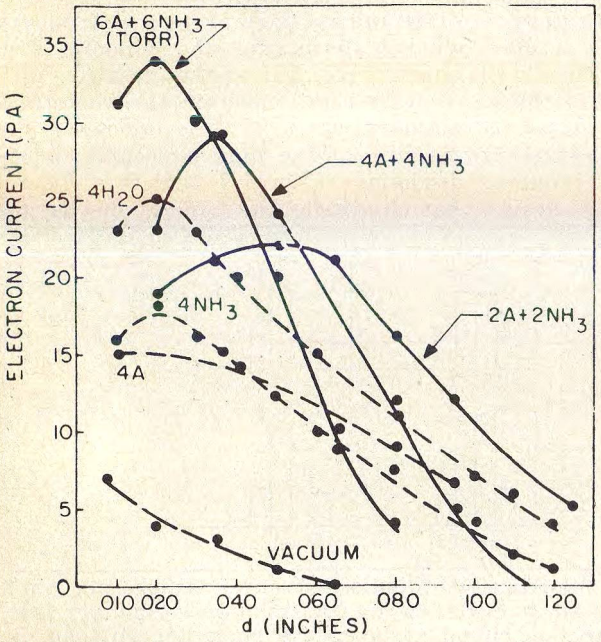

5. **Various gas mixtures** can be used with a tritium ignitor. Both the gas mixture and the interelectrode spacing influence the electron densities that result at zero bias.

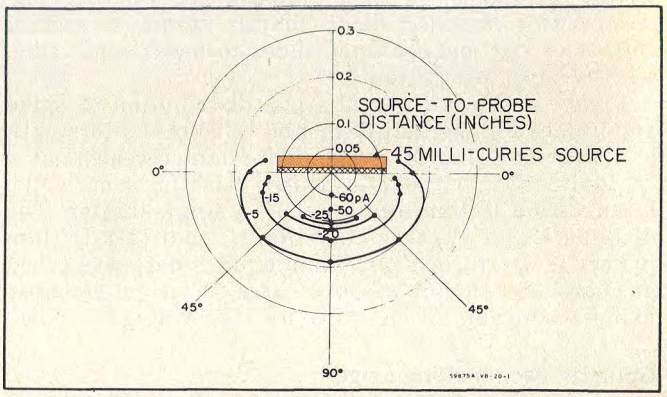

6. **The current in the ion chamber** of a tritium ignitor has an elliptical distribution which varies inversely with the source-to-probe distance.

ENGELMANN MAKES IT!

50 WATT ATTENUATOR IN 2 CUBIC INCHES

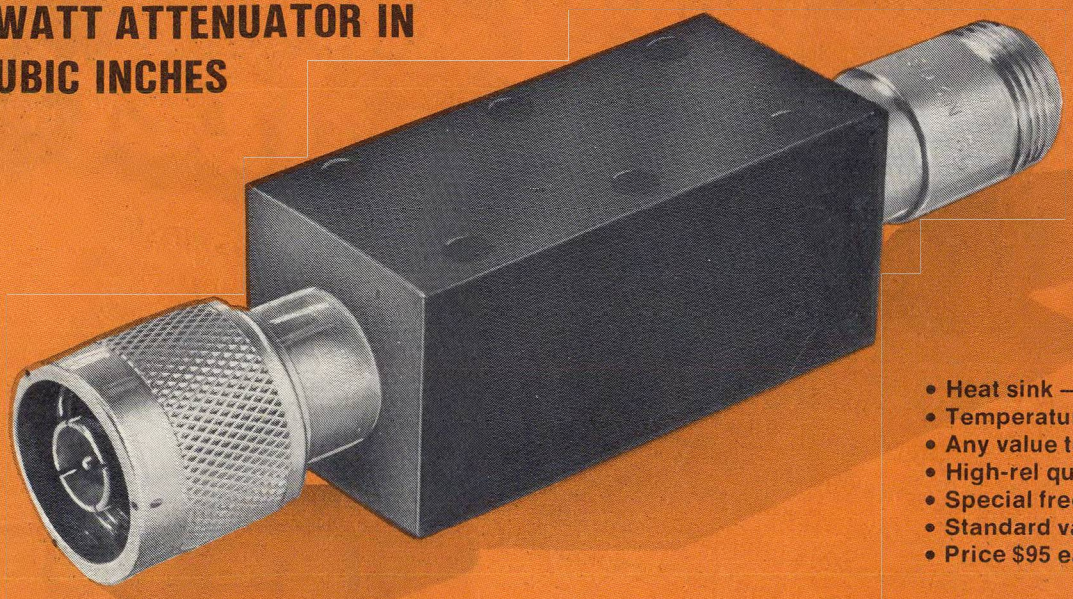

- Heat sink — compact size
- Temperature to +125°C
- Any value to 50 db
- High-rel qualified
- Special frequency to KU band
- Standard values in stock
- Price $95 each

For detailed literature or custom design information, contact **ENGELMANN** Microwave Co., Skyline Drive, Montville, N.J. 07045, (201) 334-5700

Setting New Standards in Reliability

ENGELMANN

Engelmann Microwave Co. — Subsidiary of Pyrofilm Corporation

READER SERVICE NUMBER 49

The front or pre-TR stage that limits the highest power levels has been the subject of a large number of recent life experiments since diode limiters are not capable of switching kilowatts of average microwave power. Ferrite limiters operated in the subsidiary resonance mode are inherently absorbtive and slow acting and cannot operate at kW average power levels. The simple pre-TR quartz vial is highly cost effective since it limits kilowatts of rf average power and is composed of two parts: a quartz vial and aluminum mount.

Leakage amplitudes and recovery time as a function of incident power, with and without a dual-diode limiter, is shown in Figs. 8, 9 and 10. The spike and flat amplitudes are under 50 and 20 mW, respectively, up to 10 kW over a 10% frequency range in X-band. Figure 10 shows 3 dB recovery periods and 400 nanoseconds from 100 watts to 5 kW. Note that, at power levels above the vial threshold, the leakage and recovery remain low and stable from 0.1 to 10 kW; no window discharge occurs. Equivalent parameters at C-band over a 12% bandwidth and at S-band over and 8% bandwidth are shown in the table.

(continued on p. 52)

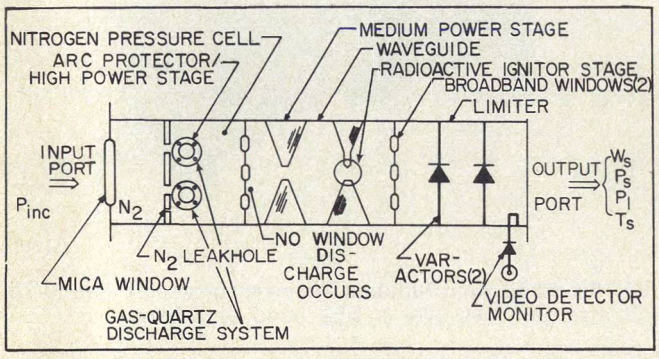

7. **Discrete three-stage design** eliminates the window discharge in the ignitor stage by transferring it to a gas-filled quartz vial. The varactor limiter stage limits spike and high leakage amplitude.

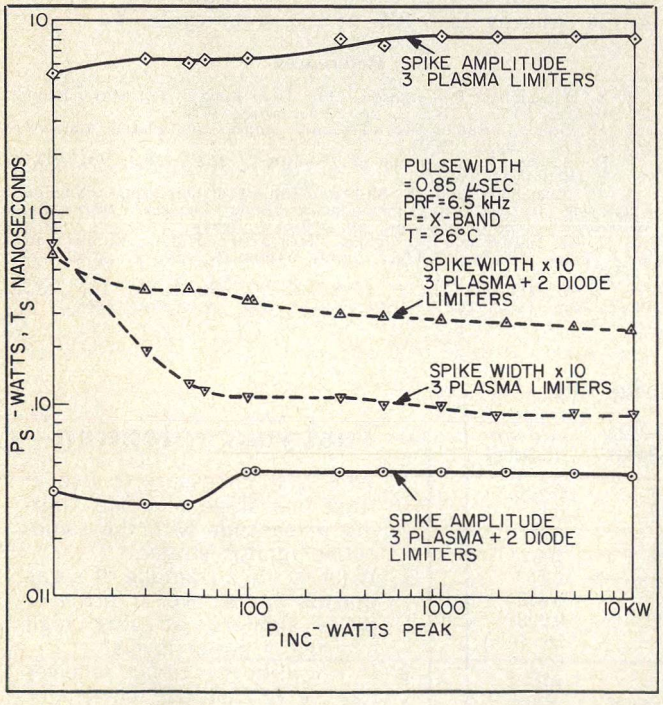

8. **Spike amplitude drops sharply** by adding diode limiter stages but spike width increases while leakage energy remains under 0.005 ergs at all power levels.

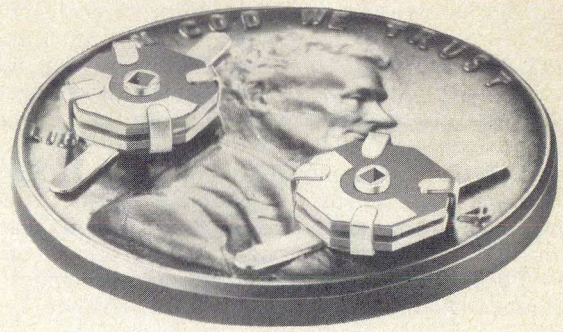

THIN-TRIM CAPACITORS FOR HYBRIDS AND MIC'S

Series 9410 Thin-Trims are sub-miniature variable capacitors for applications where size and performance are critical. Featured are high Q's for low circuit losses, high capacity values for broadband applications and low profile for "gap trimming" in tiny MIC's. Body size .200" x .200" x .060"T. Available in 5 capacitance ranges from 1.0 - 4.5 pf to 7.0 - 45.0 pf.

Johanson®

MANUFACTURING CORPORATION
Rockaway Valley Road
Boonton, N.J. 07005
(201) 334-2676 TWX 710-987-8367

READER SERVICE NUMBER 51

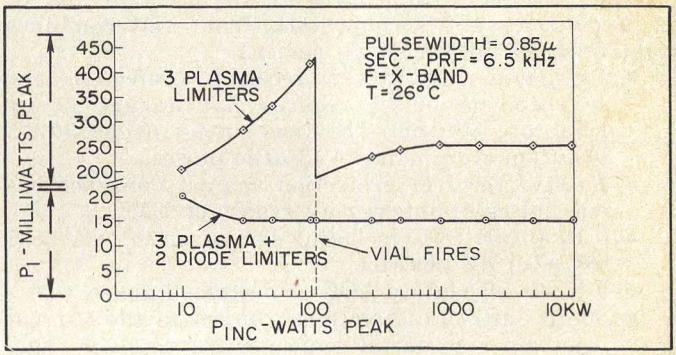

9. **Addition of diode limiter** smooths out flat leakage characteristic 30 dB range of incident power.

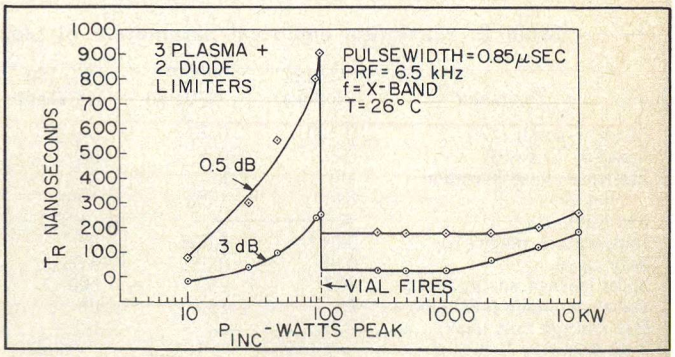

10. **3 dB recovery time is well** under 250 ns up to 10 kW power levels.

RECEIVER PROTECTORS

Life testing, while simultaneously temperature cycling at 200 watts of average power on an X-band pre-TR/radioactive ignitor/diode-limiter-receiver-protector shows no significant degradation in leakage recovery time or insertion loss properties for 5,600 hours. Indications are that the plasma/diode protector with discrete stage optimization has an rf operating life in excess of 10,000 hours.

The principle of separate stage optimization of plasma/diode receiver protectors has yielded low-loss ignitorless RPs that are capable of protecting radar receivers using Schottky barrier diode mixers or other LNAs. They provide a significant improvement in performance over single-envelope TRs with dc keep-alives.

The seven-stage (WD-132A) S-band receiver protector in Fig. 11 has been successfully field evaluated and is now in production. It contains five individual stages, each of which is optimized at the appropriate rf power level. The first four are a double-vial stage to handle 100 kW peak and 4 kW average, a single-vial stage to operate at 1 kW peak, a capillary stage to handle 10 watts peak and tritium ignitor stage to operate at 0.2 watt peak. The fifth section, composed of three PIN diodes, decreases the peak power to 20 mW flat leakage and 400 mW spike leakage. Recovery period is under 350 nsec for this unit. The unit may be gated to achieve an additional 25 dB of attenuation. When not gated, the device will satisfactorily protect a receiver in the passive mode.

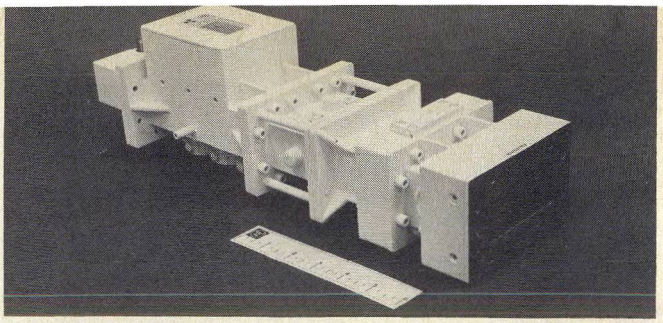

11. **Seven-stage receiver protector** consists of a double vial stage, single vial stage, a capillary stage and a PIN diode stage. Recovery is under 350 ns and it reduces 100 kW peak, 4 kW average to 20 mW leakage and 400 mW spike leakage.

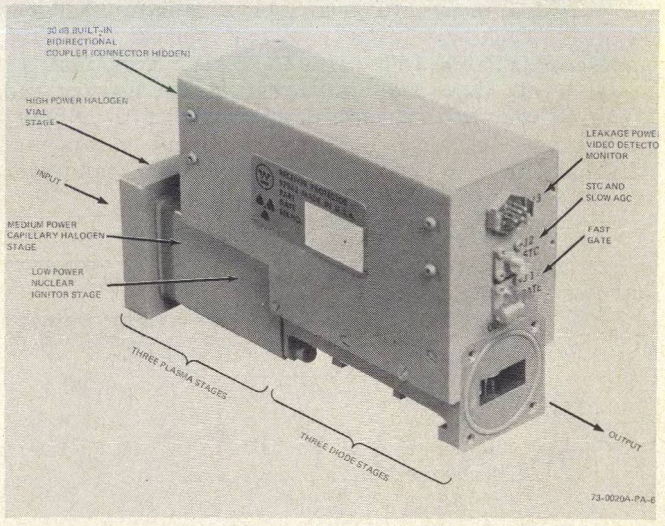

12. **Six-stage multifunction receiver** protector has 0.75 dB insertion loss over a 5% band at X-band.

Multifunction receiver protectors

Another recent trend in receiver protectors is to combine several functions into the receiver protectors. This is possible only if the insertion loss does not increase substantially. Figure 12 shows a six-stage X-band receiver protector with an insertion loss of 0.75 dB over a 5% bandwidth. This unit combines six functions into a single device.

- Pre-gated high-power receiver protection for synchronous pulses reduces flat leakage power level to −30 dBm. The diode gate provides 50 dB of attenuation using +13 dBm pulses.
- Passive receiver protection against nonsynchronous pulses of interfering radars or EMI.
- 0 to 40 dB STC including linearizer to provide 5 dB ±0.1 dB per volt.
- 0 to 40 dB clutter AGC as described above.
- 30 dB built-in bidirectional coupler to allow signal injection via coaxial connector for receiver tests.
- Video detector to monitor output leakage amplitude.

This multifunction receiver protector uses two halogen stages in front of the nuclear ignitor stage to recover within 10% of the cold loss in 200 nsec at power levels ranging to 5 kW at 2% duty cycle. ••

References

1. R. Dokken and P. Ferguson, "For High Power—Try Multipacting," *MicroWaves*, Vol. 13, No. 7, pp. 52-53, (July, 1974).
2. H. Goldie, "Radioactive (Tritium) Ignitors for Plasma Limiters," *IEEE-GED*, (August, 1972).
3. H. Maddix, "Gas Cleanup in TR Tubes," *IEEE-GED*, Vol. ED-15, No. 2, (February, 1968).
4. R. Tenenholtz and P. Basken, "Improved Duplexing Techniques Employing Gas T-R and Semiconductor Limiter Devices," *International Microwave Symposium Record*, pp. 209-212, (1964).
5. T. M. Nelson and H. Goldie, "Fast-Acting X-Band Receiver Protector Using Varactors," *IEEE SMTT Symposium Digest*, pp. 176-177, (1974).
6. D. W. Downton and P. D. Lomer, "A Pre-TR For High Mean Power Duplexing," *IEEE-GMTT*, pp. 654-670, (November, 1960).

Table 2. Maximum electrical parameters of plasma/diode RPs

Parameter	WD-132 (S-Band)	WD-191 (C-Band)	WD-160 (X-Band)	WD-242A (X-Band)	WD-256 (L-Band)
Incident power (kW)	0-100	0-70	0-0.5	0-10	0-500
Insertion loss (dB)	0.6	0.7	0.7	0.8	0.6
Insertion phase deviation -deg	10	8	8	10	N/A
Bandwidth (%)	8%	12%	10%	10%	7%
Temperature range (°C)	← −50° to +80° →				0-50°
Duty cycle	0.04	0.006	0.5	0.01	0.006
Spike leakage energy (ergs)	0.05	0.05	0.05	0.05	0.008
Spike amplitude (kW peak)	400	250	500	50	30
Flat leakage (mW peak)	25	15	25	20	5
3-dB Recovery time (μs)	0.35	20	0.15	0.4	10
RF operating life (hr)	>10,000	>10,000	>10,000	>10,000	20,000
Protects	Paramp + Mixer	FET	Paramp + Mixer	Paramp + Mixer	Bipolar transistor amplifier

Test your retention

1. Why is it necessary to use at least one stage of diode limiting in cascade with the radioactive ignitor stage?
2. What is the advantage of a gas plasma limiter over a ferrite or diode limiters at very high average rf power levels?
3. If an airborne radar receiver has an FET ultrasensitive amplifier as a low-noise front end, which type of RP would you use?

zie Microwaves october 1976, pag 89

How Noisy Is That Load?

The output power of a noise standard is considered proportional to temperature and independent of frequency. But at mm frequencies, this assumption is wrong. An error curve shows how much.

CALIBRATION of microwave radiometers and other low-noise receivers requires noise sources emitting a known amount of noise power. Noise standards frequently consist of a well-matched termination held at a constant temperature. Cold loads have a temperature defined by the boiling point of a cryogenic coolant, such as liquid nitrogen or helium. Hot loads may be designed in a similar manner, using a liquid with a high-boiling point or a carefully controlled heater to maintain the termination at known temperature.

In all hot or cold loads, it is generally assumed that the termination emits a noise power N expressed by:

$$N = kTB \qquad (1)$$

where: $k = 1.3804 \cdot 10^{-23}$ J/°K (Boltzman's constant)
T = Temperature in degrees Kelvin (K).
B = Bandwidth in Hz.

However, Eqn. (1) is an approximation of the general blackbody radiation formula originally derived by Planck. For low temperatures and high frequencies, such as in the millimeter range, use of this approximation can lead to errors which are significant in many applications.

This article presents a derivation of the error limits inherent in the expression $N = kTB$, using higher order approximations to the exact formula. The results are presented graphically in the form of correction terms vs. temperature and frequency.

Derivation of errors

The exact formula for noise power N, emitted within a narrow frequency interval of B Hz by a matched termination held at a physical temperature T°K is:

$$N = kTB \frac{2x}{e^{2x} - 1} \text{ (Watts)} \qquad (2)$$

where: $2x = hf/kT$,
$h = 6.625 \cdot 10^{-20}$ J s (Planck's constant)

If the frequency f is expressed in GHz, then

$$x = 0.0240 \cdot f/T$$

When $x << 1$, the denominator of Eqn. (2) is approximately 2x, which leads to the first order approximation given in Eqn. (1).

To derive higher order approximations, it is convenient to rearrange Eqn. (2) as follows:

$$N = kTB \cdot x \cdot (\text{cotanh } x - 1) \qquad (1)$$

Expanding the cotanh function in a power series, gives:

$$N/kB = T - 0.0240 \cdot f + 1.920 \cdot 10^{-4} \cdot f^2/T \ldots . \quad (4)$$

Retaining the well established definition of noise temperature, $T_N = N/kB$, it's apparent that T_N is lower than the physical temperature T. For low frequencies, the difference is negligible, but in the millimeter-wave region, the error may be significant in certain applications, such as precision radiometry.

How big is the error?

In the expansion shown in Eqn. (4), additional terms of the series are less than 0.1°K for frequencies below 100 GHz and temperatures above 2°K. With these limitations in mind, Eqn. (4) can be approximated by:

$$T_N \approx T - T_1 + T_2 \qquad (5)$$

where:
$T_1 = 0.0240$ f (f in GHz)
$T_2 = 1.920\ 10^{-4}\ f^2/T$

Values of the correction terms T_1 and T_2 are plotted in Fig. 1 for the frequency range 1 to 100 GHz. In this region, T_2 is significant only for very low temperatures and when frequency is close to 100 GHz.

(continued on p. 56)

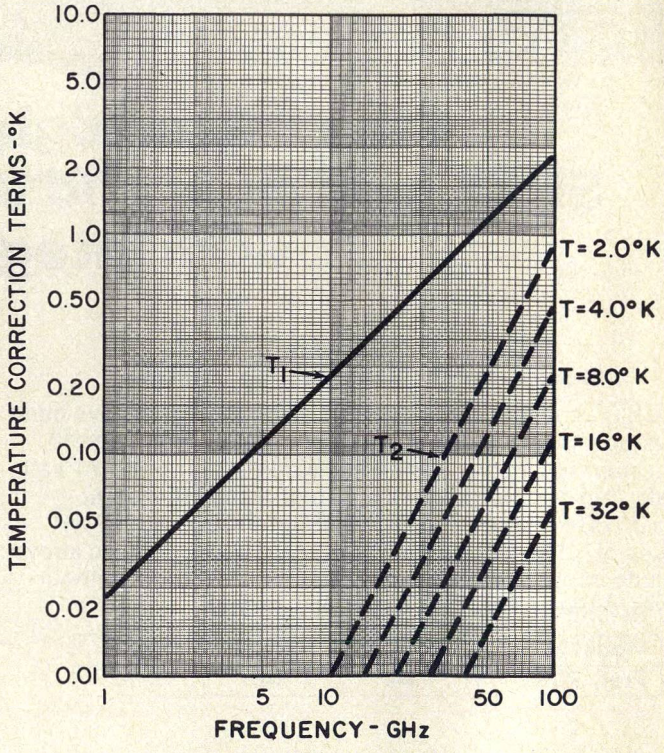

1. Error curves for obtaining temperature correction factors, T_1 and T_2. T_1 is temperature independent while T_2 is significant only at low temperatures and in the millimeter region.

Dr. Mats E. Viggh, Vice President, Transmission Lines, Inc., P. O. Box 292, Ipswich, MA 01938.

Correction term T_1 exceeds 0.1°K for frequencies above 4 GHz, regardless of temperature. The correction terms T_1 and T_2 derived here are of a significant magnitude when compared to other corrections normally applied to cold loads.

There are two important sources of error to consider in this context:

- impedance mismatch
- losses in the transmission line connecting the cooled termination to the output port.

The physical temperature of the termination determines the *available* noise power. However, unless the cold load is well matched, the actual power delivered to a receiver-under-test will be lower than the available power.

The output port of the cold load is normally at or near room temperature. The physical temperature and the ohmic losses will change gradually along the transmission line between the cooled termination and the output port. The noise radiated into the line by the lossy walls will thus be different at different locations along the transmission line.

Stelzreid[1] has described a method for determining the noise temperature corrections due to transmission line losses of this kind. For a liquid helium load ($T \approx 4°K$) operating near 3 GHz, he finds that the effective output noise temperature is 5.0°K, with a probable uncertainty in order of 0.1°K. However, from Eqn. (5) and Fig. 1, we find that the correction term T_1 is really about 0.07°K at 3 GHz, i.e., of the same order as the uncertainty claimed by Stelzreid. Thus, already at 3 GHz, the error in Eqn. (1) can be significant when compared to other sources of uncertainty.

In the millimeter wave region, this error becomes even more pronounced. As an example, consider a liquid nitrogen cooled load ($T = 77°K$ at 760 mm Hg pressure) operating in the 83 to 86 GHz band[2]. For this load, the line-loss correction is about 12°K and in addition, corrections in the order of 0.2 to 0.7°K are made for load impedance mismatch (VSWR). From Eqn. (5) or Fig. 1 we find T_1 to be about 2.0°K line-loss correction and significantly larger than the correction for VSWR.

When liquid nitrogen is used as a coolant, the physical temperature of the termination is about 77°K. From Eqn. (5) and Fig. 1, the correction term T_2 is small (below 0.1°K) at this temperature and at frequencies in the 83-86 GHz range. However, if liquid helium were used, with a temperature of about 4°K, the term T_2 would be about 0.3°K in this frequency band, i.e., of the same order of magnitude as the VSWR corrections considered in Reference 2. ••

References

1. C. T. Stelzried, "Temperature Calibration of Microwave Thermal Noise Sources," *IEEE Transactions on Microwave Theory and Techniques*, Vol. MTT-13, No. 1, pp. 120-130, (January, 1965).

2. R. C. Menon, N. P. Albaugh and J. W. Dozier, "Cooled Loads As Calibration Standards For The MM-Wavelength Range," *Proc. IEEE*, Vol. 54, No. 10, pp. 1501-1502, (October, 1966).

Test your retention

1. Why can noise power emitted by a matched termination be approximately expressed in terms of physical temperature?
2. Under which of these conditions does the approximation $P_N = kTB$ become invalid: (a) high T and high F; (b) high T and low F; (c) low T and low f; (d) low T and high f?
3. Is the actual noise power emitted by a cold termination higher or lower than the approximate formula $P_N = kTB$ indicates? (T = physical temperature of the termination).

From the first family of fixed filters...
TUNABLES

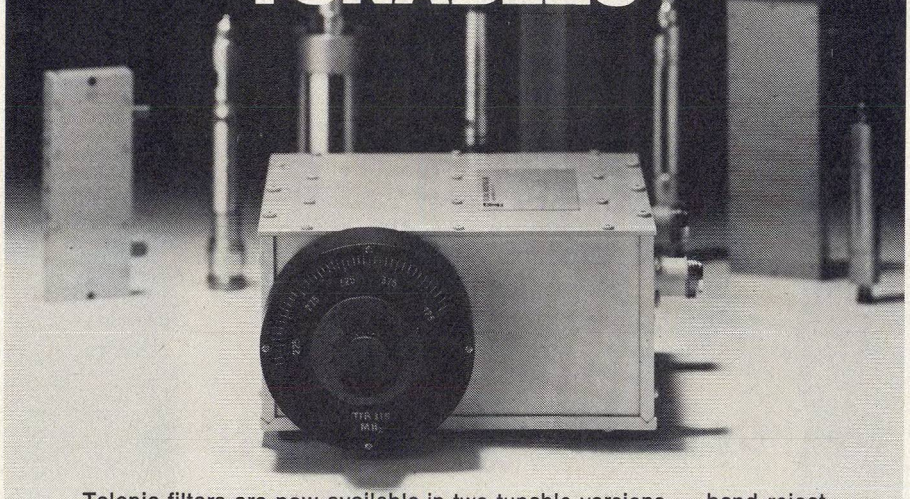

Telonic filters are now available in two tunable versions — band reject and band pass. Band reject models cover 1 octave, up to 1 GHz, with notch depths to 70 dB. Band pass types also cover an octave, up to 4 GHz, with pass bands of 1% to 10%.
These tunable models are another reason Telonic should be your first source for RF and microwave filters. The wide range of our product line lets you select a standard filter for your special applications.
We supply tubular low pass and band pass filters, cavities, interdigital and combline types to a broad spectrum of OEM and end users. Let us know your needs. We'll make a recommendation or forward our 50-page catalog of complete filter data.

TelonicAltair
2825 Laguna Canyon Rd. · Box 277
Laguna Beach, California 92652
Tel: 714 494-9401 · TWX: 910 596-1320 · Cable: TELENG

READER SERVICE NUMBER 56

EBRUARY
76

MICROWAVES

laser technology

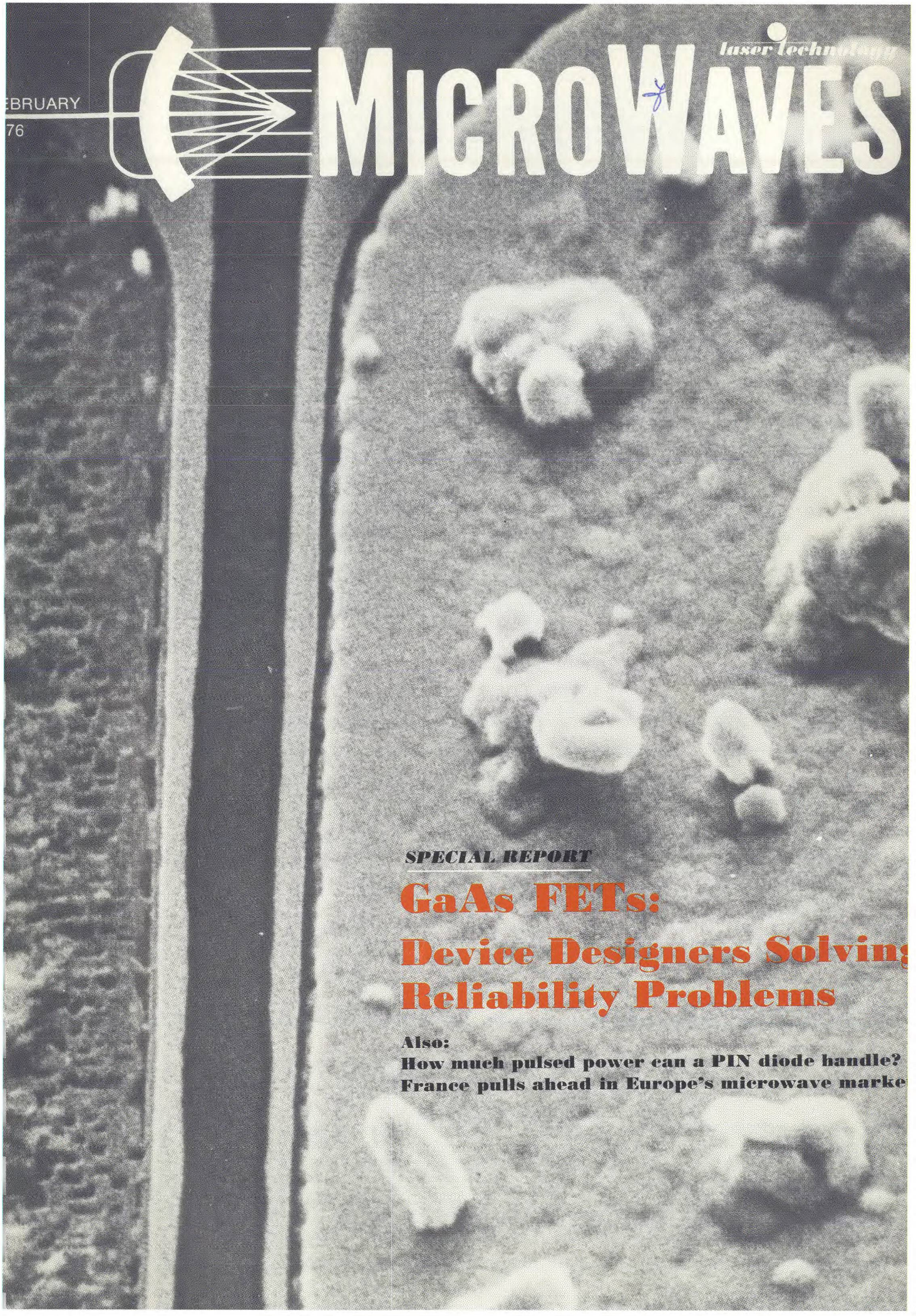

SPECIAL REPORT

GaAs FETs:
Device Designers Solving Reliability Problems

Also:
How much pulsed power can a PIN diode handle?
France pulls ahead in Europe's microwave marke

MICROWAVES

February 1976
Vol. 15, No. 2

news

9 France Extends Lead in W. Europe's Communications And Radar Markets
10 14.5 GHz Transponder Developed For Airport Surface Detection Radar
14 R & D Funding Predicted To Increase 11% In '76
17 R & D
19 Washington
22 International
24 Meetings
26 Industry
28 For Your Personal Interest . . .

editorial

30 How Credible Is The Brain Bank?

technical section

Semiconductors

32 **GaAs FETs: Device Designers Solving Reliability Problems.** Although GaAs FETs have been in use for quite some time, researchers are just beginning to overcome drift and reliability problems. Improvements should be evident in the avalanche of new devices planned for 1976.
54 **How Much Pulsed Power Can A PIN Diode Handle?** Frederick Dominick of GHz Devices develops a thermal analysis to determine the peak pulsed power that a PIN diode can safely switch.
62 **Power Amp Design For 900 MHz Mobile Radio.** Junius Taylor and Gordon McIntosh of Motorola Semiconductor Products Division discuss design techniques for 12.5 V power amps. A 15 W design is described in detail.

products and departments

70 **Product Feature:** $6200 Frequency Counter Extends Automatic Measments To 24 GHz
70 New Products
81 Application Notes
82 New Literature
83 Advertisers' Index
84 Product Index

About The Cover: Electromigration of GaAs FET drain and source contact metal is dramatically illustrated by this SEM taken at Plessey's Allen Clark Research Centre. This effect has been observed during step-stress tests, and does not appear to constrain normal usage. Story on page 32.

coming next month: Millimeter Waves

Staff Report On Millimeter Wave Technology. New systems' needs in the millimeter bands are pushing the development of microstrip and stripline designs up to 60 GHz. Also, competing for these new system applications is a new entry—dielectric waveguide. Electro-forming methods for making complex waveguide components are also covered.

The Case For Dielectric Waveguide. Robert Knox of Epsilon-Lambda in Batavia, IL, reviews millimeter wave integrated circuits using dielectric waveguide. Their advantages are described as well as their potential for cost-effective millimeter wave systems design. Principles are covered as well as some of the latest image-guide components that have recently been developed.

GaAs or Si: What Makes a M-M Wave Mixer? F. Bernues, H. J. Kuno and P. A. Crandell of Hughes Electron Dynamics Division in Torrance, CA, analyze the performance of mixer diodes in the 90 to 110 GHz range. Gallium arsenide is generally believed to be a superior material for Schottky barrier diodes in this frequency range. However, when other factors are considered, there is no significant difference in mixer performance using either material.

Publisher/Editor
Howard Bierman

Managing Editor
Richard T. Davis

Associate Editor
Stacy V. Bearse

Contributing Editor
Harvey J. Hindin

Washington Editor
Paul Harris
Snyder Associates
1050 Potomac St., NW
Washington, DC 20007
(202) 965-3700

Editorial Assistant
Gail Murphy

Production Editor
Sherry Lynne Karpen

Art
Robert Meehan, Dir.

Production
Dollie S. Viebig, Mgr.
Dan Coakley

Circulation
Trish Edelmann, Mgr.
Sherry Karpen,
Reader Service

Promotion Manager
Albert B. Stempel

Directory Coordinator
Janice Tapp

Editorial Office
50 Essex St.,
Rochelle Park, N.J. 07662
Phone (201) 843-0550
TWX 710-990-5071

A Hayden Publication
James S. Mulholland, Jr., President

MICROWAVES is sent free to individuals actively engaged in microwave work at companies located in the U.S., Canada and Western Europe. Subscription price for non-qualified copies is $10.00 for U.S., $15.00 a year elsewhere. Additional single copies $1.50 ea. (U.S.); $2.00 ea. (foreign); except additional Product Data Directory reference issue, $10.00 ea. (U.S.); $18.00 (foreign). POSTMASTER, please send Form 3579 to Fulfillment Manager, MICROWAVES, P.O. Box 13801, Philadelphia, PA 19101.

Back Issues of MicroWaves are available on microfilm, microfiche, 16mm or 35mm roll film. They can be ordered from Xerox University Microfilms, 300 North Zeeb Road, Ann Arbor, MI 48106. For immediate information, call (313) 761-4700.

Hayden Publishing Co., Inc., James S. Mulholland, President, printed at Brown Printing Co., Inc., Waseca, MN.
Copyright © 1976 Hayden Publishing Co., Inc., all rights reserved.

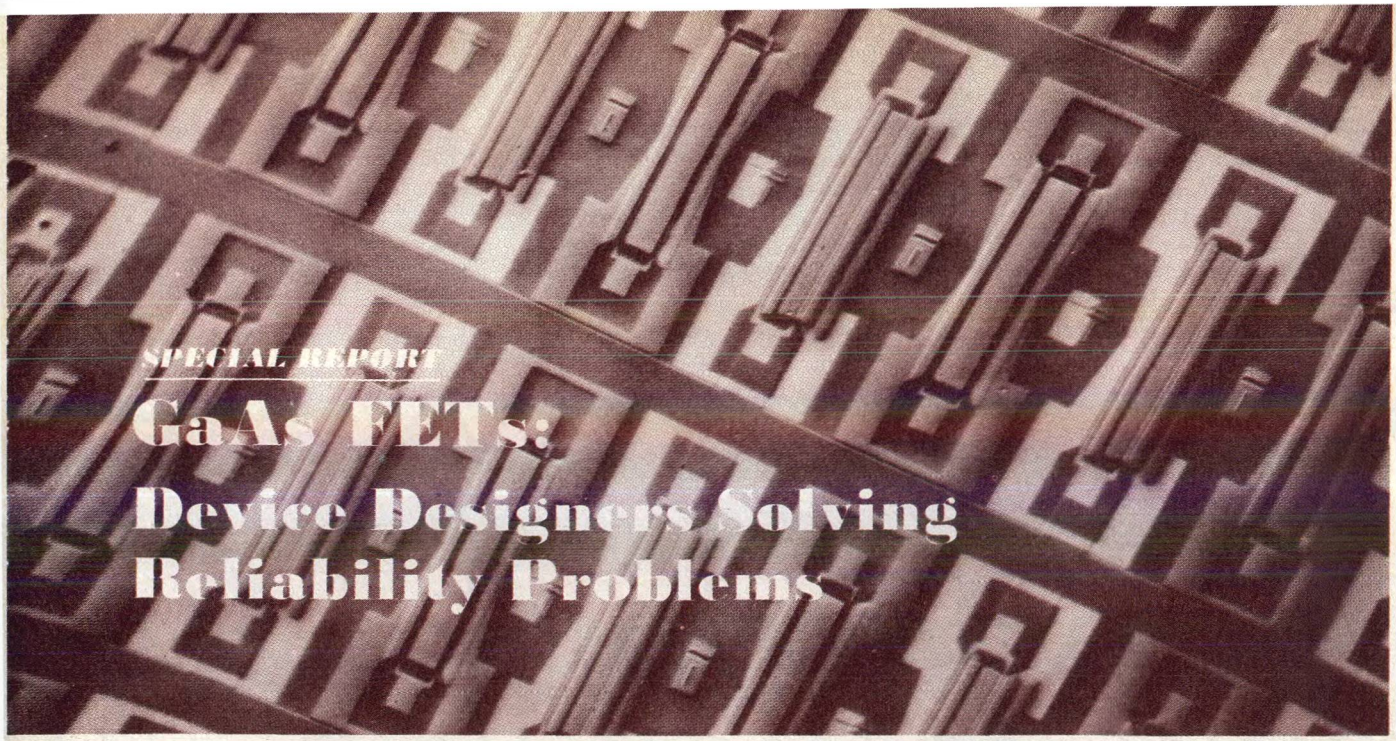

SEM COURTESY OF AVANTEK

SPECIAL REPORT

GaAs FETs: Device Designers Solving Reliability Problems

Stacy V. Bearse
Associate Editor

THERE'S no question about it: The high-frequency field-effect transistor is experiencing a glowing present, with the promise of a very bright future. As an efficient, low-voltage, low-noise amplifier, it threatens to replace virtually all low-noise TWTS, at frequencies from 4 GHz through K-band. As a three-terminal oscillator element, it's an attractive substitute for hard-to-make Gunn diodes in the 4 to 8 GHz range.[1,2,3] Monolithically realized as a logic gate, it may someday enable logic speeds of several GHz.[4] Power amplification properties are just beginning to be exploited, with commercial devices now offering 1W at 8 GHz, and laboratory specimens producing 185 mW at 21 GHz.[5]

In short, the FET could eventually replace a lot of more complex circuitry. But in spite of the fact that the device is nearly ten years old, it is not yet a mature, "plug-in" product. The FET is still a young device caught in the middle of its evolution from the laboratory to the production line.

Today, a fairly broad selection of off-the-shelf low-noise devices is offered by three companies (Plessey, Nippon Electric Co. and Hitachi) and performance, according to the specification sheets, is very impressive. But going beyond the manufacturers' specs, the designer quickly finds that the devices are quite expensive, easily burned out and until recently, that sales were backed with relatively little solid reliability information. On top of this, deliveries are reported to be erratic, partially due to the increasing demand, but primarily, according to industry sources, due to chronic material problems experienced by manufacturers. "We don't know enough about the devices yet," summarizes James A. Turner, FET group leader at Plessey's Allen Clark Research Centre in Towcester, England.

Perhaps the most serious questions in the minds of circuit designers deal with the stability of the GaAs FET's electrical parameters and with its reliability in general. Many designers have carefully characterized a device and designed an appropriate circuit, only to find that the FET's characteristic has drifted after only a couple of hours of operation. "FET amplifier deliveries in the industry have been plagued by problems just like this," notes Richard E. Hejmanowski, manager of semiconductor

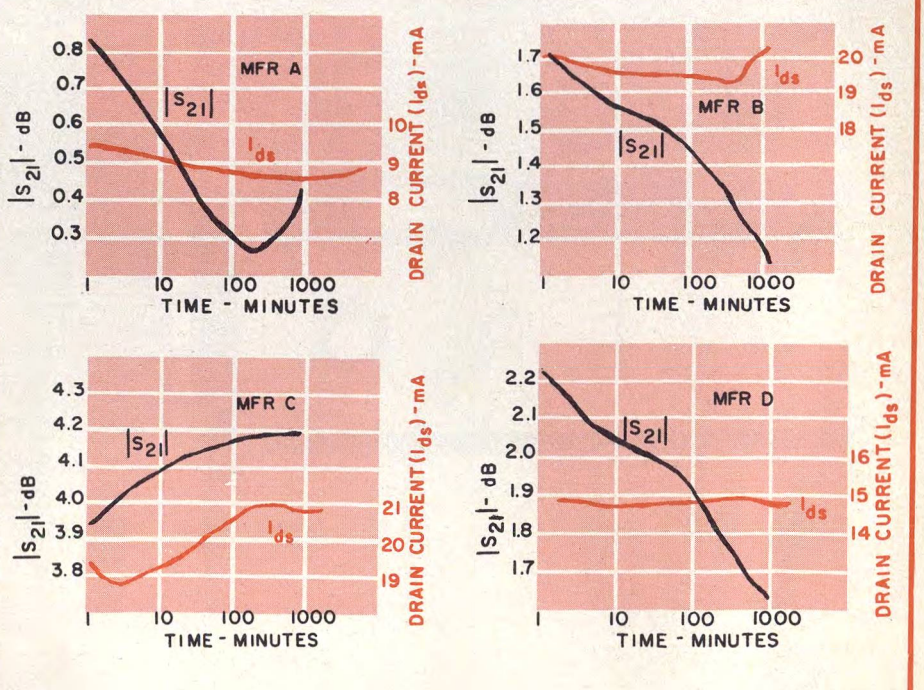

1. **Severe drift** is evident in these devices which were purchased through normal marketing channels from four manufacturers. Frequency is 3 GHz.

development at Avantek, Santa Clara, CA. "I don't think that there is a manufacturer of FET amplifiers who hasn't had difficulty in getting the amplifiers out as quickly as he would like."

These problems have not escaped the attention of the government, which is primarily looking at the GaAs FET as a low-power TWT replacement at frequencies through K-band. The Army Electronics Command at Ft. Monmouth, NJ, and the Naval Research Laboratory in Washington, DC, are both sponsoring intensive investigations into the related problems of stability and reliability. The Air Force has plans to support stringent reliability studies from Rome Air Development Center in 1976, but as of this writing, the contract has not been let. Sources say this program may be in jeopardy, however, due to congressional cuts in funds destined for RADC.

The question of gain drift surfaced a few years ago when 8 to 12.4 GHz developmental amplifiers made for ECOM by both Watkins-Johnson and Avantek began to drift out of their 2 dB gain windows, notes Vladimir Gelnovatch. an engineer at the Fort Monmouth facility. The most severe problems centered on drifts of the rf S_{21} parameter and dc drain current.

In an effort to assess the magnitude of the problem, researchers at Avantek purchased typical over-the-counter devices from four manufacturers and tested them, in addition to in-house devices, for periods up to 1,000 minutes. The evaluation was at room temperature, under normal bias conditions.

The reported results of the experiment[6] are disturbing. Each device apparently drifted in a different manner, some showing increased S_{12} with time, others displaying a gain characteristic with a negative slope, as shown in Fig. 1. One device reportedly exhibited a gain change of nearly 30%.

"Each device seems to have its own signature; no two are alike," notes Dr. Daniel Ch'en, senior scientist at Avantek. "Similarly, a great deal of variation was noted from device to device from the same manufacturer. Some manufacturers show a very wide spread in the severity of the drift characteristic. It was also found that there was a variation in the drift characteristic of the devices from lot to lot, and to some extent, of devices on the same slice."

"The only thing that is consistent is that every one (GaAs FET) we tested showed some change with time," adds Hejmanowski.

Avantek's findings are supported, to some extent, by independent work carried out by Nippon Electric Company Ltd., Kawasaki, Japan. At the 1975 International Electron Devices Meeting[7], Hideaki Kozu of NEC reported that a serious drift of electrical parameters was observed immediately after some devices were turned on, as shown in Fig. 2. However, Kozu reports that when the device was turned off, the parameters recovered to their original values after some time, at almost the same speed of the drift in the turn-on state. Although Fig. 2 shows an example of severe drift within 30 minutes, the NEC researcher claimed that the drift differed from sample to sample, and time constants ranged from seconds to hours.

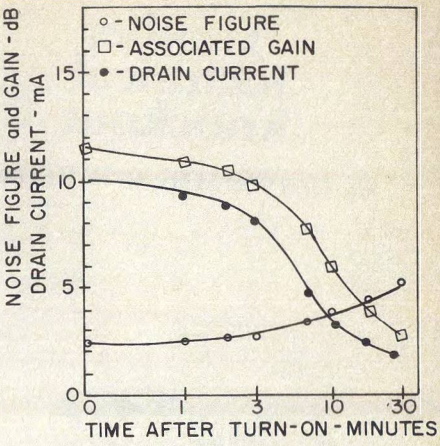

2. **Although this drift is in terms of minutes,** NEC reports other devices with time constants of seconds and hours. Measurement is at 4 GHz.

But Carl Peterson, vice president of California Eastern Laboratories, the Burlingame, CA-based distributor of NEC devices, carefully differentiates what he calls short-term drift problems ("a matter of a few minutes" per Peterson) from the relatively long-term drift apparently observed in the Avantek study. With regard to Avantek's findings, Peterson claims: "We (NEC) do not have that problem now, and we never had that problem." Plessey's James Turner also believes that the results of Avantek's experiments do not accurately reflect the performance of his company's products. Turner simply states: "Our devices don't show the S_{21} droop either!"

(continued on p. 36)

Some facts about FETs

Are you working with active components above 4 GHz? If so, the metal-epitaxial semiconductor field-effect transistor (MESFET, or simply FET) is likely to impact your work. MESFETs have the largest current-gain bandwidth (20 GHz) and the highest frequency of oscillation (80 GHz) of all transistors.[22]

To review some basics, the FET is a three-terminal, unipolar device: Its operation depends upon the flow of majority carriers only. Electrons have higher mobility than holes in all materials commonly used for high-frequency FETs (Si, GaAs and InP, for example). Consequently, n-channel FETs are used exclusively in the microwave region.[22] Carriers move through a very thin (2000 Å, or so) active layer, which is formed by epitaxial growth or ion implantation on top of a high-resistivity (10^8 ohm-cm) substrate. Often, a high sensitivity buffer layer is grown at the interface to isolate the sensitive active layer from defects in the substrate.

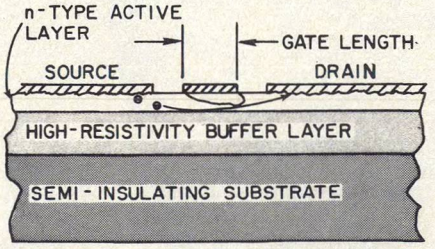

Electron concentration in the active n-type layer typically ranges from 10^{15} to 10^{17} cm^{-3}.

Majority carriers are introduced through the source contact and leave the device through the drain contact, both of which are ohmically alloyed to the active layer.

A gate, located between source and drain, controls the flow of carriers by setting up a depletion region when reverse biased. Early, high-frequency FETs used a diffused gate,[15] but it was soon discovered that a Schottky barrier gate greatly enhanced performance.[23] Contrary to common usage, gate length specifies the narrow dimension of the metal gate stripe (the direction perpendicular to the edges of the source and drain contacts). There is an inverse relationship between gate length and frequency of operation, as detailed in the text. Gate width describes the longer dimension of stripe, which parallels the edges of the source and drain contacts. Gate width influences the maximum amount of power that a device can safely handle.

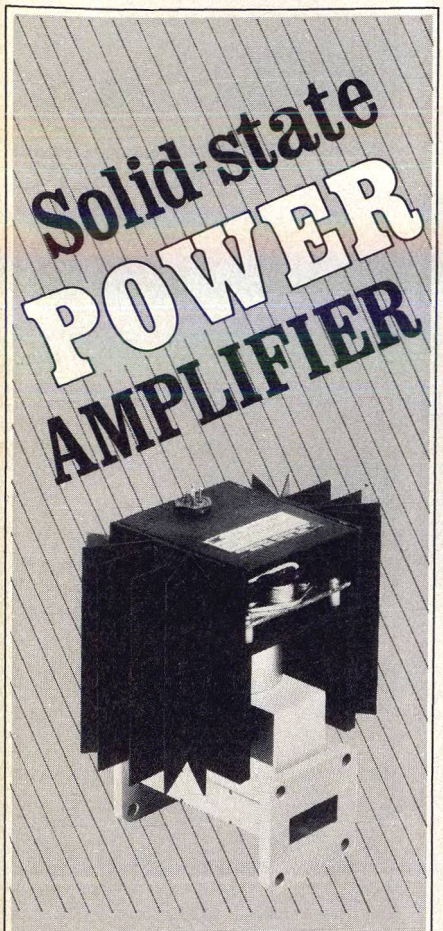

IMPATT AMPLIFIERS...

...The **NOW** Alternative to Tube Amplifiers
For Today's Communications Systems

REPRESENTATIVE UNITS

FREQ. (GHz)	BAND-WIDTH	POWER OUTPUT (Watts)*	DC POWER
4.4-5.0	FULL	0.5-5.0	130 V
5.9-6.4	FULL	0.5-5.0	130 V
7.1-8.5	5%	0.5-5.0	130 V
10.7-13.0	5%	0.5-2.0	130 V
14.0-22.0	5%	0.5-1.0	130 V

*Driver Amplifiers Available

FOR YOUR SPECIFIC REQUIREMENTS CONTACT

International Microwave Corp.

33 River Rd.,
COS COB, Ct. 06807
Tel. 203 661-6277

READER SERVICE NUMBER 36

GaAs FET RELIABILITY

Does passivation help?

Investigations into the origins of drift phenomena are in the early stages, but work thus far suggests two culprits: (1) impurities or traps (crystal dislocations or vacancies) inside the FET at the interface between the semi-insulating substrate and the active layer, and (2) surface depletion effects. Avantek researchers believe that the major cause of the drift problem is a depletion layer, sensitive to time, temperature and electric field, which forms on the surface of the FET due to trapped surface charges on the GaAs. "The problem then, became how to alter the surface charges of the GaAs in such a way that they do not vary with time and environmental changes," Ch'en explains.

The solution, according to Avantek, is to passivate the device with a thin layer of polycrystalline gallium arsenide (PGA), so that the GaAs epitaxial surface takes on the characteristics of bulk material. The characteristics of an experimental Avantek device before and after passivation are shown in Fig. 3.

Avantek is currently evaluating PGA passivated FETs to meet the tight, ±1.5 dB gain flatness spec of an ultra-broadband amplifier it is building for the Naval Research Laboratory. The two-phase project initially calls for a delivery of a 7 to 15 GHz amplifier in June, 1976, with 25 ±1.5 dB gain, +6 dBm output, less than 10 dB noise figure and ±10 degree phase deviation from linear. In 1977, the company hopes to meet the same specifications over a 7 to 18 GHz bandwidth. Devices used in these amplifiers will have a 0.5 micron gate length.

Device designers at Hewlett-Packard, which plans to introduce a line of one micron devices early this year, agree that surface phenomena can influence an FET's performance with time. "Many semiconductors, when exposed to an improper ambient, can either deplete or accumulate carriers at the surface, giving a virtual gating effect," explains Joseph Barrera, member of the technical staff at the Microwave Component Division (formerly part of HPA) in Palo Alto, CA. "It's like taking the one-micron gate, stretching it out and modifying the current." The active area of HP's new FET, including the gate, source and drain, will be coated by a proprietary dielectric layer. Technically, it is not a passivation, notes Barrera, but a protection.

Neither Plessey nor NEC currently passivate or glassivate their devices. However, NEC claims that at some point in the future, all their devices will be glassivated by a layer of SiO_2. California Eastern's Peterson makes it very clear that the thin glass layer is solely for mechanical protection, and will not influence the electrical performance of the device.

Better substrates called for

Most manufacturers feel that surface effects are only a small part of the overall stability problem. "Usually, the devices that exhibit drift phenomena come from epitaxial wafers which show some anomalous capacitance-voltage relation used for doping profile measurement," notes Hideaki Kozu of NEC. "The C-V relation suggests that a high density of deep lying carrier trapping centers (dislocations or vacancies in the crystal) exist near the interface between the active layer and the semi-insulating substrate."

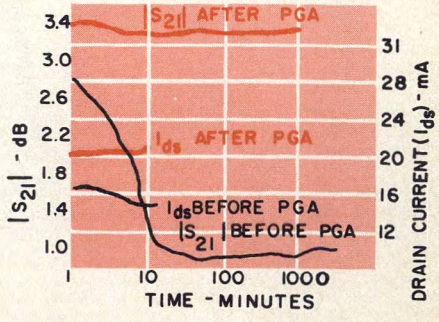

3. **Passivation with pollycrystaline gallium arsenide** (PGA) stabilized this Avantek device. Before and after curves were taken on the same FET at 3 GHz.

A high-resistivity buffer layer is commonly grown between the semi-insulating substrate and the thin epitaxial layer to prevent diffusion of impurities from the substrate, which is often of inferior quality, into the sensitive active region. But HP's Barrera points out that this buffer layer itself must be "super pure." Any impurity centers in this relatively thick layer could cause deep-lying traps with time constants on the order of minutes, he notes.

"The whole substrate issue is probably the largest problem area," adds Bert Berson, laboratory R&D manager at HP's Microwave Component Division. "The available supply of semi-insulating GaAs substrate in the U.S. has been sporadic at best. And, when available, the quality is just not as good as it should be."

(continued on p. 38)

Another technical knockout

the first microwave, micropower transistor

When every microwatt counts...save power with the MRF931!

Offering impressive 10 dB power gain at 1 gigahertz, the MRF931 can be biased at a minuscule 250 uA...a level traditionally associated with leakage currents.

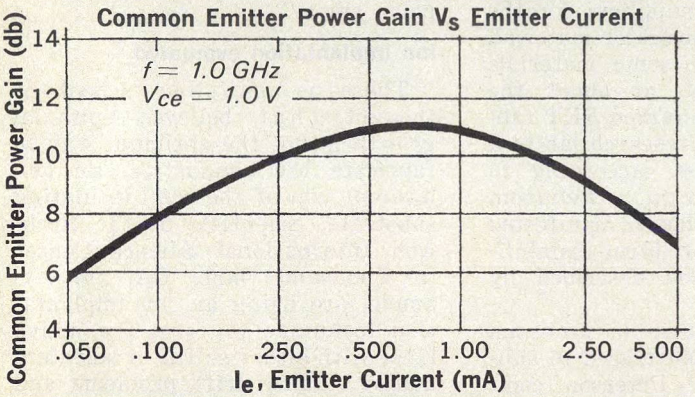

It's super for applications sensitive to power consumption – low-voltage, low-current equipment and ultra-sensitive instruments where long-haul battery power is critical – as in pagers and personal portables.

Save bucks, too. It's OEM-priced at only $2.30, 100-499.

The ion-implanted, gold-metallized chip is packaged in the .188 dia. plastic stripline case with 4-lead opposed-emitter construction to maximize performance. Other packages (or the MRF931 chip) are available to meet specialized needs.

There is one macro-spec: availability. Thousands are ready for evaluation or production from factory, field or distributors.

Big brothers of this mighty mite include metal, plastic and ceramic 4.5 to 5 gigahertz types in the BFR90/91...MRF902/914 families costing far less than traditional microwave transistors.

Send for complete data on all.

Be first with the first...

MOTOROLA RF

Box 20912/Phoenix, AZ 85036

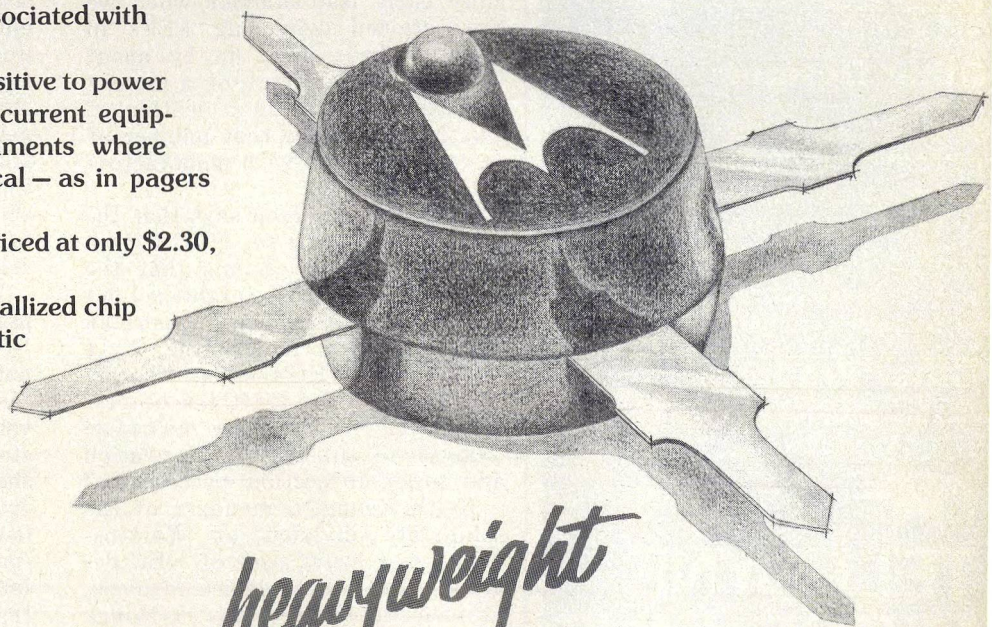

heavyweight

from Motorola, the RF producer.

READER SERVICE NUMBER 37

ISOLATORS

Com-Band Isolators

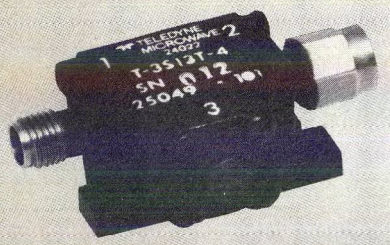

3.7 - 4.2 GHz
Isolation: 25 dB
Insertion Loss: .25 dB
VSWR: 1.10:1
Size: 0.75 × 0.75 × 0.50
CIRCLE NO. 100

5.9 - 6.4 GHz
Isolation: 26 dB
Insertion Loss: 0.3 dB
VSWR: 1.10:1
Size: 0.75 × 0.75 × 0.69
CIRCLE NO. 101

Other Designs

- Octave Bandwidths 0.5 - 20 GHz
- Octave "Plus" Bandwidth (85-90%)
- Multi-Octave Bandwidths
- Narrow Bandwidths 200 mHz - 20 GHz
- Multi-Junction
- Custom Configurations

Other Products
Switches - Filters
Multiplexers - V.C.O.

TELEDYNE MICROWAVE
1290 Terra Bella, Mt. View, CA 94043
(415) 968-2211 TWX (910) 379-6939

GaAs FET RELIABILITY

HP is one of the few FET manufacturers to grow its own substrate, and according to Berson, they "can do it as well or better than anyone else in the industry." Each substrate grown at HP undergoes a rigorous qualification procedure[8] to determine which substrates require a buffer layer, and which are good enough to accept an epitaxially-grown active layer directly. HP relies on liquid phase epitaxial (LPE) growth, and claims to have the first such production facility capable of growing a large number of substrates economically. Two other manufacturers, Avantek and Dexcel, of Santa Clara, CA, also use LPE. Vapor phase epitaxial (VPE) growth or ion implantation can also be used to form the active layer. VPE is employed by the majority of firms, including NEC, Hitachi and Varian.

Interestingly, the world's largest commercial producer of GaAs FETs, Nippon Electric Company, relies on outside suppliers for the bulk of its semiconductor material. NEC encountered some materials problems recently, at about the time when it transferred FET fabrication from the research lab to a production facility. According to California Eastern's Peterson, these problems have manifested themselves as short-term instabilities, such as those described by Kozu.

"Our recent turn-on problems have definitely been traced to substrate materials," Peterson comments. "Customer requirements since early last summer when we first started delivering FETs in quantity have gone up by about ten times, and to turn on a factory and its suppliers in a matter of months to produce that number of devices has to do with manufacturing capacity."

Although Peterson says that the material problems set NEC back a month or so, he claims that the situation has been straightened out and deliveries are back to normal. "In the production of the GaAs FET," adds NEC's Kozu, "the device showing the drift can be preventatively rejected by careful analysis of substrate C-V relation and other inspection procedures."

Keith Kennedy, manager of the solid-state division at Watkins-Johnson, a heavy user of NEC devices, says that device delivery problems definitely slowed things down for a while at W-J's Palo Alto production facility. According to Kennedy, even though W-J maintains "a very large inventory of devices," it was forced to extend lead times in late 1975. However, he confirms that the problems of instability which plagued NEC devices for two or three months late last year have apparently been solved. "Our vendors have identified the problem, and we are now not getting any devices with poor stability. The GaAs FET is a new device, and it merely had a hiccup in it," he suggests. W-J is currently accepting orders for FET amplifiers with a 60 to 90 day turnaround time.

Kennedy is careful to note that W-J simply could not use the bad devices, and never shipped an amplifier built with one. "Every amplifier is carefully screened and burned in before it is shipped," he explains. "In fact, I believe that we were the first to bring the problems to the vendor's attention. Interestingly, we have experienced a smaller percentage of field returns with our FET amplifiers than with our other product lines, even bipolar amps."

Ion implantation evaluated

There is another school of thought that believes epitaxial growth is not the optimum way to fabricate the conductive, active layer on top of the semi-insulating substrate. Scientists at the Rockwell International Science Center in Thousand Oaks, CA, for example, are using an ion implantation technique to form the active layer with either sulfur or selenium doping.[9] "The drift problems and sensitivity of noise figure to drain-source voltage which occur in epitaxial transistors are omens of undesirable interface states between the epi layer and the substrate," comments J. Aiden Higgens, a member of the technical staff at Rockwell. "We have found that ion implanted transistors have shown considerably less tendency to drift than the epitaxial transistors."

In Rockwell's experiments, comparable epitaxial and ion implanted FETs were biased for optimum noise figure. Initially, the gate biases were quickly reduced by one volt, held at that level, then restored to the optimum voltage, as shown in Fig. 4. "Note that the epitaxial transistor returns to a lower noise figure, then slowly comes back to the normal level," interprets Higgens. "This implies that if it were not for something undesirable in the structure of the transistor, the device would actually be operating at this lower noise figure under optimum bias condi-

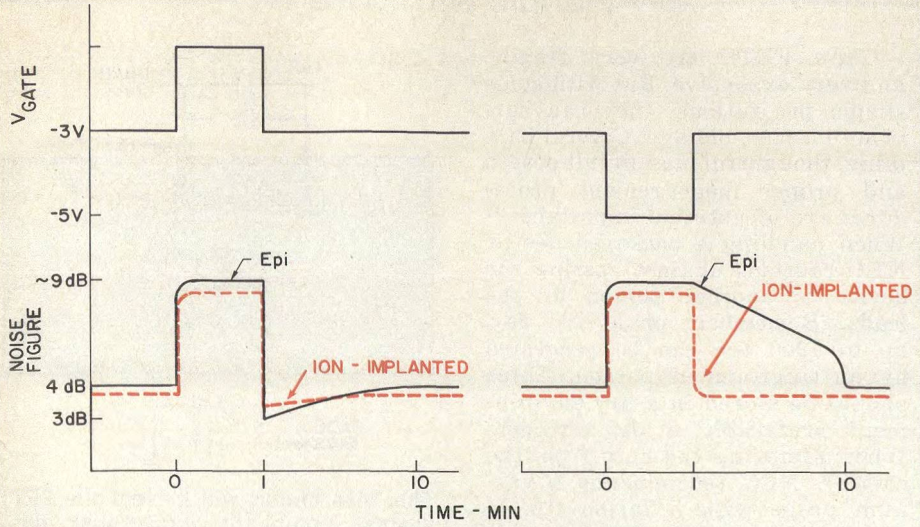

4. **Time variations in noise figure** as a result of bias perturbations may suggest extra trapping levels in epitaxial structures.

tion. When I go the other way (increase gate bias to −5 V, then return it to −3 V), I put more electric field at the interface (of the substrate and the active layer) and the noise figure goes up and stays up for a long time." The researcher believes that the fact that the ion implanted transistor returns to normal much more quickly is a strong indication of fewer interface trapping levels.

Rockwell uses a substrate qualification procedure, which is very similar to Hewlett-Packard's method, to select the best substrates. Sulfur or selenium implants are carried out into the selected, chrome-doped semi-insulating GaAs material to produce suitable n-type channels for the active layer. The substrate samples are heated to 350°C and implanted with 100 keV sulfur or 400 keV selenium ions. Following the implantation, a 2400 Å of reactively sputtered Si_3N_4 is deposited on the substrate to prevent dissociation of the GaAs during the annealing cycle. Both sulfur and selenium doped substrates are annealed at 850°C for 30 minutes.

MTTFs are very good

Under normal operating conditions, just how reliable are low-noise GaAs FETs? "Intrinsically, the devices are very reliable," answers Plessey's James Turner, "and where failures have occurred, there are certainly ways to get around the problem." Plessey's life tests have been going on longer than anyone elses in the industry and appear to support Turner's prediction. In fact, at Plessey, 11 four micron devices with outputs of about 300 mW have been on the test stands for seven years now, running at junction temperatures of 80 to 90°C without a single failure.

At last December's International Electron Devices Meeting, Turner predicted a mean time to failure (MTTF) of about 10^7 hours, at a junction temperature of 70°C, for well-made, low-noise GaAs FETs.[10] The prediction was based on the results of step-stress testing of a number of one-micron X-band devices with a variety of metalization systems.

A more optimistic estimate of MTTF comes from Hideaki Kozu, of NEC, who, at the same meeting, predicted an MTTF of 10^9 hours for one micron GaAs FETs operating at a junction temperature of 80°C. Using the simple rule of thumb that MTTF is halved for every 10°C rise in junction temperature, Plessey's estimate for an 80°C junction would be 5×10^6. Kozu's prediction is the result of high-temperature storage, power burn-in and high-temperature gate biasing tests on more than 200 sample devices.

NEC's mean time to failure estimate is based on a failure mode not reported by Plessey: gradual degradation of source and drain contact resistance. Based on the results of preliminary acceleration life tests and high temperature storage tests, NEC researchers report that for a good device, all dc parameters are likely to remain within a specification window of ±10%, with the exception of I_{DS}, the specific drain current in the unsaturated region. By NEC standards, a device failure occurs when I_{DS} falls 25%, which results in a 0.5 dB increase in noise figure. Since no evidence of variations in the physical properties of the de-

(continued on p. 40)

ECCOAMP

ELECTRICALLY CONDUCTIVE ADHESIVES & COATINGS

New four page folder describes materials from 0.0001 to 100 ohm-cm. Adhesive pastes to replace hot solder, thin liquids, silver lacquer in aerosol spray, lossy coatings, etc.

READER SERVICE NUMBER 85

ECCOSORB®
ANECHOIC CHAMBERS

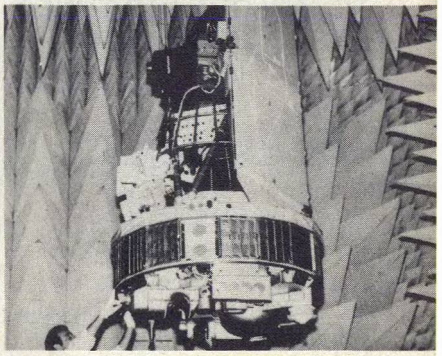

The most advanced anechoic and shielded chambers . . . used worldwide for antenna pattern, radar cross-section, VSWR and RF compatibility measurements. Send for data.

READER SERVICE NUMBER 86

CASTABLE HIGH LOSS MICROWAVE ABSORBER

ECCOSORB® CR is an epoxy casting resin which cures to a rigid high-loss material for waveguide and coax terminations and more complex shapes. ECCOSORB® CR-S is a castable high-loss RTV silicone. Flexible and good high temp. Send for technical bulletins.

READER SERVICE NUMBER 87

Emerson & Cuming, Inc.

CANTON, MASS.
GARDENA, CALIF.
NORTHBROOK, ILL.
Sales Offices in Principal Cities

EMERSON & CUMING EUROPE N.V., Oevel, Belgium

Handle with care!

GaAs FETS are very fragile, and **very** expensive. But with some simple precautions, they can survive to a ripe, old age. Careful handling, thoughtful bias circuit design and proper measurement procedures are of extreme importance.[11] When handling a packaged device, NEC cautions against passing the device to another person by the leads. Remember, on a dry day, up to 1200 erg can be generated by an ungrounded person. Chips should be stored in a dry environment, preferably, in dry nitrogen. When removing the chip from the carrier, NEC recommends a vacuum probe with a teflon tip. If tweezers are used, extreme caution is mandatory: GaAs is considerably softer than Si, and dust may break off and become lodged in the channel of unprotected devices. All soldering, die attach and bonding equipment must be properly grounded to prevent large transients.

In measurement and bias circuits, the importance of providing adequate protection against transients and changes in I_{DSS} cannot be over emphasized. NEC recommends that a battery and series resistor of 1 to 10 kilohms be used for gate bias during characterization. Never insert a packaged FET into a pre-biased test fixture, warns NEC. Once the device is soldered in the inactive test circuit, don't just turn on gate and drain bias supplies: Even regulated power supplies can generate large in-rush transients due to their stability-limited gain-bandwidth product. Always adjust V_{GS} first to about −1.0 V, then slowly increase V_{DS} to the proper bias point, NEC suggests. Finally, readjust V_{GS} to obtain the desired drain current. If something is suspect, don't use a digital multimeter to check resistance, for the voltage supply within the meter can easily destroy the gate.

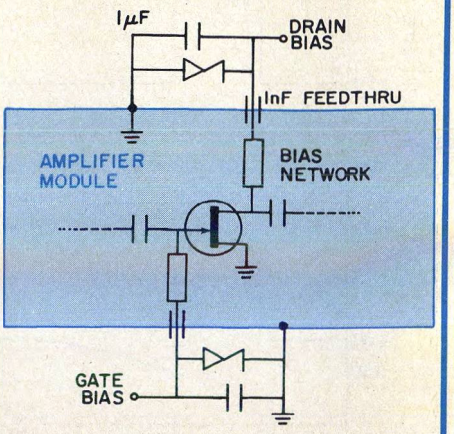

This bias circuit will protect the FET against potentially dangerous voltage transients.

NEC also cautions against the use of curve tracers: the high-voltage transformers used in most curve tracers have high leakage currents which, can if not properly grounded, destroy the FET. If a device's dc charcteristic must be measured, ground the curve tracer to earth, set V_{GS} to zero, increase V_{DS} slowly to about +3 V, then adjust V_{GS} to the desired value.

A little extra attention paid to the design of the bias circuit will also help protect the sensitive Schottky barrier gate. Plessey recommends that bias ports be decoupled near the device with a low inductance, 1 μF tantalum capacitor, shunted with a zener diode (approximately 5.8 V, 1.3 W), as shown in the figure. [12] In addition to limiting transients, the zener gives protection against over voltage and reverse biasing.

vice's GaAs layers were detected, the Japanese scientists conclude that the gradual decrease of I_{DS} is due to an increase in the contact resistance of the ohmic source and drain electrodes. From the temperature dependence of the change in I_{DS}, NEC concludes that the FET's activation energy is about 1.8 eV. Plessey assumes an activation energy of 1.0 eV in its MTTF calculation.

Both research programs indicate that breakdown of the Schottky barrier gate, either by static discharge or switching transients, is the leading killer of GaAs FETs. As a rule, resistance to breakdown is proportional to gate to source separation. Thus, the newer 0.5 and one micron devices are more susceptible to burnout than their two and four micron predecessors. Tests at Plessey indicate that energy levels as small as 0.3 erg are sufficient to melt the thin, aluminum gate stripe. Plessey's findings show that the gate can burn out without warning: the noise figure of the device does not change, even when subjected to potentially dangerous voltage spikes, until the moment the device ultimately fails.

Data from NEC (Fig. 5) shows that the critical voltage for gate

(continued on p. 43)

FROM STOCK...

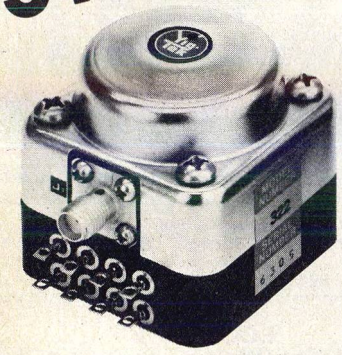

1.8 TO 4.2 GHz YIG-TUNED BUFFERED OSCILLATOR

- **Lowest cost**
- **Military version available**
- **Guaranteed 5 day delivery**
- **Fully magnetically shielded**
- **RFI filtering on all DC lines**

The YIG-TEK standard S-band oscillator, Model 322, is a fundamental, transistor oscillator with a MIC buffer amplifier which provides approximately 30 milliwatts of power output across the frequency range of 1.8 to 4.2 GHz. The buffer amplifier ensures stable performance in widely varying VSWR loads.

.. 1.8 to 4.2 GHz
.. 30 mw typical output power
.. <1 MHz pulling (1.5:1 VSWR)
.. Temperature drift (0° to +60°C) <6 MHz
.. Size 1.54" x 1.54" x 1.6"
.. Weight 8 oz.
.. Bias +20 VDC @ 100 mA

NEW CATALOG — send today for complete information on our full line of YIG components.

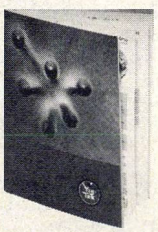

YIG-TEK CORPORATION
A CUTLER-HAMMER COMPANY
1725 De La Cruz Blvd. ■ Santa Clara, CA 95050
(408) 244-3240 ■ TWX 910-338-0293

READER SERVICE NUMBER 40

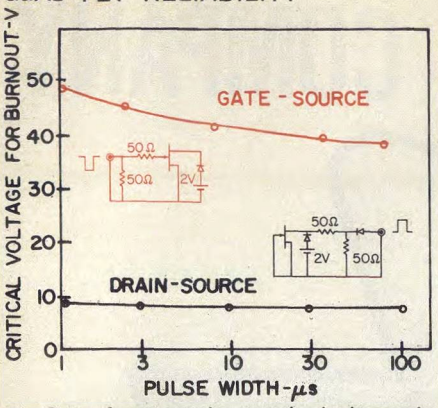

5. **Gate burnout** is nearly independent of pulse width, according to an NEC study.

burnout does not depend strongly on pulsewidth. Tests were conducted by applying a rectangular voltage pulse between gate and source, and drain and source. Inspection of damaged devices indicated that localized burnout occurs mostly at the edge of the active layer mesa, (Fig. 6), leading the researchers to believe that the damage is triggered by localized high electric fields. The largest field in common-source operation is between the drain and gate, and NEC recommends that this potential never exceed 10 volts.

Manufacturers are currently evaluating the use of high melting-point refractory metals to increase the resistance of the gate to burnout. Plessey has demonstrated that Schottky barrier gates constructed of nickel metalization can typically withstand energy levels up to 2.3 erg, which is more than two orders of magnitude higher than aluminum gates. Unfortunately, these devices are still in the lab.

But while researchers are working to improve the FET's resistance to gate burnout, manufacturers emphasize that the majority of gate failures can be prevented by simple precautions on the part of the user. Some fundamental protective procedures are outlined in

(continued on p. 45)

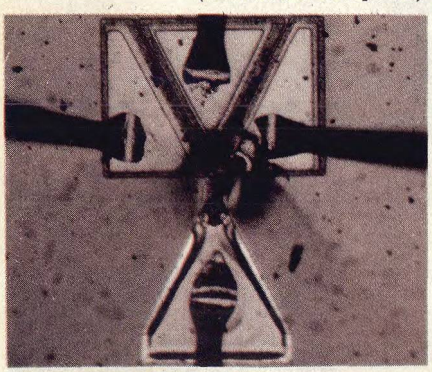

6. **A large voltage surge** burns out gate near the edge of the active area mesa, says NEC.

GX approved

DI-CLAD 527 laminates

offer consistent low loss at X Band.

Di-Clad 527 PTFE/glass/copper laminates have now received GX approval under MIL-P-13949 E. Produced under special "clean room" conditions, Di-Clad 527 offers reproducible dielectric constant control plus a maximum loss of .0022 at X Band.

Di-Clad 527 laminates less than 1/32-inch thick are also available. We make and test them by the same method that has earned GX approval. And we hold them to tight thickness tolerances—down to ± .0005 inch for a base thickness of .004 inch. All Di-Clad 527 laminates are engineered for plated-through-hole applications.

New free bulletins.

To help you meet your microwave design objectives, we've prepared detailed technical bulletins covering Di-Clad 527 laminate characteristics, plated-through-hole processing techniques, and computer-produced design parameters. To receive your copies, circle the reader service card. Keene Corporation, Chase-Foster Division, 199 Amaral St., East Providence, R.I. 02914.

KEENE CORPORATION

CHASE-FOSTER DIVISION

READER SERVICE NUMBER 43

the box on page 40. With a device as young as the GaAs FET, it really pays to keep in close contact with the various vendors, and heed what they have learned from other's mistakes.

Electromigration failures identified

Although there is good industry agreement on the gate diode failure mechanism, electromigration is the subject of some debate. Results of research at Plessey show that metal migration does indeed occur, but only noticeably at junction temperatures around 250°C.[10] NEC's Kozu, speaking at the 1975 IEDM, emphatically claimed that "we have observed no effects of electromigration with our FETs." It should be noted, however, that NEC's high temperature tests were storage tests, not rf or dc bias tests. In rf step stress test conducted at the Naval Research Laboratory, where the device was biased for maximum gain and heated in increments up to 150°C, researchers report seeing some effects of electromigration in NEC devices.

Three ohmic contact metalization systems were evaluated at Plessey for their susceptance to electromigration in high-temperature environments. The devices were dc biased at an ambient temperature of 200°C and migration effects

(continued on p. 47)

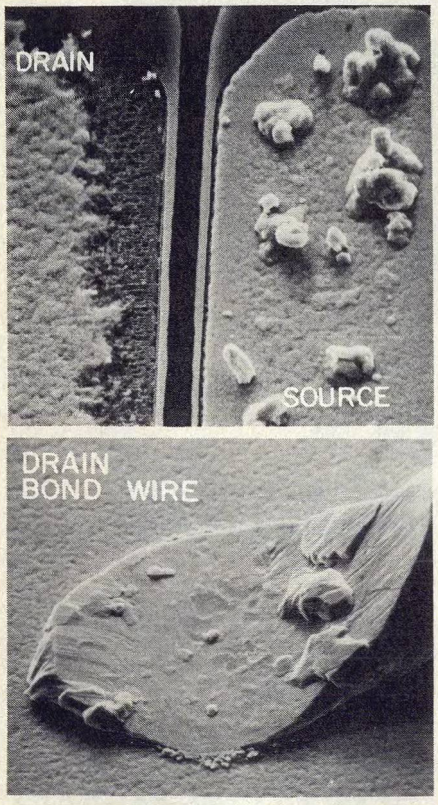

7. **Electromigration of source and drain contact metal** has been observed at very high (250°C) temperatures.

NEC GaAs FET option now available

Quick Change Artist

7025 Transistor Test Fixture

A fixture you can configure for most existing stripline transistor packages in only five minutes with only a screwdriver.

- ☐ **S-Parameter and Noise Figure measurement to 10 GHz.**
- ☐ **Slab-line construction means low loss.**
- ☐ **Shipped complete with parts for 3 packages and computer-tested reference plane locations.**

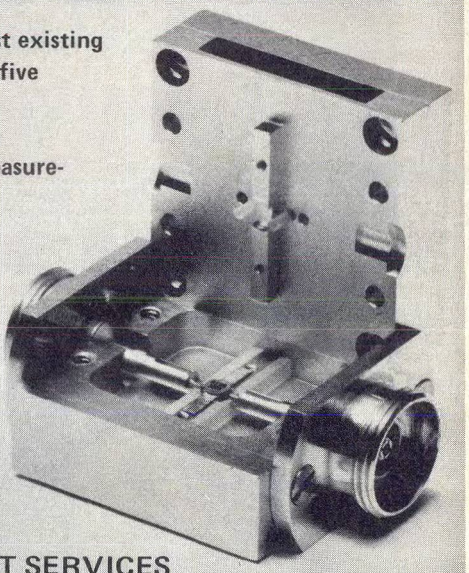

WATS

WESTERN AUTOMATIC TEST SERVICES
955 BENICIA AVE., SUNNYVALE, CALIF. 94086
(408) 736-0941 TWX: 910-339-9365

READER SERVICE NUMBER 45

Half-Rack Low Power TWT Amplifiers

These compact, light weight instruments contain reliable, solid state power supplies and operate in the 1 to 18 GHz frequency range with minimum CW power outputs from 1 to 20 watts. The TWT is protected by helix current and voltage sensors, filament surge limiting, solid state delay circuitry and thermal overload sensors. LogiMetrics low power TWT amplifiers are available or can be modified for special military and commercial systems applications.

Standard communication band units can be used as IPA's or HPA's in single or redundant configurations, meeting stringent specifications. Write or call for details.

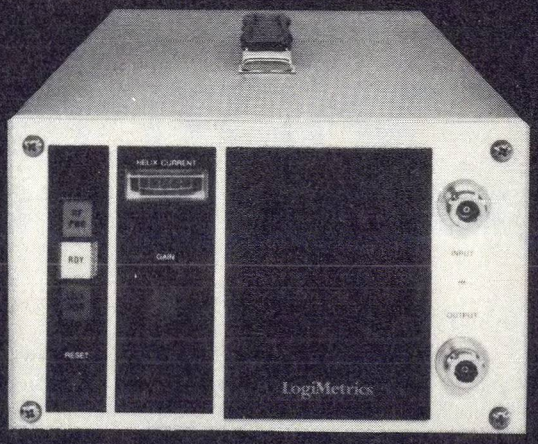

LogiMetrics

121-03 Dupont Street, Plainview, New York, 11803, (516) 681-4700/TWX: 510-221-1833
RF Signal Generators, Frequency Synthesizers, Traveling Wave Tube Amplifiers

READER SERVICE NUMBER 46

were observed on all devices tested within 1,000 hours. With gold/germanium (Au/Ge) and indium/gold/germanium (In/Au/Ge) contacts, material tends to accumulate at the edge of the source contact adjacent to the etched channel and deplete from the drain contact at a similar place (Fig. 7). "It looks like the metal sort of jumps across the channel!," jokes Turner. "In fact, what happens is that material is being transported from the source bond area and deposited at the edge of the source contact. Metal from the edge of the drain contact is deposited on the drain bond area. This is in the direction of the electron flow, and is electromigration of the contact metal," he concludes. Failure ultimately occurs when the source build up becomes large enough to bridge across and touch the gate.

A platinum gold/germanium (Pt/Au/Ge) system is also under evaluation at Plessey, however, it is too early to draw conclusions.

According to Turner, high-temperature metal migration can be minimized in several ways. "The current density can be reduced by making the metalization thicker," he suggests, "but due to limits imposed by the floatoff process used to define the contact area, plating up of the contacts is necessary to achieve maximum effect. As the migration is dependent on junction temperature, improvements in mounting techniques to reduce the thermal impedance could also give improvements in reliability."

To obtain optimum noise performance, FETs are often biased at a low drain current. Turner notes that this is beneficial to the device lifetime as it reduces both current density and junction temperature.

It must be stressed that Plessey noticed electromigration only under severe temperature conditions. Under the normal military specification of −55 to +71°C, "it does not present a serious hazard to high reliability usage," Turner claims. To support this point, Plessey conducted tests on X-band amplifiers, built with devices using In/Ge/Au ohmic contacts and aluminum gates. The amplifiers were operated in a 100°C ambient, with inputs of 2 mW cw and 150 mW dc. "After 2,000 hours (10,000 device hours) of testing under these conditions, there were negligible changes in the amplifier gain and noise characteristics," Turner

(continued on p. 49)

NEW RF Amplifiers under $20.*

Now You Have a Choice!

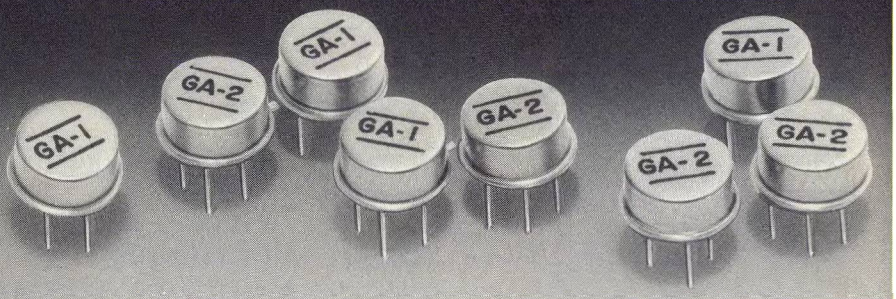

Our new "GA" Series of compatible GPD (General Purpose Device), cascadable amplifiers feature **GUARANTEED SPECIFICATIONS** (not typical), **LOW COST** (From under $30 to under $20*) gain insensitivity to input voltage variations (from 10 to 15 volts) and small size (TO-12).

*OEM Quantities

SPECIFICATIONS INCLUDE:

Frequency Response: 5-400 MHz; **Gain:** 13 dB min.; **Flatness:** 1 dB; **Noise Figure:** 4.0 dB (GA1), 5.5 dB (GA2); **VSWR (50 ohms):** 2.0 In and Out; **Input Power:** 15V, 17 ma (GA1), 15V, 25 ma (GA2). The units weigh 1.0 gram and measure 0.355" dia. by 0.175" high.

Send for detailed specifications, application information and a suppliers' Cross Reference List.

AYDIN VECTOR division

Newtown Industrial Commons • P.O. Box 328, Newtown, Pa. 18940
Phone 215-968-4271 / TWX 510-667-2320

RF/HYBRID REPRESENTATIVES

METRO. NEW YORK
Scientific Devices, East
(201) 945-3962

UPSTATE NEW YORK
Scientific Devices, N.Y.
(716) 334-2445

WASHINGTON, D.C.
Eastern Instrumentation
(301) 681-6500

SOUTHEAST — FLORIDA
Gentry Associates
(305) 894-4401

NEW ENGLAND
O'Sullivan & Murphy
(617) 449-4141

MID WEST
Harris Hanson
(314) MI 7-4350
(816) HI 4-9494

COLORADO, N.M.
Bob Callister, Assoc.
(303) 761-0992

PENNSYLVANIA
Schibley Associates
(215) MU 8-7207

OHIO
Ron Makin Associates
(513) 232-5588

NORTHERN CALIFORNIA
Hoeke/Reeser
(415) 941-4080

SOUTHERN CALIFORNIA/ARIZONA
Interstate Marketing
(213) 883-7606 in California
(602) 957-1220 in Arizona

READER SERVICE NUMBER 48

reports. "None of the devices showed signals of metal migration or any other physical deterioration." Amplifiers of this type are being flown on the Canadian-US Communications Technology Satellite.

New materials under evaluation

While work proceeds toward filling the remaining information gaps and perfecting X-band devices, FET device designers are eagerly eyeing higher frequencies. According to Gelnovatch of ECOM, Ku-band will be one of the Army's biggest priorities for 1976. The military is especially interested in the FET for high-frequency mini-RPV, electronic warfare and airborne equipment programs.

The high-frequency performance of an FET is fundamentally limited by the dimensions of the channel and by the mobility of carriers within the channel.[13] In short-gate devices, such as those required for microwave applications, the electric fields in the channel region are so high (>3.5 kV/cm) that carriers reach their limiting velocities. Thus, according to simple theory, for a given channel length the maximum frequency of operation is determined by the peak carrier velocity of the material.[14]

Early devices were fabricated on silicon. However, researchers soon took advantage of the better mobility of GaAs, and found that they could raise the maximum frequency of operation by a factor of about four times by resorting to the high-velocity material.[15] Recently, another III-V semiconductor compound, indium phosphide (InP), has attracted a lot of attention since it offers a maximum drift velocity that is about 1.5 times that of GaAs (see Fig. 8).

InP research programs are given high priority in Great Britain[16], where sources estimate that government-backed programs in InP far outnumber those in GaAs. InP work has lagged behind in the U.S., and just now appears to be picking up momentum. One important program is nearing conclusion at Hewlett-Packard Laboratories in Palo Alto, CA, under the sponsorship of Army ECOM. According to Dr. Lothar Wandinger, a phyicist at ECOM, the results of this two-phase program will give the Army a definite answer to the question of whether or not InP is worth pursuing for FET applications. The first phase of this project includes the development of a LPE process for growing thin InP layers on semi-insulating InP substrates, the adaptation of the GaAs FET fabrication technology to InP, and the comparison of InP devices to GaAs FETs of similar structure.[17]

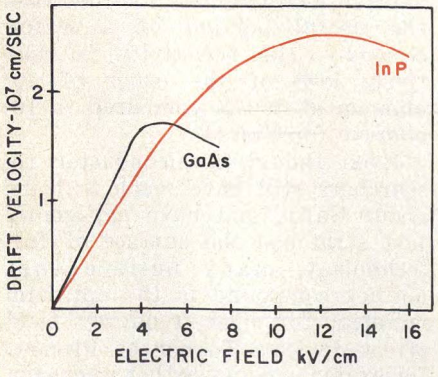

8. **A higher drift velocity** may give InP an advantage for high-frequency devices. Curves are valid at 300°K, for doping levels of 10^{17} cm^{-3}.

"We expected that InP would have higher f_{max} and higher gain than GaAs," comments Joseph Barrera, who was with HPL during the initial phases of the program. "We also predicted a 30 to 40% increase in f_t, the point where the current gain goes to unity."

Performance of the experimental InP devices exceeds HP's predictions for current-gain cutoff, but is rather disappointing in terms of power-gain cutoff. The best devices tested had current-gain cutoff frequencies of about 20 GHz, which is greater than the best analogous GaAs FET by a factor of 1.5. But the highest power-gain cutoff frequency (f_{max}) for the best InP devices is 33 GHz, which is somewhat lower than the 40 GHz figure reported for a similar GaAs FET. Minimum noise figure at 10 GHz was 3.9 dB with an associated gain of 4.8 dB for these first InP devices. The best result for the GaAs counterpart is 3.2 dB, with an associated gain of 7.8 dB. Barrera is careful to note that the main thrust of this program was not to minimize noise figure: "My feeling is that if optimized, the difference in noise figure would be marginal."

"Most of our expectations were realized," he notes. "Current gain is substantially larger, and the 50% higher f_t values are in accord with the higher maximum drift velocity of electrons in InP. But the hooker is that the power gains of these first InP MESFETs are somewhat poorer than those of corresponding GaAs devices." According to Barrera, the InP device offers lower power-gain than com-

(continued on p. 50)

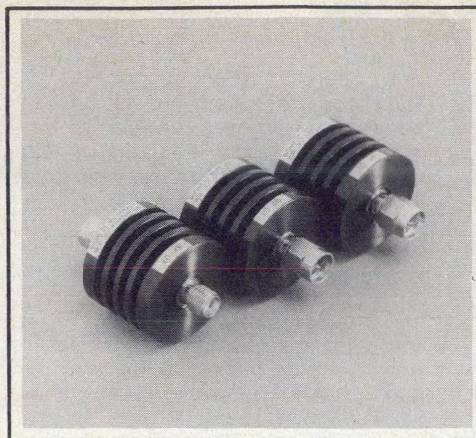

High Performance/Low Price

5 watt sma attenuators

SPECIFICATIONS			
MODEL:	307	Price:	$89.50 each
Frequency Range:	DC to 18.0 GHz	Delivery:	Stock to 30 Days A.R.O.
Attenuation Values:	3, 6, 10, 20, 30dB		
Attenuation Accuracy:	3dB ±0.3dB 6dB,10dB ±0.5dB 20dB,30dB ±1.0dB		
Maximum VSWR:	1.07+0.015fGHz		
Connectors:	Stainless Steel SMA		
Maximum Input Power:	5 watts at 25°C derated linearly to 0 watts at 125°C		
Temperature Range:	−54°C to +125°C		

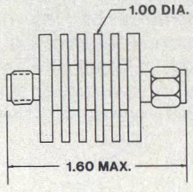

MIDWEST MICROWAVE

3800 Packard Road, Ann Arbor, Michigan 48104 • (313) 971-1992 • TWX 810-223-6031

FRANCE: S.C.I.E.-D.I.M.E.S. 928-38-65

READER SERVICE NUMBER 50

New devices surface

The metal-epitaxial-semiconductor field-effect transistor, or MESFET (in this discussion, we simply use FET), is currently attracting more interest than any other microwave semiconductor. In fact, market predictions by Frost and Sullivan, of New York City, project a 37% annual growth for the GaAs FET device market to 1980. According to a 1975 study by Frost and Sullivan,[20] the annual sales volume, which was estimated to be $600,000 in 1974, will increase to $4-million by 1980 and to $8-million by 1985.

It must be noted, however, that the volitility of the GaAs FET market clouds even the most carefully prepared marketing predictions. For example, last year there were three major suppliers of low-noise GaAs FETs: Nippon Electric Co., Fairchild and Plessey. Power FETs were not commercially available and sub-micron devices were, at best, in preproduction cycles. Now, in 1976, Fairchild has dropped its entire GaAs FET effort, Hitachi has already entered the market with one-half and one micron devices, Hewlett-Packard will hit the market with one micron chips plus two new packaged devices, Varian will toss their hat in the ring with a line of low-noise devices, Dexcel, a new company headed by Dr. Yoso Satoda, a former director of research at Avantek, will introduce commercial, sub-micron GaAs FETs, Plessey, NEC and Fujitsu will offer power FETs and NEC plans to announce the first commercial dual-gate device. And these are only the companies who have announced commercial intentions. Firms such as Hughes, Avantek, Rockwell International, RCA, Westinghouse, Phillips, Siemens, Raytheon and Aertech all have in-house development programs under way, and in many labs, the question is still open whether or not to assault the marketplace.

Pre-matched packaging previews

It's noteworthy that the FET's major asset at low frequencies—high impedance levels—is its chief drawback at microwave frequencies. A well-designed GaAs FET, with low parasitics, is inherently a broadband device and its bandwidth is, in practice, limited by the matching of its very high input and output impedances to 50-ohm lines. Many amplifier designers would like to work with packaged FETs that are internally matched to 50 ohms over broad bandwidths like bipolar transistors. However, FET manufacturers claim that at this time it is not possible to design such a package without seriously degrading the performance of the chip. A compromise solution, which should impact the market in 1976, is the "pre-matched" package.

"On a Smith Chart, an FET's S_{22} characteristic covers a pretty short reactance arc, but it covers a large range of output resistance values," notes Len Lea, product marketing manager at Hewlett-Packard's Microwave Component Division, in Palo Alto, CA. "Inside our new package, we try to shorten the reactance arc, and get it on a constant resistance circle toward 50 ohms. It does not match 50 ohms exactly, but given your choice of an output S_{22} that goes from 150 ohms to 15 ohms and covers many, many degrees versus a line that stays on, say, the 35-ohm circle and covers a few less degrees, which one would you take?" questions Lea.

Sampling quantities of HP's packaged FET are expected to be made available this month, and production devices should be introduced by mid-year. Two packages will be offered, one designed for the 4 to 8 GHz band, and a second for 8 to 12 GHz. Both will be built around the same chip, which covers dc to 18 GHz, and which will be offered separately. The packages are strictly microstrip structures with no stripline sections. Hermetically sealed, they consist of a beryllia slab with copper parts and measure 100 x 170 mils.

A dual-gate device debuts

NEC, meanwhile, is intent on maintaining its lead in the GaAs FET market and will introduce at least three new devices this year. Perhaps the most interesting is a dual-gate design intended for X-band low-noise amplification and automatic gain control (AGC). According to an early spec sheet, model V463 displays a noise figure of 1.8 dB @ 4 GHz, 18 dB maximum available gain, 20 mmho transconductance and a maximum frequency of oscillation of 45 GHz. At 4 GHz, 20 dB of automatic gain control will be available by controlling the second Schottky-barrier gate.

Two medium power devices will also augment NEC's product line. Model V464A is intended for 250 mW amplifier and oscillator applications up to X-band. Preliminary specifications include 7 dB gain at the 1 dB compression point, 80 mmho transconductance and a maximum frequency of oscillation of 30 GHz. A more powerful version, model V464B, will handle up to 500 mW. Maximum frequency of oscillation

parable GaAs FETs primarily due to degenerative feedback resulting from an exceptionally large gate-to-drain capacitance combined with a small output resistance.

Under the second phase of the ECOM contract, HP will try to determine whether major cause of the feedback, gate-to-drain capacitance is intrinsic to the material, or if it can be reduced with improvements in processing. "That this loss may be intrinsic and irremediable is suggested by the fact that an analogous SI device has the same magnitude C_{dg} as the InP MESFET," Barrera cautions, "but we expect that it is remediable. And, if the problem of a high feedback capacitance and a low output resistance were corrected in InP, you could indeed talk about devices with an f_{max} of 80 to 100 GHz, versus about 40 to 60 GHz for GaAs with equivalent structures. On paper, to our way of thinking, it promises a better device."

But even if prototype InP devices are shown to perform better in all respects than corresponding GaAs devices, there are several practical hurdles to overcome. First of all, until recently it was very hard to obtain InP substrates in the U.S.; it is estimated that the status of InP technology in the U.S. today is comparable to the status of GaAs a decade ago. Varian, in Palo Alto, is about the only domestic producer of InP, and has just recently begun selling substrates to other firms. In the past, American labs usually turned to the Royal Radar Establishment (RRE) in England for the material, as HP did.

And, even though InP is available, it is very expensive, available in limited quantities, subject to long delivery delays and may be of poor quality. According to Barrera, the Cr-doped InP boules purchased from the RRE for HP's developmental FETs are poorer in two respects than corresponding GaAs material. "Firstly," he notes, "there are sometimes macroscopic occulsions of CrP particles that decrease the useful portion of a wafer. Secondly, the resistivity is relatively low—of the order of 10^4 ohm-cm at 300 K compared to 10^8 ohm-cm for GaAs."

Even though semiconductor researchers still have much to learn about GaAs, and have apparently just scratched the surface of InP technology, many believe that neither compound is the optimum material for high-frequency field effect devices. Turner of Plessey, for example, believes that a ternary alloy, such as gallium-indium-arsenide (GaInAs) could eventually result in a superior high-frequency

npetition intensifies

for this model is also 30 GHz, but transconductance will be in the neighborhood of 110 mmho and gain at the 1 dB compression point will be about 6 dB.

According to Carl Peterson of California Eastern Laboratories, model NE388, NEC's half-micron FET, has moved from preproduction to full production status, with an expected improvement in deliveries. Final specs on this device include 80 GHz f_{max}, 13 dB gain at 8 GHz and 2.5 dB noise figure at 8 GHz. NEC's one-micron FET, the NE244, currently the most popular commercial FET in the industry, provides 11 dB gain at 8 GHz, 3 dB noise figure at 8 GHz and an f_{max} of 55 GHz.

Plessey, with U. S. offices in Santa Ana, CA, sells a one micron device, the GAT-3, which has been in a neck and neck specification race with NEC's NE244. "Last March, we came out with some FETs that we thought were comparable with NEC's, in terms of gain and noise figure. But just when Plessey drew even, NEC rapidly improved their technology," comments Will Foster, a Plessey application engineer.

Plessey's GAT-3 chip currently offers a noise figure of 5.5 dB at 8 GHz (4.0 dB with low-noise option 010), which is clearly poorer than the present 3 dB spec claimed by NEC. But Foster notes: "We think that we are on the track of why our noise figures are worse, and believe that it has to do with the interface between the epitaxial layer and the substrate. We are, at the moment, growing new combinations which we hope will improve the spec." In a more recent interview, James Turner of Plessey said: "By modifying our technique for GaAs epitaxial growth, we have improved our material such that our device noise figures at 8 GHz are 2.0 dB, which I believe, is the lowest yet published for a one-micron gate length device. We believe we can push this lower, too."

High powers to ponder

As detailed in MicroWaves last November[16], Plessey intends to market FETs for power amplification in 1976. "Our latest power FET result is 0.6 W at 8 GHz, with an associated gain of 6 dB, from a 1.5 micron long, 1.4 mm wide gate. The power-added efficiency is 34%," Turner reports.

Last month, Fujitsu's Component Division in Tokyo, Japan, introduced the first truly high-power GaAs FET's to the commercial marketplace. New models in the FLC series are intended for common source Class A linear power amplifier and oscillator applications. Model FLC30 offers power outputs of 3.0, 2.4 and 1.0 watts at 4, 6 and 8 GHz, respectively. Model FLC15 is rated at 1.5, 1.2 and 1.0 watts, while model FLC08 is speced at 0.8, 0.7 and 0.6 watts, at the same frequencies. At 8 GHz, power added efficiency ranges from 24 to 38%, depending on model. The devices use a multi-finger, overlay gate structure.[21] High power does not come cheaply, however. Prices for these hermetically-packaged FETs are $740, $980 and $1,200. Thus, rf semiconductor costs for a 5 watt, 6 GHz amplifier would exceed $5,300.

Here comes more competition

Hitachi has committed itself more deeply to the GaAs FET market by discontinuing its old model 84, which was only characterized to 4 GHz, and replacing it with two new devices. Model HCRL-85 is a one-micron device that provides 11 dB maximum available gain, 3 dB noise figure at 8 GHz and an f_{max} of 60 GHz. Model HCRL-87, a half-micron device, offers 13 dB maximum available gain at 8 GHz, 2.5 dB noise figure and a 70 GHz f_{max}. According to Hank Inoue, manager of the millimeter wave division at the Hitachi Shibaden Corporation in Woodside, NY, the half-micron devices are available in sampling quantities only, and delivery of both devices is very limited.

Dexcel, located in Santa Clara, CA, has just celebrated its six-month birthday yet hopes to have sampling quantities of a new half-micron FET out the door early this year. President Yoso Satoda plans to keep Dexcel strictly a device house catering to component manufacturers. Satoda says that his company will rely on liquid phase epitaxial deposition to fabricate a complete line of half and one-micron devices. Although performance figures were not available at press time. Satoda indicates that his goal is to reach a 3 dB noise figure at 18 GHz with 9 dB gain by the end of the year.

According to Berin Fank, manager of business development at the Solid-State West Division, Varian will also offer one-micron devices midway through 1976. "Right now, we are doing life testing," he comments. "What we have now is certainly adequate for the 4 to 8 GHz range and probably up to 12 GHz, but there are still many improvements to be made." Although Varian is doing extensive work with InP, their initial products will be built on GaAs. "Most of our InP work is with Gunn devices," Fank says. "There are still too many pros and cons concerning InP FETs for us to devote full manpower to it now."

device. Early work at Varian with another ternary compound, gallium-indium-phosphide (GaInP), looks encouraging.[18] However, the practical implementation of these more exotic materials is conceded to be quite far in the future.

Shorter gates seen in future

Resorting to materials with higher mobility is only one way to boost the FET higher in frequency. A more obvious technique is to shorten the gate length of a GaAs device, thus reducing the electron transit time in the channel region and improving frequency response. To illustrate the effect of reducing gate length, consider the specifications for two NEC products: the half-micron gate NE388 and the one-micron gate NE244. The one-micron device exhibits an f_{max} of 55 GHz, compared to 80 GHz for the NE388. At 8 GHz, the gain of the NE388 is 2 dB higher, while the noise figure is 0.5 dB lower.

Reducing the gate dimension to sub-micron lengths poses two fundamental problems. First, most FET manufacturers claim that the close resolution required to deposit a metal gate stripe one-micron wide is pushing optical lithography to the limit for the high yields and large volume required of production runs. "Pushed to the absolute limit, these techniques can go to 0.5 micron resolution, but it would be terribly difficult to do on an everyday basis," comments HPA's Barrera.

Although some manufacturers, including NEC and Avantek, have apparently devised photolithographic processes capable of repeatable half-micron structures, many experts claim that electron-beam lithography must be used for truly large scale production. E-beam techniques can produce repeatable structures down to two-tenths micron, but presently, commercial machines are not suitable for volume production. For example, Plessey, which used to fabricate its one-micron device with electron-beam techniques, recently switched to an optical system to increase production capacity.

The second fundamental challenge to building a satisfactory device with a sub-micron gate length centers on the fabrication of an ultra-thin active layer. There is currently quite a bit of controversy in the industry whether LPE and VPE processes can be accurately controlled, in terms of both doping and thickness, when the active layer dimension shrinks to a micron or less. NEC, which uses a VPE process, says that it can control epitaxial thickness to within ±0.04 micron

(continued on p. 52)

Eliminate Watts For Pennies!

ATTENUATOR KITS

For the over-efficient engineer

Now available, the ideal tool for breadboarding, enabling you to determine the exact attenuation value needed for your circuit. Each chip has three large Pt/Au land areas which can easily be tabbed or soldered. Mounting recommendations are included. This chip attenuator, model AC0100, is available in production quantities for as low as $1.00 each. For complete information and full product catalog featuring a variety of attenuators for applications up to 18 GHz and up to 5 watts power, call or write today.

- ☐ **Attenuator Chip:** For 50Ω line
- ☐ **Frequency Range:** DC to 1 GHz
- ☐ **Power Rating:** 1.0W @ 25°C
- ☐ **Peak Voltage:** 100V
- ☐ **Size:** .240 x .240 x .035 max. (T-Configuration)
- ☐ **VSWR:** 1.25 max
- ☐ **Accuracy:** ±0.5 db or 10% whichever is greater
- ☐ **Operating Temp.:** −55°C to +150°C

ATTENUATOR CHIP KIT KA0100
Contains 5 chips each of 1dB to 10dB (in 1 dB steps)
A total of 50 chips Price $100.00 per kit

EMC TECHNOLOGY, INC.

1971 Old Cuthbert Road
Cherry Hill, New Jersey 08034
Phone (609) 429-7800 TWX 710-896-0193

READER SERVICE NUMBER 52

(continued from p. 51)

of the design value. HP, a proponent of LPE, claims a typical accuracy of ±7% with some runs being as good as ±4%

The alternative to epitaxial growth, as mentioned previously, is ion implantation. Experiments at the Rockwell Science Center have shown less than ±5% typical variation in maximum carrier concentration and film thickness with the process. Relatively few ion-implanted FETs have been actually fabricated, and those that have been reported show gain parity with epitaxial FETs, but display slightly higher noise figures. At Rockwell, a selenium-implanted device with a 1.1 micron gate produced better than 10 dB maximum available gain up to 10 GHz. S-parameter measurements on this device predict a maximum frequency of oscillation in excess of 30 GHz. Noise figure at 10 GHz was measured to be 3.4 dB, which compares with 3.2 dB for a comparable epitaxial transistor.

Sulfur-implanted devices developed at Siemens AG in Munich, Germany, also display acceptable gains, but rather poor noise figures. [19] A 1.5 micron device reported by Siemens produces a maximum available gain of 10 dB at 10 GHz and a maximum frequency of oscillation of 30 GHz. Noise figure is greater than 8 dB at 10 GHz.

Today, there are a couple of half-micron devices on the market, and the question naturally arises whether or not higher frequency performance could be obtained by resorting to even shorter gate lengths. There are the obvious constraints of manufacturing processes, but there are some electrical problems as well. By shrinking the gate size, dc resistance, and therefore rf resistance, increases appreciably. Also, field-effect devices are very sensitive to capacitance in the conductive channel, and when the gate is shrunk, its fringing capacitance is modified considerably.

To investigate the merits of very short gate lengths, Army ECOM plans to fund the development of a quarter-micron gate length device in 1976. The K-band device is designed to operate in the 20 to 22 GHz region, and will be fabricated on a GaAs substrate using electron-beam lithography for gate metalization and ion implantation to fabricate the thin n-type active layer. Implantation will also be used to form an n+ layer under the source and drain contacts in an effort to reduce contact resistance. ••

References

1. S. Okazaki, S. Takahashi, M. Maeda and H. Kodera, "Microwave Oscillation with GaAs FET," *Journal of Japan Society of Applied Physics,*" Vol. 44, pp. 157-161, (1975).

2. M. Maeda, K. Kimura and H. Kodera, "Design and Performance of X-Band Oscillator with GaAs Schottky-Gate Field-Effect Transistors," *IEEE Transactions on MTT,* Vol. MTT-23, No. 8, pp. 661-667, (August, 1975).

3. D. C. James, G. Painchaud, E. Minkus and W. J. R. Hoefer, "Stabilized 12 GHz MIC Oscillators Using GaAs FETs," *Proceedings of the Fifth European Microwave Conference,* pp. 296-300. Hamburg, Germany, (September 1-4, 1975).

4. R. L. Van Tuyl and C. A. Liechti, "High-Speed Integrated Logic With GaAs MESFETs," *IEEE Journal of Solid-State Circuits,* Vol. SC-9, No. 5, pp. 269-276, (October, 1974).

5. H. C. Huang, I. Drukier, R. L. Camisa, S. T. Jolly and S. Y. Narayan, "GaAs MESFET Performance," *Technical Digest of IEDM,* pp. 235-237, (December, 1975).

6. D. R. Ch'en, H. F. Cooke and J. N. Wholey, "Long Term Stability of Microwave FETs," *Microwave Journal,* Vol. 18, pp. 60-61, (November, 1975).

7. H. Kozu, I. Nagasako, M. Ogawa and N. Kawamura, "Reliability Studies of One-Micron Schottky Gate GaAs FET," *Technical Digest of IEDM,* pp. 247-250, (December, 1975).

8. J. Barrera, "The Importance of Substrate Properties on GaAs FET Performance," *Proceedings of Fifth Biennial Conference on Active Semiconductor Devices for Microwaves and Optics,* Paper 3.3, (August, 1975).

9. J. A. Higgens, B. M. Welch, F. H. Eisen and G. D. Robinson, "Performance of Ion-Implanted GaAs MESFETs," *Technical Digest of IEDM, Late News Supplement,* pp. 5-6, (December, 1975).

10. D. A. Abbott and J. A. Turner, "Some Aspects of GaAs FET Reliability," *Technical Digest of IEDM,* pp. 243-246, (December, 1975).

11. NEC Technical Note, "The Design and Applications of the NEC GaAs FET," (October, 1975).

12. Plessey Application Note, "Plessey GaAs FET Handling Precautions."

13. W. Gosling, W. G. Townsend, J. Watson, *Field Effect Electronics,* pp. 62-68, Wiley Interscience, (1971).

14. J. A. Turner and S. Arnold, "Schottky Barrier FETS . . . Next Low Noise Designs," *MicroWaves,* pp. 44-49, (April, 1972).

15. J. A. Turner, "Gallium Arsenide Field-Effect Transistors," *Proceedings: 1966 Symposia on GaAs,* pp. 213-218, (1966).

16. R. T. Davis, "A Look At West Europe's Priorities IN R&D," *MicroWaves,* pp. 38-51, (November, 1975).

17. J. S. Barrera and R. J. Archer, "InP Schottky-Gate Field Effect Transistors," *IEEE Transactions On Electron Devices,* Vol. ED22, No. 11, pp. 1023-1030, (November, 1975).

18. D. R. Decker, R. D. Fairman and C. K. Nishimoto, "Microwave In_xGa_{1-x} As Schottky-Barrier Field Effect Transistors—Preliminary Results," *Proceedings of Fifth Biennial Conference on Active Semiconductor Devices for Microwaves and Integrated Optics,* Paper 5.6, (August, 1975).

19. W. Keller, H. Kniepkamp, D. Ristow and H. Boroffka, "Microwave Field-Effect Transistors From Sulphur-Implanted GaAs," *Technical Digest of IEDM,* pp. 238-242, (December, 1975).

20. Frost & Sullivan, Inc., *The U. S. Microwave Device and Components Market,* No. 352, (August, 1975).

21. M. Fukuta, H. Ishikawa, K. Suyama and M. Maeda, "GaAs 8 GHz-Band High Power FET," *Technical Digest of IEDM,* pp. 285-287, (December, 1974).

22. C. A. Liechti, "Recent Advances in High-Frequency Field-Effect Transistors," Technical Digest of IEDM, pp. 6-10, (December, 1975).

23. G. A. Mead, "Schottky-Barrier FET," Proceedings of IEEE, Vol. 54, No. 2, pg. 307, (February, 1966).

How Much Pulsed Power Can A PIN Diode Handle?

A thermal analysis is necessary to determine the peak pulsed power that a PIN diode can safely switch. The problem is easily solved, however, once physical and pulse parameters are known.

DETERMINING the maximum peak power a PIN diode can safely handle and switch need not be a matter of guesswork. Although manufacturers do not specify peak power capability, it's relatively easy to calculate given the thermal characteristics of the device and the pulse interval and pulse width of the incident pulse train.

A PIN diode, mounted in shunt with a transmission line, presents a low impedance to incident rf power when biased in the forward direction. In this low impedance state, the device reflects a large amount of incident power, but not totally. The portion of power not reflected is dissipated in the device causing a temperature rise in the junction. A safe operation junction temperature, which should never be exceeded, is 175°C.

Thus, the maximum power handling problem is thermal in nature, involving a heat flow analysis. Figure 1 represents a simplified heat flow model for a PIN device, where θ_{jc} is the thermal resistance between the junction and the heat sink and the C_{th} is the heat capacity of the semiconductor chip. Using this equivalent circuit and assuming a junction that is cooled by conduction, the maximum power that can be applied to a junction device without exceeding its rated junction temperature can be calculated.

Incident rf power will raise the junction temperature of a shunt-mounted PIN diode according to:

$$T_j = T_A + P_d \theta_{jc} (1 - e^{-t/\tau_{th}}) \quad (1)$$

where:

T_A = heat sink temperature (°C)
P_d = power dissipated per diode (W)

Frederick Dominick, Applications Manager, GHz Devices, Inc., 16 Maple Road, Chelmsford, MA 01824.

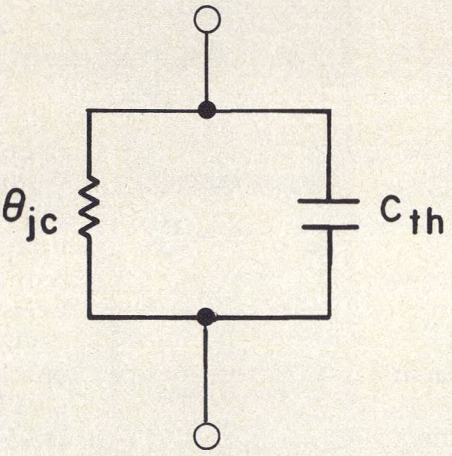

1. A simple thermal equivalent circuit includes thermal resistance (θ_{jc}) and heat capacity (C_{th}).

θ_{jc} = thermal resistance (°C/W)
t = time during which power is applied (sec)
τ_{th} = thermal time constant (sec)

If the incident rf power is applied continuously (cw), $t/K >> 1$, and Eqn. 1 may be expressed as:

$$T_{max} = T_A + P_d \theta_{jc} \quad (2)$$

where T_{max} is 175°C, the junction temperature that cannot be exceeded.

For the non-continuous or pulsed case, the peak power that a device can handle also depends on pulse width (t_p) and pulse interval (t_r = (rep rate)$^{-1}$). In pulsed operation, the junction temperature rises when a pulse of power is incident on the device, and falls during the interval between pulses as the device cools by convection. This effect is illustrated in Fig. 2, in contrast to a typical cw temperature characteristic[1]. During the time, t_p, that pulsed power is incident on the device, the junction temperature, T_j, rises according to Eqn. (1):

$$T_j = T_A + P_d \theta_{jc} (1 - e^{-t_p/\tau_{th}}) \quad (3)$$

It also follows that during the interpulse period, At_p, the junction cools by conduction in the following manner:

$$T_j = T_A + (T_j - T_A)\, e^{-At_p/\tau_{th}} \quad (4)$$

where: $At_p = t_r - t_p$

Referring to Figure 2, the temperature increase (T_2) due to an incident rf pulse is equal to:

$$T_2 = T_1 + (T_A + P_d \theta_{jc} - T_1)(1 - e^{-t_p/\tau_{th}}) \quad (5)$$

In the same manner, the decrease in junction temperature (T_1) due to cooling during the interpulse period is equal to:

$$T_1 = T_A + (T_2 - T_A)(e^{-At_p/\tau_{th}}) \quad (6)$$

At some point in time, equilibrium will be reached and Eqns. 5 and 6 may be combined. T_2 may then be determined after the elimination of T_1 resulting in the following expression:

$$T_2 - T_A = P_d \theta_{jc} \frac{1 - e^{-t_p/\tau_{th}}}{1 - e^{-t_r/\tau_{th}}} \quad (7)$$

Note that for cw operation, $t_p/\tau_{th} \approx t_r/\tau_{th} >> 1$ and Eqn. 7 tends toward Eqn. (2):

$$T_2 = T_A + P_d \theta_{jc} \quad (8)$$

Now consider that the power dissipated in the diode in a low-impedance state is a function of its match to the transmission line:

$$P_d = P_{incident} \frac{4R_s}{n^2 Z_o} \quad (9)$$

(continued on p. 56)

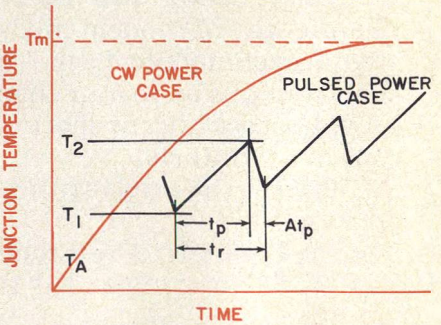

2. During pulsed operation, junction temperature rises when pulse is applied and drops in the period between pulses.

where:

R_s = series resistance of diode (ohms)
n = number of diodes in shunt
Z_o = characteristic impedance of the transmission line.

By setting a maximum value for T_2 (i.e., 175°C), the maximum cw power that a device can safely dissipate may be expressed as:

$$P_{d(cw)} = \frac{T_{max} - T_A}{\theta_{jc}} \quad (10)$$

Or, in terms of incident power:

$$P_{incident(cw)} = \left(\frac{Z_o n^2}{4R_s \theta_{jc}}\right)(T_{max} - T_A) \quad (11)$$

For example, a typical switching diode might have the following specifications:

R_s = 2.5 ohms
θ_{jc} = 9.57°C/W
T_{max} = 175°C
τ_{th} = 9.5 ms

When mounted across a 50-ohm transmission line on a heat sink that is held to a temperature of 25°C, this device can safely switch a cw power level of:

$$P_{incident(cw)} = \left(\frac{50}{(4)(2.5)(9.57)}\right)(175 - 25)$$
$$= (0.111)(150) = 78.3 \text{ watts.}$$

To obtain an expression which describes the maximum peak pulsed power that the device can safely switch, substitute T_{max} for T_2 in Eqn. (7) and subtract from Eqn. (11) to yield:

$$P_{d(pulsed)} = P_{d(cw)} \frac{1 - e^{-t_r/\tau_{th}}}{1 - e^{-t_p/\tau_{th}}}$$
$$= \left(\frac{T_{max} - T_A}{\theta_{jc}}\right)\left(\frac{1 - e^{-t_r/\tau_{th}}}{1 - e^{-t_p/\tau_{th}}}\right) \quad (12)$$

Using Eqn. (9):

$$P_{incident(pulsed)} = \frac{Z_o n^2}{4 R_s \theta_{jc}}\left(T_{max} - T_A\right)\left(\frac{1 - e^{-t_r/\tau_{th}}}{1 - e^{-t_p/\tau_{th}}}\right) \quad (13)$$

It's interesting to note from Eqn. (12) that for:

- $\frac{t_r}{\tau_{th}} < 0.3; \frac{t_p}{\tau_{th}} << 1$:
$$P_{pulsed} = P_{cw}\left(\frac{1}{\text{duty cycle}}\right)$$
- $\frac{t_r}{\tau_{th}} >> 1; \frac{t_p}{\tau_{th}} << 1$:
$$P_{pulsed} = P_{cw}\left(\frac{\tau_{th}}{t_p}\right)$$
- $t_r = t_p; P_{pulsed} = P_{cw}$

Now, given pulse specifications, it's an easy matter to calculate the maximum peak pulsed power that can be switched. Using the same conditions described in the cw example developed earlier, and assuming t_r = 1 ms and t_p = 10 μs, apply Eqn. (13):

$$P_{incident(pulsed)} = \left[\frac{50}{(4)(2.5)(9.57)}\right]\left[[175 - 25]\right]\left[\frac{1 - e^{-10^{-3}/9.5 \times 10^{-3}}}{1 - e^{-10^{-4}/9.5 \times 10^{-3}}}\right]$$
$$= [78.3]\left[\frac{1 - e^{-0.105}}{1 - e^{-0.0105}}\right]$$
$$= [78.3]\,[10]$$
$$= 783 \text{ watts}$$

Calculate thermal constants

Equation (12) contains two parameters, θ_{jc} and τ_{th}, which do not always appear on a diode's spec sheet. Both numbers can easily be calculated, however, knowing the physical parameters of the device in question. Thermal resistance, θ_{jc} is obtained from Fourier's law of heat conduction, which states that the rate of heat flow is proportional to temperature gradient:

$$P = -K_{th}\left(\frac{\Delta T}{\Delta L}\right)A \quad (14)$$

In this equation,

K_{th} = thermal conductivity (W/cm°C)
A = cross-sectional area (cm²)
L = length of conduction path (cm)

Thus, thermal resistance is defined as:

$$\theta_{jc} = \frac{L}{K_{th} A} \quad (°C/W) \quad (15)$$

To determine θ_{jc} for a particular device, the thermal resistance of each doping layer and material in the diode must be evaluated separately, then summed. For example, consider a stud-mounted PIN diode with the geometry outlined in Table 1. The thermal resistance of each doping layer of the silicon chip can be calculated using Eqn. (15) and the material constants in Table 2:

$$\theta_{jc}(Si) = \theta_{ic}(P+) + \theta_{ic}(I) + \theta_{jc}(N+)$$
$$= \frac{1}{K_{th}(Si)}\left[\frac{L}{A}(P+) + \frac{L}{A}(I) + \frac{L}{A}(N+)\right]$$
$$= 1.25\,[0.38 + 2.44 + 2.27]$$
$$= 1.25\,[5.09] = 6.36°C/W$$

The contribution due to the 50 μinch gold metalization is very small as may be seen from the following calculation:

$$\theta_{jc}(Au) = 0.33\left[\frac{L}{A}\right]$$
$$= 9.3 \times 10^{-3} \text{ °C/W}$$

If we assume that the copper pedestal on which the chip is bonded has a diameter of 40 mil (10.2×10^{-2} cm) and a thickness of 50 mil (12.8×10^{-2} cm), then its contribution to the device's thermal resistance is:

$$\theta_{jc}(ped) = \frac{1}{3.9}\left(\frac{L}{A}\right)$$
$$= 2.57 \text{ °C/W}$$

Spreading resistance through to the copper heat sink also contributes to a device's total thermal resistance:

$$\theta_{jc}(\text{spreading}) = \frac{1}{2d\ K_{th}(Cu)}$$
$$= \frac{0.125}{0.203}$$
$$= 0.62 \text{ °C/W}$$

Summing all of these components, the total resistance due to this chip mounted on a copper pedestal is:

$$\theta_{jc} = \theta_{jc}(Si) + \theta_{jc}(Au) + \theta_{jc}(ped) + \theta_{jc}(\text{spreading})$$
$$= 9.57 \text{ °C/W}$$

The second parameter which is often omitted from data sheets is

(continued on p. 59)

Table 1: Typical PIN Diode Geometry

	Thickness (L)	Area (A)
P+ Layer	$.76\times10^{-3}$ cm	2×10^{-3} cm²
I Layer	7.6×10^{-3} cm	3.12×10^{-3} cm²
N+ Layer	10.2×10^{-3} cm	4.5×10^{-3} cm²
Metallization	0.127×10^{-3} cm	4.5×10^{-3} cm²
Pedestal	10.2×10^{-2} cm	12.9×10^{-3} cm²

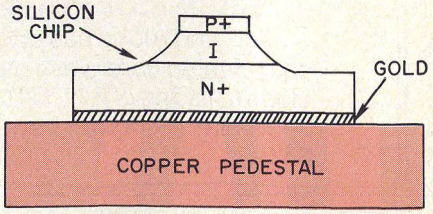

thermal time constant, τ_{th}, which is defined as:

$$\tau_{th} = \frac{\rho\, C_p\, L^2}{K_{th}}$$

where ρ is material density and C_p is specific heat (Table 2). Calculated like thermal resistance, the overall time constant is the sum of the time constants of individual materials and doping layers.

Table 2: Material Constants

	Silicon	Copper	Gold
$K_{Th}\left(\frac{\text{watts*}}{\text{cm°C}}\right)$	0.80	3.9	3.0
$C_p\left(\frac{\text{joules}}{\text{gram°C}}\right)$	0.76	0.39	0.13
$\rho\left(\frac{\text{gram}}{\text{cc}}\right)$	2.42	8.89	19.32

*Thermal conductivity at 200°C from curve published in "Physics of Semiconductor Devices" S.M. Sze page 55, Wiley Press (1969).

Using the chip geometry described in Table 1:

$\tau_{th} = \tau_{th}(Si) + \tau_{th}(Au) + \tau_{th}(Cu)$

The contribution from the thin gold layer may obviously be neglected, leaving:

$$\begin{aligned}\tau_{th} &= \tau_{th}(Si) + T\tau_{th}(Cu)\\ &= 2.28\,[L^2(P+) + L^2(I) + L^2(N+)] + 0.88\,L^2(Cu)\\ &= 2.28 - 10^{-6}\,[0.57 + -57.16 + 104] + 0.88\,(10.45 \times 10^{-3})\\ &= 2.28 \times 10^{-6} \times 161.73 + 9.2 \times 10^{-3}\\ &= 9.5 \times 10^{-3}\ \text{sec}\\ &= 9.5\ \text{ms.}\ \bullet\bullet\end{aligned}$$

References

1. H. M. Olson, "Microwave Semiconductor Devices and Their Circuit Applications," McGraw-Hill, H. A. Watson, editor; Chapter 9, p. 292, (1969).

Test your retention

1. What is a safe junction temperature for a PIN switching diode?
2. How are cw and pulsed power ratings related?
3. State the fundamental form of Fourier's law of heat conduction.
4. Does spreading resistance contribute significantly to overall thermal resistance?

letters

Check the Compression

"Take The Guesswork Out Of Compression Tests" (p. 64, October, 1975), was interesting but the more affluent among us have been using the HP network analyzer for many years to accomplish this. The basis of the analyzer is to compare two signals as Mr. Cooke shows. It also has the added advantages of measuring phase and displaying phase and amplitude vs. frequency. **B. A. Pegg, Aeronutronic Ford, Western Development Laboratories Division, 3939 Fabian Way, Palo Alto, CA 94303.**

HP's Small Wonders

The 8470B Microwave Detectors

- 10 to 18,000 MHz, ±0.6 dB overall flatness.
- New low barrier Schottky diodes for a low SWR of <1.4 at 18 GHz.
- Rugged, low-burnout, field-replaceable diodes.
- Type N, SMA, APC-7 connector options. Priced from $190*

These and more than 300 other microwave measurement items are described in our new 80 page coaxial and waveguide catalog. You can get a copy from your nearest HP field office, or write.

*Domestic US prices only.

HEWLETT hp PACKARD

Sales and service from 172 offices in 65 countries.
1501 Page Mill Road, Palo Alto, California 94304

READER SERVICE NUMBER 59

Power Amp Design For 900 MHz Mobile Radio

This discussion of design techniques for broadband, 12.5 V, 900 MHz power amplifiers concludes with detailed instructions for building a 15 watt design.

IT is anticipated that by the year 1980, the number of mobile radios operating in the 800-900 MHz band will be as large as the total number of mobile radios operating in the lower bands combined. In terms of today's dollars, this represents a potential $56-million market for discrete power transistors.

To meet the challenge of this forecast, the semiconductor industry is striving to incorporate sophisticated microwave packaging designs into low-cost, volume-production transistors (Fig. 1). What results is a device that is probably unfamiliar to designers of hf, vhf and lower uhf radios. This article reviews a new packaging technique being used for 900 MHz power transistors, and presents general design techniques for 12.5 V, 800-900 MHz amplifiers. Initial emphasis is placed on the package, since an understanding of the fundamental limitations of a packaged device can save many frustrating hours on the bench.

Presently, for output levels greater than 15-20 W, the designer is forced to use common base topology for several reasons.

First, for a given output power level and power gain requirement, the common-base transistor is inherently more rugged and less costly. To achieve comparable performance with common emitter topology, a higher figure of merit die (finer geometry) is required. The finer geometry, affects die yield inversely and therefore, influences costs directly.

Secondly, and most important, the common-base device has a 2-3 dB power gain improvement over a similar common emitter configuration. But the increased power gain does not come cheaply; you can't get something for nothing. A computer analysis of the model in Fig. 2 shows that the increased gain is caused mainly by positive regeneration afforded by base spreading resistance (r_b') and common lead inductances (net common lead inductance). The inductance is especially critical, since, if it is too large relative to the device's operating frequency-to-f_t ratio, the device becomes unstable. This problem is usually manifested by (1) a hysteresis effect in rf gain profiles (plots of P_o vs P_{in}), (2) snap-on characteristics with gradual application rf drive, (3) hard saturated output power levels which are generally less than the saturated level for the same device in common emitter configuration (4) sustained oscillations (P_o without application of P_{in}) (5) reduced operating bandwidth and (6) poor collector efficiency. *(continued on p. 65)*

Junius Taylor, Engineer, High Frequency Products, Senior Design Engineer and **Gordon McIntosh,** Motorola Semiconductor Products Division, Box 20912, Phoenix, AZ 85036.

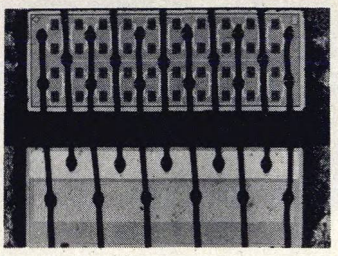

1. A typical 900 MHz geometry has 0.15 mil fingers and spaces.

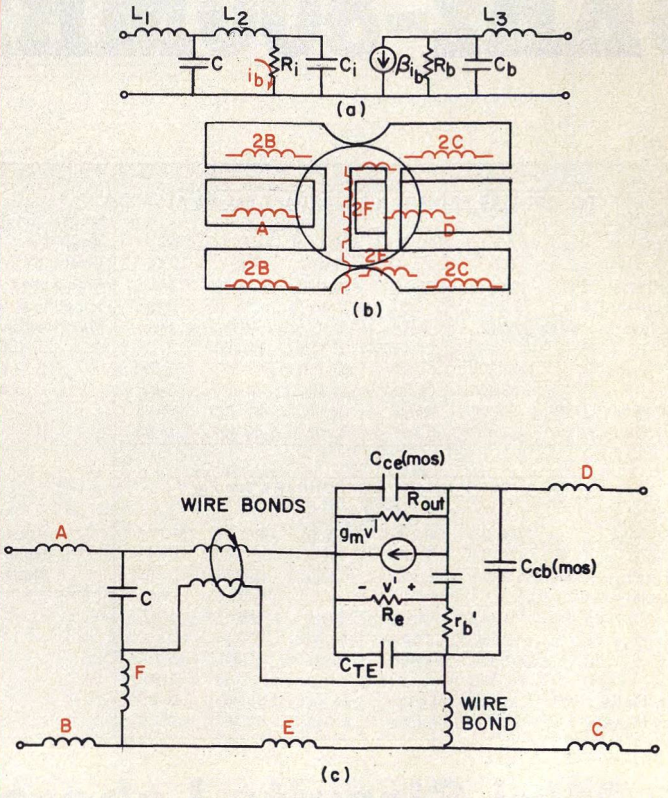

2. Package parasitic inductances (b) must be included in the model for a high-power, 900 MHz device (c). A much simpler model (a) can be used at lower frequencies.

A more subtle, but serious drawback of a common base configuration with lead inductance is a strong dependence of the packaged device's input and output impedances and apparent power gain on the base-collector capacitance (C_{bc}), collector-emitter capacitance due to MOS (C_{ce}), and ac beta. These impedance variations are added to those caused by inconsistent wire bonding and could cause chaos on any radio assembly line.

Chips present low impedance

The impedance levels of packaged devices in each configuration are approximately the same. At the chip, common lead inductance for the common emitter device is reflected as inductance and resistances. The net result is increased resistance and inductive reactance. In a common base configuration, the inductance is reflected at the input as inductive reactance and negative resistance.

Due to extremely low input impedances (0.1 to 0.6 ohm at the input of 12.5 volt chips), package parasitic inductances and I^2R losses, internal impedance transforming networks are employed in 900 MHz power transistors to improve both gain and bandwidth. Wire bond and lead inductance combine with MOS capacitors to form a low-pass impedance transforming network. At lower frequencies and lower power levels, it is reasonable to use as a first-order approximation the circuit model shown in Fig. 2(a) to represent the packaged device. In this case, classical works by Bode, Fano, Matthaei and others provide a straight forward synthesis approach to determine element values in terms of a given bandwidth requirement. At high power and high frequencies, $P_o \geq 40$ W @ 470 MHz and $P_o > 20$ W @ 900 MHz, package parasitic inductance seriously constrains the transistor's performance. In these cases, models similar to that shown in Fig. 2(c) become more useful.

In general, most rf parameters are affected by the selection of wire self and mutual inductances and MOS capacitance; computer analysis shows that bandwidth is not the sole consideration in the synthesis procedure. Collector efficiency (n_c), power gain (G_p) and stability factor (k) are also heavily dependent on the selection of internal matching elements.

Lower frequency package designs have been predicated on the concept of a perfect ground system. All ground terminals are assumed or wished to be made equi-potential. The resulting plane of points serves as a reference point, or circuit reference node. Until now, the penalties resulting from this approximation have been minor. Frequency and power demands of the new mobile band, however, demand the recognition that all points on a finite surface be isolated by some finite inductance.

One of the latest package designs, Motorola's Controlled S_{12} (CS_{12}) package, abandons the perfect ground concept. The package leads, wire bonds, package internal stray inductances, MOS capacitor and transistor chip all form a lumped element equivalent to a transmission line. In this de-

(continued on p. 66)

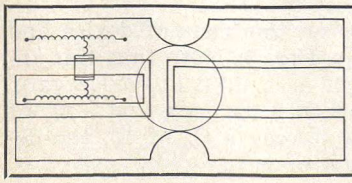

3. The capacitor must be placed as close to the case as possible. Note that the distance ($\Delta\ell$) will affect circuit performance.

THIN-TRIM CAPACITORS FOR HYBRIDS AND MIC'S

Series 9410 Thin-Trims are sub-miniature variable capacitors for applications where size and performance are critical. Featured are high Q's for low circuit losses, high capacity values for broadband applications and low profile for "gap trimming" in tiny MIC's. Body size .200" x .200" x .060"T. Available in 5 capacitance ranges from 1.0 - 4.5 pf to 7.0 - 45.0 pf.

Johanson®

MANUFACTURING CORPORATION
Rockaway Valley Road
Boonton, N.J. 07005
(201) 334-2676 TWX 710-987-8367

READER SERVICE NUMBER 65

When RFI problems get sticky, try sticky fingers®

Attaches faster, shields better than anything else!

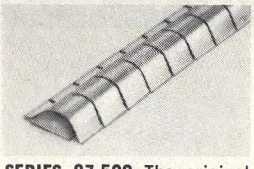

SERIES 97-500 The original Sticky Fingers with superior shielding effectiveness.

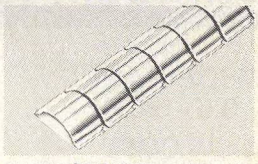

SERIES 97-520 A smaller size strip; highly effective in less space.

SERIES 97-555 New Single-Twist Series for use when space is at a premium. Measures a scant ⅜" wide.

SERIES 97-560 New ½" wide Double-Twist Series, ideal for panel divider bar cabinets.

Now you can specify the exact type beryllium copper gasket that solves just about every RFI/EMI problem. Perfect for quick, simple installation; ideal for retro-fitting. Self-adhesive eliminates need for special tools or fasteners. Write for free samples and catalog.

INSTRUMENT SPECIALTIES COMPANY, Dept. MW-57
Little Falls, N.J. 07424
Phone—201-256-3500 • TWX—710-988-5732

READER SERVICE NUMBER 66

READER SERVICE NUMBER 67

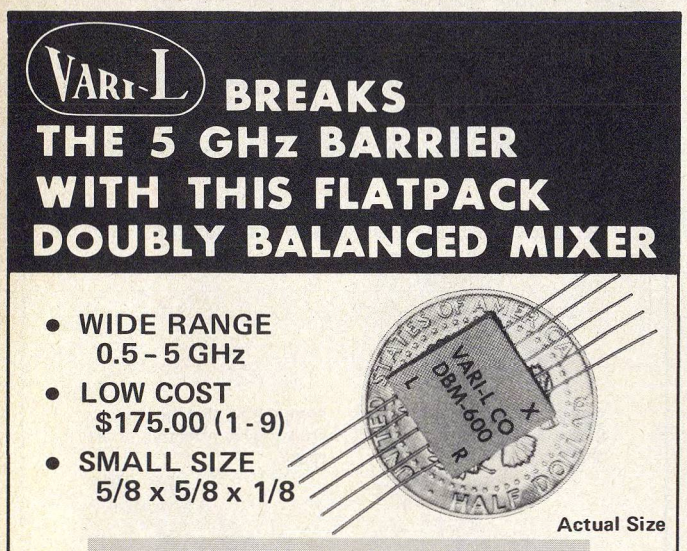

READER SERVICE NUMBER 68

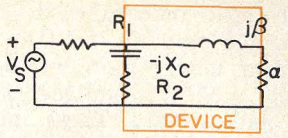

4. The transistor's impedance is represented by $\alpha + j\beta$ in this simple model.

sign, package lead inductances are exploited as matching elements, just as bonding wire inductances are used in earlier designs.

Shunt capacitance important

While distributed elements readily lend themselves to a 900 MHz amplifier, size constraints often dictate that the first external element next to the package be a shunt capacitor, since the transistor's input and output impedance have inductive reactance (Fig. 3). This is by far the most critical area in the amplifier's design. Here, the designer is faced with relatively low impedance levels, high circulating currents and consequently, the potential for high-insertion loss due to the Q of the capacitor or shunted transmission line.

The insertion loss attributed to the capacitor creates the peculiar effect where maximum output power from the amplifier stage does not occur with minimum generator VSWR. Assuming a device with an input impedance of $\alpha + j\beta_2$, the insertion loss can be calculated by considering the equivalent circuit shown in Fig. 4.

Referring to Fig. 4, the power dissipated in elements α and R_2 is found to be:

$$P_\alpha = \frac{V_s^2\,\alpha\,(R_2^2+X_c^2)}{(\alpha(R_1+R_2)+R_1R_2+\beta X_c)^2+[\beta(R_1+R_2)-X_c(R_1+\alpha)]^2}$$

$$P_{R2} = \frac{V_s^2 R_2(\alpha^2+\beta^2)}{[\alpha(R_1+R_2)+R_1R_2+\beta X_c]^2+[\beta(R_1+R_2)-X_c(R_1+\alpha)]^2}$$

Insertion loss (IL) =

$$\frac{P_\alpha}{P_\alpha + P_{R2}} = \frac{1}{1+\frac{P_{R_2}}{P_\alpha}} = \frac{1}{\left[1+\frac{R_2}{\alpha}\right]\frac{(\alpha^2+\beta^2)}{(R_2^2+X_c^2)}}$$

$$= 1 + \frac{\frac{1}{\alpha[1+(\beta/\alpha)^2]}}{\frac{R_2}{\left[1+\left(\frac{X_c}{R_2}\right)^2\right]}} = \frac{1}{1+\frac{\alpha}{R_2}\left(\frac{1+Q_d^2}{1+Q_c^2}\right)}$$

where: Q_d is the Q of the transistor; Q_c is the Q of the capacitor.

Neglecting mismatch loss at the generator:

$$\text{IL (dB)} = -10\log\left\{\frac{1+\alpha}{R_2}\left(\frac{1+Q_d^2}{1+Q_c^2}\right)\right\}$$

When we substitute the approximation

$$X_c = R_1\left(\frac{\alpha}{R_1-\alpha}\right)^{1/2} \quad \text{and} \quad R_1 = \frac{\alpha^2+\beta^2}{\alpha}$$

$$-\text{IL dB} = 10\log\left[1+\frac{Q_dQ_c}{1+Q_c^2}\right]$$

A table of insertion loss on the basis of device and capacitor Q is presented in Fig. 5. Note that this insertion loss manifests itself as a drop in device gain. For example, if a device with 8 dB gain and a Q_d of 6 is used with a capacitor having a Q_c of 10, the device will yield only 5.97 dB of gain.

The parasitic inductance of the capacitor becomes a critical consideration, since it acts to increase the effective value of the capacitor.

$$C_{eff} = \frac{C}{1 - 4\pi^2 f LC}$$

Typical values of equivalent series inductance are approximately 0.3 nH for a 50 mil chip and 0.7 nH for a 100 mil chip. The next effect of this parasitic is an overshoot of the capacitance intended, increased insertion loss and reduced bandwidth performance.

Another problem area crops up in production repeatability. The placement of capacitors near the package is critical. As would be expected, during factory assembly operation, variations on this component's seating and placement distance ($\Delta\ell$) from the package edge will cause shift in the amplifier's frequency response.

Although common base devices are more practical for high power 900 MHz output stages, low-power stages are often common emitter. A forward bias (V_{BE}) of approximately 0.3-0.6 volts on low-power level stages significantly improves the common emitter amplifier's dynamic characteristics. This technique can be used to obtain a smooth and continuous curve for P_{out} versus P_{in} at low power levels, improved stability and decreased variation of input VSWR with various drive levels. Note, however, that collector efficiency is reduced approximately five percentage points. Ideal conditions for the application of this bias is that the device be emitter ballasted and that the bias level tracks the device's V_{ce} drop with temperature.

To further improve the stability factor of a common emitter stage a series RLC feedback network can be connected from collector to base (R from collector to ground). The element values are chosen such that the network has low impedance at lower frequencies, ($f < 100$ MHz), and practically open circuited at the device's operating frequency.

A design example

The practical implementation of techniques described above will be illustrated in the design example of a three-stage, 50-ohm amplifier with direct interstage matching (Fig. 6). Distributed circuit elements

Q_c / Q_d	5	10	20	40	80	100
2	1.41	0.78	0.41	0.21	0.11	0.05
3	1.98	1.13	0.61	0.31	0.16	0.08
4	2.48	1.45	0.79	0.41	0.21	0.11
5	2.93	1.75	0.97	0.51	0.26	0.13
6	3.33	2.03	1.14	0.61	0.31	0.16
7	3.70	2.29	1.30	0.70	0.36	0.19
8	4.05	2.53	1.46	0.79	0.41	0.21
9	4.36	2.77	1.61	0.88	0.46	0.24
10	4.66	2.99	1.76	0.97	0.51	0.26

5. Drop in gain, or insertion loss, caused by the shunt capacitor can be quickly determined from this chart.

are used where possible on all stages to insure high circuit consistency since these component values and location are photographically controlled during the circuit board etching process. The amplifier was designed to deliver 15 W into 50 ohms from 800-900 MHz at 12.5 V and 25°C. Specified input power is 25 mW and input VSWR is less than 2.0:1 at band edges.

The input stage is a common emitter amplifier, in this case, a Motorola MRF816. It has approximately 11 dB gain with input power of nominally 25 mW. At this drive level, the transistor exhibits hysteresis in Class "C" operation, but a threshold of approximately 0.50 V applied to the base eliminates this tendency. Measured data also indicates that the threshold voltage increases gain, stability and raises the real part of the input impedance. This impedance increase lowers the total transform ratio from the 50-ohm input to the device impedance, thereby increasing the available bandwidth.

Input impedance matching consists of a two section, low-pass filter, which is adequate to hold a less than 2.0:1 VSWR across the desired bandwidth. The network consists entirely of distributed capacitors and transmission lines printed on the circuit board. Collector voltage and base threshold voltage are supplied to the device by $\lambda/4$ transmission lines also printed on the circuit board. These lines are terminated by rf bypass capacitors to provide a high degree of isolation between the device and its supply

(continued on p. 68)

Transmission line calculations

Occasionally, the designer is left with the task of estimating the physical size of an amplifier or the approximate length of transmission lines in the impedance transforming networks. The following rules of thumb are helpful:

1. The maximum available bandwidth is fixed by the transistor's manufacturer.
2. For an n section network, transform real part levels by a constant multiplication factor.

$$R_n = \lambda^n R_o, \quad \lambda = \left(\frac{R_n}{R_o}\right)^{1/n}$$

Where: λ = multiplication factor = $\dfrac{R_{K+1}}{R_K}$

$$X_{CK} = R_{K+1}\left(\frac{R_K}{R_{K+1} - R_K}\right)^{1/2}$$

$$X_{L\,K-1} = \sqrt{R_K\,(R_{K+1} - R_K)^{1/2}}$$

where: K = 1, 2, 3 . . . n $R_{K+1} > R_K$

Device impedance $Z = R_o + j\,X_{LO}$

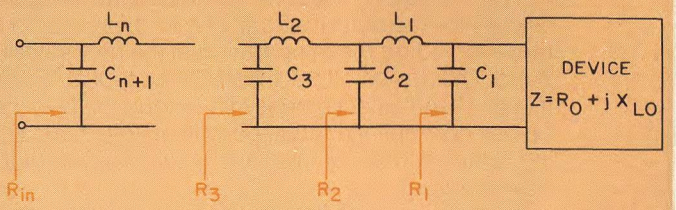

3. For high VSWR on a transmission line terminated with a low impedance and length $\ell < \dfrac{\lambda_g}{4}$:

$$jX_L \simeq j\,Z_o \tan\frac{2\pi\ell}{\lambda_g}$$

$$\ell \simeq \frac{\lambda_g}{2\pi} \tan - 1\,\frac{X_L}{Z_o}$$

For ℓ very short, $\ell \simeq \dfrac{X_L\,\lambda_g}{2\pi\,Z_o}$

Where ℓ has the same dimensions as λ_g (guide wavelength), it should be emphasized that the above are approximations.

line at the operating frequencies. A 1 μF tantalum capacitor provides the necessary low frequency decoupling.

The intermediate stage is also a common emitter amplifier. In this example, the Motorola XRF822 is used, operating at approximately 9.5 dB gain with 2.5 W power output. Direct interstage impedance matching is used to interface the two devices. The matching network is a low-pass filter consisting of printed transmission lines and a shunt capacitor.

Because the input impedance of the intermediate stage is much lower than the output impedance of the first stage, a threshold voltage is also applied to the base of the XRF822. The resulting increase in its input impedance lowers the transform ratio between the devices, increasing available bandwidth. Dc feed and decoupling are identical to the input stage. A selective low frequency network shunts the collector of the XRF822 to damp oscillations at frequencies less than 50 MHz during load mismatches.

The final stage is an XRF835 which has approximately 7.8 dB gain with a 3.5 W input. Direct interstage matching is suggested, used in the form of a bandpass filter consisting of shunt and series ceramic capacitors. This network is very critical and components specified in the parts list must be used to duplicate amplifier performance. Dc return currents of the output device are carried by a printed $\lambda/4$ transmission line terminated by an rf bypass capacitor and through a ferrite bead to ground. This combination isolates the dc return from the circuit at the operating frequencies and provides a lossy load for frequencies below 50 MHz.

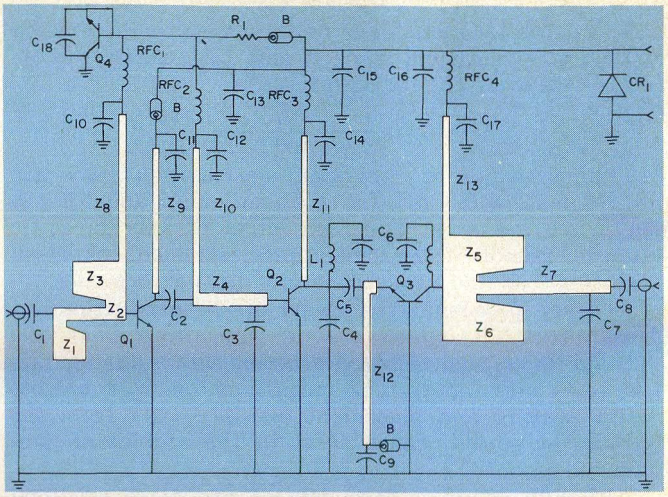

6. This three-stage amplifier boosts a 25 mW input to 15 W.

The output impedance of the amplifier is transformed to the 50-ohm level by a two section low-pass filter. The network is made up of distributed capacitors and transmission lines printed on the board, and one ceramic chip capacitor. A low frequency loading network is also used on the output to stabilize the stage during load mismatch.

The threshold voltages applied to the MRF816 and XRF822 are established by the base-emitter to collector forward voltage drop of a silicon power transistor. The device is attached to the heat sink and temperature tracks the device's base-to-emitter forward voltage drop from less than —50°C to greater

New from Litton: 15 GHz, 1 Watt, Injection Locked Amplifier

The M-1034-01 Injection Locked Amplifier is designed specifically for the output stages of microwave radio transmitters—including those operating in the new satellite band. The device offers 1-watt CW output at 15 GHz. It uses Gunn-Effect diodes in a unique, high-efficiency, power-combining circuit, permitting low diode operating temperatures for increased reliability and high power output.

Look to Litton as the source for your solid-state source requirements. Send today for full information. Electron Tube Division, 960 Industrial Road, San Carlos, California 94070. (415) 591-8411.

M-1034-01 Injection Locked Amplifier: Power output; 1 W, CW ☐ Frequency; 14.40 to 15.25 GHz ☐ Mechanical tuning range; 850 MHz ☐ Locking bandwidth; 50 MHz min (70 MHz typical) ☐ Locking gain; more than 15 dB (17 dB typical) ☐ Waveguide output; WR 62.

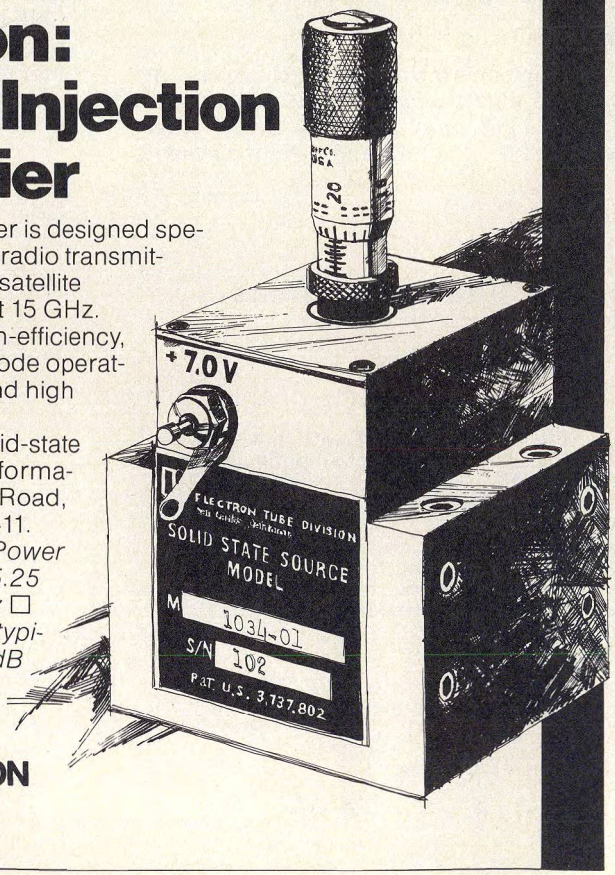

Litton ELECTRON TUBE DIVISION

READER SERVICE NUMBER 69

Parts list

C_1, C_8	56pf ERIE Chip Capacitor
C_2, C_9 – C_{12}, C_{14}, C_{17}	39pf ATC 50 mil Chip Capacitor
C_3	10pf ERIE 100 mil Chip Capacitor
C_4	15pf ATC 100 mil Chip Capacitor
C_5	2 – 12pf ATC Chip Capacitor
C_6, C_{18}	.1μf ERIE Ceramic Capacitor
C_7	2.2pf ATC 100 mil Chip Capacitor
C_{13}, C_{15}, C_{16}	1μf 35V Tantalum Capacitor
Z_1, Z_3, Z_5, Z_6	Distributed Capacitors (See Photomask for Dimensions)
Z_2	45 ohm Microstrip .10" × 1.10"
Z_4	25 ohm Microstrip .20" × 1.00"
Z_7	45 ohm Microstrip .10" × 1.30"
Z_8 – Z_{13}	100 ohm Microstrip .025" × 2.4" (λ/4 @ 870MHz)
RFC_1 – RFC_4	VK200B – 20 – 4B
B	Ferroxcube Bead 56-590-65-3B
L_1, L_2	3T #24 AWG .1" ID
CR_1	Motorola IN5353B 16V Zener Diode
Q_1	Motorola MRF816 Transistor Case 249-01
Q_2	Motorola XRF822 Controlled Q Transistor Case
Q_3	Motorola XRF835 Controlled Q Transistor Case
Q_4	Motorola MJE341 Plastic Encapsulated Transistor Case 77
Board	3M Glass Teflon 2 oz .03125" Dielectric ε_R — 2.55 δ — .002 (Lot 40092-4-EL-1-105, 108)

than +120°C. Forward current through the device is limited to about 120 mA by a 2 W, 100-ohm resistor. Connected as shown, the threshold voltage developed by the MJE341 will never exceed the forward voltage of the MRF816 or the XRF822.

The maximum amount of DC and RF circuitry has been printed on the circuit board specifically to reduce component and assembly costs. The circuit board is double-sided, 2-ounce copper clad glass reinforced teflon. This material was selected for dielectric consistency and low-loss tangent (δ = 0.002). Board thickness is 31.5 mil and was chosen to enable the use of distributed capacitors and still maintain current carrying capability on the higher impedance transmission lines. The bottom side of the board is solid foil and eyelets are used to connect from circuit side ground pads to this ground plane.

The 12.5 V DC and the 0.50V threshold distribution lines are both printed on the circuit board. These distribution lines are connected to the appropriate λ/4 line to each device by Ferroxcube VK200 RF chokes. Further decoupling is provided by 3, 0.1μf ceramic capacitors and 4, 1μf tantalum capacitors placed along the distribution line. This combination of λ/4 transmission lines, RF chokes, and capacitors provides the necessary isolation between devices both at the operating frequencies and at the lower frequencies where parasitic oscillations are likely to occur. ••

References

1) Octavius Pitzalis, Jr. and Russell A. Gibson, "Broadband Microwave Class-C Transistor Amplifier," IEEE Transactions on Microwave Theory and Technique, VOL-MTT-21, No: 11, (November, 1973).

2) George L. Matthaei, "Tables of Chebyshev Impedance-transforming Networks of Low-pass Filter Form," Proceedings of the IRE, VOL 52, p. 939 (August, 1964).

3) R. M. Faro, "Theoretical Limitations on the Broadband Matching of Arbitrary Impedances," Journal Franklin Inst., VOL 249, pp. 57 and 139.

4) John G. Tatum, "VHF/UHF Power Transistor Amplifier Design," Application Note AN-1-1, ITT Semiconductors.

5) Julius Lange, "A Survey of the Present State of Microwave Transistor Modeling and Simulation as Applied to Circuit Design," IEEE Transactions on Electron Devices, VOL. ED 18, No. 12, (December, 1971).

6) Julius Lange and William N. Carr, "An Application of Device Modeling to Microwave Transistors," IEEE Journal of Solid State Circuits, VOL. SC-7, No. 1, (February, 1972).

7) Stacy V. Bearse, "The Year of Giant Growth Arrives For Land-Mobile Communications," *MicroWaves,* Vol. 13, No. 1, pp. 38-47, (January, 1974).

ENGELMANN MAKES IT!

ULTRA-MINIATURE COUPLERS FEATURE 0.375" THICKNESS

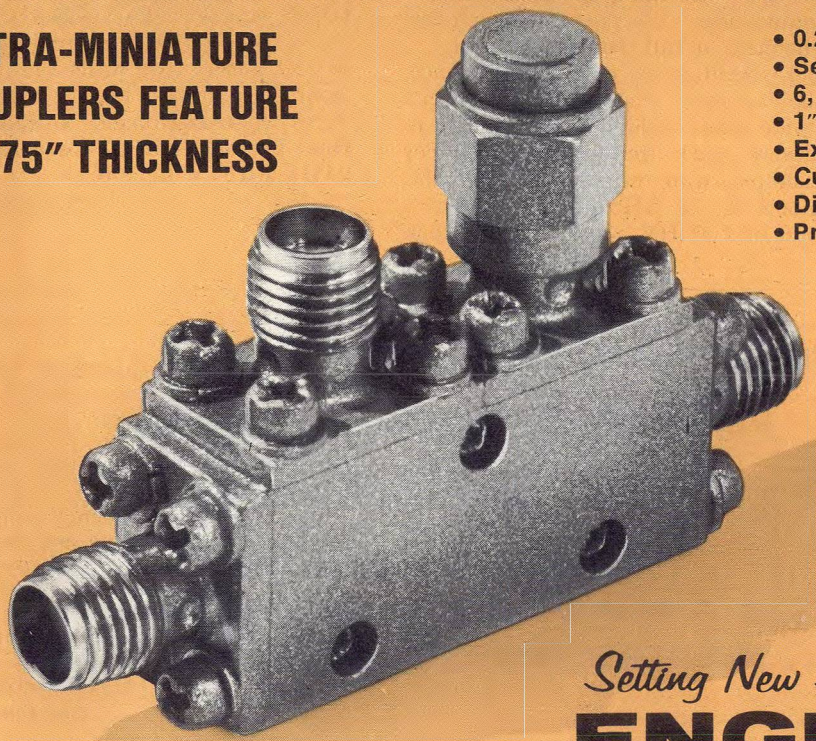

- 0.2-18 GHz in Octave + B.W.
- Sealed Stripline Construction
- 6, 10, 20, 30 db standard values
- 1" x 0.5" x 0.375", 4 GHz & UP
- Exceeds requirements of MIL-C-15370C
- Custom coupling values available
- Directivity typically > 20 db
- Price $110 ea.

For detailed literature or custom design information, contact **ENGELMANN** Microwave Co., Skyline Drive, Montville, N.J. 07045, (201) 334-5700.

Setting New Standards in Reliability

ENGELMANN

Engelmann Microwave Co. — Subsidiary of Pyrofilm Corporation

READER SERVICE NUMBER 70

$6200 frequency counter extends automatic measurements to 24 GHz

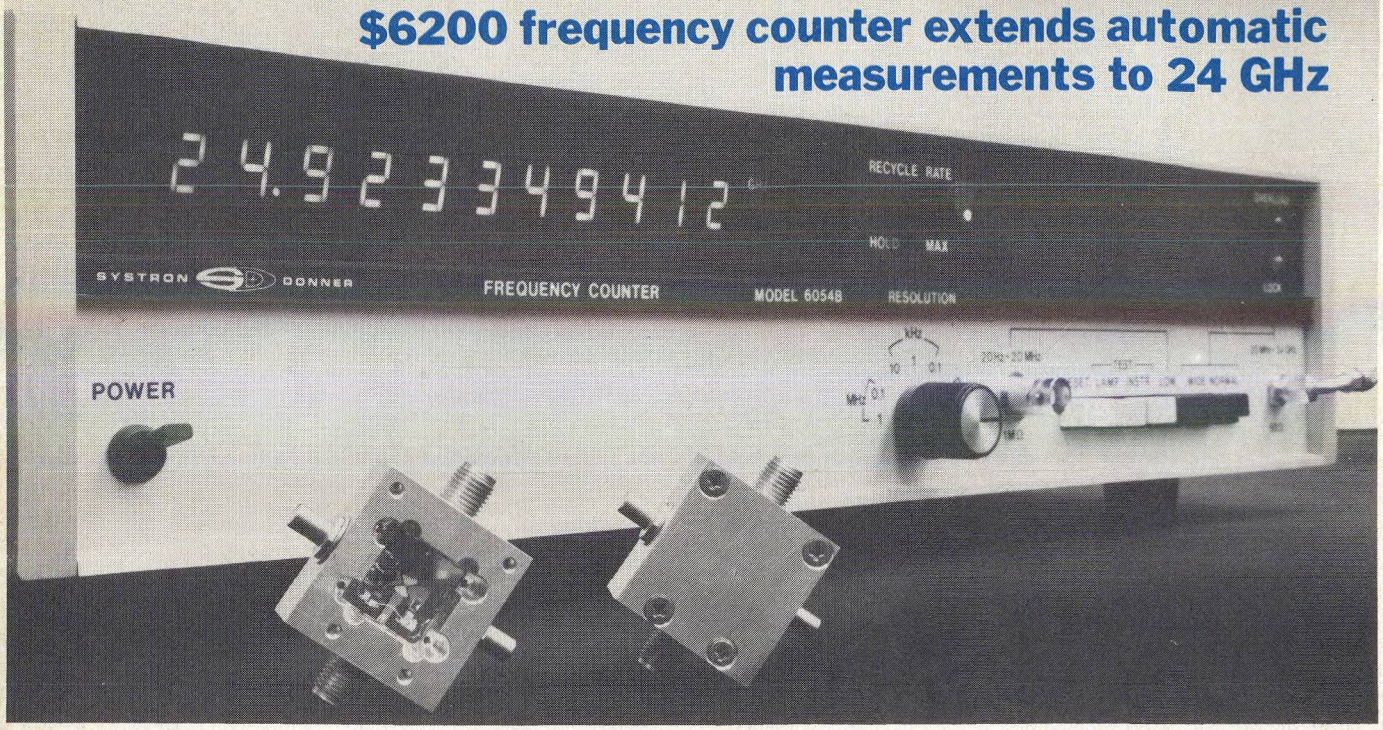

This frequency counter, model 6054B, measures inputs from 20 Hz through 24 GHz, and displays the proper frequency on an 11-digit LED readout. A single type-N connector accepts inputs from 20 MHz to 24 GHz, while lower frequency signals can be fed to a BNC port. The counter exhibits state-of-the-art sensitivity across its entire frequency range, and includes a special "wide mode" for broadband frequency tracking.

Developments in sampling mixer circuitry give this counter high sensitivity without sacrificing dynamic range. Sensitivity of the new instrument is rated at −30 dBm from 20 MHz to 10 GHz, −25 dBm from 10 GHz to 18 GHz and −20 dBm from 18 GHz to the 24 GHz maximum. However, even with this degree of sensitivity, the manufacturer guarantees operation at levels of up to +30 dBm (1 watt) for a dynamic range of greater than 50 dB anywhere in the frequency band.

Two indicators mounted on the counter's front panel, quickly show whether an input is within the instrument's dynamic range. A green LED turns on when an input of adequate strength is fed to the counter. If the input exceeds +20 dBm (100 mW), a red LED activates to warn of a potential overload.

Model 6054B relies on a frequency-lock technique as opposed to a phase-lock method, thus, according to the manufacturer, it tolerates 10 MHz peak-to-peak frequency modulation at any rate up to 10 MHz. For example, the counter is capable of measuring a −20 dBm, 6.5 GHz telecommunications carrier with 1,200 channels of full data under voice.

In addition to good fm tolerance, the counter incorporates a special "wide mode" which forces the LO to closely track the input signal. For example, with the instrument in this mode, an 18 GHz input, swept at a rate of 100 Hz, could vary as much as 3000 MHz and remain in lock.

It should be noted that the 6054B produces a very low level of output noise, an important parameter often neglected on most instrument spec sheets. Since the counter itself produces a noise level of less than −65 dBm, many measurements involving receivers and other noise-sensitive equipment can be made without isolators.

Normally, the counter provides 1 Hz resolution, with a sampling speed of one second across the entire band to 24 GHz. Faster sampling speeds can be obtained by selecting another resolution setting (up to 1 MHz). The 6054B weighs 30 lbs, measures 3.5 × 16.76 × 17.5 inches, requires 115 or 230 Vac @ 106 watts and is rated from 0 to 50°C. P&A: $6,200; 60 days. **Systron-Donner Corporation, One Systron Drive, Concord, CA 94518 (415) 676-5000.**

CIRCLE NO. 103

TEST INSTRUMENTS

CATV sweeper covers 35 channels

Thirty-five channel CATV sweeper, model 1402A, covers 1 to 400 MHz and includes a 36 position programming switch. The switch presets the center frequency of the instrument to i-f (43.0 MHz), broadcast channels 2 to 13 and lettered channels A to W. In addition, crystal-controlled, pulse-type markers are included at the picture and sound carriers of each and every channel. Attenuation is 55 dB. Optional features include: five extra i-f markers for processor and modulator i-f alignment and local oscillator tracking markers allowing a double conversion CATV converter to be completely aligned with no auxiliary equipment. The unit may also be programmed to sweep any or all of its 1 to 400 MHz frequency range for the other CATV testing and measurement. Flatness is ±0.1 dB over any of the 35 channels and better than ±0.25 dB over its entire range. P&A: $1,395; 3 to 4 wks. **Wavetek Indiana, Inc., 66 North First Avenue, Beech Grove, IN 46107 (317) 783-3221.**

CIRCLE NO. 104

MARCH
1976

MICROWAVES

laser technology

Millimeter-Wave Technology:

Designers ponder options for transmission media

Dielectric waveguide: A low-cost option for ICs

GaAs or Si: What makes a better mixer diode?

Also: Microwaves probe for cancer cells

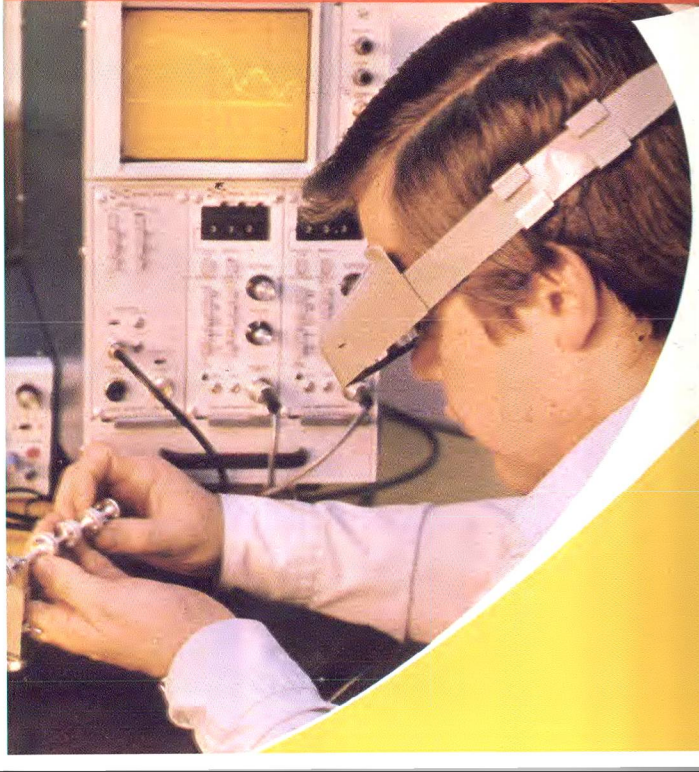

Synthesizer purity and am/fm combined in 2-18 GHz generator

MICROWAVES
March 1976
Vol. 15, No. 3

news

9 GaAs FET and Impatt Amplifiers Deliver Watts of Power
Researchers Say Parametric Effect Upsets Class A Transistor Amplifiers
10 Microwaves Probe For Cancer Cells
14 Increases In Defense Spending Characterize Ford's Budget
17 R & D
19 Washington
22 International
24 Meetings
26 Industry
28 For Your Personal Interest . . .

editorial

30 Think Metric!

technical section

Millimeter-waves
32 **Controversy Brews Over Transmission Media.** Industry leaders explain the trade-offs between microstrip and dielectric waveguide, the two most promising candidates for tomorrow's millimeter-wave ICs, from the aspects of economy and performance.
46 **GaAs or Si: What Makes A Better Mixer Diode?** F. Bernues, P. A. Crandell and H. J. Kuno of Hughes Aircraft point out that mobility is not the only factor to consider when choosing a material for millimeter-wave mixer diodes.
56 **Dielectric Waveguide: A Low-Cost Option For ICs.** Robert M. Knox of Epsilon Lambda investigates a promising new transmission media for future millimeter-wave integrated circuits.

products and departments

68 **Cover Feature:** Synthesizer Purity and AM/FM Combined in 2-18 GHz generator.
70 **Product Feature:** Millimeter Thermistor Mounts Don't Shift.
72 New Products
81 Application Notes
82 New Literature
83 Advertisers' Index
84 Product Index

About the cover: The test setup at the top of this month's cover is a 50-75 GHz network analyzer/reflectometer test unit developed by TRW. It offers continuous measurement of a 10 GHz band with a single sweep. Just below is a skilled machinist at Baytron making precision parts for millimeter-wave components. The test instrument sharing the cover is Hewlett-Packard's latest synthesized signal generator, see page 68.

coming next month: Electronic Warfare

Keep Track Of That Low Flying Attack. Peter Dax of Westinghouse describes the challenges facing designers of shipborne tracking radar. Off bore-sight and double-null tracking techniques applied to monopulse conical scan antennas are investigated as solutions to the problems of specular reflections.

Guided Missiles For Air Defense. Alex Ivanov of Raytheon explores the role of microwave technology in three types of missile guidance systems. The homing missile guidance technique which relies on a tracking radar for target illumination, is examined in detail.

Design A Ka-Band Polar Frequency Discriminator. David Saul of the Naval Electronics Laboratory Center details a new design approach for 26.5 to 40 GHz polar frequency discriminators. All coupled-line components, which are exceptionally difficult to build at Ka-band frequencies, have been eliminated.

Publisher/Editor
Howard Bierman

Managing Editor
Richard T. Davis

Associate Editor
Stacy V. Bearse

Contributing Editor
Harvey J. Hindin

Washington Editor
Paul Harris
Snyder Associates
1050 Potomac St., NW
Washington, DC 20007
(202) 965-3700

Editorial Assistant
Gail Murphy

Production Editor
Sherry Lynne Karpen

Art
Robert Meehan, Dir.

Production
Dollie S. Viebig, Mgr.
Dan Coakley

Circulation
Trish Edelmann, Mgr.
Sherry Karpen,
Reader Service

Promotion Production Manager
Albert B. Stempel

Directory Coordinator
Janice Tapp

Editorial Office
50 Essex St.,
Rochelle Park, N.J. 07662
Phone (201) 843-0550
TWX 710-990-5071

A Hayden Publication
James S. Mulholland, Jr., President

MICROWAVES is sent free to individuals actively engaged in microwave work. Subscription prices for non-qualified copies:

	1 Yr.	2 Yr.	3 Yr.	Single Copy
U.S.	$15	$25	$35	$2.50
FOREIGN	$20	$35	$50	$2.50

Additional Product Data Directory reference issue, $10.00 each (U.S.), $18.00 (Foreign). POSTMASTER, please send Form 3579 to Fulfillment Manager, MicroWaves, P.O. Box 13801, Philadelphia, PA. 19101.

Back Issues of MicroWaves are available on microfilm, microfiche, 16mm or 35mm roll film. They can be ordered from Xerox University Microfilms, 300 North Zeeb Road, Ann Arbor, MI 48106. For immediate information, call (313) 761-4700.

Hayden Publishing Co., Inc., James S. Mulholland, President, printed at Brown Printing Co., Inc., Waseca, MN.
Copyright © 1976 Hayden Publishing Co., Inc., all rights reserved.

Millimeter-Waves:

Controversy Brews Over Transmission Media

Richard T. Davis Managing Editor

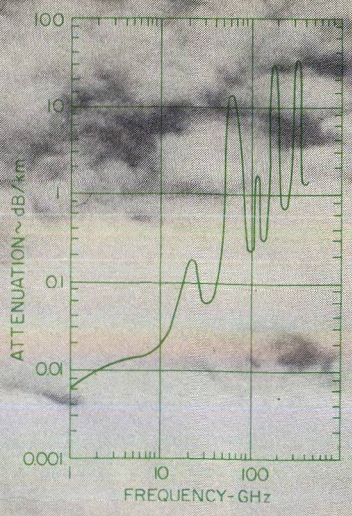

SIT down with three or four millimeter-wave experts over coffee someday, and you'll find the conversation could go something like this:

"Dielectric waveguide has merit for many systems applications in the millimeter wavelengths. While its most attractive feature, the promise of low cost in volume production, has yet to be demonstrated in a specific system application, the accomplishments of early development efforts provides a basis for pursuing additional component development."

"But the government has already dumped lots of money into dielectric waveguide without great success. It has limited bandwidth and radiation problems that has led a large segment of the technical community to question its advantages for cost-effective millimeter-wave systems."

"Photolithographic integrated circuits are probably a more viable and cost-effective approach to circuit integration. And remember, standard waveguide technology can't be discounted for many millimeter wave system applications. In fact, I doubt if any of the millimeter IC methods will ever achieve performance truly comparable to that available through conventional waveguide."

"Oh sure, microstrip has been built at millimeter wavelengths, but it's an extremely difficult design and fabrication process. Because dimensions are so small and tolerances must be within a fraction of a mil, photolithographic ICs just don't lend themselves to low-cost, high-volume methods."

"Wait a minute. For low-cost and relatively unsophisticated millimeter systems in quantities, dielectric waveguide may be the way to go. Frankly, I see a need for all these techniques, and I doubt if any of them will ever become dominant."

Although the above conversation is contrived, it represents a concensus of divergent viewpoints from a number of industry experts recently interviewed by *MicroWaves*. It points up a growing controversy over millimeter-wave transmission media. Unfortunately, the tradeoffs are not as clear cut as our coffee-break characters would lead us to believe, as will be shown later in this report.

Because of the growing interest in the millimeter-wave spectrum brought on by new spectrum needs, there is a resurgency of development in millimeter-wave technology. In particular, it is the military's potential needs for millimeter-wave weapons systems that really have millimeter-wave researchers scrambling to come up with some cost-effective designs. (See, "Spectrum Needs Spur mm Developments.")

Dielectric waveguide vs. microstrip

Presently, there are two rather diverse types of integrated circuits that are competing as "low-cost" millimeter-wave systems—printed circuits and dielectric waveguide.

The accompanying section entitled, "Transmission Media—What's Suitable at mm Wavelengths" on p. 36, provides a brief description of those transmission line techniques that look most promising for millimeter wavelengths. According to Ashok Gorwara, project supervisor at Stanford Research Institute (SRI), the use of a particular planar transmission media depends on the particular application and performance required. "In many millimeter-wave component or subsystem designs, it may even be useful to use different types of transmission media to achieve optimum performance."

Martin Schneider, a supervisor in the Radio Research Department of Bell Telephone Laboratories, Holmdel, NJ, pioneered the technique of using hybrid-transmission media. He, with other BTL researchers, developed components at 30, 60 and 90 GHz using combinations of microstrip, suspended stripline and slotline on a single substrate to achieve optimum performance.[1]

Dielectric waveguide is the newer and less proven technology. It represents an extension of optical techniques to the millimeter bands. Image and insular line, basically consist of solid dielectric waveguide mounted on an image plane. Propagation is confined by refraction within the dielectric. (See, "Dielectric Waveguide: A Low-Cost Option For ICs", p. 56, this issue). Materials such as silicon, gallium arsenide and alumina are being used as the dielectric media. One of the principal advantages of dielectric waveguide is that active components can be directly implanted into the dielectric without mechanical supports to disturb the fields.

Ultimately, it is hoped that monolithic designs may be possible. The objective would be to use ion implantation on single crystal substrates to form active devices (such as transistors or diodes) along with various passive components, forming a complete circuit, on the same substrate. Depending on whom you talk to, there are a variety of answers to the question of how high

(continued on p. 34)

in frequency these circuits can effectively operate.

John Cotton, TRG division manager of Alpha Industries, Woburn, MA, feels microstrip is viable to 40 GHz or higher, depending on the losses one can sustain. "Gold-on-sapphire looks most attractive," claims Cotton.

"We are presently putting most of our millimeter-wave R&D money into developing GaAs beam-lead diodes for use on these substrates. So we do see a future for printed circuit techniques in the millimeter bands." Gorwara of SRI claims "microstrip circuits, using low dielectric constant media, can go as high as 60 or 80 GHz if you can stand the losses." The Naval Electronics Lab, San Diego, has proven this up to 60 GHz in passive component designs using teflon fiberglass."

Barry Spielman, head millimeter wave techniques section at the Naval Research Labs (NRL), Washington, DC, also thinks millimeter ICs are feasible to at least 60 GHz. "We are investigating millimeter-integrated circuits in the 40 to 60 GHz range during the current year and are quantitatively addressing aspects of basic propagation and loss phenomena," says Spielman. "There are special problems in pushing up into these millimeter bands including tolerances and discontinuities, dissipative and radiation losses and higher order moding phenomena. We have developed several computer-aided methods to account for these problems in designing these frequencies."

Right now, NRL is developing single-channel preselector, mixers and LOs, using microstrip-type transmission lines, operating the 40 to 60 GHz bands. We hope to have a prototype downconverter finished by October of this year."

Design problems exist

Speilman sees photolithographic integrated circuits as a more viable and cost effective approach than the dielectric waveguide for developing millimeter-wave systems.

"An aggregate of over a million dollars from both the Army and Navy has been put into dielectric waveguide programs. The activity has gone on now for about 4 years and has not produced a broad scope of capabilities. Before the dielectric waveguide approach can be expected to meet complicated systems' requirements, the technology must be more fully developed," claims Spielman.

Why isn't NRL aggressively pursuing dielectric waveguide? Two dielectric waveguide programs for Navy agencies were conducted during 1973 and 1974. The first for the Naval Air Systems Command and Air Development Center was a J-band (10-20 GHz) integrated receiver with a 2-4 GHz i-f.

"This program was reasonably successful but used conventional waveguide for the balanced mixer and local oscillator. Dielectric waveguide was used only for the hybrids employed," says Spielman. The subsequent program for the Naval Electronics Systems Command called for an integrated six-channel surveillance receiver covering 18-42 GHz with each channel 4 GHz wide. The receiver was to consist of six mixers with image rejection filters and three LOs on a single planar

(continued on p. 36)

Spectrum Needs Spur mm Developments

After several false starts, millimeter-wave technology in the U. S. is on the move again. Today, there is both commercial and military incentives to develop the millimeter-wave spectrum, generally considered to cover 30-300 GHz. One reason is the crowded spectrum conditions in the microwave bands. In the commercial sector, Bell Labs, for example, is developing millimeter-wave trunks for tomorrow's long-distance phone lines. But it is the military's potential needs and the possible funding behind them that are stirring the most interest.

One major military application is in military mapping, such as in satellites for reconaissance and in missiles for terminal guidance. Being entirely passive, the millimeter radiometer is not easily jammed—a major asset for any weapons system.

The Army is interested in compact and rugged cold-seeking radiometers, which can be put into artillery shells and which would home in on large cold targets. Such targets as tanks or trucks could then be differentiated from the warmer background vegetation and selectively destroyed.

Because of the small diameter of the artillery shell, the receiving antenna woud be limited in size. To achieve the necessary gain, the window at 94 GHz looks attractive for this particular Army application.

Millimeter-wave target designators are also being considered for roles where laser designators are presently being used. Their ability to penetrate fog is a distinct advantage for a standoff-weapons system. High resolution radars at 35, 70 and 94 GHz where atmospheric windows exist, is also being eyed for low-on-the-horizon tracking radars and airborne terrain avoidance radars.

For covert communications, millimeter line-of-sight radios have already been developed as shown. At 60 GHz where an attenuation peak occurs, secure short-range communications can be achieved but without concern over enemy eavesdropping. The Navy is particularly interested in this for ship-to-ship communication and the Army for short-range battle field communications.

The wavelength at 60 GHz is also being looked at for satellite-to-satellite communications. Because there is no attenuation in space, range is not limited as on earth. But being in orbit, these satellite links are secure from earth listeners and can't be jammed from earth because of the high attenuation of the atmosphere.

Millimeter-wave radiometers are under development for the terminal guidance of strategic cruise missiles. This 21 ft long cruise missile is built by General Dynamics, San Diego, CA, for the Navy. The strategic version is powered by a turbo-fan engine and carries a nuclear warhead. Its status under the strategic arms limitation treaty is an issue between the U. S. and Russia.

Spread-spectrum communications, such as those used to provide a secure air-to-ground data link, is still another application area. Its enormous appetite for bandwidth leaves little alternative but to use the frequencies available in the millimeter spectrum.

Is there millimeter-wave ECM? Not yet . . . according to one industry source but the U. S. is doing a lot of listening. As a result there is a considerable amount of millimeter-wave receiver design under way in the U. S. ●●

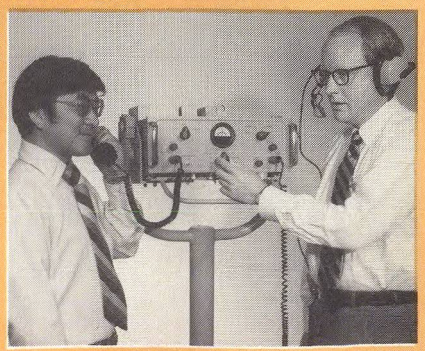

K-band communications set was developed by Hughes for line-of-sight data and voice communications.

Transmission Media—What's Suitable At MM Wavelengths?

At microwave frequencies, MIC technology is widely used for low-cost, compact modules. In particular, stripline and microstrip have been found quite successful. Figure 1 shows some of the more common transmission media for microwave and millimeter wave-lengths as shown divided in non-TEM and TEM and quasi-TEM lines. There are several other types of transmission lines still in R&D, such as microguide,[5] which looks like microstrip, but is wider and propagates a waveguide mode.

The lowest-loss transmission lines are dielectric wavguide, conventional metal waveguide and dielectric-filled waveguide. Unfortunately, none of them can be considered planar, a distinct disadvantage over those that may be processed in volume using photolithographic techniques. Conductor loss of more convenient microstrip is about 0.2 dB/wavelength.[3,4]

For ease of fabrication and compatibility with semiconductor devices, those transmission lines that are particularly promising at millimeter wavelengths are:

- Coplanar waveguide
- Slotline
- Fin line
- Image line
- Microstrip
- Suspended stripline

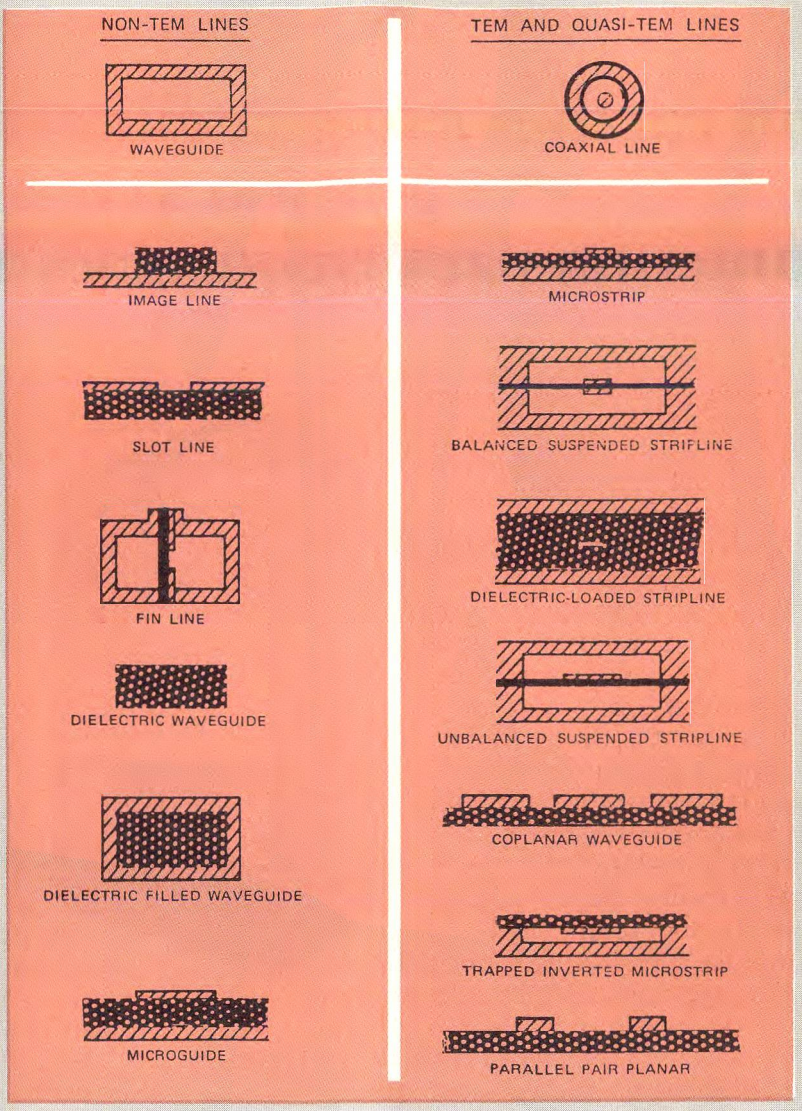

A. Various microwave transmission media are listed by mode and according to their proficiency to operate at millimeter wavelengths.

Coplanar line eases shunt conections

A coplanar transmission line consists of a strip of thin-metallic film deposited on the surface of a dielectric substrate with two ground electrodes running adjacent and parallel to it on the same surface.[6] The rf energy is confined to a closed area and the conducting elements permit easy connection of active devices in hybrid integrated circuits. It is ideal for shunt connection elements in monolithic MIC systems. Coplanar line has the advantage of having all the conducting elements on the same side of a dielectric substrate; standard MIC photolithographic and etching techniques are applicable. Coplanar line, enclosed in a channel, has been successfully used at frequencies to 60 GHz.

Slotline allows easy coupling

Slot transmission line was introduced by S. D. Cohn in 1968 as an alternative transmission line for microminiature componets.[7] It is particularly useful for applications requiring regions of circularly polarized magnetic field and/or shunt-mounted elements. Slotline consists of two conductors separated by a gap on one side of a dielectric substrate. Combined microstrip and slotline circuitry seem to offer possibilities with the advantage of easy coupling through the substrate from one medium to the other.

Slotline is well understood and can be fabricated using standard MIC photolithographic and etching techniques. Such transmission line techniques, enclosed in a channel, have been successfully used for the design of tapered transformers to 60 GHz.

Fin line broadens bandwidth

When slotline is used in a channel—that is, when the slotline substrate bridges the broad walls of a rectangular waveguide—it is sometimes called fin line.[8] In effect, the line is a printed ridged waveguide and can be designed to have a wider useful bandwidth than conventional line can provide bandwidths in exridged waveguide.[9,10] Integrated fin cess of an octave with less attenuation than microstrip.[10,11] This adaptation of ridged-loaded waveguide permits circuit elements to be fabricated at low cost and is compatible with thin-film hybrid techniques.

In passive circuits, such as filters, the fins may be directly grounded to the waveguide, and lumped elements, such as beam-lead capacitors, may be added. The gap between the fins can be varied along the longitudinal

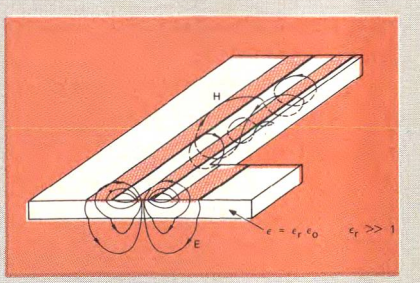

B. In coplanar line, axial and transverse H-field components exist.

Ashok K. Gorwara, Project Supervisor, Stanford Research Institute, 333 Ravenswood Avenue, Menlo Park, CA 94025.

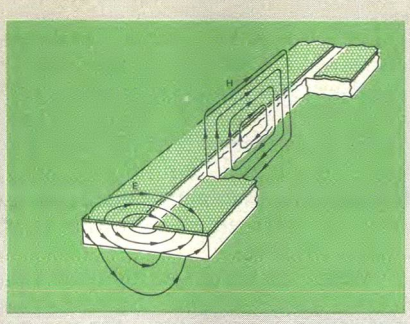

C. **A slotline supports a dominant TE mode** which resembles the dominant mode of rectangular waveguide and provides natural regions of circularly polarized magnetic fields.

axis to provide low-cost circuit elements. When semiconductor devices are to be added, at least one of the fins must be dc isolated from ground to permit the application of bias.[33] In both approaches, the waveguide is parted along a plane where the current flow is parallel to the break, as in a common slotted line.

During the past few years, fin line components have been fabricated successfully up to 40 GHz, and existing beam-lead devices in a simple fin-line mount may be useful beyond 80 GHz.[8] However, it is expected that mechanical tolerance of the assembly may become important much above 60 GHz.

Image-line, active IC construction

Low-loss propagation at millimeter wave, submillimeter wave and even optical frequencies is theoretically realizable using refractive dielectric guides and image guides.[12-16] In theory, image guide is suitable for active integrated-circuit construction because the image plane can provide mechanical support to the dielectric material and also serve as heat sink and electrical ground to the integrated active devices. However, there are many practical fabrication and process problems that some researchers are trying to resolve at this point. In addition, metallic shielding around the image-guide is often necessary to reduce any radiation losses and eliminate any external electromagnetic interference.

Although rectangular dielectric guide has been applied at optical frequencies using low-dielectric constant materials,[17-26] only recently has this type of guide been used at millimeter-wave frequencies using high-dielectric constant materials.[27,28,29]* The potential of rectangular dielectric guide millimeter-wave integrated circuits has been greatly enhanced with the recent demonstration by Chrepta and Jacobs[27,29] using high-resistivity semiconductors such as silicon and GaAs as dielectric material.

Microstrip line the popular media

Standard microstrip is one media where considerable effort had been directed towards exploiting the advantages of MIC technology to higher frequencies. Impatt oscillators have been developed at 30 GHz, 60 GHz and 100 GHz using quartz substrates at Bell Laboratories.[1] Similarly, microstrip techniques have been applied to design 18-26 GHz balanced and image-rejection mixers and 18-26 GHz and 26-40 GHz polar discriminators using 0.010-inch thick sapphire substrates.[30,31] Also, several researchers have used MIC techniques to fabricate broadband components up to 60 GHz using low dielectric substrates with dielectric constant of $\epsilon \approx 2.5$.[32]

There are several difficulties that arise in extending microstrip over 60 GHz for low-loss circuits. These include critical tolerances, fragile substrates and radiation losses. The radiation losses can be eliminated by properly spacing the microstrip circuit in a channel. Some researchers have demonstrated the use of microstrip techniques up to a frequency of 100 GHz using fused silicon as the base substrate.[1] The mechanical problems can be overcome with careful design techniques.

Suspended stripline, useful to 60 GHz

Suspended stripline is essentially the same as conventional stripline. However, the transmission line is inhomogeneous because of the presence of the dielectric. As a result, high-order modes can propagate. Also, the presence of any discontinuity can cause radiation losses and higher-order modes. These can be suppressed if the suspended stripline is enclosed in a rectangular guide. The dimension tolerances and surface finish on the metallic surroundings are not critical, as compared to a standard waveguide transmission line. Such transmission line techniques enclosed in a channel have successfully been used up to 60 GHz.

Shielding important for all

Regardless of the type of planar transmission media chosen, it appears that all the millimeter circuits require metallic shielding in order to control higher-order modes, reduce radiation losses and eliminate external electromagnetic radiation interference. Generally, mode control becomes critical at higher frequencies and for broad bandwidth circuits.

In the selection of a particular transmission line, the following characteristics should be considered:

- Maximum achievable bandwidth
- Low loss or high unloaded Q
- Low-cost processing and fabrication techniques
- Ease in bonding or attaching active componets
- Radiation losses
- Susceptibility to external electromagnetic interference. ••

*Additional information and references on image-line are found on p. 42.

package. It was also to occupy a space of 44 cu. in (723 cm³)

"The required specifications proved too tough for this new technology and the program did not meets its goals. Only a single mixer/filter channel was finally developed," says Spielman. "Program dollars got chewed up developing standard waveguide parts not related to the dielectric waveguide technology. As a result of this program, the Navy is taking a more cautious wait-and-see attitude regarding dielectric waveguide technology.

That isn't to say that there have not been problems associated with the printed circuit designs. Stripline and microstrip designs are also struggling as they get into higher millimeter bands. This is to be expected, however, since both technologies are still in fairly early stages of development.

In a recent project for ECOM for example, an 18-40 GHz six-channel receiver was developed by Microwave Associates in Burlington, MA, using air and teflon dielectric stripline and teflon-fiberglass microstrip in the millimeter-wave circuitry.[2] According to Dr. Charles Buntschuh, senior scientist in MA's R&D Group, "There were problems in the Wilkinson power splitters so that interactions between the following diplexing filters were troublesome." Also, mixer insertion loss tended to be quite high. "This wasn't a serious problem, just a tedious nuisance," explained Buntschuh.

Army pursues dielectric approach

At the present time, one of the strongest supporters for dielectric waveguide is Dr. Harold Jacobs head of ECOM's Electronics Technology and Device Laboratories at Fort Monmouth, NJ. According to Jacobs, "dielectric waveguides potentially offer great cost reductions for millimeter-wave components and circuitry due to the simplicity of machining waveguide from the outside and batch-fabrication techniques.

"We still have an open mind over the various approaches to millimeter-wave integrated circuits. But we have had some of our most successful results in the dielectric waveguide area."

Comparing the three approaches waveguide, stripline and dielectric waveguide, Jacobs sees waveguide technology as offering certain advantages such as being almost immediately available and having high

(continued on p. 38)

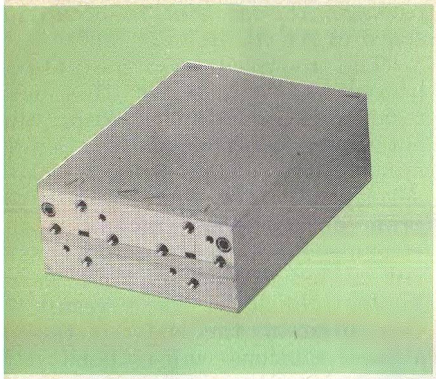

1. **Model 4394, dielectric waveguide double balanced mixer** operates at 94 GHz. The two waveguide parts are for the rf and LO. It is built by Epsilon Lambda and price is $5800.

Q and low-loss properties. However, its cost in the past has been prohibitively high.

Suspended stripline appears attractive in the future and is being investigated for use as millimeter-wave ICs because of its wide bandwidth and potentially low cost. "However, as frequencies go higher, say above 30 GHz, the conductor losses in stripline or the other planar technologies may become excessively high," cautions Jacobs.

"Dielectric waveguides," he claims, "offer very great potential in obtaining low loss as well as meeting simpler, and lower-cost construction goals. The approach, however, is still in a research and development phase and considerable expenditures will be required before each circuitry becomes more generally available for use."

Dielectric waveguide mixers for sale

According to Robert Knox, President of Epsilon-Lambda, the concept of planar integrated circuits using high permitivity dielectric waveguide was originally developed at IIT Research Institute (IITRI) in 1969, simulated by related activities in integrated optics and in surface acoustic wave technology. "I realize dielectric waveguide is a controversial subject," explains Knox. "Some claim it doesn't work and only looks good on paper. The fact is, however, it does work. The particular approach we're taking, that of insular-line-integrated-circuits, using inexpensive alumina dielectric as the waveguide medium, lends itself to low cost from both a materials and fabrication point of view."

Epsilon-Lambda sells the only dielectric waveguide component available today, a 94 GHz balanced mixer/preamp, Fig. 1. Its price is $5,800 in unit quantities.

"The price is comparable to metal waveguide devices for this frequency," notes Knox. "But I see the potential for lower costs and think that in quantities of about 300, a price of $1,875 is realistic. The mixer diodes are at present a principal cost factor, however. Fabrication of the ceramic parts while not trivial, allows cost reductions for large volume production."

"We're planning to go into production with this mixer in the next few months and to sell 'insular-line' balanced mixers/preamps at 35 and 60 GHz as well. Unit prices should be around $3,900 and $5,100, respectively."

"I don't know of any integrated circuit components that are presently being sold commercially above 18 GHz," observes Knox, "although I do expect to eventually see certain components offered for operation to 40 GHz."

"Many people tend to draw a line at 18 GHz, where microstrip or stripline techniques work," he continues. "Since there are no fundamental frequency limits, efforts continue to extend printed circuit designs higher into the millimeter region. While they work in a fashion, they require specialized techniques, which make them less cost effective."

Dr. H. John Kuno, manager, Microwave Circuits Department at Hughes Electron Dynamics Division, Torrance, CA, also acknowledges that microstrip circuits have been built at millimeter wavelengths but also considers it an extremely difficult design and fabrication process.

"With our image-guide technique, active devices can be combined right into the dielectric guide, (Fig. 2.). The image plane serves as a heat sink and mechanical support as well as a ground plane," Kuno notes. Biasing is achieved by connecting a printed circuit lead, like microstrip, on top of the dielectric without affecting the fields in the waveguide.

According to Kuno, Hughes is using single crystal silicon for their dielectric waveguide because "it is a well known semiconductor material, can be chemically processed easily, and by selecting the proper crystal orientation one can make use of preferential etching techniques."

"It will eventually allow us to go to monolithic integrated circuits," claims Kuno, "but this is still several years away. We are not working on monolithic designs right now, because there are some tremendously complex processing steps involved, and we don't feel this is the right time or place to spend R&D money."

(continued on p. 40)

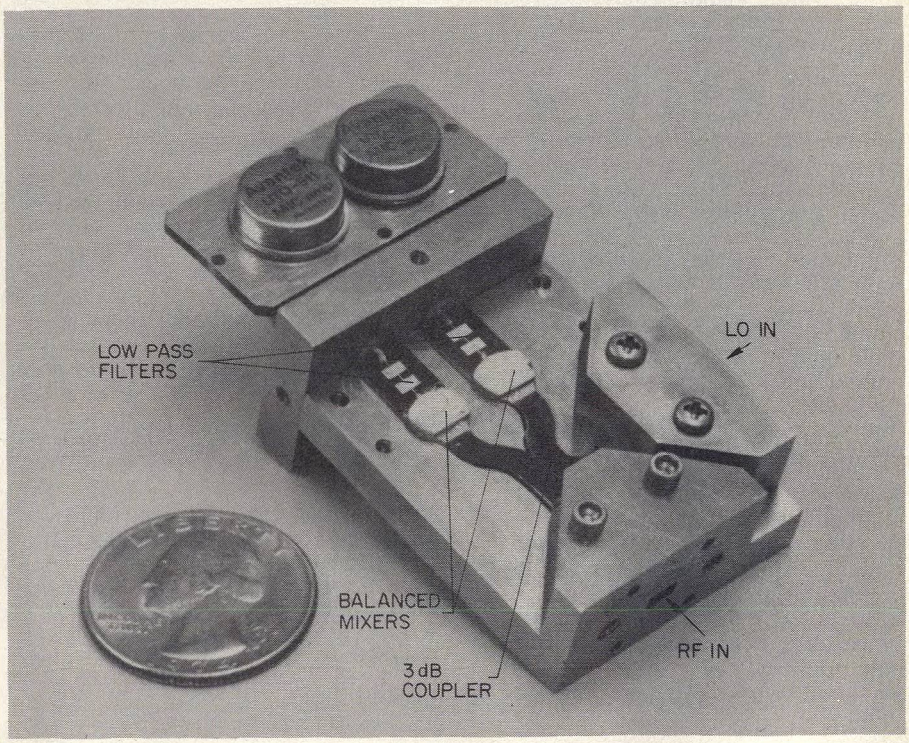

2. Balanced mixer in silicon image-guide developed by Hughes uses two Schottky barrier mixer diodes imbedded in silicon dielectic. Transitions are for the LO and rf inputs. The Avantek thin-film amps are used as i-f amps.

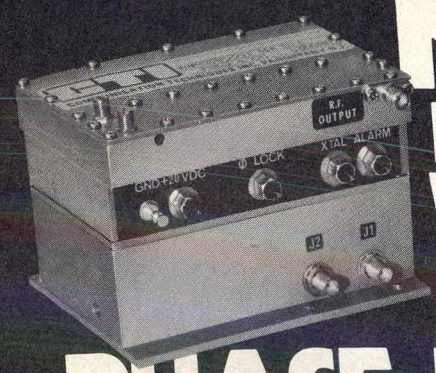

NOW! Lowest Noise & Widest Bandwidth in MODULATABLE PHASE-LOCKED SOURCES

CTI's new all-solid-state modulatable phase-locked sources are ideal for color-video, service/message-channel and digital-data transmission, and many other broadband microwave relay applications.

SERIES FMPL *(shown)* employs state-of-the-art, proprietary digital phase-lock circuitry that results in extremely low close-in noise. Typical specs: modulation BW, 100Hz-12MHz; peak deviation to 1MHz (6MHz optionally); stability, 5PPM. Available in all communication bands to 18GHz. Special features: exceptionally high modulation linearity (high NPR performance); easily field-changeable crystals: simplified mechanical retuning; adjustable modulation level; phase-lock alarm.

SERIES FMPX provides modulation BW of DC to 60kHz, with many of the same features.

Call or write for the complete data file on CTI phase-locked sources.

COMMUNICATION TECHNIQUES INC.
1279 Route 46, Parsippany, N.J. 07054, CALL: (201) 263-7200, TWX: 710-987-8341

READER SERVICE NUMBER 40

TRANSMISSION MEDIA

Waveguide . . . alive and well

Efforts in dielectric waveguide as well as printed-circuit technique are basically intended for modest performance applications at a reasonable cost. If low cost is not the most significant design factor, then conventional waveguide is also in the running for millimeter systems design.

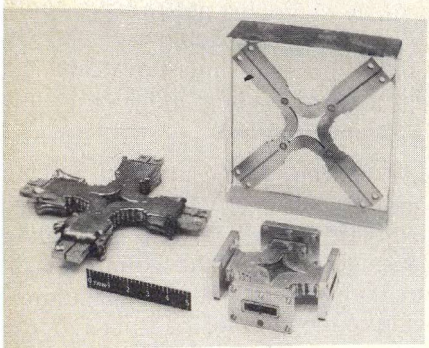

3. Various stages of electroforming, shows mandrel in transparent block, electro-formed part before aluminum mandrel is dissolved away and the final part with waveguide flanges attached. This 35 GHz four-way hybrid power divider/combiner by TRW has 0.3 dB insertion loss (two hybrids), over 20 dB of isolation and a coupling flatness of ±0.25 dB over a 5 GHz bandwidth.

According to Dr. Jorg Raue, senior technical staff member in TRW Systems Communications and Antenna Laboratory, Redondo Beach, CA, the conventional waveguide approach will be with us for quite some time, particularly when the need is for just a few highly reliable systems, such as in space applications. In the lower portion of the millimeter spectrum, 28-35 GHz, Aeronutronic Ford, Palo Alto, CA, builds graphite-epoxy waveguide components for their satellite programs. According to Al Giddis, microwave engineering manager, the components weigh about one-third less than if built in aluminum and have a coefficient of expansion that's an order of magnitude less. "But they have the same strength as aluminum. Antennas have been built to 60 GHz using graphite-epoxy material."

TRW is presently active in practically all facets of millimeter-wave technology—printed circuits, metal waveguide and dielectric waveguide. "In the dielectric waveguide area, we are using high resistivity, single crystal GaAs as a medium," Raue comments. "For low-cost and relatively unsophisticated millimeter systems in quantities, dielectric waveguide may very well turn out the way to go. I don't feel, however, that purely monolithic designs will be practical. There are just too many processing steps involved for high yield," he predicts.

"If you came to me with a fairly involved millimeter wave receiver design requiring many channels, several mixers and several LOs, I would be hard put to develop it in dielectric waveguide. Adequate filtering would be a very difficult task in dielectric guide and coupled with the radiation problem would pose a major challenge to keep spurs down,'" continues Raue. "I see image line as best for simple receiver/transmitter applications-perhaps with only a single mixer and one LO and without any switching requirements." Gorwara feels image-line may be suitable for certain communication applications. "While it has been developed with bandwidths of 5 to 10 GHz, this may be enough for communications circuits. In fact, as the millimeter spectrum fills up, channelizing may be required and image-line, despite its narrow-bandwidth capability, might even be considered for EW applications.

Waveguide integrated circuits

While standard millimeter-waveguide techniques are fairly well developed, improvements are still being made today. For some of the more complicated waveguide components, electro-forming is being used not only to achieve top performance, but also to reduce size, weight, and interfaces.

"Through electroforming, a waveguide-integrated circuit can be realized," explains Raue. "For example, a mixer assembly consisting of adapters, hybrids, filters, transitions and mixer mounts are good candidates for electroforming. If each of these parts were individually machined and then assembled together, the resultant performance would not be comparable to that achieved by a single electroformed part."

Components at TRW typically made by electroforming are mixers, upconverters, transitions, hybrids, isolators and circulators. Copper is used to provide the electrical surface followed by nickel for strength if weight is critical.

In electroforming copper, for example, each component forms around a mandrel, Fig. 3, which serves as a cathode in an electrolytic bath of copper sulfate. A solid ingot of copper is used as an anode. Copper is transferred from the ingot to the mandrel by ionic conduction, Fig. 4. Typically 1 mil per hour deposition rate is used. The plating current density is about 50 to 60 amperes/sq. ft. of plating area at a low dc voltage.

According to Carlton Goss, president of Gamma-F Corporation, El Segundo, CA, which specializes in electroforming, different types of copper formulations are used. For high tensile strength, a GFC #2 copper is used. For a more intricate design, in which the flux density of the solution will vary, GFC #1 copper is used which has a higher "throwing power" to get into small crevasses.

"Electroforming is about the

(continued on p. 42)

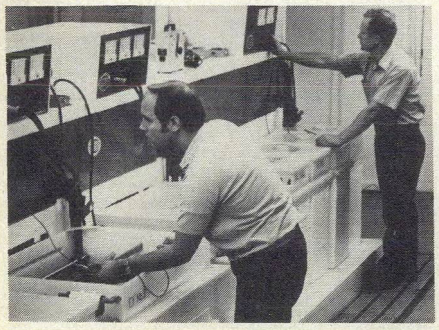

4. **Electro-forming process at Gamma-F Corporation** uses an electrolytic bath of copper sulfate to plate precision components onto a mandrel.

Table 1. Performance of electroformed passive components

Component	Center Frequency (GHz)	Bandwidth	Insertion Loss (dB)	Isolation (dB)	VSWR
3 dB short slot hybrid	30-37	4 GHz	0.2	25	1.1
	55-63	8 GHz	0.5	20	1.2
Fixed tuned band-pass filters	30-38	400 MHz	0.2	—	1.1
	55-65	200 MHz	0.3	—	1.2
High pass filters	30-38	—	0.12	30*	1.2
	55-60	—	0.5	50*	1.25
Circulators	32-36	8 GHz	0.2**	20	1.1
	55-65	2 GHz	0.3	20	1.2
WG-coaxial transition	35	10 GHz	0.2	—	1.2
Passive power divider	37	6 GHz	0.2	20	1.2

*1.0 GHz Below Design Pass Frequency **0.1 dB Over 5 GHz

TRG millimeter experience translates into reliability...

Challenge us! Our 68-page catalog wraps up over 16 years of millimeter experience that includes many state-of-the-art advances. We offer the broadest line.... at budget-considerate prices.. with the kind of reliability that only experience can give. That is why TRG is considered THE millimeter company. For example, we have been using cold hobbing techniques for years, while other companies are just beginning to talk about it. And we're no strangers to hi-rel either. TRG produces components and sub-systems for laboratory test, communications, radar, radiometry and radio astronomy for use in ground, air and space applications.

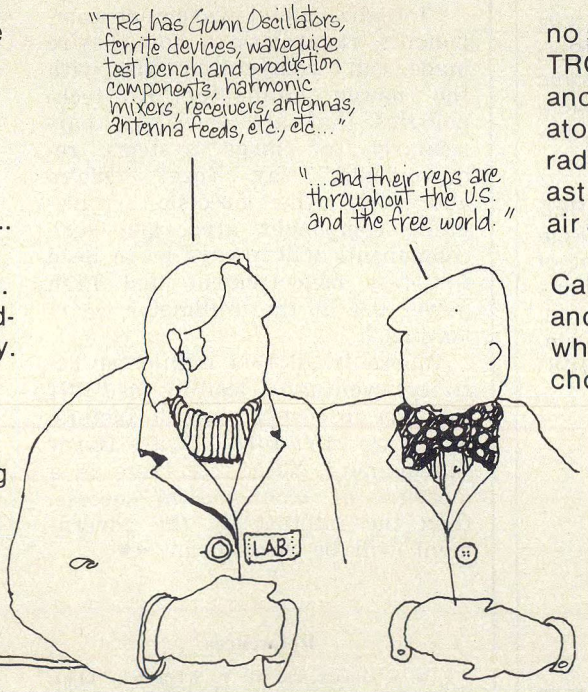

Call or write for our catalog and decide for yourself whether we offer you more choice than anyone else.

TRG DIVISION Alpha

ALPHA INDUSTRIES, INC. • 20 Sylvan Road, Woburn, Massachusetts 01801 (617) 935-5150 • TWX: 710-393-1236 • TELEX 949436

READER SERVICE NUMBER 41

Our Oscillators won't let you down.

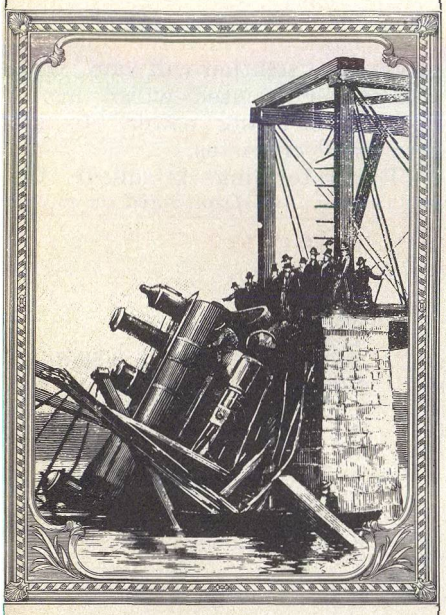

YIG-tuned oscillators so reliable we back 'em with a 2-year warranty!

Off-the-shelf models include:
SDYX-3000 (7-12.4 GHz, >25 mW), and
SDYX-3001 (12.4-18 GHz, >30 mW).

Need something special? Our YIG capabilities span 0.6 to 26.5 GHz in oscillators, filters, and harmonic generators. Try us for fast delivery and attractive OEM pricing. Evaluation samples available from stock.

For a new brochure and your **FREE** 18" x 20" copy of this poster, circle bingo or for fast action contact Jim Johnson at Systron-Donner's Advanced Components Division, 735 Palomar Avenue, Sunnyvale, California 94086. Phone (408) 735-9660.

SYSTRON-DONNER

READER SERVICE NUMBER 42

only fabrication technique that will meet the close tolerance production requirements of complex millimeter devices," claims Goss.

Mandrels major expense

Some electro-formed components can be made from the same stainless steel mandrel over and over again.

"The mandrel represents about two-thirds of the cost in making electroformed components," claims Raue.

Typically, the mandrel must be polished to a surface finish of 8 to 16 micro inches since a 1:1 transfer of dimension takes place with electroformed parts. At TRW, a 5 micro-inch surface finish is used in their space qualified millimeter components.

Is an electroformed part less expensive than one machined by hand? According to Ted Kozul, President of Baytron in Medford, MA, it can be, depending on the component.

"Transitions are one type of component best made by electroforming." Kozul claims that because of a transition's shape, making six of them by the sheet stock method with a 30-micron finish would take 40 man hours of brazing and machining.

"A machinist with six or seven years experience would be required and at an average rate of $6/hour and assuming 200% overhead, it gets quite costly," explains Kozul.

"The same part could be made by electroforming, using reuseable mandrels which cost about $150.

"I realize metal waveguide components, regardless of how they're made, can't compete costwise with the newer millimeter IC technologies that are emerging, particularly for large systems requirements," say Kozul. "We're addressing the precision waveguide component area, and such components will always be in need for test measurement and high power use at the millimeter wavelengths."

Where is all this millimeter activity eventually leading us? "It depends on several outside factors, which we can't forsee," says Barry Spielman of NRL. "If there is a measure of technological success, then the interest by the government will be sustained." ••

References

1. B. S. Glance and M. V. Schneider, "Millimeter-Wave Microstrip Oscillators," *IEEE Trans. on Microwave Theory and Techniques*, pp. 1281-1283, (December, 1974).
2. C. Buntschuh, "Integrated Circuit 18-40 GHz Receiver," *Microwave Systems News*, Vol. 5, No. 5, pp. 33-39, (October/November, 1975).
3. S. Mao, S. Jones and G. D. Vendelin, "Millimeter-Wave Integrated Circuits," *IEEE Trans. on Microwave Theory and Techniques*, Vol. MTT-16, pp. 455-461, (July, 1968).
4. S. Mao, S. Jones, E. W. Mehl and R. C. Hooper, "Integrated Microwave Receivers," Technical Report AFAL-TR-68-339, Air Force Avionics Laboratory, Wright-Patterson AFB, Dayton, OH, (December, 1968).
5. E. G. Cristal, A. F. Podell and D. Parker, "Microguide, A New Microwave Integrated Circuit Transmission Line," *1972 IEEE G-MTT Symposium Digest*, p. 212, (1972).
6. C. P. Wen, "Coplanar Waveguide," *1969 IEEE G-MTT Symposium Digest*, pp 110-115, (May, 1969).
7. S. B. Cohn, "Slot Line—An Alternative Transmission Medium for Integrated Circuits," *1968 G-MTT Symposium Digest*, (1968).
8. P. J. Meier, "Integrated Fin-Line Components," *IEEE Trans. on Microwave Theory and Techniques*, Vol. MTT-22, pp. 1209-1216, (December, 1974).
9. S. B. Cohn, *Proc. IRE*, Vol. 35, pp. 783-788, (August, 1947).
10. S. Hopfer, *IRE Trans.*, Vol. MTT-3, pp. 20-29, (October, 1955).
11. F. E. Gardiol, *IEEE Trans.*, Vol. MTT-16, pp. 919-924, (November, 1968).
12. D. D. King, "Circuit Components in Dielectric Image Lines," *IRE Trans. on Microwave Theory and Techniques*, Vol. MTT-3, pp. 35-39, (December, 1955).
13. D. D. King and S. P. Schlesinger, "Losses in Dielectric Image Lines," *IRE Trans. on Microwave Theory and Techniques*, Vol. MTT-5, pp. 31-35, (January, 1957).
14. S. P. Schlesinger and D. D. King, "Dielectric Image Lines," *IRE Trans. on Microwave Theory and Techniques*, Vol. MTT-6, pp. 291-300, (July, 1958).
15. J. C. Wiltse, "Some Characteristics of Dielectric Image Lines at Millimeter Wavelengths," *IRE Trans. on Microwave Theory and Techniques*, Vol. MTT-7, pp. 65-70, (January, 1959).
16. W. Schlosser and H. Unger, "Partially Filled Waveguides and Surface Waveguides of Rectangular Cross Section," *Advances in Microwaves*, Vol. 1, pp. 319-387, (Academic Press, NY and London), (1966).
17. S. E. Miller, "Integrated Optics: An Introduction," *Bell Syst. Tech. Journal*, Vol. 48, pp. 2059-2069, (September, 1969).
18. A. Yariv, "Coupled-Mode Theory for Guided-Wave Optics," *IEEE J. Quant. Elect.*, Vol. QE-9, pp. 919-933, (September, 1973).
19. E. A. J. Marcatili, "Dielectric Rectangular Waveguide and Directional Coupler for Integrated Optics," *Bell Syst. Tech. J.*, Vol. 48, pp. 2071-2102, (September, 1969).
20. J. E. Goell, "A Circular-Harmonic Computer Analysis of Rectangular Dielectric Waveguides," *Bell Syst. Tech. J.*, Vol. 48, pp. 2133-2160, (September, 1969).
21. E. A. J. Marcatili, "Bends in Optical Dielectric Guides," *Bell Syst. Tech. J.*, Vol. 48, pp. 2103-2132, (September, 1969).
22. S. D. Personick, "Time Dispersion in Dielectric Waveguides," *Bell Syst. Tech. J.*, Vol. 50, pp. 843-859, (March, 1971).
23. D. Marcuse, "Power Distribution and Radiation Losses in Multimode Dielectric Slab Waveguides," *Bell Syst. Tech. J.*, Vol. 51, pp. 429-454, (February, 1972).
24. D. Marcuse, "Mode Conversion Caused by surface Imperfections of a Dielectric Slab Waveguide," *Bell Syst. Tech. J.*, Vol. 48, pp. 3187-3215, (December, 1969).
25. D. Marcuse, "Radiation Losses of Dielectric Waveguides in Terms of the Power Spectrum of Wall Distortion Function," *Bell Syst. Tech. J.*, Vol. 48, pp. 3233-3242, (December, 1969).
26. E. A. J. Marcatili and S. E. Miller, "Improved Relations Describing Directional Control in Electromagnetic Wave Guidance," *Bell Syst. Tech. J.*, Vol. 48, pp. 2161-2188, (September, 1969).
27. M. M. Chrepta and J. H. Jacobs, "Bulk Semiconductor Quasi-Optical Concept of Guided Waves for Advanced Millimeter-Wave Devices," USAECOM TR No. 3482, (September, 1971).
28. M. M. Chrepta and H. Jacobs, "A Bulk Semiconductor Millimeter-Wave Phase Shifter," USAECOM TR No. 3513, (November, 1971).
29. H. Jacobs and M. M. Chrepta, "Semiconductor Dielectric Waveguides for Millimeter-Wave Functional Circuits," *Digest of 1973 IEEE G-MTT International Microwave Symposium*, pp. 28-29, (1973).
30. A. K. Gorwara, et al., "Design and Performance of a Broadband MIC Low Noise K-Band Balanced Mixer and Related Components," *1975 MTT-S Symposium Digest*, pp. 140-142, (May, 1975).
31. A. K. Gorwara, et al., "Design and Performance of a Broadband Low-Noise K-Band Microstrip Image Reject Mixer," submitted for presentation at the 1976 IEEE MTT-S International Microwave Symposium.
32. Richard T. Davis, "MICs Invade Millimeter Wavelengths," *Microwaves*, Vol. 13, No. 8, p. 14, (August, 1974).
33. P. J. Meier, *1972 IEEE G-MTT Symposium Digest*, pp. 221-223, (May, 1972).

GaAs or Si: What Makes a Better Mixer Diode?

GaAs is favored by many for millimeter-wave mixer diodes due to its high mobility. But a detailed expression for cut-off frequency reveals that mobility does not tell the whole story.

CONVERSION loss in millimeter-wave mixers is influenced by many factors. Initially, the optimum conversion loss of a mixer is dictated by the properties of the semiconductor chosen for the Schottky-barrier mixing diodes. However, once a suitable diode has been selected, its optimum conversion loss is degraded by parasitics, circuit losses and impedance mismatches.

Quite a bit of controversy exists over the relative merits of gallium arsenide and silicon diodes for millimeter-wave mixer applications. Superficially, GaAs appears to be superior by virtue of the fact that its mobility is greater than five times that of Si. But contrary to popular belief, there is little significant difference in mixer performance between GaAs and Si Schottky-barrier diodes in the millimeter-wave region. This will be demonstrated theoretically and experimentally for the 90 to 110 GHz frequency range.

In order to compare the relative theoretical behavior of unpackaged GaAs and Si diode wafers, it is necessary to first choose a valid figure of merit. Optimum conversion loss, perhaps the most important diode-related parameter for mixer applications, improves as cut-off frequency increases. Since cut-off frequency is easily calculated on the basis of a device's geometry and material characteristics, we will assume this as a figure of merit for comparison. Cut-off frequency (f_c) is defined by[2,3,4]:

$$f_c = [2\pi R_s C_j]^{-1} \qquad (1)$$

where R_s is series resistance and C_j is junction capacitance.

Using the cross-sectional view of a typical Schottky-barrier mixer diode shown in Fig. 1, it is possible to derive more detailed expressions for the resistive and capactive elements that determine cut-off frequency. Junction capacitance (C_j) is given by:

$$C_j = \pi r^2 [q \epsilon N_{epi}/2 (V - \phi)]^{1/2} \qquad (2)$$

where r is the junction radius, q is the electron charge, ϵ is the dielectric constant of the semiconductor material, N_{epi} is the effective doping density of the epitaxial layer, V is the externally applied voltage (defined as positive when the junction is biased in forward direction) and ϕ is the built-in potential determined by the barrier.

Series resistance basically consists of two components, resistance due to the epitaxial layer outside the depletion region, and spreading resistance in the relatively thick substrate material. These elements are given by:

F. Bernues, member of the technical staff, **H. J. Kuno,** department manager and **P. A. Crandell,** section head, Hughes Aircraft Company, Electron Dynamics Division, 3100 W. Lomita Blvd., Torrance, CA 90509.

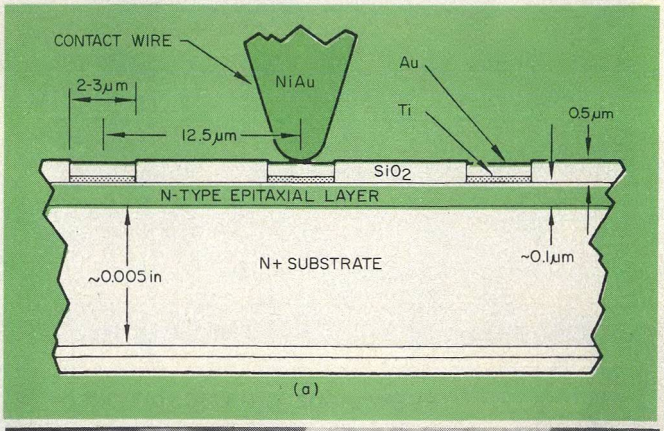

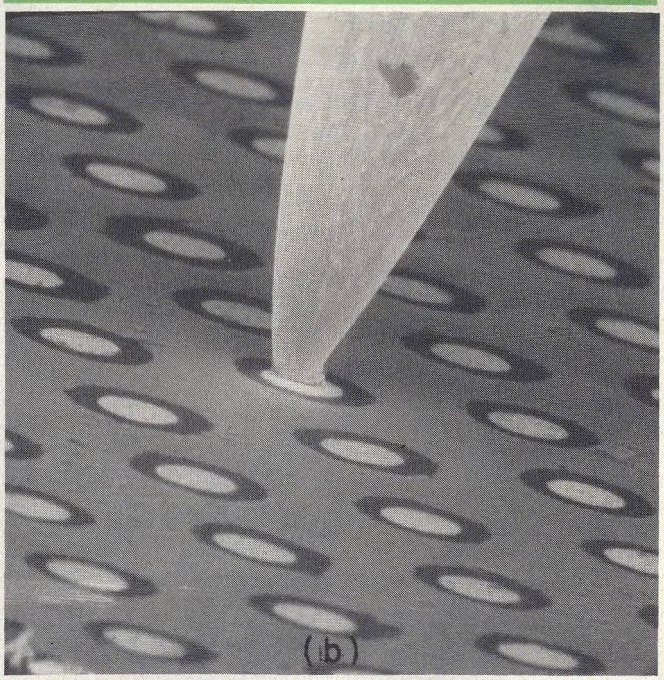

1. Schottky-barrier diodes for millimeter-wave mixers rely on a hyper-thin epitaxially grown layer (a). Pressure holds a tapered whisker in contact with a diode in this array (b).

$$R_{epi} = \frac{1}{q\mu\pi r^2} \cdot \int_{w_o}^{W_{epi}} \frac{dx}{N} = \frac{W_{eff}}{q\mu\pi r^2 N_{epi}} \qquad (3a)$$

$$R_{sub} = \frac{1}{q\mu 4 r N_{sub}} \qquad (3b)$$

where μ is electron mobility, N_{sub} is the substrate doping density and W_{eff} is the effective thickness of the epitaxial layer outside the depletion region, as

defined by Eq. (2).

Combining Eqs. (1), (2) and (3), cut-off frequency may be expressed as:

$$\frac{1}{f_c} = \frac{\pi W_{eff}}{q\mu N_{epi}}\left[\frac{2q\epsilon N_{epi}}{(V-\phi)}\right]^{1/2} + \frac{\pi^2 r}{4q\mu N_{sub}}\left[\frac{2q\epsilon N_{epi}}{(V-\phi)}\right]^{1/2} \quad (4)$$

This expression serves as a good working equation for evaluating the relative merits of GaAs and Si, since it expresses cut-off frequency strictly in terms of physical parameters and material constants. Mobility (μ) and dielectric constant (ϵ) are both intrinsic to the particular semiconductor material. On the other hand, N_{epi} and N_{sub} are controlled by the individual semiconductor material process, while W_{eff} and r are dictated by the diode's fabrication process. A simple examination of Eq. (4) reveals that for a high cut-off frequency, a semiconductor material (and associated process) with large values of μ and N_{sub} is desirable. W_{eff} and r should be made as small as practically possible. On the surface, it is hard to evaluate the influence of N_{epi}, since there is a conflict between the two terms on the right hand side of the equation.

From Eq. (4), it can be seen that junction diameter should be minimized to achieve a high cutoff frequency. Diameter is mainly limited by the diode fabrication process and electrical contacting technique. For this reason, the smallest millimeter-wave mixer diodes have 2-3 μm diameter Schottky-barrier junctions. Smaller junctions are difficult to fabricate on a reproducible basis with present photochemical etching technology, but ion-machining techniques[6] are being developed to overcome this limitation.

Mobility is not the whole story

Now, let's look more closely at the material co stants of GaAs and Si which appear in Eq. (4). Th dielectric constants of the two semiconductor mat rials are nearly equal (11.8 for Si versus 10.9 fo GaAs). However, the electron mobility of GaAs i about 5.6 times greater than that of Si (8500 cm² volt-second compared to 1500 cm²/volt-second). Fo this reason, it is commonly believed that GaAs i superior to Si as a millimeter-wave mixer diode ma terial. However, a more thorough examination of Eq (4) reveals that mobility alone is not the whole story

With the refined manufacturing processes develope over the past several years, hyper-thin epitaxial ma terials can be grown with well-controlled thickness and doping density. As a result, for a well-designe millimeter-wave mixer diode the first term on th right hand side of Eq. (4) becomes negligibly sma compared with the second term. Under this condition the product of μ and N_{sub}, not μ alone, becomes im portant. It happens that with arsenic-doped Si, dopin densities as high as 10^{20} cm^{-3} are practical, yieldin substrate resistivities ($\rho_{sub} = q\ \mu\ N_{sub}^{-1}$) as low a 0.001 ohm-cm, while with GaAs, the maximum achiev able doping density is limited to about 10^{18} cm^{-} ($\rho_{sub} = 0.0008$ ohm-cm) due to the solid solubilit limitation of the donor impurity in GaAs. Consequent ly, when other factors are weighed the advantage o higher electron mobility that GaAs holds over Si be comes much less important.

This is especially true when other factors ar weighed. For example, a Ti-Si Schottky-barrier junc tion presents a relatively low barrier height (0.5 V) compared with that created by any of the commo

(continued on p. 48)

ENGELMANN MAKES IT!

ULTRA-MINIATURE COUPLERS / HYBRIDS 0.375" THICK

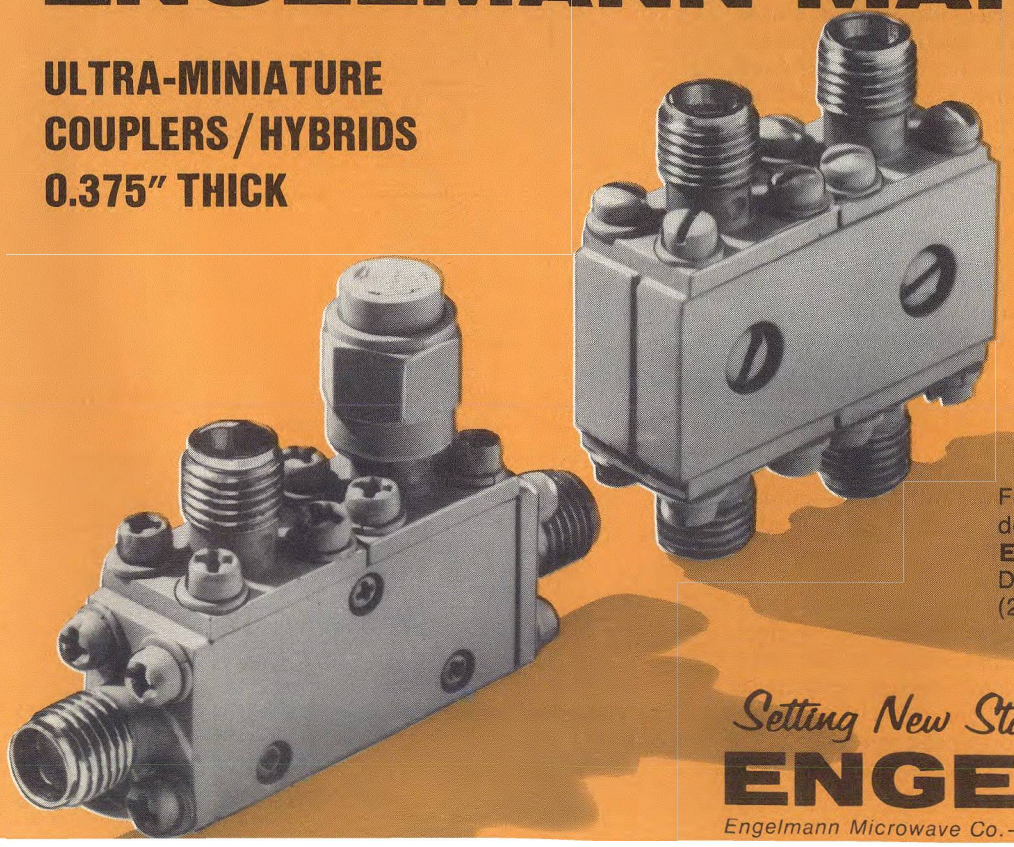

- 0.2-18 GHz in Octave + B.W.
- Sealed Stripline Constructio
- 3, 6, 10, 20, 30 db standard va
- 1" x 0.5" x 0.375", 4 GHz & UP
- Exceeds requirements of MIL-C-15370C
- Custom coupling values avai
- Directivity typically > 20 db
- Price $105 ea.

For detailed literature or custom design information, contact **ENGELMANN** Microwave Co., Sk Drive, Montville, N.J. 07045, (201) 334-5700.

Setting New Standards in Reliabilit

ENGELMANN

Engelmann Microwave Co. — Subsidiary of Pyrofilm Corporati

metal-GaAs Schottky barrier junctions (>0.8 V). The use of a diode with a lower barrier height should result in a mixer circuit with lower LO power drain, and with no external bias current requirements. In addition, the doping density profile and thickness of the epitaxial layer can generally be more finely controlled with Si than with GaAs. This is an important consideration for microwave diodes in general and for millimeter-wave mixer diodes in particular. Remember, the parasitics associated with excessive epitaxial material have increasingly adverse effects on performance at high frequencies.

Measurements support analysis

Thus, looking strictly at an unpackaged wafer from a theoretical standpoint, there appears to be no distinctive difference in the performance of Si and GaAs, Schottky-barrier mixer diodes at millimeter wavelengths. To test this theory mixers were designed for the 90 to 110 GHz range using both GaAs and Si Schottky barrier diodes mounted in similar packages (see Fig. 2). Cut-off frequency of the 2 μm junction devices is estimated to exceed 1000 GHz.

Conversion loss as a function of LO power is shown in Fig. 3 for both types of mixers. As the LO frequency was varied, the mixers were tuned with a sliding short. Note that there is no significant variation in conversion loss as a function of frequency for either type of mixer.

No significant difference is apparent in the measured optimum conversion loss between the Si and GaAs diodes in this experiment, supporting the theoretical predictions. However, there is a significant difference in the LO power requirement for self-biased mixers, which was predicted earlier on the basis of the higher voltage barrier in GaAs. The measurements confirm that an optimum conversion loss of 6.5 to 7 dB can be expected with high-quality diodes fabricated from either material.

What degrades conversion loss?

Optimum conversion loss is seldom realized in a mixer due to the effects of parasitics, circuit losses and impedance mismatches. An ideal Schottky-barrier junction diode without parasitics can be assumed to display a frequency independent current-voltage (I-V) characteristic of the form:

$$I(V) = I_s(e^{\alpha v} - 1) = I_s[\exp(nqv/kt) - 1] \quad (5)$$

where I_s is constant, V is the voltage across the junction, q is the electron charge, k is the Boltzman constant, T is the absolute temperature and n is the slope factor (n = 1 for an ideal junction).

Depending on whether the diode is voltage or current pumped and which harmonics and modulation products are shorted or open-circuited, mixers are commonly classified into Y, Z, G or H types.[1] The Z-type model, shown in Fig. 4, is the best representation of a typical millimeter-wave mixer. The current pumped through the diode by the LO is given by:

$$I_d = I_{dc} + I_{LO}\cos(\omega_{LO}t) \quad (6)$$

Theoretically, for an ideal, broadband Z-type mixer, the optimum conversion loss is a function of bias and LO current according to[1]:

$$L_c \simeq 2(1 + 2b)$$

$$\text{where } b = \{1 - [I_{LO}/(I_{dc} + I_s)]^2\}^{1/4} \quad (7)$$

It is important to note that Eqs. (5) and (7) neglect the adverse influences of diode parasitics, which may be analyzed using the equivalent circuit shown in Fig. 5. In this mixer model, only the current through R_b, the time-varying barrier non-linear resistance, is

(continued on p. 51)

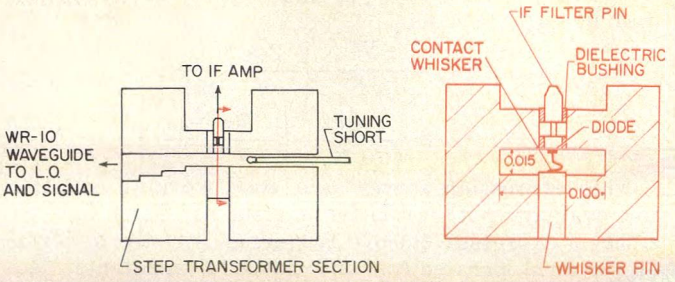

2. A reduced-height wafer package is necessary to minimize parasitics. Ideally, standard waveguide height should be reduced by a factor of three to five.

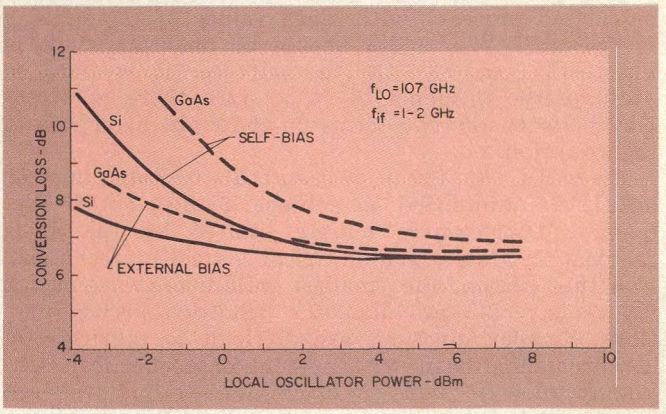

3. GaAs diodes require higher LO drive than Si devices for a given conversion loss.

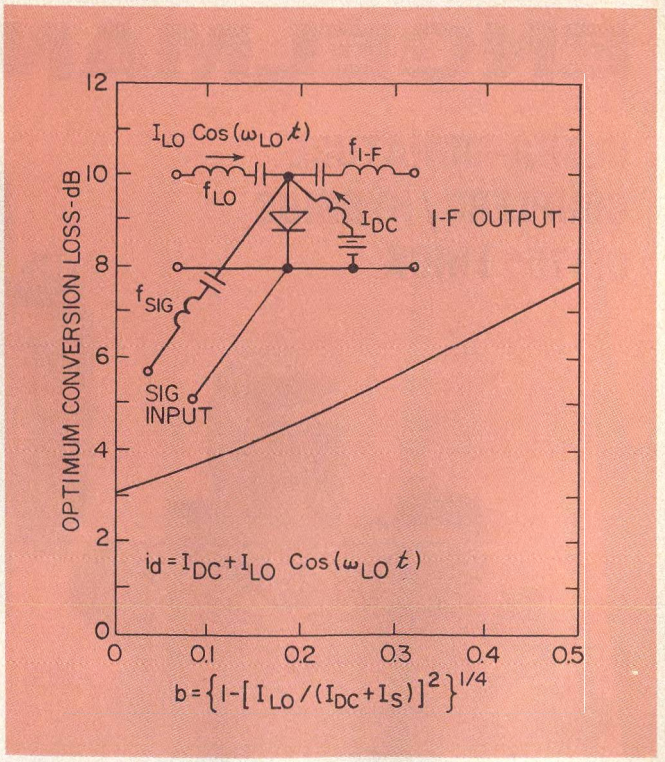

4. Optimum conversion loss varies with bias and LO current.

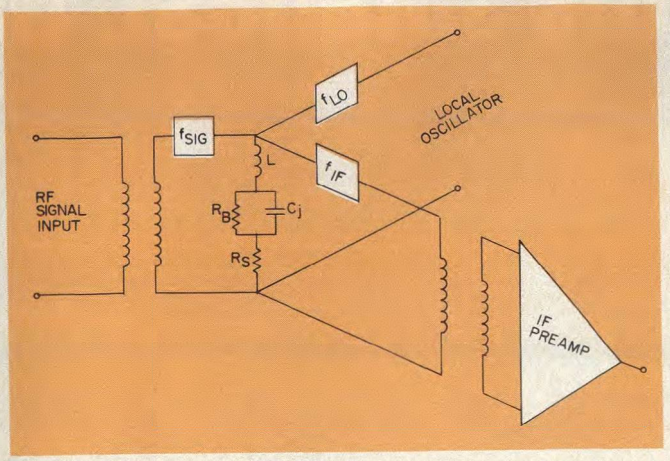

5. A diode's non linear barrier resistance (R_b) performs the mixing action. Capacitance and series resistance merely introduce loss.

(continued from p. 48)

effective in the mixing process. Although, strictly speaking, the junction capacitance C_j varies with applied voltage, the current through C_j contributes little to the mixing action. Thus, C_j is treated as constant, neglecting parametric effect. Series resistance, R_s, results in ohmic loss at both signal and i-f frequencies, and also does not contribute to mixing.

Obviously, the losses associated with C_j and R_s must be minimized if a diode is to approach optimum conversion loss. Although lossy elements will always be present, their magnitude can be reduced by careful processing. Equation (4) indicates that low epitaxial layer doping density results in low junction capacitance but high series resistance in the epitaxial layer. Thus, a tradeoff between series resistance and junction capacitance must be made when determining an optimum value for epitaxial layer doping density. The optimum value lies in the low 10^{17} cm^{-3} range for millimeter—wave mixer diodes. With $N_{epi} = 10^{17}$ cm^{-3}, the epitaxial layer thickness should be less than 0.1 μm. Considering that there is a transition region between the substrate and the epitaxial layer and that the zero bias depletion layer width is about 0.05 μm when $N_{epi} = 10^{17}$ cm^{-3}, the optimum value for W_{epi} is about 0.1 μm.

While the designer is pretty much forced to accept the loss due to series resistance, the effect of junction capacitance can be minimized by reducing the rf component of the signal current passing through C_j. Thus, it is desirable to choose a diode with a cut-off frequency that is considerably higher than the mixer's signal frequency. This may be demonstrated by considering the relation between actual and optimum conversion loss:

$$L_c = F \cdot L'_c$$

where F is a degradation factor described by:

$$F = \left(\frac{R_s}{R_{sig}}\right)\left(1 + \frac{R_s}{R_{i-f}}\right)\left[1 + \frac{R_{sig}}{R_s} + \left(\frac{R_{sig}}{R_s}\right)^2\left(\frac{f_{sig}}{f_c}\right)^2\right] \quad (8)$$

R_{i-f} = component of R_b

R_{sig} = signal frequency component of R_b

In Eq. (8), R_s, R_{i-f} and f_c are relatively easy to measure, but R_{sig} is not so easily determined for a milli-

(continued on p. 55)

PYROFILM MAKES IT!

PILLSHAPE ATTENUATORS AND CHIP ATTENUATORS

- Ground Plane Spacing .125
- Guaranteed VSWR
- DC to 4 GHz VSWR 1.25 Max.
  4 to 8 GHz VSWR 1.35 Max.
  8 to 12 GHz VSWR 1.5 Max.
- Attenuation Accuracy at 1 GHz: ±½ db or 5% whichever is greater
- Standard db values: 3, 6, 10, and 20 d

For a complete descriptive literature, write to: **PYROFILM**, 60 South Jefferson Road, Whippany, N.J. 07981 or discuss your design with one of our application engineers by calling (201) 887-8100.

Setting New Standards in Reliabilit

PYROFILM

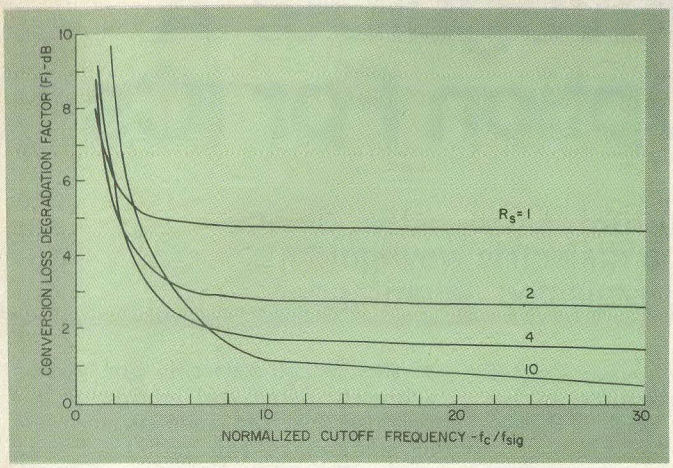

6. Diode cut-off frequency must be at least 10 times a mixer's signal frequency to near optimum conversion loss.

(continued from p. 51)

meter-wave mixer. However, for a broadband Z-type mixer:

$$R_{i-f} = R_{sig}/2 \simeq (\alpha I_{dc} b)^{-1} \quad (9)$$

Thus, Eq. (8) may be rewritten in terms of readily measurable parameters:

$$F \simeq \left(\frac{R_s}{2R_{i-f}}\right)\left(1+\frac{R_s}{R_{i-f}}\right)\left[1+\left(\frac{2R_{i-f}}{R_s}\right)+\left(\frac{2R_{i-f}}{R_s}\right)^2\left(\frac{f_{sig}}{f_c}\right)\right] \quad (10)$$

A plot of the variation of this degradation factor as a function of the cutoff frequency to signal frequency ratio for typical diodes (Fig. 6) reveals three important points:

(1) For $f_c/f_{sig} > 10$, cut-off frequency has very little effect on the degradation of conversion loss.

(2) The ratio of R_{i-f} to R_s has a great influence on a mixer's ultimate conversion loss.

(3) To keep the degradation of the optimum conversion loss less than 1 dB, it is required that $f_c/f_{sig} > 10$ and $R_{i-f}/R_s > 10$. ••

Acknowledgement

The authors wish to thank J. W. Tully for his efforts in manufacturing the diodes used in these mixers, D. Wong for assembling the packages and A. Cardiksnenos of the University of Massachusetts for valuable discussions.

References

1. A. A. M. Saleh, *Theory of Resistive Mixers*, MIT Press, Cambridge, Mass., (1971).

2. J. C. Irvin and N. C. Vanderwal, "Schottky Barrier Devices," *Microwave Semiconductor Devices and Their Applications*, H. A. Watson, ed., McGraw-Hill Book Company, New York, N.Y., (1969).

3. H. E. Elder and V. J. Glinski, *Detector and Mixer Diodes and Circuits*, Microwave Semiconductor, McGraw-Hill Book Company, New York, N.Y., (1969).

4. S. M. Sze, *Physics of Semiconductor Devices*, McGraw-Hill Book Company, New York, N.Y., (1969).

5. A. R. Kerr, "Low Noise Room Temperature and Cryogenic Mixers for 80-120 GHz," *IEEE Transactions on Microwave Theory and Techniques*, vol. MTT-23, pp. 781-787, (October, 1975).

6. H. L. Stover, H. M. Leedy, and H. G. Morehead, "Solid-State Devices and Components for Millimeter-Wave Receiver-Transmitter Systems," *Microwave Journal*, Vol. 16, pp. 35-41, (February 1973).

If you haven't **RENEWED IN 1976,** your **Micro-Waves** subscription will **EXPIRE.** See card inside front cover.

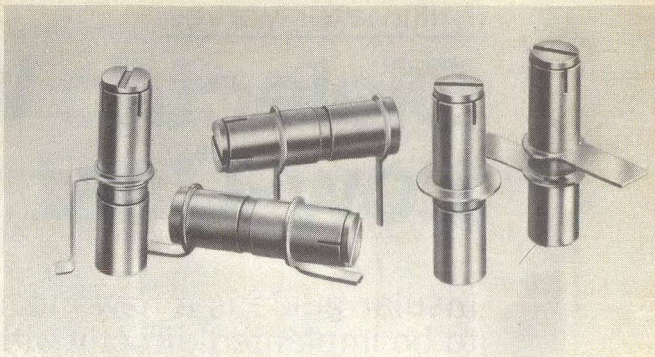

GIGA-TRIM CAPACITORS FOR MICROWAVE DESIGNERS

GIGA-TRIM (gigahertz-trimmers) are tiny variable capacitors which provide a beautifully straightforward technique to fine tune RF hybrid circuits and MIC's into proper behavior.

APPLICATIONS

- Impedance matching of GHz transistor circuits
- Series or shunt "gap trimming" of microstrips
- External tweaking of cavities

Available in 5 sizes and 5 mounting styles with capacitance ranges from .3 - 1.2 pf to 7 - 30 pf.

Johanson®

MANUFACTURING CORPORATION
Rockaway Valley Road
Boonton, N.J. 07005
(201) 334-2676 TWX 710-987-8367

READER SERVICE NUMBER 55

MINIATURIZED
Coaxial Switch

- only 2.625" OD, max height 2"
- 8 positions with indicators and suppression diode
- VSWR 1.5:1 up to 15 GHz
- isolation better than 60 dB
- insertion loss 0.4 dB
- guaranteed 2 x 10^6 cycles per pole

We have 326 switches designed—single, double throw, multiple position, failsafe or latching, transfer switches with logic, etc.

Write for new catalog

UZ Manufacturing Inc.

Transtel Products
1101 Colorado Avenue, Santa Monica, CA 90404
(213) 393-0567

READER SERVICE NUMBER 56

Millimeter-waves

Dielectric Waveguide: A Low-Cost Option For ICs

Insular guide is a new medium that allows active devices to be implanted directly within a dielectric waveguide. Cost and low circuit losses are projected advantages.

ONE of the most promising techniques for implementing low-cost millimeter-wave systems is dielectric-waveguide integrated circuits. Instead of confining an electro-magnetic wave by conductive walls as in conventional metal waveguide, dielectric waveguide combined with a conductive plane, can be used to confine and propagate energy using its refractive properties, much like optical fibers do with light.

Why the interest in dielectric waveguide? In the design of microwave integrated circuits using microstrip, the losses become prohibitively high for many system applications at frequencies around 20 to 30 GHz. Although specialized techniques are available to overcome some of the objectionable features of millimeter microstrip MICs, these circuits lose appeal because of higher fabrication costs.

Metal waveguide components, of course, have traditionally fulfilled the requirements for millimeter-wave systems. However, the close tolerances required to build metal waveguide components makes it very difficult to implement batch processing methods for components in any large scale system applications. Waveguide components continue to be very expensive and no practical means to mass produce them seems forthcoming.

In addition, metal waveguide does not lend itself to integration techniques. This is largely the reason that dielectric waveguide has evolved—to develop a planar transmission/circuit media at millimeter wavelengths that can provide reasonably good performance but which also lends itself to mass-production techniques. Incidentally dielectric-waveguide should not be confused with dielectric-loaded-waveguide, in which the size of standard metal waveguide is reduced by loading it with a dielectric.

A millimeter-wave dielectric integrated circuit is somewhat analogous to optical fibers.[1,2] The principle of guiding is the same, i.e. single mode propagation in a refractive waveguide, but there are several important differences.

The main distinction between optical dielectric waveguides and those used at the millimeter wavelengths lies in the dielectric material and fabrication techniques used.[3] Optical dielectric waveguides, for example, are often made of strips, thin films of glass or semiconductors and are formed using sputtering, ion implantation, diffusion, reverse sputtering or, ion beam or chemical etching techniques. Guide widths are typically a few microns when a small index ratio between the guide and surrounding medium is used. Millimeter dielectric waveguides, on the other hand, use a high dielectric constant material ratio between the guide and surrounding medium which in the optical spectrum would result in guide wavelengths that are sub-micron in width and extremely difficult to fabricate. Presently, single crystal, high resistivity silicon and GaAs is being used as well as high purity amorphous alumina for millimeter MICs. Techniques for low-cost, mass-production of alumina waveguides are under development. Some investigators favor the use of semiconductor waveguides because ultimately active devices might be fabricated directly in the waveguide.

Microstrip vs. dielectric waveguide

Emerging millimeter systems requirements, such as communications, radar and radiometric sensors clearly indicate that some form of practical and cost effective integrated circuit technique must be developed. There are two schools of thought on how this can best be achieved. Some feel microwave integrated circuits such as stripline or microstrip can be scaled into the millimeter bands, for operation as high as 60 GHz or more. Although there are certain specialized techniques, such as use of machined channels, that allow microstrip to be used at millimeter wavelengths, this is often done at the expense of reduced performance. While there is no fundamental frequency limit for microstrip circuits, loss and mode problems tend to reduce their usefulness to around the 20 GHz range, but not much more.

Dielectric waveguide MICs have some limitations as well. For instance, bends must be made with a moderately large radius to limit radiation to acceptable levels. They also have a useful single-mode frequency range limited by higher-order modes on the upper end and poor "guidability" on the lower end of its bandwidth. Another disadvantage lies with dielectric waveguide directional couplers which are based on the coupling of two fundamental asymmetrical modes. Because they propagate at different velocities, the coupling bandwidth is reduced to just a few percent.

(continued on p. 58)

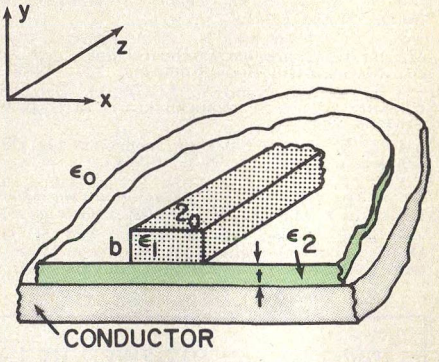

1. Dielectric waveguide, separated from a conducting ground plane, by a thick dielectric film ε_2, is called insular-guide. Note that $\varepsilon_1 >> \varepsilon_2 > \varepsilon$.

Robert M. Knox, President, Epsilon Lambda Electronics Corporation, 28 South Water Street, Batavia, IL 60510.

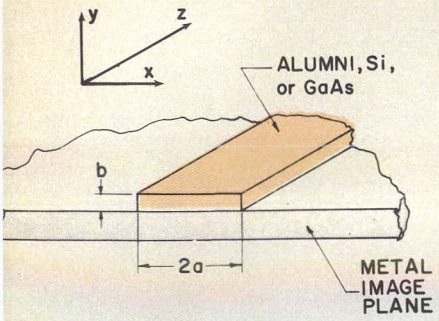

2. Image-waveguide is a special case of insular-waveguide where t = 0. Single crystal semiconducting materials, such as silicon and GaAs as well as alumina are used to form the dielectric guide.

Nonetheless, in the millimeter bands, which for present purposes assume to be 30 to 300 GHz, dielectric waveguide clearly has several potential advantages. For one thing, active devices can be directly integrated into the dielectric guide. It is less lossy than other types of integrated circuits as shown in Table 1. Note that unloaded, the Qs of various resonant structures are surprisingly high. For example, a dielectric waveguide made of alumina is about four times less lossy (theoretically) than microstrip (on alumina) at 60 GHz.[4,5] Experimental measurements show that this theoretical comparison is conservative and that in practice, the insular guide is approximately an order of magnitude lower in loss than microstrip. Compared with silverplated rectangular metal waveguide, the dielectric waveguide is only slightly more lossy at millimeter wavelengths.[6]

Insular and image-waveguide

Dielectric waveguide, as envisioned for millimeter integrated circuits,[7] Fig. 1, consists of a rectangular core of relative dielectric, ϵ_r surrounded by semi-infinite medium of dielectric constant, ϵ_o

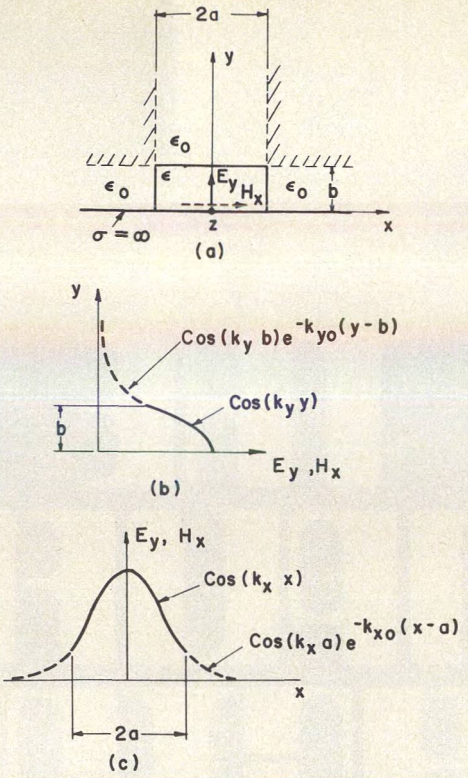

3. Rectangular image-guide immersed in air dielectric, ε_o, has a cosine field distribution inside the dielectric and exponential outside.

(usually air) and attached to a conducting ground plane by a thick dielectric film (ϵ_2). The conducting ground plane is important for minimizing spurious higher-order modes. As depicted in Fig. 1, propagation is in the z direction. This structure is called insular-guide. A special case of insular guide is image-guide, Fig. 2, where the film thickness is zero. Both can support a discrete spectrum of guide modes, E^y_{mm} (m = 1, 2, 3 . . . ; n = 1, 3, 5 . . .) and a continuous spectrum of unguided modes. As a result, cross sectional dimensions and operating frequencies must be properly selected for just propagating the fundamental mode. The fundamental mode is the E^y_{11} mode, which has an electric field polarization in the y

Comparison of Insular, Microstrip, and Metal Waveguide

Description	Frequency (GHz)	λ_g (cm)	2a (cm)	t (cm)	Attenuation Factor α (dB/cm)	α (dB/λ_g)	Unloaded Q Q_u	$Q_{insular}$
Insular Dielectric	15	0.955	0.534	0.053	0.0093	0.0089	3063	1
Waveguide	30	0.476	0.268	0.027	0.0224	0.0107	2551	1
(Alumina)	60	0.237	0.134	0.013	0.0554	0.0131	2072	1
	90	0.158	0.090	0.009	0.0955	0.0151	1802	1
Microstrip-Gold	15	1.210	0.108	0.054	0.0200	0.0242	1124	2.72
on Fused	30	0.605	0.054	0.027	0.0562	0.0340	800	3.18
Quartz	60	0.302	0.027	0.014	0.1542	0.0466	583	3.55
(50 ohm)	90	0.201	0.018	0.009	0.2802	0.0563	483	3.73
Rectangular	15	2.58	1.580		0.0019	0.0049	5551	.55
Metal Wave-	30	1.40	1.067		0.0066	0.0092	2956	.86
guide-Silver	60	0.669	0.376		0.0156	0.0104	2615	.79
plated	90	0.441	0.245		0.0300	0.0132	2060	.87

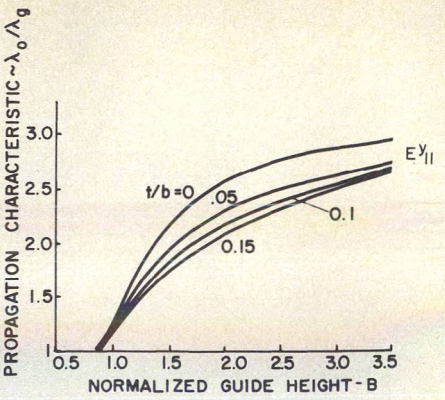

4. Fundamental mode propagation characteristics for insular-guide are influenced by the guide height and somewhat less by the thickness of plastic film which is under the dielectric guide. Here a/b = 1, ε_1 = 9.8 (alumina) and ε_2 = 2.25 (polyethylene).

(vertical) direction. As shown in Fig. 3, the field variation with the dielectric image guide is a cosine function, while outside the guide (on top and on both sides), it decays exponentially.

There exists for any rectangular dielectric waveguide in free space, a degenerate or nearly degenerate mode, the E^x_{11} mode, which has a polarization transverse to the E^y_{11} mode. Imperfections, discontinuities or bends will cause coupling of the modes. To suppress the E^x_{11} mode over a limited frequency range, an aspect ratio of a/b which is somewhat greater than one can be used. However, the best method for achieving single mode operation is to increase the cutoff frequency of the E^x_{11} mode by using the electric field shorting effect of the image plane.

One disadvantage to image-guide in practical circuits, is the difficulty of achieving a zero gap between the ground plane and the dielectric waveguide due to fabrication tolerances. These air gaps seriously affect the velocity of propagation and thus the guide-wavelength in image-guide. A second disadvantage is the adhesive, used to bond the image-waveguide to the image-plane, introduces losses. One way to circumvent this gap and bonding problem is to deposit a conducting film on the underside of the image-guide. This requires an extremely fine surface finish on the dielectric waveguide, which can lead to increased fabrication costs. It is particularly difficult to achieve with alumina.

Transmission line properties

Figure 4 shows the propagation characteristics of an alumina dielectric waveguide (ϵ_1 = 9.8) supported by various thicknesses of

(continued on p. 60)

polyethylene film ($\epsilon_2 = 2.25$) and a ground plane. The guide wavelength λ_g, is dependent on B, the normalized height of the guide, defined as:

$$B = \frac{4\,b}{\lambda_o}\sqrt{\epsilon_1 - 1}$$

where λ_o = free space wavelength

The parameter B becomes the frequency variable for a fixed guide configuration and may also be presented as:

$$B = \frac{4\,b}{11.8}\, f_{GHz}\sqrt{\epsilon_1 - 1}$$

The a/b = 1 cross section, where the guide width is twice the guide height, yields an electrical equivalent which is square due to the imaging of the fields when the polyethylene film thickness is zero (t/b = 0). This aspect ratio is a good choice for image-guide because it offers maximum percent bandwidth for single-mode operation.

The dispersion curves for square guide (a/b = 0.5) are shown in Fig. 5 along with the two most probable higher order modes that can limit the upper frequency of single mode operation. Typically a 30 to 40 percent bandwidth can be achieved with image or insular-guide. Square waveguide is the choice usually made for insular-guide because the polyethylene film somewhat diminishes the image of the electromagnetic fields. This effectively reduces the electrical height of the guide and to increase it, the physical height must be increased correspondingly.

The effect of a gap between the dielectric waveguide and the image-plane upon the propagation characteristics is shown in Fig. 6, where t is the film thickness. The slope of this curve for a square guide and a fixed frequency (B = 1.9) is greatest for very small gaps. This curve demonstrates one of the main advantages of insular-guide relative to image-guide—it allows circuits to be fabricated with a uniform small gap and this provides a uniform propagation velocity.

Inspection of Fig. 5 reveals that increasing the t/b ratio causes the E^x_{11} mode cutoff to decrease in frequency. As a result, a compromise for the t/b ratio in the range of 0.05 to 0.15 is usually made in order to obtain maximum single-mode bandwidth with minimum dependence of the guide wavelength on variations in the film thickness.

The attenuation constant, α, of insular-waveguide is shown in Fig. 7. Note how ohmic losses in the ground plane decrease with increasing frequency (B) due to the greater field confinement to the high dielectric guide. Also the conductor loss of an insular guide having a t/b = 0.1 is lower by a factor of two or more than that of image-guide where t/b = 0. Figure 7 neglects losses due to adhesives which would also increase overall image-guide attenuation. Conductor surface roughness for both insular and image-guide also increase attenuation but is not included in Fig. 7.

Radiation losses in curved sections

Curved sections of dielectric image-guide also suffer from radiation losses.[8] As a result, there are minimum allowable bending radii that can be designed into dielectric waveguide circuits. The radiation loss also depends on the dielectric constant of the waveguide used and its cross-sectional dimensions. The higher the dielectric constant, the less the radiation from curved sections.

Radiation loss for a typical alumina insular guide, Fig. 8, can be minimized to acceptable levels if a minimum operating frequency (B value) is observed for a given waveguide cross section. Also a minimum normalized circuit bend radius (R/2a) in excess of four is usually observed.

There is one other loss mechanism in alumina dielectric guide —that of the E^y_{11} fundamental

(continued on p. 62)

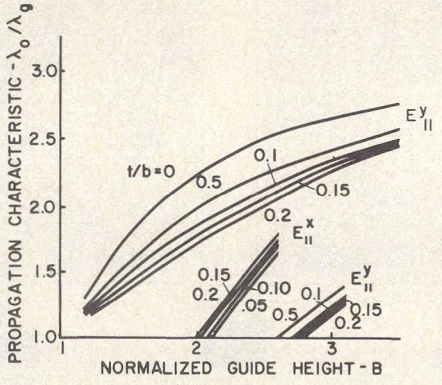

5. Mode propagation for square dielectric guide (common with insular-guide design) shows conditions where higher-order modes will propagate. Here a/b = 0.5, ε_1 = 9.8 and ε_2 = 2.25.

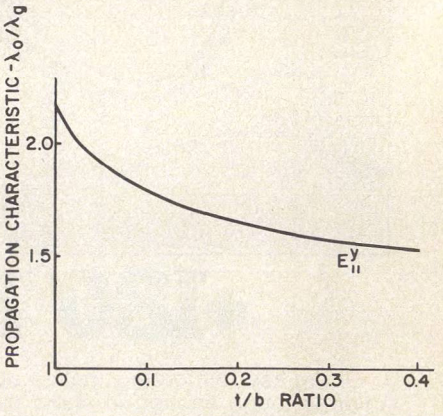

6. Guide wavelength is influenced by the thickness of the plastic film in insular guide. Here B = 1.9, a/b = 0.5, ε_1 = 9.8 and ε_2 = 2.25.

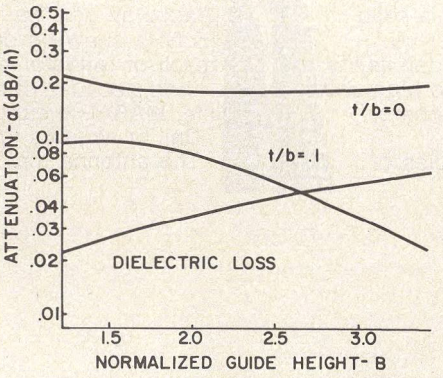

7. Attenuation in alumina insular waveguide on an aluminum ground plane is due to both conductor ohmic loss and dielectric absorption loss. Insular conductor loss is typically less than half that of image-guide. In this case, a/b = 0.5, tan = 10^{-4} (Al_2O_3) α = 3.72 × 10^7 mhos/m (Al). Other loss mechanisms not included are adhesive losses (image-guide) or film losses (insular guide), radiation at bends and scattering from guide surface roughness.

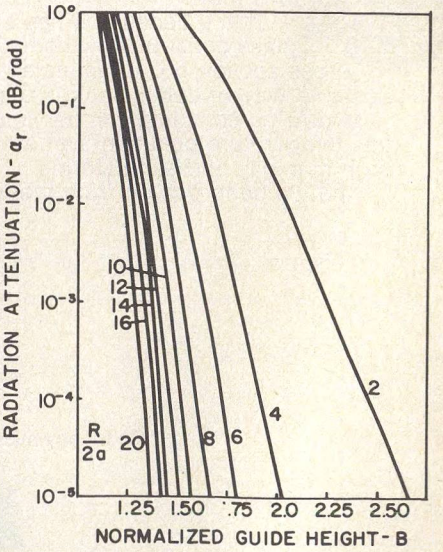

8. Attenuation due to radiation occurs in image and insular guide at curves and bends. The normalized bend radius (R/2a) is generally kept above four to minimize losses. In this graph, the guide material is Al_2O_3, a/b = 0.5 and t/b = 0.1.

Divide and Conquer.

DC to 3 GHz Attenuators, Terminations, & Impedance Transformers from APPLIED RESEARCH.

For Types BNC, TNC, C, N, SMA & other connectors.

Our integrated line of fixed pad attenuators, terminations and impedance-matching transformers conquers the problem of RF measurements and system integration by providing isolation between RF components over the frequency range of DC to 3 GHz. Also provides for the matching of different impedances with minimum loss over a broad frequency band. Unit cost is practical for large and small equipment users.

GENERAL CHARACTERISTICS
Frequency Range: DC—3 GHz
VSWR: 1.25:1
Attenuation Accuracy: +0.5 dB
Impedances (nominal): 50, 75, 90 ohms
Attenuation values: 1, 2, 3, 4, 6, 10, 12, 15, 20 dB (standard)
Temp. Range: —55°C to 100°C

U.S. PAT. NO. 2,891,223/2,974,403

For details, contact: Applied Research, 76 So. Bayles Ave., Port Washington, N.Y. 11050, (516) 883-5700, TWX #510-223-0822.

Applied Research
INCORPORATED
Filters, Converters, Multicouplers, Signal Sources, Amplifiers, Multipliers

READER SERVICE NUMBER 62

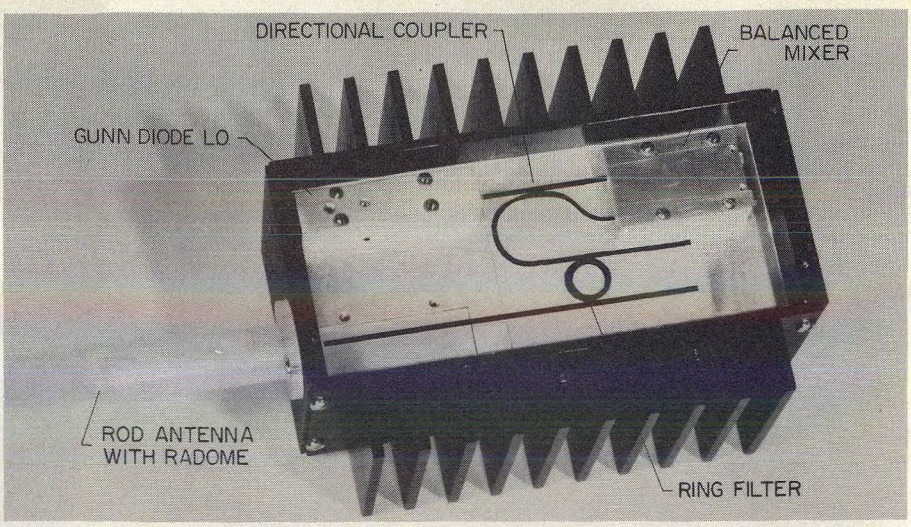

9. V-band communications receiver, developed at IIT Research Institute, incorporates a directional coupler and ring resonator made in Al_2O_3 insular guide. It works with a companion fm transmitter, Fig. 14, and is intended for covert communication at 60 GHz where an attenuation peak exists.

mode fields, coupling to higher-order radiation modes. This results from wall imperfections in the dielectric waveguide.[9]

Unfortunately, there is little quantitative data available on this loss mechanism. Circuit Qs have been measured (see Table 1) and found higher than theoretically predicted, encouraging the conclusion that scattering losses are not significant for well guided fundamental modes.

Passive component

Directional couplers are basic to many circuit designs. As a result, one of the first components developed using image-guide was the parallel waveguide directional coupler.[9] The dielectric guide parallel line coupler, such as shown in Fig. 9, tends to be narrow band because the coupling results from the interference of two waveguide modes each propagating at different velocities. These two modes, called the symmetrical and asymmetrical mode, are the lowest order modes which can propagate in the coupling region of the coupler. Other higher-order modes are necessary to satisfy exactly the boundary conditions but have much smaller amplitudes and hence have a small net effect, especially when the coupling between the guides is weak.

For single mode operation, the choice of the coupler dimensions must be based on the dispersion curves, such as shown in Fig. 5, for alumina ($\epsilon_r = 9.8$). It is found that the normalized height of the guide must lie approximately in the range $1.0 \leq B \leq 1.34$ where the upper bound is dictated by the cutoff of the E^y_{21} mode and the lower bound by the practical requirement of good guidability at low frequencies.

A typical insular guide coupler response is shown in Fig. 10.[10,11] This is a 3 dB quadrature coupler designed to operate at 61.2 GHz and is used in the V-band communications receiver module, in Fig. 9 developed at IIT Research Institute in Chicago. This coupler can be made less frequency dependent and, therefore, useable over a wider band by shortening the coupling region and decreasing the gap.

Achieving small coupling factors (3 dB or less) is not difficult even in very short couplers if the waveguide cross-sectional dimensions are appropriate for the operating frequency. Couplers which are symmetrical about both planes of symmetry (parallel and normal to the waveguide direction of propagation) will always have a frequency independent quadrature phase shift between transmitted and coupled waves.

Bandpass or band-reject filters having one or more resonators can be built in insular-guide using ring resonators. A single resonator bandpass filter is shown in the 61.2 GHz superheterodyne receiver in Fig. 9. The ring resonator response is given in Fig. 11. One disadvantage of this type of filter is the multiple bandpass responses that occur. The separation of the spurious responses from the desired response is a function of the diameter of the ring resonator. However, the increase of the sepa-

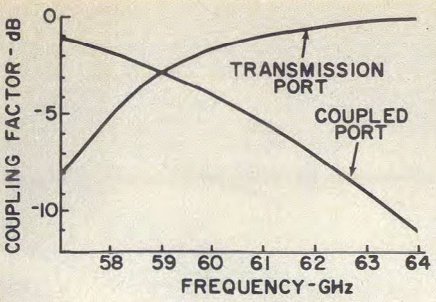

10. Typical coupling characteristics for a quadrature hybrid in insular-guide are shown here at V-band. Tight coupling is easy to achieve but due to the mode conditions, wide-band coupling is restricted to a few percent for a given coupling ratio.

ration of the spurs through diameter reduction is limited by the minimum radius-of-curvature considerations, discussed earlier.

Analyses for single and double ring resonator filters have shown theoretically that if the frequency selectivity nature of the interstage and input/output couplers is used (Fig. 10), these spurious responses can be significantly suppressed.

Phase shifters and attenuators

One of the major advantages of dielectric waveguide is that the electromagnetic fields are accessible for introducing an attenuating or phase shifting media. For example, lossy thin ferrite slabs or thin films can be placed external to the guide, with only the fundamental mode affected and without coupling to higher order or radiating modes.

An example of a 70.5 GHz electronic phase modulator developed by the Army Electronics Com-

(continued on p. 64)

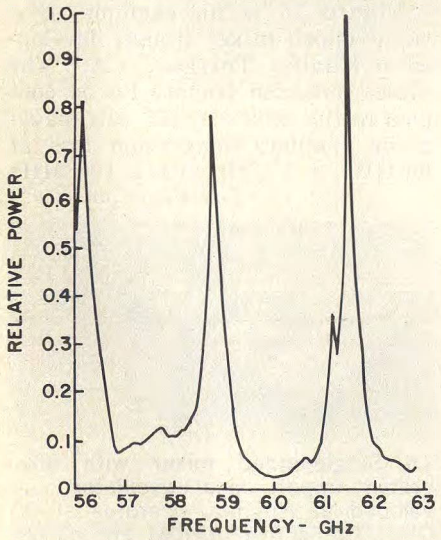

11. Ring preselector filter ($Q \approx 3500$) used in V-band receiver Fig. 9, has multiple bandpass responses. The diameter of the ring determines response separation.

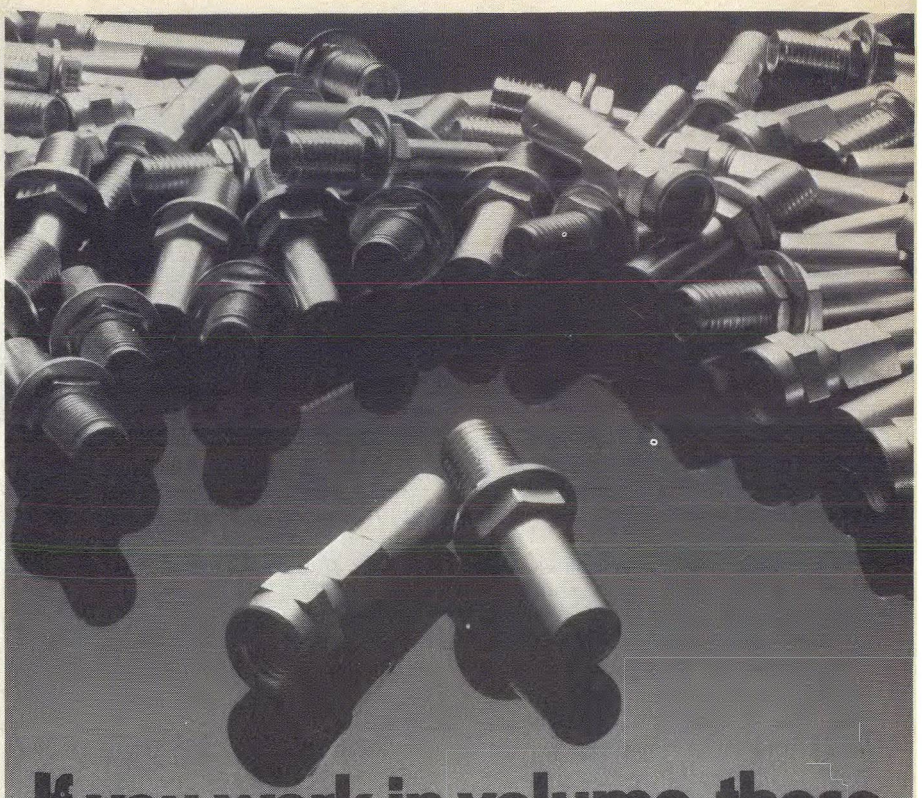

If you work in volume, these can mean less work for you.

If you use miniature coaxial connectors in quantity, you'll be interested in the latest additions to the Johnson JCM family: Crimp-type straight cable plugs, and crimp-type straight cable jacks.

You use a standard crimping tool, so they're quicker to assemble. And when you're a volume user, the savings in labor can really mount up.

Like all other Johnson JCM's, these feature gold or nickel plating, brass body, Teflon® insulator, and beryllium copper center contact. There are five or fewer parts to assemble.

They are fully compatible with SMA types, yet cost less than SMA equivalents. Designed for frequencies into the microwave range.

New Johnson crimp-style connectors. We've put a lot of work into them.

To make less work for you.

E. F. Johnson Company
3005 Tenth Avenue S.W., Waseca, MN 56093

☐ Please send me technical information on JCM miniature coaxial connectors.

☐ Please send me samples. You can call me at

(____) _____

NAME _____

TITLE _____

FIRM _____

ADDRESS _____

CITY _____ STATE _____ ZIP _____

E. F. Johnson Company

READER SERVICE NUMBER 63

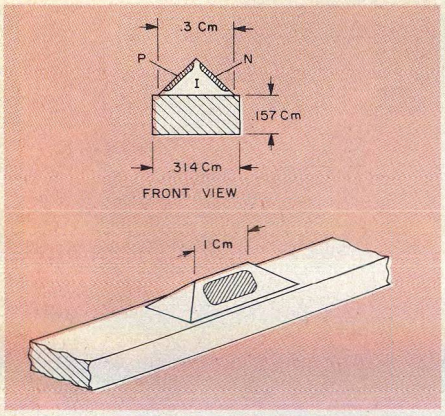

12. PIN diode phase shifter, developed at AECOM, operates at 70.5 GHz and is seated on top surface of a silicon image-guide.

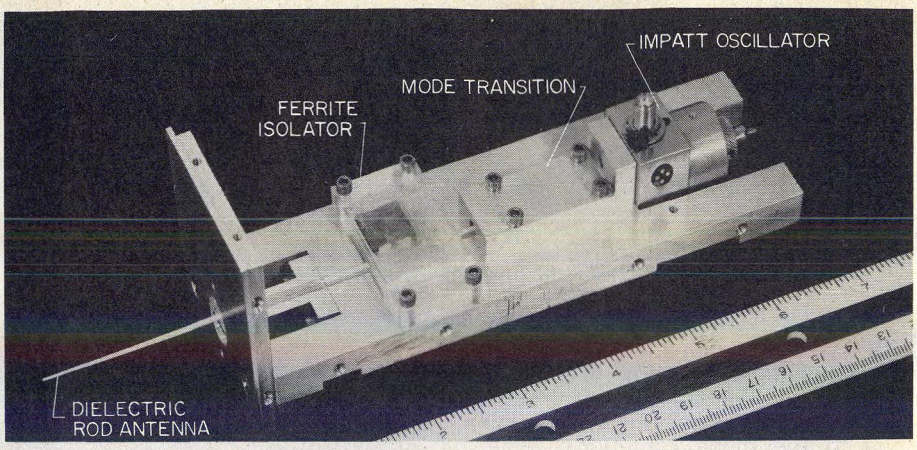

14. V-band insular transmitter operates at 60 GHz. It uses a tapered alumina guide to form a rod antenna with 15 dB of gain.

mand is[12,13,14] shown in Fig. 12. The triangular PIN semiconductor plate is first cut, ground and polished to the dimensions shown and then attached to the upper surface of the silicon dielectric waveguide.

The PIN junction is formed by metal arcing in a forming gas atmosphere. Mismatch loss in placing the modulator on the silicon semiconductor guide is less than 2 dB. When bias current is increased from 0 to 1.75 amperes, a 0 to 35-degree phase shift occurs in a reasonably linear fashion. As the current increases, the conductivity of the PIN structure increases in a downward motion from the upper most edge of the triangular piece—essentially introducing a conducting (image) plane above the silicon dielectric guide. The downward motion of the conducting plane has the same effect as reducing the film thickness, (ϵ_z) in the insular-waveguide. Therefore, the effective t/b ratio is changing which alters the guide wavelength.

Additional work on this device has occurred at Martin-Marietta, Orlando, FL.[15] By using a layered PIN structure, the phase shifter can provide over 40 degrees of phase shift but with a bias current, of less than 50 mA as shown in Fig. 13.

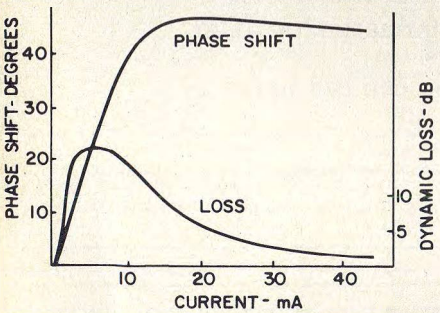

13. Layered PIN diode phase shifter developed at Martin-Marietta, offers linear phase variations with just a few mA of bias current.

One potential use for the dielectric-guide phase shifter is as a low-cost element in a phased-array antenna. These devices do require additional work, however, to improve efficiency and reduce insertion loss.

Isolators have also been developed in insular-guide. The V-band transmitter, Fig. 14, developed by IIT Research Institute, contains a field-displacement isolator. A ferrite slab replaces a portion of the dielectric waveguide material along one side of the cross section. An absorbing film is then placed at the outside edge of the ferrite slab which is between two biasing magnets. The measured isolation ratio is 10 dB at 60 GHz and insertion loss is 1 dB. A similar Ku-band isolator demonstrated 15 dB isolation. A Y-junction, three-port circulator using a ferrite post is also under development.

As can be noted in the receiver and transmitter of Figs. 9 and 14, radiating elements can be directly connected to insular-guide without using a launcher or transition. A suitably tapered dielectric guide will form an aperature having 10 to 15 dB of gain. An array of such radiators can form even higher-gain antennas.

Active components

Several types of mixers and integrated receivers have been developed in image- and insular-guide using two approaches to device mounting. One approach is to use split-block mounts where the active devices are mounted in rectangular air-filled metal waveguide, which allow control of possible radiation or mode conversion losses.[10,11] This technique requires using a mode transition, such as shown for the mixer in Fig. 15, to convert the E^{y}_{11} dielectric guide mode to the TE_{10} mode for the metal waveguide. In fact, whenever measurements are made of insulator-guide components, transitions are necessary since virtually all millimeter wave test equipment has waveguide output ports.

Another approach, which makes use of one of the principal advantages of insular-guide, is to mount the active devices directly in the dielectric waveguide. This technique is still in a fairly early development stage and conversion to higher order or radiating modes can easily occur and must be suppressed.

Figure 16 is an example of a single-ended mixer design developed at Hughes, Torrance, CA.[16] The direct mounted Impatt LO is coupled to the mixer by a 3 dB image-guide coupler. Conversion loss at 60 GHz is 6.1 dB with a 100 MHz

(continued on p. 67)

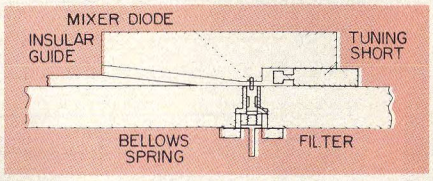

15. Transitions are used to go from insular-guide to the waveguide mixer shown in Fig. 9. An E-plane taper such as shown can be used.

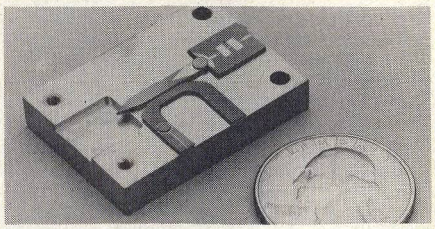

16. Single-ended mixer with integrated Impatt local oscillator, developed at Hughes, operates at 60 GHz. The active devices are placed in high resistivity (7900 ohm-cm) silicon. The dielectric is tapered to an angle of about 30° to insure a smooth transition to WR-15 waveguide.

miniature SMA terminations

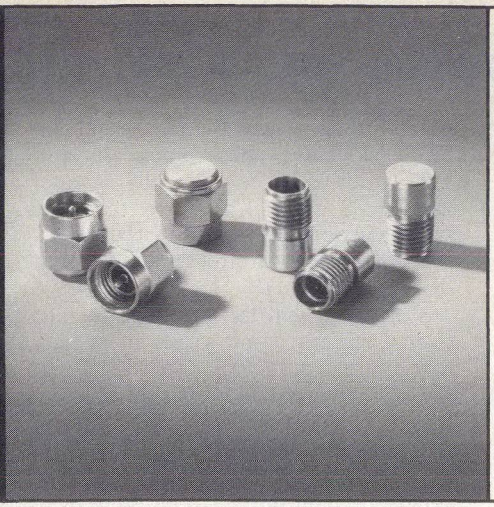

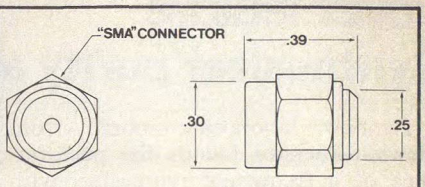

SPECIFICATIONS	
MODEL:	4444
Frequency Range:	DC to 18.0 GHz
Input Power:	0.5 watts
Connector:	SMA M/F
Maximum VSWR:	1.05 + 0.008f (GHz)
Temperature Range:	—54°C to +125°C
Construction:	Stainless Steel
Delivery:	Stock
Price	17.50 Each

MIDWEST MICROWAVE

3800 Packard Road, Ann Arbor, Michigan 48104 (313) 971-1992/TWX 810-223-6031

FRANCE: S.C.I.E.-D.I.M.E.S. 928-38-65

READER SERVICE NUMBER 67

DIELECTRIC WAVEGUIDE

(continued from p. 64)

i-f and with the LO power estimated at 5 to 10 mW. The mixer can operate over a 5 to 10% bandwidth.

A self-oscillating mixer fabricated in silicon dielectric waveguide was developed at the Army Electronics Command at Ft. Monmouth, NJ. Injection-locking tests showed an oscillator loaded Q of 350. Measurements of the device as a mixer indicated noise figures of about 10 dB. The conversion loss ranged from —10 dB to +10 dB where the conversion gain is attributed to the negative resistance of the Gunn diode.

Figure 17 (top) shows an integrated Impatt oscillator in silicon imageguide, designed by Hughes, consisting of a packaged Impatt diode connected to a radial ring resonator via metal ribbon contact.[16] The radial ring is a thin film deposited on the top surface of the silicon-image waveguide while the diode is mounted in a hole in the image-guide. Bias is supplied through a filtered thin-film line also deposited on the top of the silicon image-guide. Measured power output is 120 mW at 60 GHz. The device just below is a similar 60 GHz source but with a microstrip-type bias line filter.

Another active device developed at Hughes is an integrated, image-guide detector, incorporating a low-pass filter. Measured detector sensitivity from 56 to 64 GHz varies from 250 mV/mW to about 750 mV/mW.

The Army Electronics Command has also worked with radial disks

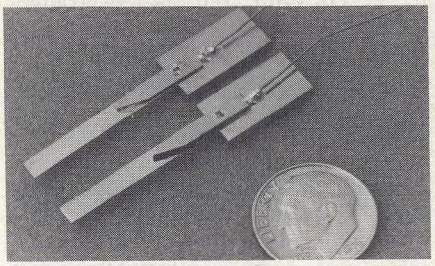

17. Image-guide Impatt oscillators (top), developed at Hughes, delivers 120 mW at 60 GHz.

on silicon image-guide for building oscillators using packaged Gunn and Impatt diodes. These tests were conducted at Ku and V-band.

Gunn oscillators, self-oscillating mixers and Schottky-barrier mixers for direct mounting in dielectric waveguide are also under development at the Systems Research Center of Minneapolis Honeywell. They have demonstrated Gunn oscillators in Ka-band and current development is at 60 GHz. In the Honeywell approach, the resonator is a separate longitudinal block of high thermal conductivity, such as beryllium oxide. The diode is attached to a metallized pattern on the transverse face of the block. The oscillator block is then mounted to an external dielectric waveguide having similar cross section. ••

Acknowledgements

The author wishes to gratefully acknowledge contributions made by Dr. P. P. Toulios (Epsilon Lambda Electronics), M. M. Chrepta and Dr. H. Jacobs (Army Electronics Command), G. R. Vanier (Martin Marietta Aerospace), Dr. G. E. Webber and S. Kofol (Honeywell Systems Research), Dr. Y. Chang (Hughes Ele tron Dynamics Div.) and A. Kaurs (IIT Research Institute).

References

1. H. Kogelnik, "An Introduction To Integrated Optics," *IEEE MTT-S Transactions*, Vol. MTT-23, (January, 1975).
2. E. A. J. Marcatili,, "Dielectric Rectangular Waveguide and Directional Coupler For Integrated Optics," *Bell System Technical Journal*, Vol. 48, (September, 1969).
3. R. M. Knox and P. P. Toulios, "Integrated Dielectric Image Lines For Millimeter Through Optical Frequency Range," *Proc. of the Symposium on Submillimeter Waves*, (March, 1970).
4. P. P. Toulios and R. M. Knox, "Rectangular Dielectric Image Lines For Millimeter Integrated Circuits," Western Electronic Show and Convention, Los Angeles, CA, (August, 1970).
5. R. A. Pucel, et al, "Losses In Mictrostrip," *IEEE MTT-S Transactions*, Vol. MTT-16, (June, 1968).
6. *Microwave Engineers Handbook*, Horizon House, Vol. 1, pg. 40, (1971).
7. P. P. Toulios and R. M. Knox, "Image Line Integrated Circuits For System Applications At Millimeter Wavelengths," U. S. Army Electronics Command Final Report No. ECOM-73-0217-F, (July, 1974).
8. R. M. Knox, P. P. Toulios and J. Q. Howell, "Radiation Losses In Curved Dielectric Image Waveguides Of Rectangular Cross Section," IEEE MTT-S International Microwave Symposium, Boulder, CO, (June, 1973).
9. P. P. Toulios, "Image Line Millimeter Integrated Circuits-Directional Coupler Design, *Proc. of the National Electronics Conference*, Chicago, IL, (December, 1970).
10. B. J. Levin and J. E. Kietzer, "Hybrid Millimeter-wave Integrated Circuits," U. S. Army Electronics Command Final Report No. ECOM-74-0577-F, (October, 1975).
11. R. J. Knox and P. P. Toulios, "A V-Band Receiver Using Image Line Integrated Circuits," *Proc. of the National Electronics Conference*, Chicago, IL, (October, 1974).
12. H. Jacobs and M. M. Chrepta, "Electronic Phase Shifter For Millimeter-Wave Semiconductor Dielectric Integrated Circuits," *IEEE MTT-S Transactions*, Vol. MTT-22, (April, 1974).
13. M. M. Chrepta and H. Jacobs, "Millimeter-Wave Integrated Circuits," *Microwave Journal*, Vol. 17, (November, 1974).
14. H. J. Kuno, Y. Chang, H. Jacobs and M. M. Chrepta, "Active Millimeter Wave Integrated Circuits," *Proc. of the Government Microcircuits Application Conference*, (June, 1974).
15. G. R. Vanier and R. M. Mindock, "Diode Structures For A Millimeter Wave Phase Shifter," IEEE MTT-S International Microwave Symposium, San Francisco, CA, (May, 1975).
16. H. J. Kuno and Y. Chang. "Millimeter Wave Integrated Circuits," U. S. Army Electronics Command Final Report No. ECOM-73-0279-F, (June, 1974).

If you haven't **RENEWED IN 1976,** your **MicroWaves** subscription will **EXPIRE.** See card inside front cover.

cover feature

Synthesizer purity and am/fm combined in 2-18 GHz generator

A new laboratory source from Hewlett-Packard blends the performance of a frequency synthesizer with the convenience of a signal generator. Called a synthesized signal generator, model 8672A provides a virtually noise-free calibrated output from 2 to 18 GHz with the option of the selecting amplitude or frequency modulation. A lower cost companion model, the 8671A synthesizer, offers a stable, low-noise output from 2 to 6.2 GHz with fm modulation only.

The 8672A relies on a 2 to 6.2 GHz YIG-tuned transistor oscillator cascaded with a YIG-tuned multiplier circuit to cover the 2 to 18 GHz range. Band switching of the multiplier is completely automatic and "glitch-free" in both manual and remote modes. Frequency resolution is 1 kHz in the 2 to 6.2 GHz range, decreasing to 2 kHz in the 6.2 to 12.4 GHz region and to 3 kHz above 12.4 GHz. An internal 10 MHz standard locks the generator to achieve an overall frequency stability of 5 parts in 10^{10} per day, or a 5 or 10 MHz rubidium or cesium standard can be used as an external reference.

Spectral purity is where this new generator excels. Spurious signals (excluding line-related noise) are greater than 70 dB below the carrier at 6 GHz. Even at 18 GHz, they are still greater than 60 dB below the carrier. Single-sideband phase noise (in a 1 Hz bandwidth) is typically greater than −83 dBc 1 kHz away from a 6 GHz carrier. At a 100 kHz offset, the noise drops to greater than −114 dBc (see Fig. 1).

For tests that must be performed over a wide dynamic range or at very low input signal levels, the 8672A features an internal 110 dB step attenuator with convenient vernier control. Attenuation settings are displayed on a 2-1/2 digit LED readout and the generator's output is monitored by a front-panel meter. Once adjusted, internal power leveling is typically ±1 dB at any power setting across the band, as shown in Fig. 2. Normal power output ranges from +3 dBm to −120 dBm, but an "overrange" setting typically allows outputs of +10 dBm up to 6.2 GHz and to +7 dBm across the generator's full 2 to 18 GHz range.

Calibrated am/fm modulation is another feature of the new instrument. The amplitude modulated 3 dB bandwidth is greater than 500 kHz at 6 GHz and greater than 100 kHz at 18 GHz. AM depth is selectable on two ranges, 30%/V and 100%/V, and is linearly controlled by varying the input signal amplitude (0 to 1 V) fed to a 600-ohm BNC port. Fm rates to 10 MHz are possible with peak deviations to 10 MHz. Six ranges of peak deviations, 30 kHz/V, 100 kHz/V, 300 kHz/V, 1 MHz/V, 3 MHz/V and 10 MHz/V are offered. The amplitude of the modulation input signal controls the actual peak deviation which is displayed on the meter. This fm function is completely independent of am.

It should be noted that the 8672A is fully programmable; all front panel functions, including frequency, output level and modulation ranges can be remotely controlled. Frequency may be remotely selected with the same resolution as in the manual mode with switching speeds typically less than 15 msec. Compatibility with the Hewlett-Packard Interface Bus System is included at no additional cost.

Frequency synthesizer, model 8671-A, offers similar signal purity and switching speeds in the 2 to 6.2 GHz band. Although lacking a calibrated rf output attenuator and am capability, this model offers the same fm performance and a +9 dBm minimum output level. Both instruments are standard rack size and measure only 5.25 inches high. P&A: Tentative prices: model 8672A: $27,000; model 8671A: $17,000; 24 wks. **Hewlett-Packard Company, 1501 Page Mill Road, Palo Alto, CA 94304 (415) 493-1501.** CIRCLE NO. 152

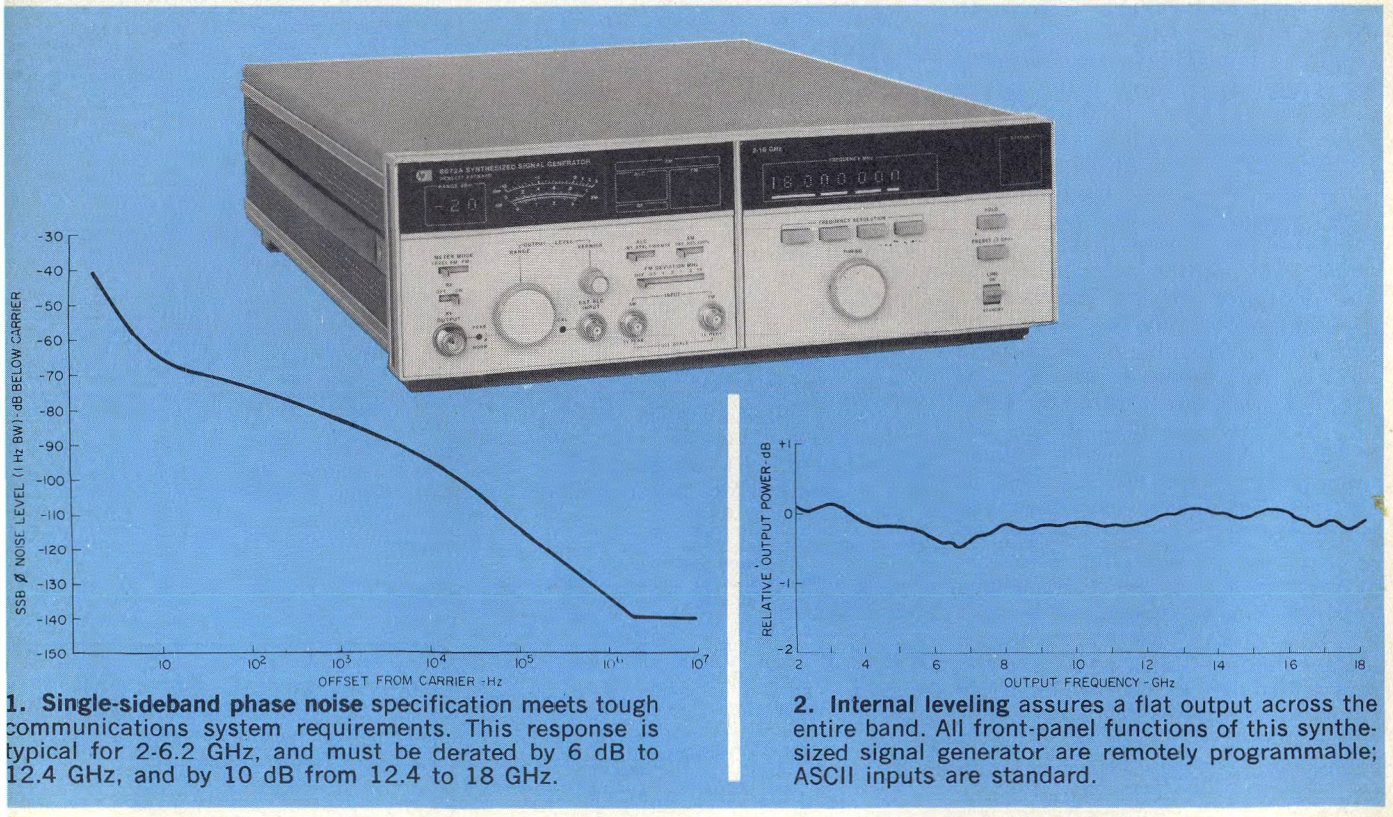

1. Single-sideband phase noise specification meets tough communications system requirements. This response is typical for 2-6.2 GHz, and must be derated by 6 dB to 12.4 GHz, and by 10 dB from 12.4 to 18 GHz.

2. Internal leveling assures a flat output across the entire band. All front-panel functions of this synthesized signal generator are remotely programmable; ASCII inputs are standard.

laser technology

MICROWAVES

RIL
976

ELECTRONIC WARFARE

Keep Track Of That Low-Angle Attack

Improved Radars Outwit Complex Threats

Design A Ka-Band Polar Frequency Discriminator

ALSO: Improved Devices Debut At Solid-State Conference

Frequency Counter Automates Pulsed RF Measurements To 18 GHz

MICROWAVES
April 1976
Vol. 15, No. 4

news

9 Improved Devices Debut At Solid-State Conference
13 Overall Radar Market Looks Flat, But Funding Shifts Are Detected
17 Varactor Doubler Boasts 80% Efficiency
19 Washington
23 R & D
24 International
26 Meetings
28 Industry
32 For Your Personal Interest . . .

editorial

30 R & D Cutbacks—Today's Savings Are Tomorrow's Losses

technical section

Electronic Warfare

36 **Keep Track Of That Low-Flying Attack.** Peter R. Dax of Westinghouse Electric Corporation explains how off-boresight and double-null tracking can be used to overcome the influence of specular and diffuse reflections on radars tracking low-flying targets.

54 **Improved Radar Designs Outwit Complex Threats.** Alex Ivanov of Raytheon Company describes three guidance systems for air-defense missiles, homing in on cw semi-active radar for detailed discussion.

74 **Design A Ka-Band Polar Frequency Discriminator.** David L. Saul of the Naval Electronics Laboratory Center illustrates how common MIC components, such as hybrids and couplers, must be modified to suit the design of a 26.5 to 40 GHz discriminator.

products and departments

82 **Cover Feature:** Frequency Counter Automates Pulsed RF Measurements To 18 GHz
83 New Products
93 Application Notes
94 New Literature
95 Advertisers' Index
96 Product Index

About the cover: EIP's new model 451, the first counter to automatically measure the frequency of pulsed rf to 18 GHz, should find many interesting applications in electronic warfare systems. Carrier photo courtesy of Watkins-Johnson; cover composition by Tycer-Fultz, Palo Alto, CA.

coming next month: Passive Components

Transform Impedance With Branch-Line Couplers. Dr. Chen Y. Ho of Rockwell's Collins Radio Group shows how to eliminate several interstage impedance transformers in hybrid-coupled amplifiers by designing branch-line couplers with unequal input and output impedances. Circuit size may be reduced by up to 50 per cent.

Specifying Isolators To Limit Frequency Pulling. Arthur Vemis of Block Engineering explains how to calculate the minimum isolation necessary to keep an oscillator's pulling specification within limits under changing load VSWR and phase.

Graphs Simplify Offset Stripline Conductor Design. Sachs Rimmon of Israel's Ministry of Defense examines the problem of designing components with stripline conductors spaced unequal distances between two ground planes. Graphs speed calculation of impedance and conductor width.

Publisher/Editor
Howard Bierman

Managing Editor
Stacy V. Bearse

Associate Editor
Joseph Ligori

Contributing Editor
Harvey J. Hindin

Washington Editor
Paul Harris
Snyder Associates
1050 Potomac St., NW
Washington, DC 20007
(202) 965-3700

Editorial Assistant
Gail Murphy

Production Editor
Sherry Lynne Karpen

Art Director
Robert Meehan

Production
Dollie S. Viebig, Mgr.
Dan Coakley

Circulation
Barbara Freundlich, Dir.
Trish Edelmann
Gene M. Corrado
Sherry Karpen,
Reader Service

Promotion Production Manager
Albert B. Stempel

Directory Coordinator
Janice Tapp

Editorial Office
50 Essex St.,
Rochelle Park, NJ 07662
Phone (201) 843-0550
TWX 710-990-5071

A Hayden Publication
James S. Mulholland, Jr., President

MICROWAVES is sent free to individuals actively engaged in microwave work. Subscription prices for non-qualified copies:

	1 Yr.	2 Yr.	3 Yr.	Single Copy
U.S.	$15	$25	$35	$2.50
FOREIGN	$20	$35	$50	$2.50

Additional Product Data Directory reference issue, $10.00 each (U.S.), $18.00 (Foreign). POSTMASTER, please send Form 3579 to Fulfillment Manager, MicroWaves, P.O. Box 13801, Philadelphia, PA. 19101.

Back Issues of MicroWaves are available on microfilm, microfiche, 16mm or 35mm roll film. They can be ordered from Xerox University Microfilms, 300 North Zeeb Road, Ann Arbor, MI 48106. For immediate information, call (313) 761-4700.

Hayden Publishing Co., Inc., James S. Mulholland, President, printed at Brown Printing Co., Inc., Waseca, MN.
Copyright © 1976 Hayden Publishing Co., Inc., all rights reserved.

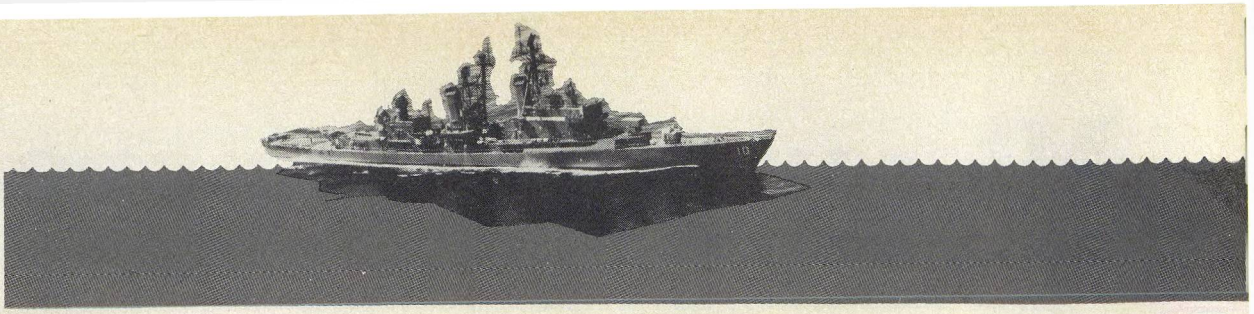

Keep Track Of That Low-Flying Attack

Shipborne radars have a difficult task tracking low-flying targets. Specular and diffuse reflections can swing the boresight erratically about the horizon, causing the radar to eventually lose track.

ONE of the toughest tasks of a shipboard fire control system is racking and hitting targets that lie low on the water, uch as a cruise missile. The associated tracking radar tarts behaving erratically in the vertical plane and requently loses track altogether. The problem is aused by reflection of target energy off the surface f the sea and occurs when the separation between he target and its image is less than the resolving ower of the antenna, (Fig. 1).

In view of the complexity of the problem, it is referable to avoid solutions that depend on a specific model" of the phenomenon. A system that discrimiates on the basis of angle against both clutter and eflected energy is theoretically ideal. Maximum discrimination requires high resolution to which there s a limit in practice.

An obvious approach for overcoming multipath problems with shipboard fire control radars is to increase the frequency or the aperture of the radar. The resolution of the system will then be improved and hence the multipath problem is reduced. This, however, is a somewhat drastic measure involving usually the complete replacement of the existing radar equipment.

Other solutions that might appear more practical include a screen or filters based on time of arrival, polarization or frequency differentials of the true and image return. Unfortunately, most of these techniques don't work, particularly in a sea environment. As will be described, off boresight tracking and double null tracking offer the best practical solution to this problem.

Actually, the observed behavior of a tracking radar

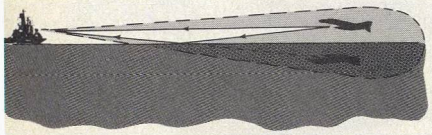

. **Multipath problems associated ith a tracking radar** occur when ıe separation between the target ıd its image is less than the reolving power of the radar. In the ase of a very smooth sea where pecular reflection dominates and here the reflection coefficient is ose to unity, the radar is effecvely presented with two identical rgets at the same range, reıring coherent signals that are arying slowly in relative phase.

eter R. Dax, Advisory Engineer, estinghouse Electric Corporaon, Friendship International Airort, Box 1897, Baltimore, MD 1203.

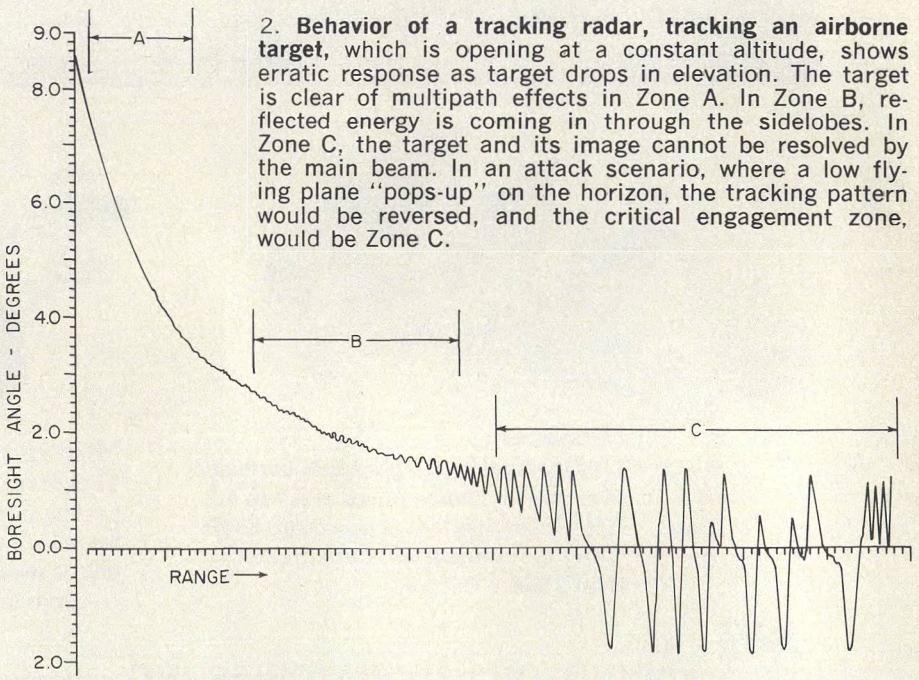

2. **Behavior of a tracking radar, tracking an airborne target,** which is opening at a constant altitude, shows erratic response as target drops in elevation. The target is clear of multipath effects in Zone A. In Zone B, reflected energy is coming in through the sidelobes. In Zone C, the target and its image cannot be resolved by the main beam. In an attack scenario, where a low flying plane "pops-up" on the horizon, the tracking pattern would be reversed, and the critical engagement zone, would be Zone C.

results from a combination of three factors:

- specular reflection
- diffuse reflection
- clutter or energy returned directly from the surface of the sea in the same radar cell as the target.

The contribution of each factor will vary, depending on the sea state. If the sea is glassy smooth, the specular reflection will dominate. As the sea gets rougher, most of the disturbing energy will come from the diffuse component and from the clutter.

Of the three factors that inhibit tracking low flying targets, specular reflection can be considered the "basic" disturbance observed with a smooth sea. Effects of specular reflections can be predicted by using geometric optics.

Consider Fig. 2, where a target is opening in range at constant altitude. As can be seen, its apparent elevation is constantly decreasing and the following can be observed:

- At high angles of elevation with the main sidelobes well clear of the sea, the radar tracks within the normal limits of accuracy. (Zone A).
- As the target approaches an elevation angle such that noticeable energy can enter the antenna via the sidelobes after reflection from the sea, the antenna can be seen to oscillate regularly about its mean position. (Zone B).
- At some point when the reflected energy enters the main beam, the oscillations increase in amplitude very rapidly until the radar oscillates from about two thirds of a beamwidth above the horizon to two thirds of a beamwidth below. This erratic tracking is irrespective of actual target elevation and continues until the target disappears over the horizon. (Zone C).

In this last phase, the radar's behavior may become very erratic and target track is frequently lost.

How multipath affects monopulse tracking radars

An amplitude comparison monopulse radar has two basic antenna patterns: the sum or reference pattern, Σ (which is an even function) and the difference pattern, Δ (which is an odd function). These patterns are sometimes derived at the rf frequency, by taking the sum and difference of two identical beams overlapping at their 3 dB points. In the absence of multipath, the two receiver outputs corresponding to the Σ and Δ patterns are either in phase or 180 degrees out of phase.

In a standard monopulse system, the Δ function is normalized (usually in an agc system) and compared with Σ in a phase detector. In free space, the detected output is zero for a target on boresight and approximately linearly proportional to the off boresight angle when the target is within the beamwidth. The error signal is of the approximate polarity to drive the antenna, via the servo system, to the equilibrium position of target-on-boresight. This basic scheme is shown in Fig. 3.

In the presence of multipath, the two available signals out of the sum and difference channels are Σ_R and Δ_R which are the resultants of the contributions from the direct and reflected paths; Σ_d, $A\Sigma_i$ and Δ_d, $A\Delta_i$ respectively, as shown in Fig. 4. (A) is the amplitude ratio of the direct and reflected signals arriving at the antenna. (A) is made up of the difference in gains in the target re-radiation pattern and of the reflection coefficient (ρ) at the sea surface. Note that Σ_R and Δ_R are not normally in phase.

The error signal developed at the output of the phase detector by the standard circuit of Fig. 3 is the projection of Δ_R on Σ_R, normalized with respect to Σ_R. From a simple trigonometrical analysis of Fig. 4, it can be shown that the normalized error voltage is given by:

$$E = \frac{\Sigma_d \Delta_d + A^2 \Sigma_i \Delta_i + A \cos\phi\,(\Sigma_d \Delta_i + \Sigma_i \Delta_d)}{\Sigma_d^2 + A^2 \Sigma_i^2 + 2A \cos\phi\, \Sigma_d \Sigma_i} \quad (1)$$

(continued on p.. 38)

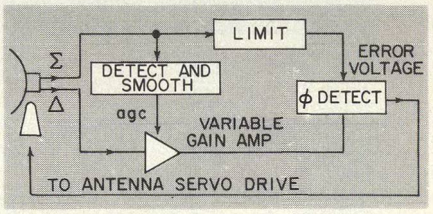

3. **In standard monopulse processing,** the error signal derived is the in-phase component of the Δ signal after normalization. The Σ signal is used as a reference.

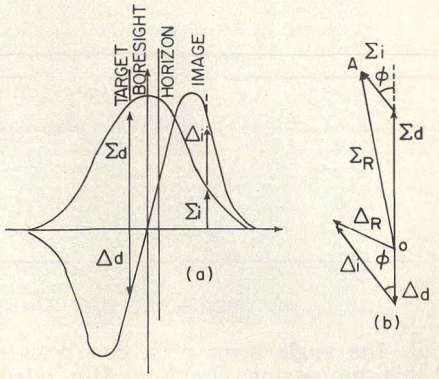

4. **A monopulse radar with multipath results in** Σ_d and Δ_d signals from the target combining with the corresponding Σ_i and Δ_i signals from the image. The resultant Σ_R and Δ_R vectors are not normally in phase.

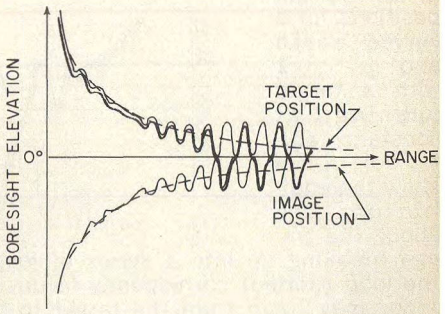

5. **Equilibrium positions for a target** opening at constant altitude under conditions of a flat earth and $\rho = 1$ show the radar tracking either the actual target or the image. Occasionally, it jumps from one to the other (as indicated in color).

LOW-ANGLE TRACKING

With normal closed loop operation, the boresight will be driven until the error is zero.

In a practical situation where the target is moving rapidly in range and slowly in elevation, the equilibrium position will vary cyclically, depending on ϕ, the relative phase of target and image signals. The amplitude of the oscillations will be a function of the strength of the reflected signal. What is not so clear from Eqn. (1) is that there are usually two stable positions of equilibrium where $E = 0$, one near the target and the other near the image.

If the quantity (A) is unity and if a flat earth is assumed, there must be symmetry of the equilibrium positions about the reflecting surface, as shown in Fig. 5. Therefore, there are at least two elevation angles where the boresight is in equilibrium.

Each "cycle" in Fig. 5 corresponds to the target flying through a lobe of the antenna pattern as modified by multipath. The "density" of the "cycles" depends, therefore, on the height of the radar above sea level (in wavelengths). The upper portion of the oscillations about the true target elevation corresponds to target positions where the direct and reflected rays are out of phase, hence to instants where the signal-to-noise ratio is at a minimum. Conversely, the lower portions correspond to instants when the signal-to-noise ratio is at a maximum (with the boresight close to 0 degrees in this case).

When the target is opening in range and tracking has started at a relatively high angle, the boresight will follow the line of equilibrium about the true target within the limits of the mechanical capabilities of the antenna mount. It will also track as long as the target moves fast enough so as not to remain for any extended period of time in a null of the pattern.

In a practical situation, the lobes of the pattern may be close enough together, and the target may be flying through these lobes fast enough so that the inertia of the mount will have an appreciable effect on boresight behavior. In this case, boresight may move over to positions of equilibrium about the image, as shown in Fig. 5 (in color). This is what is happening in Fig. 2.

Figure 5 has been drawn for a reflection coefficient of unity and for a flat earth. When ρ is less than unity, the equilibrium positions about the true target will still remain continuous but the equilibrium positions about the image break up into a series of loops, Fig. 6. The upper half of the loops correspond to the unstable equilibium positions. The boresight is then driven as indicated by the arrows. If the target is moving relatively slowly so that the inertia of the mount does not affect the ability of the radar to follow the equilibrium position, the boresight will follow the upper curve. If, however, the inertia of the mount modifies the boresight's response or if the reflection coefficient, ρ, of the surface changes with time and occasionally becomes close to unity (as the point of reflection changes for instance), then the radar can jump over to the image equilibrium line. This could result in losing track as the target moves to a range where no equilibrium position exists about the image (as shown in Fig. 6 in color).

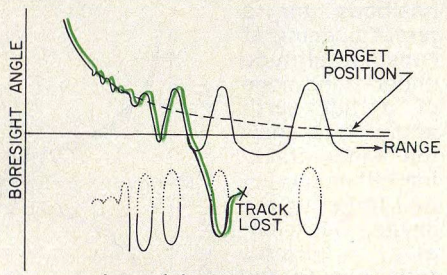

6. **Equilibrium positions for a curved earth** and $\rho < 1$ with a target opening at constant altitude now show the equilibrium line about the image breaking up into a series of loops. The top half of the loop (dotted) corresponds to unstable positions. The radar may jump from the target to the image and lose track as shown in color.

How multipath affects con-scan radars

A conical scan radar performs sequentially what a monopulse radar accomplishes on a single pulse basis, by mechanically scanning the beam in a circular motion at a typical rate of 30 Hz. The output video, Fig. 7, is modulated in amplitude at the scan rate if the target is off boresight. The normalized amplitude of the modulation is a measure of the angle off boresight and its phase relative to reference sine and cosine waves is a measure of the direction of the error (up, down, left or right). If the boresight is made to move slowly across the target elevation, the error voltage developed as a function of the off-boresight angle is similar to a monopulse radar error function and the agc voltage at (E) in Fig. 8 is similar to a monopulse Σ function.

The main relevant difference between a conical-scan radar and a monopulse radar is that the derivation of the error voltage by the circuitry of Fig. 8 requires appreciable time. This is because the time constant

(continued on p. 40)

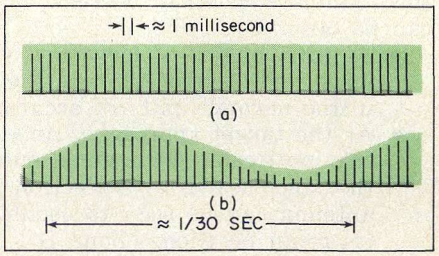

7. **Conical scan video display** shows the target on boresight (a) and off (b). The amplitude of the video pulses that occur at a rate of typically 1000 Hz is constant for boresight. If the target is off boresight, the video is modulated at the scan rate.

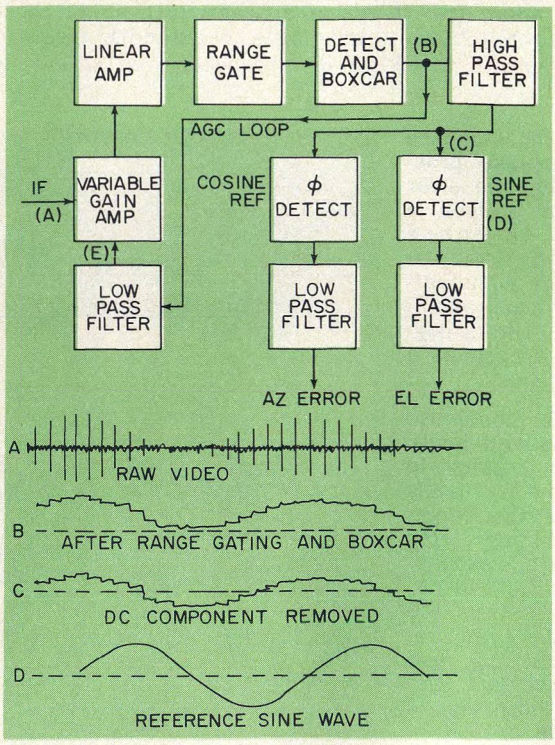

8. **The angle error** of a con scan radar is derived by this processing circuitry. The relevant waveforms are shown.

MICRO-COAX® ASSEMBLIES SAVE TIME, SPACE, AND MONEY

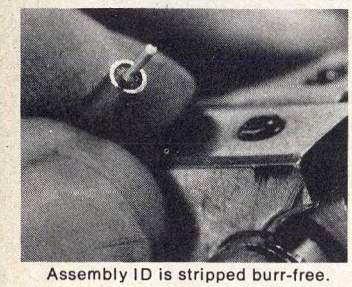

Assembly ID is stripped burr-free.

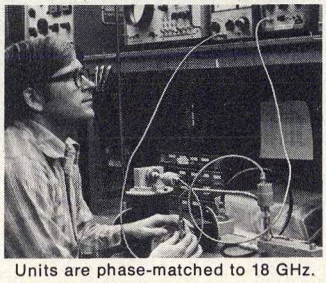

Units are phase-matched to 18 GHz.

That's why so many equipment manufacturers depend on Uniform Tubes for finished coaxial cable assemblies. The stripping is already done; the connectors are attached; the testing has been completed; Micro-Coax Assemblies are ready for installation. There is no need to develop assembly equipment or techniques, train personnel, set up testing procedures, or become involved in rejects or fluctuating connector and cable scrap rates.

Uniform, because of its expertise in coaxial cable and fabrication, and special assembly equipment, can provide simple or complex assembly configurations that deliver maximum power in minimum space. Micro-Coax Assemblies meet rigid mechanical and environmental requirements in phase matching, attenuation, and VSWR optimization.

Talk with a coaxial engineer at Uniform about your toughest problem today. Or better yet, send a print of a problem assembly — he may be able to point you in the direction of a solution.

UNIFORM TUBES, INC.
. . . . a UTI Company

Collegeville, Pa. 19426 • Phone: 215/539-0700
TWX: 510-660-6107 • Telex: 84-6428

READER SERVICE NUMBER 40

of the agc circuit must be long when compared to the scan period (typically 1/30 second) in order to remove the 30 Hz component at point E, Fig. 8. Thus, if the boresight moves appreciably with respect to the target over a time corresponding to the agc time constant, a source of error not present in monopulse radars will be present and, in particular, crosstalk between the elevation and azimuth channels will occur. The effect of this agc time constant can be eliminated by using logarithmic amplifiers, but there still remains the problem of boresight motion during the 1/30 second scan time (appreciably shorter than the agc time constant) which cannot be eliminated.

The observed behavior of conical-scan radar under multipath conditions is very similar to that of a monopulse radar. Simulation of the actual con-scan process generates the same equilibrium positions as those given for the monopulse radar in Figs. 5 and 6.

Attacking the problems of multipath

There are many theoretical solutions to multipath problems, but the majority can be discarded at the outset as being impractical. Increasing the frequency or aperture of the radar is an obvious, yet impractical solution, as is the use of a screen in front of and below the antenna to intercept the indirect reflected signal. Quite apart from the impracticality of such an arrangement at sea, it has been found when this was tried out on land, that the multipath problem was replaced by a diffraction problem over the top of the screen.

Filter processes are also inadequate to handle this problem. Conceptually, if the direct and indirect signals differ sufficiently in certain characteristics, then the two signals can be separated by some form of filtering in the receiver/data processor. The characteristics that could be used include time of arrival, frequency and polarization. Time-of-arrival filtering of multipath is based on the fact that the reflected signal lags behind the direct signal by a time corresponding to the extra path length it must travel. The path length difference is, however, very small: on the order of a few wavelengths. In a radar located at a height of 250 wavelengths over the sea, the path lengths difference is only 5 λ for a 0.5-degree elevation. It would be necessary to have a receiver with a 20% bandwidth to resolve two signals 5 λ apart. The situation rapidly becomes impossible at lower elevations.

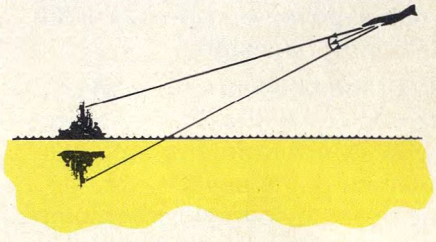

9. **Doppler difference between direct and reflected signals** is very small, for example, in the case of a missile diving at a ship.

As shown in Fig. 9, there could be a difference between the frequency of the direct signal and the frequency of the reflected signal. This difference will be very small, however, and in some cases, it's practically non-existent. To distinguish the direct from the reflected signals on the basis of frequency would require exceptional doppler resolution and even then the solution would not be applicable to all situations.

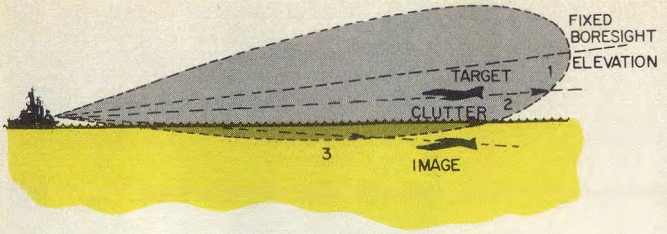

10. **In off-boresight tracking, it is necessary to maintain the boresight fixed at some angle** (of the order of 0.7 × beamwidth) **above the horizon.** This provides angular discrimination against both clutter and image. The numbers 1, 2, 3 on the beam refer to gain in direction of the target, the clutter, of the image, respectively.

At the frequencies and elevations considered, the grazing angle of the reflected ray is always less than the Brewster angle and therefore, the sense of circular polarization is not reversed. Since, in addition, the sea surface cannot convert a vertically polarized wave to a horizontally polarized one (or vice versa), no discrimination can be made on the basis of polarization.

In short, the separation of the direct from the reflected signal by simple filtering is not a viable solution.

Off-boresight and double null techniques maintain track

If the normal tracking operation of a radar is stopped by breaking the tracking loop, then while the target is still within the beam, its position can be determined by converting the error voltages to off boresight angles in azimuth and elevation.

In the "off-boresight tracking" method of dealing with multipath problems, the boresight is held at some angle (β) which is the order of 0.7 × beamwidth above the horizon. The error voltage is taken as giving the target elevation below this angle. By this method, some discrimination in angle is achieved since the image signal is attenuated by being appreciably further off boresight than the target (Fig. 10). In addition, the antenna is prevented from latching onto the image and perhaps losing track as in Fig. 6. This is by far the simplest approach since the changes required in the radar are minimal.

A monopulse radar with off-boresight tracking has circuitry designed to switch over smoothly from closed loop to open-loop operation (Fig. 11). The conversion of a conical-scan radar for off-boresight tracking at low angles is shown in Fig. 12. A boresight-control unit is added in the elevation tracking loop. (Note that the azimuth tracking loop remains unchanged since multipath only affects elevation tracking.) This boresight control unit senses when the

(continued on p. 42)

11. **Simple off-boresight tracking equipment** actually doesn't use switches which are only shown here to explain the principle of operation. In practice, the circuit automatically and smoothly changes from one mode to the other.

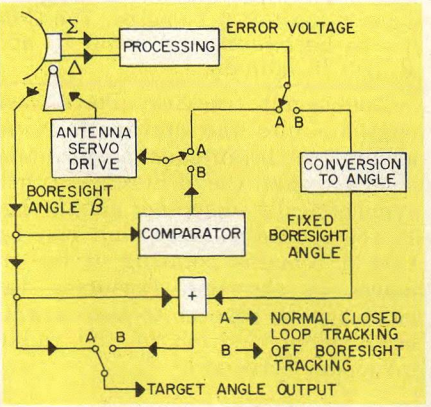

Fundamental Transistor Oscillators

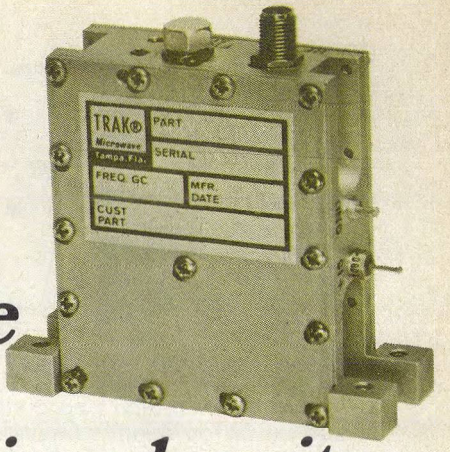

Solve Your Packing density Problems

Fit these oscillators into a very limited area and generate stable signals from 2500 MHz to 5000 MHz. All connections and tuning mechanism conveniently located to maximize use of small space. Check these specifications.

Frequency: 2500 MHz to 5000 MHz
f_C specified by customer within ±1 MHz
Tuning Range: Mechanical, ±1% min of f_C
Stability Over Temperature: ±0.05% (−20°C to +77°C)
±0.1% (−54°C to +77°C)
Pushing: ±0.005%/volt from DC to 3 kHz;
±0.001%/ volt, typical
Pulling: ±0.05% into 3.0:1 load VSWR, all phases;
±0.01%, typical
Output VSWR: 1.7:1 within ±300 MHz of f_C
RF Power Out: +10 dbm min
Power vs. Temperature: ±3 dB max; ±1 dB, typical
Turn-on Time: Full power within 1 second
Freq. within 0.1% of f_C < 1 min; 5 sec, typical
DC Power: +15V nom. @ 40 mA max; 25 mA, typical
Harmonics: −30 dB; −50 dBc, typical
Spurs: −80 dB
Size: 2.75" L x 1.0" W x 2.5" H
Weight: 5.0 oz max; 4.3 oz, typical
Connectors: SMA-F (RF), solder pin (DC)
Operating Temperature: −54°C to +77°C
Mounting: Base plate—Flange
Vibration: 25g, 10-100 cps
7g, 100-200 cps
Acceleration: 12g's any axis

TRAK

For further information, contact
TRAK Microwave Corporation
4726 Eisenhower Boulevard
Tampa, Florida 33614
Telephone 813- 884-1411
Telex 52-827

LITERATURE PRICES QUOTATIONS

☐ Please send me a free 96-page catalog today.

Name _____
Title _____
Firm _____
Address _____
City _____ State ____ Zip ____
Telephone _____

M4/6

READER SERVICE NUMBER 41

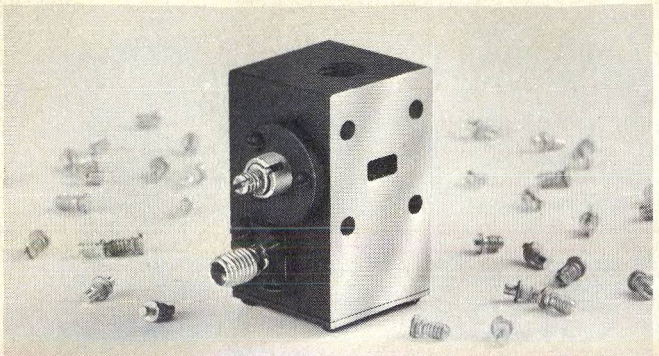

LOOK OUT—GUNNS FROM 6 TO 60
They said it couldn't be done but a better source of top quality, low cost, quick turn around GaAs Microwave Components is here

STANDARD
Lines consist of Gunn Diodes from 100 mw at 50 GHz to 500 mw in X-Band. Paramp pumps from 75 mw at 50 GHz to 150 mw in K-Band.

EXOTIC
If you have a requirement for a GaAs semiconductor or source and other people laugh, try us, we might be working on it now.

CMC central microwave company
1232 Harvestowne Industrial Dr., St. Charles, Mo. 63301
314-441-1455

READER SERVICE NUMBER 42

Safely house your communication and electronic equipment anywhere

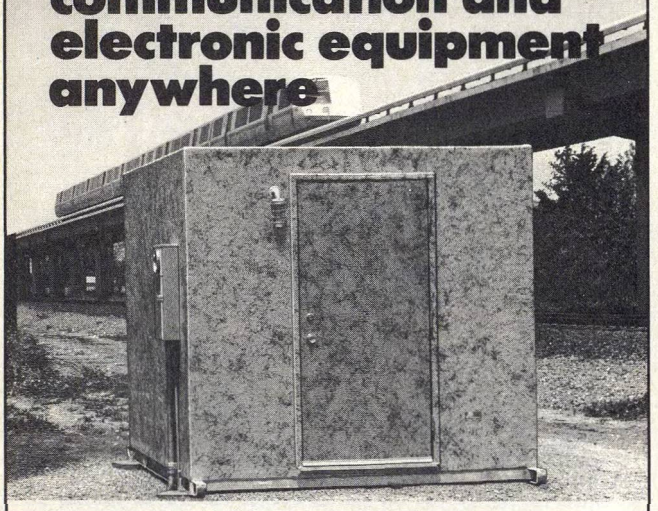

From the bitter-cold Arctic north to the blistering-hot desert south, Portatronic re-inforced fiberglass shelters are now housing sophisticated electronic equipment under the world's harshest climatic conditions.

Maintenance-free, prefabricated Portatronic shelters are more economical than building similar structures on the job site. Standard models are available or Portatronic can build to any specification. Wiring and equipment of your choice are factory installed. Call or write for free information.

PORTATRONIC
A Division of PORTA HOUSE, INC.
717 Kevin Court Oakland, CA (415) 562-9311

READER SERVICE NUMBER 38

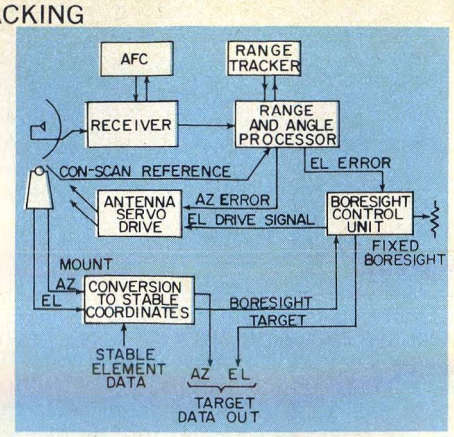

12. **A conical-scan radar modified for off-boresight tracking** has its elevation tracking loop broken so the "boresight control unit" can be inserted. The target elevation output is obtained by summing the boresight elevation with the off-boresight angle. The rest of the radar remains the same.

boresight reaches the required angle above the horizon and stops it at this angle for as long as the error voltage remains negative (indicating that the target is below the boresight). The elevation output is the boresight angle corrected by the estimated off-boresight angle derived from the error voltage.

A simulation of off-boresight tracking is shown in Fig. 13. Notice that the peak value of the error has been reduced by a factor of at least three, even with the assumption that the tracking radar in the normal mode does not nose dive and lock onto the image.

In trials at sea with this scheme, aircraft were flown in on a radial course at altitudes of about 100 ft. The radar operated in its normal mode on alternate runs and in the off-boresight mode on the other runs. The radar consistently lost track in the normal mode but never did in the off-boresight mode.

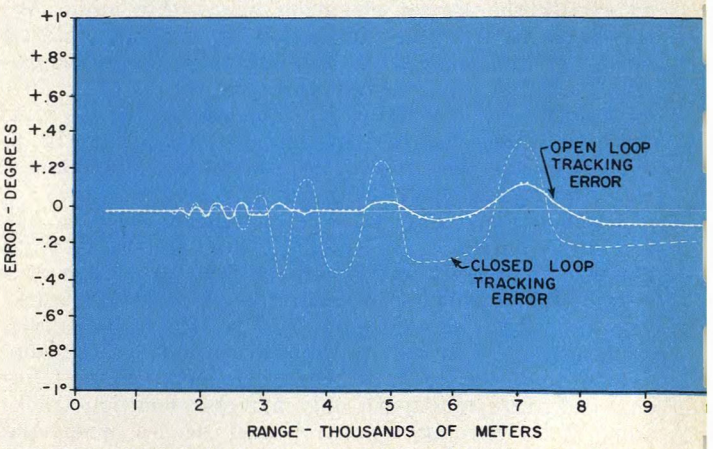

13. **Typical error in target elevation** estimation is shown here for normal and off-boresight tracking. The boresight is fixed at 0.7 degree. The C-band radar has a one degree beamwidth and is 50 ft. above water. Target is at 100 ft. altitude.

Double null tracking allows closed loop tracking to continue into the multipath region. It is based on generating an antenna pattern in a monopulse radar such as that the difference function has two nulls symmetrically disposed about the horizon, Fig. 14. If the second (lower) null can be made to move so that it remains pointing at the image as the target moves in elevation (assumed to be symmetrically located with respect to the target), then the normal equilibrium position of the radar will be with the target on boresight.[4]

(continued on p. 47)

Making use of quadrature components

Before we can obtain an even cursory understanding of how the quadrature components at the output can be used, let us first review some of the signals available in the receiver of a monopulse tracking radar. Basically, there are four unknowns in the general multipath situation: the angles at which the signals return relative to boresight (α_1 and α_2) and their phase and amplitude relations (ϕ and A). It is necessary, therefore, to make four independent measurements (i.e., obtain four independent equations) to solve the general problem.

Some simplifications are possible if certain assumptions are made:

- Assuming a flat earth and target range large with respect to antenna height. Then target elevation equals image depression.
- If a curved earth is assumed and if range can be measured (which is usually the case), then the image depression angle can be computed from the target elevation resulting in one fewer variable.
- Assuming the target re-radiation pattern is the same in the direction of the true radar as in the direction of the radar's image, then $A = \rho$. If the grazing angle is small, then $\rho \simeq 1$ and $A \simeq 1$.
- The phase change at the surface of the sea, can be assumed to be 180 degrees since the grazing angle is always small (this applies to both vertical and horizontal polarization). For a flat earth and a distant target, the total phase change is then simply a function of elevation: $\phi = (4\pi nh/\lambda) \cdot \sin\theta + 180°$.

Thus the problem can be considered to have one to four unknowns depending on the generalizations made.

Referring back to Fig. 4, the amplitude ratio and phase angle of Σ_R and Δ_R can be measured. This can best be carried out in practice by measuring the normalized in-phase and quadrature components of Δ_R using Σ_R as a reference. The standard monopulse radar tracking circuit already measures the in-phase component (Fig. 3). It is only necessary to add a 90 degree phase change in the Δ channel and a second phase detector as shown in Fig. 15 to measure the quadrature component.

For each additional independent beam, two more measurable quantities can be obtained in a similar fashion. Thus, if no assumptions are made as to the target immage symmetry or the reflection characteristics of the sea, then three independent beams are

(continued on p. 48)

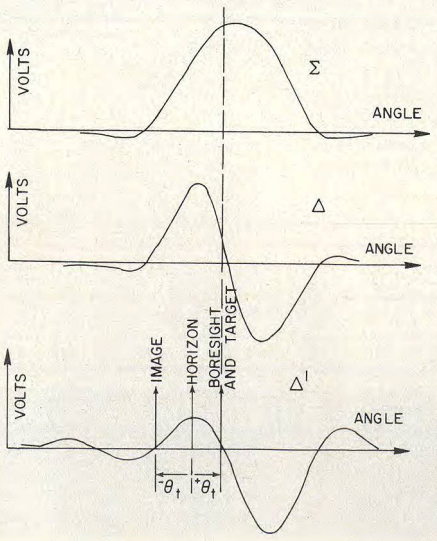

14. Modified Δ function for double-null tracking. Σ and Δ are the normal patterns for tracking in the clear. As the target approaches the horizon, a null is automatically generated in the Δ pattern (Δ′) at an angle $= -\Theta_t$ where Θ_t is the target elevation.

New from Sanders

Microwave Switches

SPST
SPDT

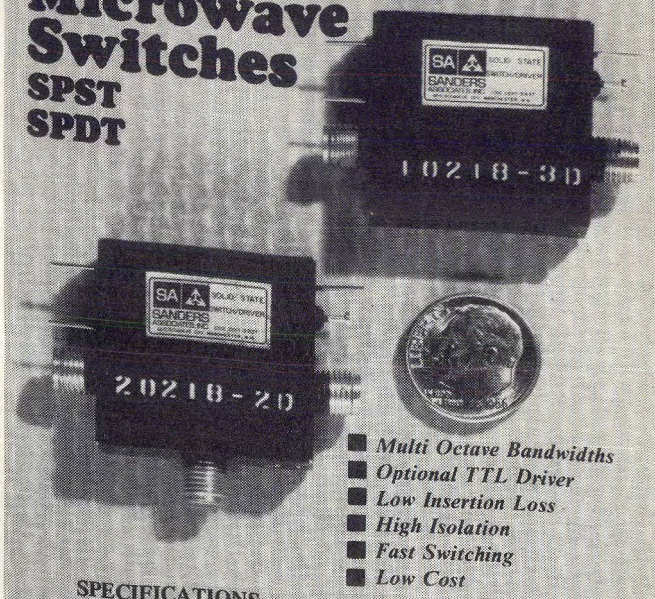

- *Multi Octave Bandwidths*
- *Optional TTL Driver*
- *Low Insertion Loss*
- *High Isolation*
- *Fast Switching*
- *Low Cost*

SPECIFICATIONS

Single Throw (without TTL Driver)

Model No.	Freq (GHz)	I.L.	Speed (N. Sec.)
DS10112	.5 – 12	1.0	5
DS10218	2 – 18	1.6	5
DS11002	.5 – 2	0.9	5
DS10208	2 – 8	0.5	5
DS10816	8 – 16	1.2	5

(1) Isolation > 20 db all units
(2) VSWR < 1.7:1 all units
(3) Size 1.1 X 1.1 X .038
(4) Integral Drivers

Double Throw (without TTL Driver)

Model No.	Freq (GHz)	I.L.	Speed (N. Sec.)
DS20112	.5 – 12	1.6	10
DS20218	2 – 18	2.0	10
DS21002	.5 – 2	0.7	10
DS20208	2 – 8	1.0	10
DS20816	8 – 16	1.6	10

(1) Isolation > 30 db all units
(2) VSWR < 1.7:1 all units
(3) Size 1.1 X 1.1 X 0.38
(4) Integral Drivers

SA SANDERS ASSOCIATES, INC.

MICROWAVE DIVISION
Grenier Field
Manchester, NH 03103
(603) 669-4615, ext. 447

READER SERVICE NUMBER 47

required with in-phase and quadrature measurements of the received signals as shown in Fig. 16. (A three-beam monopulse system is described in Reference 1).

In order to be able to solve the problem with a conventional two-beam monopulse system, either some of the assumptions listed above must be made, to cut down the number of unknowns; or some nulling process must be employed to eliminate the effect of at least two of the unknowns.

If the quadrature components E_p and E_q in Fig. 15, are plotted in x and y coordinates for a fixed boresight and varying elevation, a rough spiral is obtained, Fig. 17. This spiral can be calibrated in terms of elevation. This calibration, however, is only valid for a given situation where the reflection coefficient, ρ, does not change.[2,3].

Each complete loop of spiral corresponds to the target crossing a lobe in the pattern. If the radar is at normal height above the sea, however, (say 500 wavelengths), there will be a great many "cycles" in the spiral with the resultant ambiguities that are obvious from Fig. 17. It would seem, therefore, that this scheme is only applicable to radars that are located at only a few wavelengths above the reflecting surface.

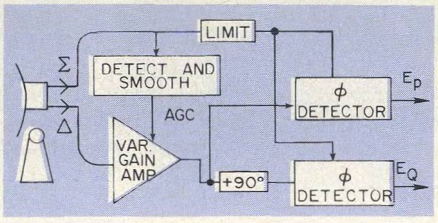

15. **Addition of another phase detector and a 90° phase shift** in the Δ channel enables the quadrature component of error to be determined as well as the in-phase component.

Nulling of quadrature components

If Fig. 4a is redrawn for a different boresight elevation angle, ϕ, the vector diagram of Fig. 4b will change and, in particular, the phase angle between Δ_R and Σ_R will change. If a boresight angle can be found such that Δ_R is in phase (or 180 degrees out of phase) with Σ_R, then Fig. 4 will reduce to the vector

(continued on p. 50)

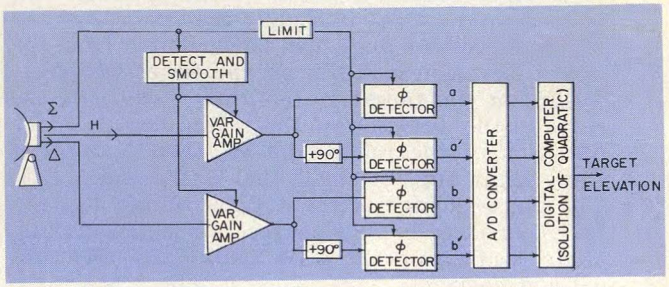

16. **This monopulse radar has three independent beams.** By adding a third beam to a conventional monopulse system and associated circuitry, four measurements can be made from which four unknowns can be derived.

BROADBAND SPIRAL ANTENNAS

Model A2200 1 to 18 GHz

- Gain: 0 dB min.
- Polarization: RHC or LHC
- Axial Ratio: 3 dB max.
- 3 dB Beamwidth: 80° nom.
- VSWR: 1.8:1 max.
- Size: 6.9" D, 4.2" H
- Weight: 2 lbs, 9 oz.
- Environ. Spec.: Mil. E 16400

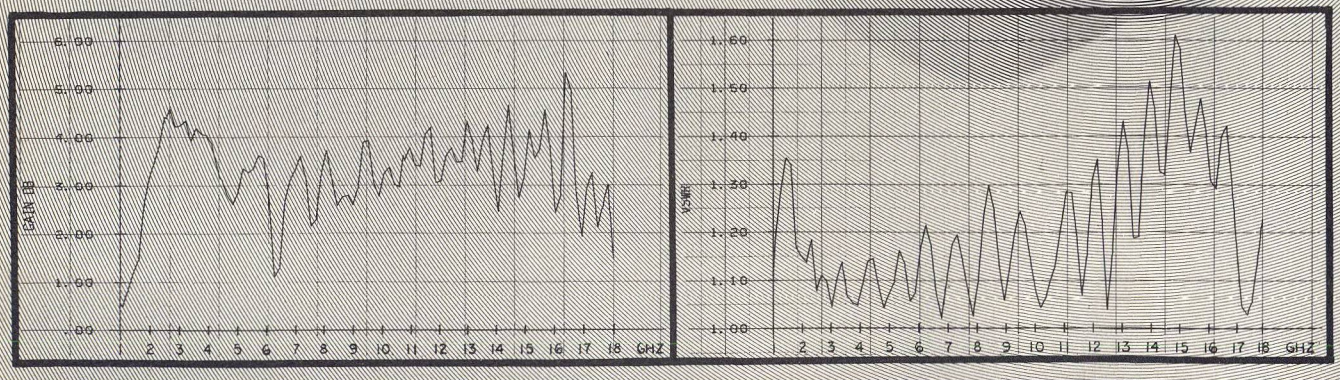

Planar spirals from 0.1 to 40 GHz
Conical spiral omnis from 0.1 to 18 GHz
Complete DF systems including controls and displays

EM Systems, Inc. 750 Kifer Road, Sunnyvale, California 94086 Telephone (408) 733-0611

READER SERVICE NUMBER 48

NEW CMOS Low Current R.F. Switches

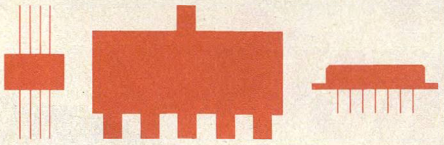

A New Series of Multipole RF Switches now available from Daico Industries have extremely low current requirements. One milliamp from a five volt supply will operate a Daico CMOS switch with up to five poles. A five to 15 volt level is also acceptable. The low current CMOS switch is directly compatible with open collector T²L logic.

These diode switches exhibit excellent performance over the range 20 MHz to 500 MHz and in multi-octave frequency bands from one MHz to 1500 MHz.

Daico CMOS Series solid-state switches may be ordered in FLAT PACK, DIP or with conventional connector packaging.

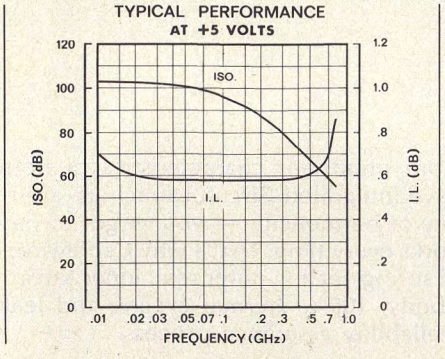

Low-Current Step Attenuators & Step Delay Line/Phase Shifters are also available.

DAICO INDUSTRIES, INC.

2351 East Del Amo Blvd., Compton, Calif. 90220
Telephone: (213) 631-1143 · TWX 910-346-6741
©1976 Daico Industries, Inc. mp 76401

READER SERVICE NUMBER 50

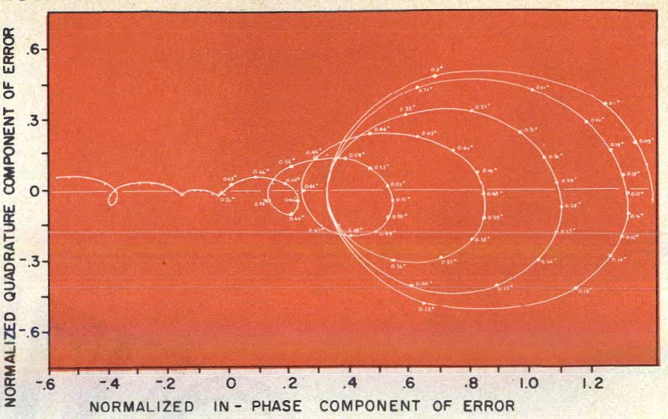

17. **Relationship between in-phase and quadrature components** of the error voltage in a 2 beam monopulse radar has this spiral relationship. Each complete loop corresponds to the target crossing a lobe in the pattern. In this case, the C-band radar has a beamwidth of one degree and is 50 ft. above water. Boresight is fixed at 0.7°. Flat earth is assumed.

diagram of Fig. 18b. In this figure, two triangles shown are similar and,

$$\frac{\Delta_R}{\Sigma_R} = \frac{\Delta_d}{\Sigma_d} = \frac{\Delta_i}{\Sigma_i}$$

Now Δ_R/Σ_R is the measured error voltage and Δ_d/Σ_d is the error voltage that would exist if the image were not present. If therefore, the boresight can take a position such that the quadrature component of error is zero, the in-phase component of error will indicate the true off-boresight angle of the target just as though the image were not present.

It is only possible to position the boresight in this manner if the error function has the S-shape shown in Fig. 19. The easiest way to implement this technique is to have an antenna pattern such that the error function is symmetrical about the peak as shown in Fig. 20. The peak of the error function should then be pointed in the direction of the bisector of the target/image angle. It can be shown that this angle is given simply by the ratio of antenna height to target range for a curved earth so that the boresight should be programmed to vary its elevation angle accordingly[5].

Specular and diffuse reflections

So far, we have dealt mainly with the dominating problem of specular reflection even though diffuse reflection will exist simultaneously with specular reflection. If the sea is glassy smooth, the radar will behave as shown in Fig. 2. As the sea gets rougher, the specular reflection coefficient will decrease and

(continued on p. 53)

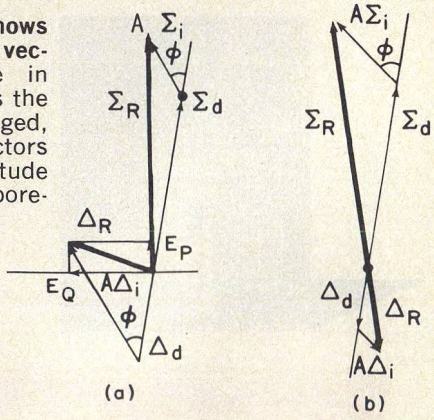

18. **This diagram shows a change in Σ, Δ vectors** with change in boresight angle. As the boresight is changed, the Σ_R and Δ_R vectors change in amplitude and phase. If a boresight is taken, such that the Δ_R is in phase or 180° out of phase with Σ_R, the error E will be the same with or without multipath.

LOW ANGLE TRACKING

19. **To achieve perfect off-boresight tracking,** the error function must have an S shape so that E_d can be made equal to E_i.

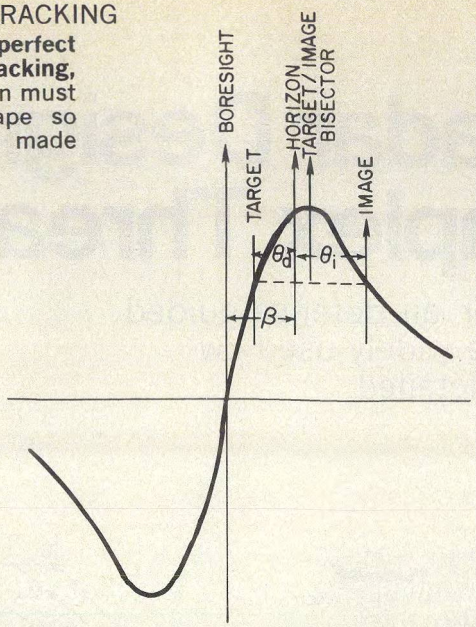

20. **With a symmetrical error function,** it is only necessary to point the peak of the error function in the direction of the target/image bisector in order to achieve $E_d = E_i$.

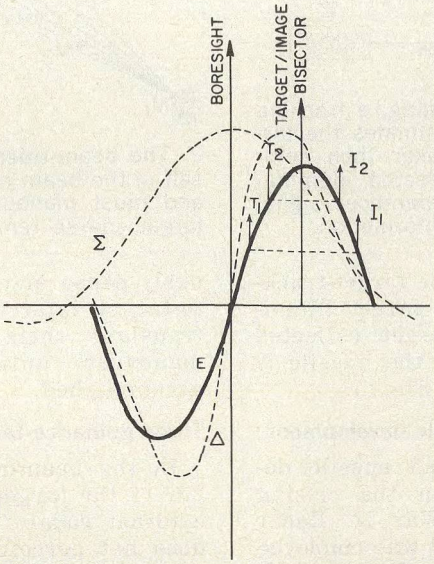

the diffuse reflection coefficient will increase. The motion of the radar will become more and more erratic and unpredictable.

In addition, since reflection will then take place from a large number of facets over a large area (the "glistening area"), there will be a noisy contribution introduced into the azimuth track as well as the elevation track.

For quantitative analysis of diffuse reflection, the reader is referred to Reference 6. However, since the off-boresight tracking technique already described discriminates on the basis of angle, it will serve just as well to reduce the effect of diffuse reflection as it does specular reflection. ••

References

1. Drabowitch and Methais, "Augmentation Du Pouvior Separateur D'Une Antenne Par Decomposition Du Champ Recu En Distributions Orthogonales," Onde Electrique. (February 1963).

2. Sherman, "Complex Indicated Angles Applied To Unresolved Radar Targets and Multipath," *IEEE Trans. Aerospace Electronic Systems,* Vol. AES-7, (January, 1971).

3. Howard, et al, "Experimental Results Of The Complex Indicated Angle Technique For Multipath Correction," *IEEE Trans. Aerospace Electronic Systems,* Vol. AES-10, (November, 1974).

4. White, "Low Angle Radar Tracking In The Presence Of Multipath," *IEEE Trans. Aerospace Electronic Systems,* Vol. AES-10, (November, 1974).

5. Dax, "Accurate Tracking Of Low Elevation Targets Over The Sea With a Monopulse Radar," "Radar, Present and Future," *IEEE Conf. Pub. London, 105,* (October, 1973).

6. Barton, "Low Angle Tracking," *Proc. IEEE,* Vol. 62, No. 6, (June, 1974).

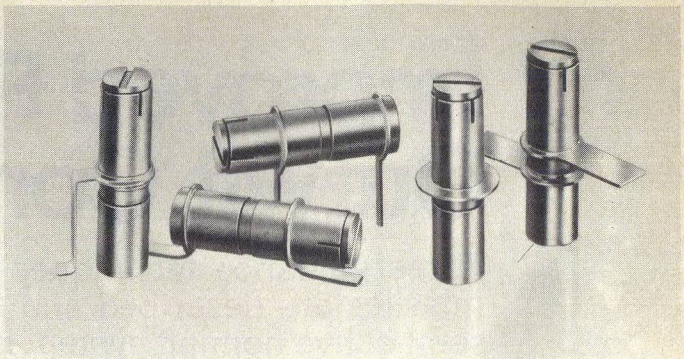

GIGA-TRIM CAPACITORS FOR MICROWAVE DESIGNERS

GIGA-TRIM (gigahertz-trimmers) are tiny variable capacitors which provide a beautifully straightforward technique to fine tune RF hybrid circuits and MIC's into proper behavior.

APPLICATIONS

- Impedance matching of GHz transistor circuits
- Series or shunt "gap trimming" of microstrips
- External tweaking of cavities

Available in 5 sizes and 5 mounting styles with capacitance ranges from .3 - 1.2 pf to 7 - 30 pf.

Johanson®

MANUFACTURING CORPORATION
Rockaway Valley Road
Boonton, N.J. 07005
(201) 334-2676 TWX 710-987-8367

READER SERVICE NUMBER 53

Solve grounding/shielding problems quickly, economically!

The wide variety of Instrument Specialties beryllium copper contact strips and contact rings in many sizes and shapes can help you solve your shielding and grounding problems. Standard catalog items work for most applications, but special adaptations are easily made and provide you with virtually a custom-designed part with only a one-time extra charge.

Send for inexpensive trial kits!

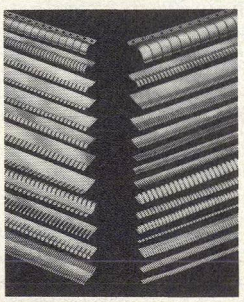

34 strips, various configurations: Assortment 97-272 . . . . . $25.00

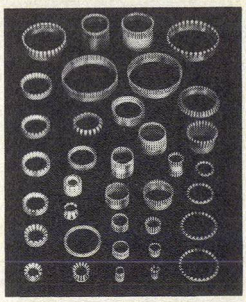

36 different contact rings: Assortment 97-273 . . . . . $20.00

FREE! Complete catalog of RFI-EMI shielding strips and rings. Write, or use Reader Service Card.

INSTRUMENT SPECIALTIES COMPANY, Dept. MW-82
Little Falls, N.J. 07424
Phone — 201-256-3500 • TWX — 710-988-5732

Specialists in beryllium copper springs since 1938

READER SERVICE NUMBER 54

Improved Radar Designs Outwit Complex Threats

Three guidance techniques for air-defense guided missiles are described and the widely-used cw semi-active homing system is detailed.

THE objectives of any air-defense missile system are to locate, track and destroy any hostile aircraft before it reaches its target. Over the years, as threat aircraft and other targets have become more sophisticated, the demands upon the design of air-defense systems have challenged the ingenuity of microwave design engineers.

Radar guided missiles today form one of the largest markets for microwave components and subsystems. In the "real world" of radar, where a quantity of more than two has been defined as production,[1] to think of over 50,000 systems may seem staggering. Yet in the past 20-25 years, this has been the magnitude of the radar guided air defense missile business. Except for phase shifters for phased arrays, no other microwave hardware is truly mass produced on such a scale.

There are many necessary functions which must be successfully performed in order to permit a lethal interception of the target by a guided missile. These include initial target detection, launching the missile, successful operation of the propulsion, guidance and control systems during flight and fuzing and detonation of the warhead at intercept. Only the guidance aspects will be discussed here.

There are three types of guidance techniques commonly used in air defense guided missiles: (1) beam riding, (2) command guidance and (3) homing. All can employ radar sensors. The most widely used is the semi-active radar homing, in which the target-tracking radar provides target illumination and the target reflected energy received by the missile is used for guidance (Fig 1).

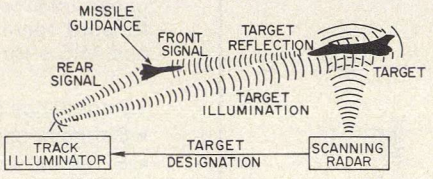

1. **In semi-active homing,** a tracking radar tracks and illuminates the target. The missile seeker then compares the target reflected illumination with its rear (reference) signal to extract guidance information.

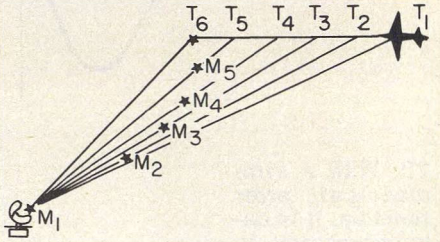

2. **The beam-rider missile** centers itself in the beam of the tracking radar and must maneuver even when the target course remains constant.

Kamikazes spur missile development

Air-defense guided missile development began in the closing months of World War II. Radar fire control of guns was employed and could extract a relatively high attrition rate from an attacking force. In the face of determined penetration attempts at low altitudes, such as Kamikaze attacks on the U.S. Pacific Fleet, a much higher degree of success was necessary. Even a handful of successful penetrators could inflict great damage.

The objectives of air defense missile systems are to achieve virtually 100% effectiveness, to prevent even a single aircraft from reaching its target. In order to approach this level of performance with a reasonable number of missiles, the accuracy of any single missile must be very high, and a high single shot kill probability is essential.

To achieve this accuracy, a guidance system substitutes automatic closed-loop control for the open-loop calculation and prediction employed in conventional artillery control. The function of the guidance system is to continuously sense errors in the missile-to-target intercept geometry and translate them into corrective maneuvers until interception is accomplished.

Three guidance techniques

In the beam-rider system, Fig. 2,[2,3,4,5] the target is tracked by an external radar. The missile itself does not perceive the target, but detects its own position relative to the radar-beam tracking the target. By keeping itself centered in the beam, it attempts, like the radar beam it rides, to pass through the target. Since the missile is always on a line between the radar and target, it must continuously maneuver to remain in this line even when the target is flying a straight-line course. This course requires severe corrective maneuvers near intercept. Another drawback is that any angular tracking error at the radar becomes a larger linear error as the range is increased. The accuracy of a beam-rider system is, therefore, inversely proportional to target range.

In a command-guidance system, (Fig. 3), the target is again tracked by an external radar. The missile itself does not perceive the target. A second radar tracks the missile. Measurements of both target and missile position are fed

(continued on p. 56)

Alex Ivanov, Staff Engineer, Division Headquarters, Raytheon Company, Missile Systems Division, Hartwell Road, Bedford, MA 01730.

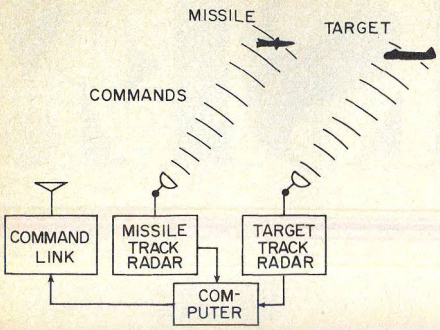

3. **Command-guidance systems** use data from separate target tracking and missile-tracking radars to compute the missile maneuver required for intercept.

to a computer which calculates the missile trajectory required for intercept and develops the needed commands. These are continuously transmitted to the missile. A more efficient trajectory can be used, since there is no need for the missile to fly along the radar target line-of-sight. A lead collision course can be plotted and prediction based on rate of change of position, rather than only-position information, can minimize the terminal maneuver. However, once again, accuracy is inversely proportional to range, since a fixed angular error at the radar is magnified at increasing ranges.

The homing missile is the most intelligent of the three, but also the most complex. It perceives the target with its own radar and computes its own control signals. Various types of homing systems exist, depending on the source of the energy which is sensed. Passive homing uses energy originating at the target. An active homing missile transmits its own radar energy at the target and receives target-reflected echoes. In a semi-active system, an external radar illuminates the target and the missile receives the reflected-target echoes.

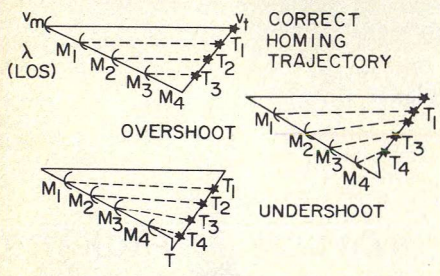

4. **Line-of-sight (LOS) rate** remains constant when missile and target are on a collision course.

Homing guidance[3,6]

In a homing missile, a collision course is characterized by a line-of-sight (LOS) from missile-to-target which does not rotate, (Fig. 4). Any rotation of the LOS is indicative of a deviation from a collision course which must be corrected by a missile maneuver.

In proportional navigation, the missile rate of turn is made proportional to the rate of turn of the LOS. The choice of the constant of proportionality (navigation ratio or N) affects the trajectory, such that increasing values of N cause early correction of collision course errors, reserving the missile's maneuver capability near intercept for countering target maneuvers and noise, the relationship being:

$$n_L = N' V_C$$

where: n_L = lateral acceleration
N' = effective navigation ratio
V_C = closing velocity
λ = rate of change of the line-of-sight

As the missile gets increasingly closer to the target, the quality of the target information continually improves, since, as range decreases, an angle error results in a lesser linear error.

The fundamental limit on accuracy is the target's own angle noise (glint or scintillation) and is independent of intercept range.

The most widely-used systems have, over the years, employed semi-active homing. Since the active system differs only by virtue of the presence of the illuminator transmitter on board the missile, the following discussion of the semi-active system can be easily extended to cover the active system as well. Similarly, passive homing can be considered a subset of the semi-active.

Illumination radar waveforms

Semi-active systems employing various waveforms such as pulse-cw, pulse doppler (pd) and more sophisticated coded pulse techniques have been designed and built over the years.[5,7] The cw is the simplest and at the same time, provides low-altitude capability by discriminating against clutter on the basis of velocity or doppler frequency. Conventional pulse systems have been used but are not suitable for high clutter environments.

The illumination for a semi-active missile system can be provided by a cw tracking radar, a cw transistor slaved to another tracking radar, or a pulse or pulse doppler tracking radar at another frequency with the cw illumination injected into the antenna system from a separate cw transmitter. The tracking cw illuminator is generally a two-dish radar, because sufficient receiver/transmitter isolation cannot usually be achieved in a single-dish system. Where space constraints preclude use of two separate antennas, such as in a fighter aircraft, the cw injection technique is used.

An alternate way to use a single dish tracking illuminator is to employ high-duty-cycle pd (30-50%) and achieve the isolation by conventional TR switching. In the receiver, however, only the central line of the pd spectrum is employed. The prf is chosen high enough to yield unambiguous doppler, thus when the receiver selects the central line, the spectrum is identical to the cw case. The receiver can use a range gate, or merely accept the loss resulting from using only the central line power of the pd spectrum. In either case, the rest of the receiver and signal processing is the same as for the cw system. The semi-active seeker implementation for a pd illuminator follows this same pattern. This is also the most common approach for an active seeker.

Low-duty-cycle pd (less than 10%) can also be used, but for this case, the loss would be prohibitive if only the central line power were used. Low-duty-cycle systems, therefore, use range gating to optimize performance. The range-gated system also provides range resolution, in addition to retaining the doppler resolution capability of the cw systems.

Phased array increases fire power

In a semi-active system, the target must be continuously illuminated, which means an illuminator must be constantly aimed at the target during an engagement.[5,7] This constrains the number of targets that a given system can engage. However, mechanically-gimballed radars are forced to live with the limitation of one radar tracking only a single target (or formation of closely-spaced targets).

The advent of phased-array radars allowed a single transmitter to illuminate many targets by sequentially jumping its agile beam from one target to the next one. Of course, the illumination would no longer be continuous, and the missile would have to operate in a sampled data mode, extracting

(continued on p. 58)

Super Power (cont'd)

NEW 3 kW AIR-COOLED JUNCTION CIRCULATOR

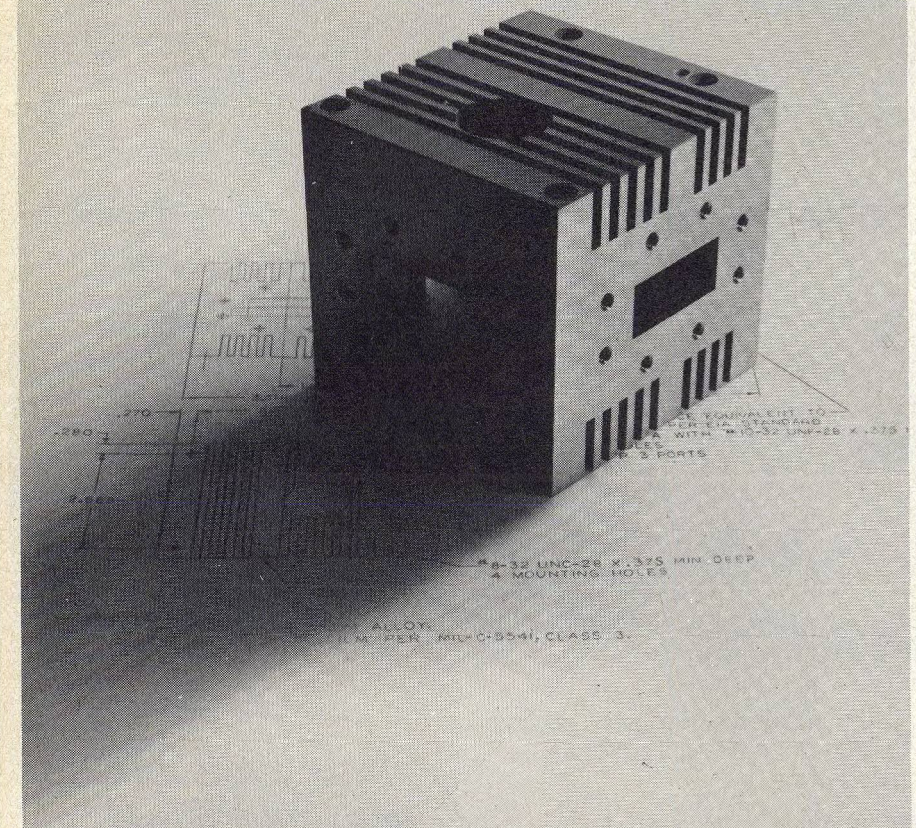

The model FCW-1528 Waveguide Junction Circulator is a new addition to Merrimac's expanding line of high power ferrite products. Designed for the 5.925 GHz to 6.425 GHz frequency range and featuring less than 0.15 db insertion loss and more than 20 db isolation, this device is ideal for protecting power amplifiers against energy reflected from mismatches.

Other "Super Power" circulators include:

- Four-port differential phase shift circulators operating from 1.12 GHz to 18 GHz with average power to 30 kW and peak power to 10 megawatts.
- Coaxial circulators from 150 MHz to 2.5 GHz with average power to 20 kW and peak power to 1 megawatt.
- Waveguide Junction Circulators from 2.4 GHz to 18 GHz with average power to 5kW and peak power to 1 megawatt.

For more information on these and other ferrite devices, call or write:

MERRIMAC INDUSTRIES, INCORPORATED
41 FAIRFIELD PLACE, WEST CALDWELL, N. J. 07006 • (201) 228-3890 • TWX 710-734-4314

READER SERVICE NUMBER 58

information during the time its target was illuminated, and then holding the information until the next sample. The illumination could be cw during the dwell time of the radar beam on the target (interrupted or keyed cw) or use a pd or more complex waveform. By removing the one radar-one target constraint, an increase in firepower can be realized.

Whereas the simple cw systems generally home all the way from launch to intercept, in the more sophisticated systems, homing is generally used for only the last few seconds of flight. In these systems, a midcourse phase (inertial, beam rider or command) is employed to get the missile to an appropriate point on its trajectory, where it acquires the target and enters the terminal homing phase of its flight. This is more efficient from the standpoint of both missile trajectory and radar power. The missile can fly out to longer ranges by a commanded or inertial up-and-over trajectory, spending less time in the denser air at low altitude. The radar power needed for illumination is seized by the terminal phase of flight, a fraction of the total intercept range. Midcourse commands impose much less severe demands on the radar power since this is a one-way transmission path.

Pulse-compression radar was introduced to achieve very fine range resolution at long ranges without extending the peak power capability of transmitters. To retain compatability with these complex waveforms, a variation of semi-active homing called TVM (target-via-missile) evolved. The target-reflected illumination is received in the missile, but instead of being processed on board is retransmitted to the illuminating radar where the complex waveform is processed and guidance information extracted. The actual steering commands are then transmitted to the missile as in a command guidance system.

Cw semi-active guidance[2,5,7]

In the semi-active system, the missile receives the target reflected illumination in its front antenna and a sample of the directly received illumination (often through sidelobes of the illuminator antenna) in its rearward-looking reference antenna. The front and rear signals are coherently detected against each other, resulting in a spectrum which contains the doppler-shifted target signal at a frequency roughly pro-

(continued on p. 60)

acronetics

Broadband Multiplexers
500 MHz to 18 GHz

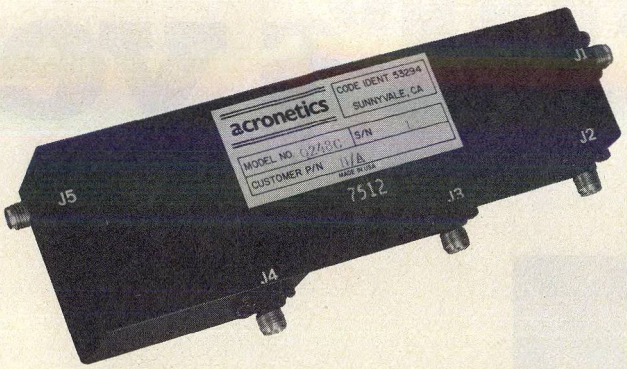

Separate or combine signals in this frequency range into up to octave contiguous bands.

Modular Design for Fast Delivery

Individual sections are pretuned for rapid assembly into diplexers, triplexers, quadruplexers or pentaplexers.

Production Capability

We are currently delivering qualified units in large quantities and are ready to meet your requirements.

Stable Crossovers

500 MHz and 1, 2, 4, 8, 12 GHz with state-of-the-art temperature drift specs from −55°C to +120°C.

Low Loss/High Rejection

- ☐ 1 dB in band
- ☐ 4.5 dB at crossover
- ☐ 60 dB within 15% of crossover

acronetics

955 BENICIA AVE., SUNNYVALE, CA. 94086
PHONE (408) 245-8000 TWX 910-339-9365

An Operating Company of Wavecom Industries

READER SERVICE NUMBER 60

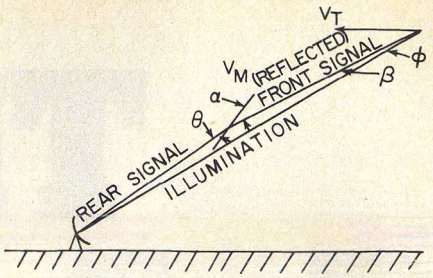

5. **Semi-active system geometry** results in a doppler-shifted target signal with a frequency roughly proportional to closing velocity.

portional to closing velocity. A narrowband frequency tracker searches the spectrum and is used to lock onto this target doppler and extract guidance information from it. The cw tracking illuminator functions the same way, except the rear signal is replaced by a sample of the transmitter output.

The doppler relationships for a ground-based semi-active system geometry (Fig. 5) are:

$$f_{d\ rear} = -\frac{f_o}{c} V_M \cos \Theta$$

$$f_{d\ front} = \frac{f_o}{c} (V_T \cos \phi + V_T \cos \beta + V_M \cos \alpha)$$

$$f_d = f_{d\ front} - f_{d\ rear} = \frac{f_o}{c} (V_M \cos \Theta + V_M \cos \alpha + V_T \cos \phi) + V_T \cos \beta)$$

$$\text{Closing Velocity} = V_c = V_M \cos \alpha + V_T \cos \beta$$

for the head on case $_1 \alpha_1 B, \Theta, \phi = 0°$

$$V_c = V_M + V_T$$

$$f_d = \frac{f_o}{c} 2 V_c$$

$$\approx 20 \text{ Hz/ft/sec at X-band}$$

For a ship-based or airborne illuminator, an additional component—illuminator velocity—must be considered. It does not fundamentally affect the spectrum except to broaden the clutter return (adding reflections from clutter patches illuminated by backlobes or sidelobes of the illuminator which now have a velocity component rather than all being at a fixed frequency). The doppler shift at X-band corresponds roughly to 20 Hz per 1 ft/sec of closing velocity. Scaling is a convenient way to handle other velocities or microwave frequencies.

A representation of the signal spectra seen by a semi-active seeker, for both fixed and airborne cases, is shown in Fig. 6. It should be noted that the target signal must compete with clutter and with feedthrough or spillover of the illumination into backlobes

(continued on p. 62)

TerraCom gives you anything you want in 1-15 GHz portable microwave radio

FIXED TUNED TCM-5 SERIES

FIXED TUNED, XTAL controlled 1.7 to 15.25 GHz for voice, video and data.

TUNABLE, direct reading calibrated dial in each frequency band.

MOBILE OPERATION, AC or DC in light weight rugged construction.

FIXED INSTALLATION, rack mount, R.F. multiplexed, hot standby and diversity.

TUNABLE TCM-6 SERIES

When you operate TerraCom microwave radios, you know you have reliable and high performance equipment working for you. More than that, you have the best factory support in the business. TerraCom makes a special effort to know, and keep on knowing, everyone who has TerraCom microwave radios and to provide them with fast, responsive service, same day dispatch of free-loaner replacements worldwide, and leasing additional portable links.

TerraCom microwave gives you all frequency bands—all types of transmission—with the best in performance and maintainability and with friendly, personal customer service. We're a high quality company with high quality microwave radio systems. You should look into it—you will like the quality.

CALL (714) 278-4100 FOR IMMEDIATE INFORMATION OR WRITE:
9020 Balboa Avenue
San Diego, California 92123

TERRACOM

RELIED ON THROUGHOUT THE WORLD

READER SERVICE NUMBER 62

When it comes to value...

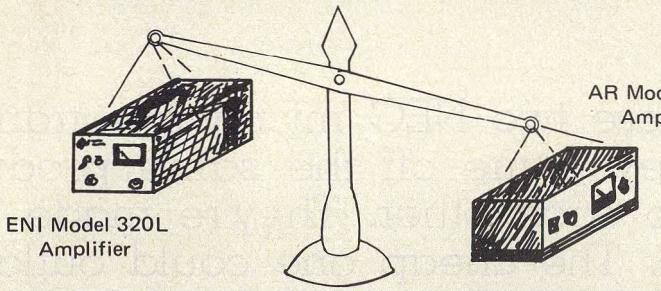

Model 30LA is a HEAVYWEIGHT

Feature-for-feature, the Amplifier Research Model 30LA broadband amplifier outweighs the ENI 320L. This rugged, high performance amplifier provides a minimum 30-watt output from 1-110 MHz. It offers a directional power meter, adjustable gain control, infinite mismatch tolerance, and low harmonic distortion.

If your considering an ENI 320L or any other ENI amplifier, send us the model number. We'll provide you with specifications on a competitive unit.

FOR COMPLETE DATA CALL 215-723-8181

ar AMPLIFIER RESEARCH

Amplifier Research
160 School House Road
Souderton, Pa. 18964

YOUR BEST SOURCE FOR RF POWER AMPLIFIERS

READER SERVICE NUMBER 64

of the seeker antenna, which can be many orders of magnitude greater than the target signal.

There are three main problems which must be addressed in connection with these large interfering signals. One is the need to prevent lock on the clutter signal, which in some geometries may be a spectrally narrow signal, resembling a target signal. This is generally accomplished by limiting the portion of the doppler spectrum which is searched during the acquisition process, to exclude the clutter frequency.

The second problem is often termed the subclutter visibility (SCV) or subfeedthrough visibility (SFV) problem. In essence, this refers to the maximum ratio of clutter (or feedthrough)-to-signal with which the system can operate. This, in its simplest form, can be related to the dynamic range of the seeker receiver, including not only possible suppression of the target signal by the clutter or feedthrough, but also potential cross modulation or intermodulation effects.

The third problem is also related to SCV (and SFV), and is concerned with the spectral purity of the transmitter and the local oscillator. The spectrum of Fig. 6 will be broadened by fm noise, so that noise sidebands will appear at the target doppler frequency and mask the target signal. Considering the magnitude of feedthrough or clutter, it can be seen that very low fm noise is required to prevent performance degradation.

The spectra for a cw tracking illuminator are similar to Fig. 6 except that clutter occurs at zero doppler, or the same frequency

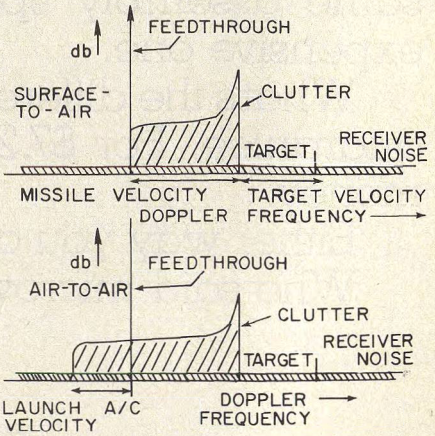

6. **The doppler spectrum contains clutter** at a maximum frequency corresponding to missile velocity. The feedthrough (or spillover) signal occurs at zero doppler.

(continued on p. 65)

as the feedthrough. Thus, the first problem—locking on clutter—does not exist. The second and third problems, however, are worse since the transmitter leakage into the receiver will usually be much higher than feedthrough in the missile seeker. Consider, for instance, a feedthrough-to-signal ratio of 100 dB. Assuming a 10 dB S/N requirement for detection, a 1 kHz detection bandwidth and a doppler of 10 kHz, the fm noise in a 1 kHz band at 10 kHz from the carrier must be 110 dB down from the carrier. A sideband-to-carrier ratio (sb/c) of −110 dB corresponds to a modulation index of 4.48×10^{-6}, or an equivalent rms noise deviation of 0.0448 Hz/kHz at 10 kHz. As transmitter power is increased, the fm noise must be correspondingly reduced to prevent it, rather than receiver noise, from limiting detection performance. For the higher-power radars, therefore, some form of feedthrough cancellation as well as transmitter noise reduction techniques are employed.

Missile seeker development

The simple missile seeker for a cw semi-active system, shown in Fig. 7, is typical of the earliest systems developed in the late 1940's and early 1950's.[5,7] It consists of rear receiver, a front receiver, a signal processor and a tracking loop to control the gimballed seeker (front) antenna. The missile also contains an autopilot to guide it and stabilize the airframe, a fuze to detonate the warhead at the optimum time, and a source of electrical and hydraulic (in most missiles) power.

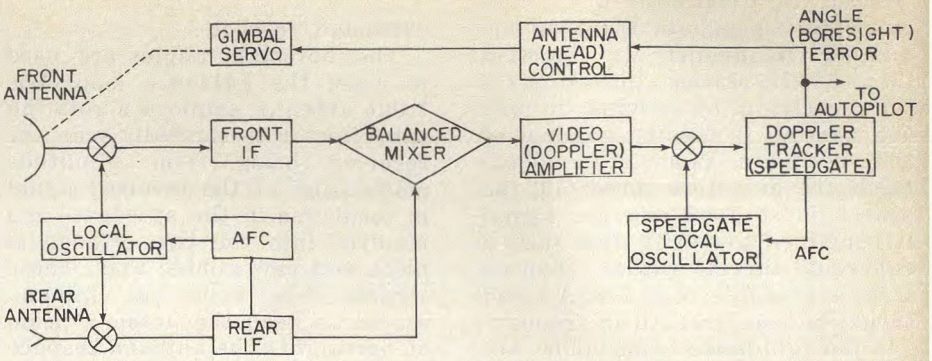

7. **The simplest cw semi-active seeker** extracts the target doppler by coherently detecting the front signal against the rear signal.

The purpose of the rear receiver is to provide a coherent reference for detection of the front (target) signal. The rear signal, after conversion to i-f, closes the afc loop around the microwave local oscillator (LO) and acts as the reference for the i-f coherent detector. The target signal, received in the front antenna, is heterodyned to i-f and amplified in a relatively wideband amplifier. It is then converted to doppler in the coherent detector. The doppler signal is amplified in the video amplifier which has a bandwidth equal to the total range of possible dopplers, and is then heterodyned with the speedgate LO, which tracks the desired signal in the narrow speedgate (sometimes called the velocity gate or doppler tracker).

Target acquisition is accomplished by sweeping the frequen-

(continued on p. 66)

ENGELMANN MAKES IT!

ULTRA-MINIATURE COUPLERS/HYBRIDS 0.375" THICK

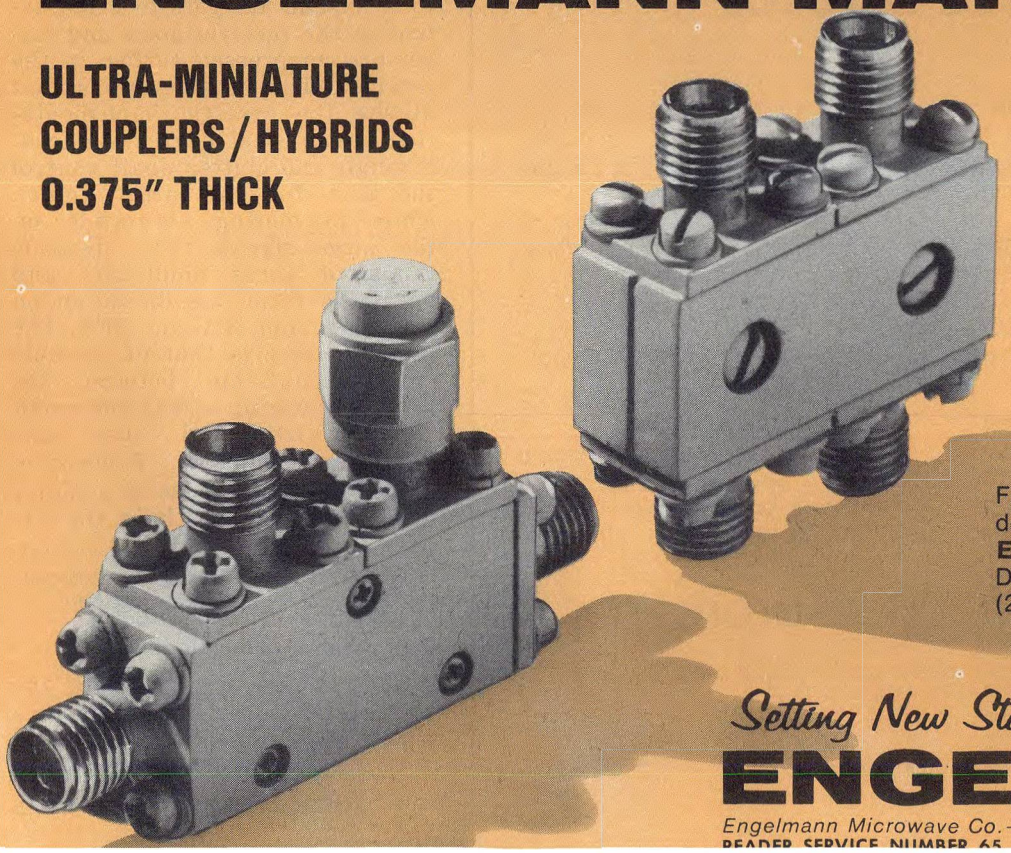

- 0.2-18 GHz in Octave + B.W.
- Sealed Stripline Construction
- 3, 6, 10, 20, 30 db standard val
- 1" x 0.5" x 0.375", 4 GHz & UP
- Exceeds requirements of MIL-C-15370C
- Custom coupling values avail
- Directivity typically > 20 db
- Price $105 ea.

For detailed literature or custom design information, contact **ENGELMANN** Microwave Co., Sky Drive, Montville, N.J. 07045, (201) 334-5700.

Setting New Standards in Reliability

ENGELMANN

Engelmann Microwave Co.— Subsidiary of Pyrofilm Corporatio

READER SERVICE NUMBER 65

cy of the speedgate LO over the doppler bandwidth (or portion thereof). In essence, this examines the spectrum by moving it past the narrow frequency window of the speedgate. When a signal exceeds the detection threshold, the search is stopped and the signal is examined to verify that it is a coherent target rather than a false alarm due to noise. A valid target is then tracked in frequency and guidance commands are extracted from it.

The boresight angles are used to close the guidance loop. The front antenna employs a rotating subreflector to conically scan the received beam. The amplitude modulation of the received signal is recovered in the speedgate and resolved into the two orthogonal pitch and yaw gimbal axes. These signals then drive the antenna servos to keep the antenna beam on boresight. The antenna is space stabilized by feedback from rate gyros mounted on the antenna, so that only target-to-missile, line-of-sight rates will result in boresight errors.

The boresight error (proportional to λ in Fig. 4) is also used by the autopilot to steer the missile along a proportional navigation trajectory to intercept the target. As has been shown, proportional navigation is based on the fact that if two objects are closing on each other, they will collide if the LOS between them does not rotate in inertial space. The important fact to note is the entire guidance function is accomplished with only a measurement of angle. The doppler tracking loop (or range tracking loops used in pulse systems) is present merely to restrict the window-in frequency (or range)—from which angle error information is extracted. The angle information is what is needed for guiding the missile.

To normalize the guidance error gain (a constant scale factor of volts/degrees off boresight is required) over the fully dynamic range of target signal amplitudes, AGC is required in the receiver. This may be done separately in the i-f, doppler amplifier and speedgate, or the agc may be derived down-stream in the receiver and used to agc an earlier section (for instance, agc derived at the doppler amplifier output may be used to control the gain of the i-f). The speedgate normally agc's on receiver noise, and can, therefore, expand its gain to some extent as the receiver noise and target are compressed earlier in the receiver. The considerations that dictate the specific implementation are to what degree the feedthrough and clutter shall control the gain for the target signal, while preventing saturation on the large signals. The dynamic range of these amplifiers and age loops form one limitation on the achievable SCV and SFV. The other concern is that of possible cross modulation between the large interfering signal and small target which could cause false guidance commands. Prevention of such nonlinearities is a major design objective, both in the circuit design and physical layout, since very high gain is concentrated in a very limited space.

Rear receiver eliminated

These early systems were the first step in an evolution that has gone through several iterations to

(continued on p. 68)

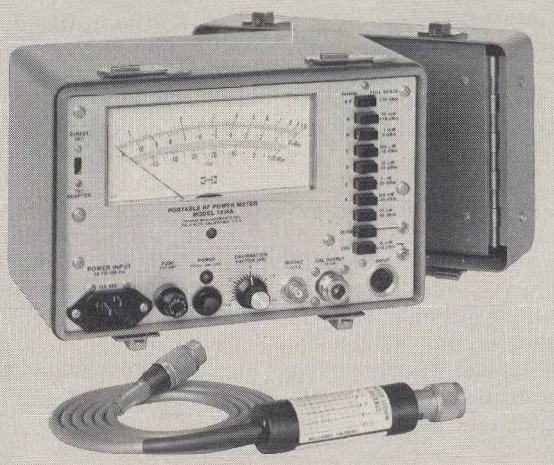

New truly-portable power meter

Self-checking/instant on

Here's a new microwave power meter you can use in the lab or field and still be sure of accurate results.

That's because this new battery- or ac-operated power meter has a built-in self-check feature.

The new Pacific 1034A also has an instant-on circuit that speeds up field measurements.

High sensitivity/low priced

Some other important features:

- Special extra meter scale gives you a 60 dB dynamic range in one meter sweep. Unbeatable when adjusting equipment.
- High sensitivity—10 nanowatts full scale. Usable to 2.5 nW (−56 dBm).
- Detectors and adapters for 50 and 75 ohms. 1 MHz to 18 GHz.
- One of the industry's lowest-priced power meters—$725. Field repairable detectors separate. Battery supply optional.

Call for data

Call Dean Armann at Pacific now and get full data on an inexpensive power meter that's a workhorse in the lab or in the field.

PM Pacific Measurements
incorporated

470 SAN ANTONIO RD., PALO ALTO, CA. 94306
(415) 494-2900 / TWX: (910) 373-1171
state-of-the-art microwave instrumentation

READER SERVICE NUMBER 67

the systems in production today or being designed for future deployment. The technology and the threat have both advanced.

An example of the former is the coherent reference, provided in the early systems by a rear receiver afc'ing a klystron. Since the early illuminators were not precisely frequency controlled (initial frequency setability and long-term drift), the missile rear receiver would have to search for and lock onto its illuminator frequency and then track it to keep the LO properly positioned. Time delay matched front and rear i-f channels reduced the klystron fm noise to tolerable values. With the development of crystal-controlled transmitters, the illumination frequency could be known precisely prior to missile launch. Thus, the microwave LO could be preset before launch, and the requirement for tunability could be replaced by a crystal-controlled LO. A fixed-frequency LO could be made sufficinetly noise free to permit use of an "on-board reference," eliminating the rear receiver entirely. Coherent detection of the front signal still results because both transmitter and LO are precisely crystal controlled, and the target-doppler shift is properly recovered. A major design simplification and advancement thus results.

Threats complicate design, too

Most of the advances in the threat, however, have brought about increased complexity of the seeker as well as the tracking illuminator. From the simple threat of a subsonic aircraft the requirements grew to much faster targets, of smaller radar cross-sections, flying at lower and higher altitudes, possessing greater maneuverability and employing increasingly powerful and more sophisticated ECM.

Thus, the need grew for a wider range of doppler-frequency coverage, greater clutter and feedthrough rejection and more ECM immunity. At some points, hardware design requirements—such as circuit Q's or percentage tuning bandwidth of oscillators—dictated use of second i-fs to avoid going to baseband (video) frequencies, double conversion in the speedgate to achieve the final narrow banding at lower frequencies and moderate circuit Qs, clutter rejection schemes. Eventually, the basic system containing three frequency conversion in the signal path grew to a system containing seven frequency conversions. Separate circuits were added to provide ECCM fixes.

This level of complexity was inconsistent with a seeker, which fundamentally is a round of ammunition. It has to perform reliably under extremes of environment-shock and vibration, low and high temperature, long-term storage and field handling—and yet be sufficiently inexpensive to be a cost-effective weapon. Since it also has to fit within a limited volume, increasing complexity makes for even denser packaging. These reliability and cost requirements demanded less complexity —not more.

The introduction of solid-state circuitry to replace the vacuum tubes of the early systems provided a step towards more reliability, but the actual parts count increased, since, in general, to fulfill the function of a single tube required two or more transistors. What was needed was an inherently simpler approach which could match or better the performance of the conventional receiver.

Crystals key to inverse receiver

This inherently simpler approach came in the form of the "inverse

(continued on p. 70)

NEW! *End Launch* waveguide to coaxial adapters — *to 40Ghz* — are here. These in-line transitions provide distinct advantages over conventional adapters for numerous systems applications. They are available with MPC2, SMA, etc., connectors and feature low VSWR and loss. Send for full details **TODAY!**

MAURY MICROWAVE
CORPORATION
CUCAMONGA CALIFORNIA 91730 • TELEPHONE 714 987 4715

READER SERVICE NUMBER 68

SINGLE-POLE DOUBLE THROW
SWITCH

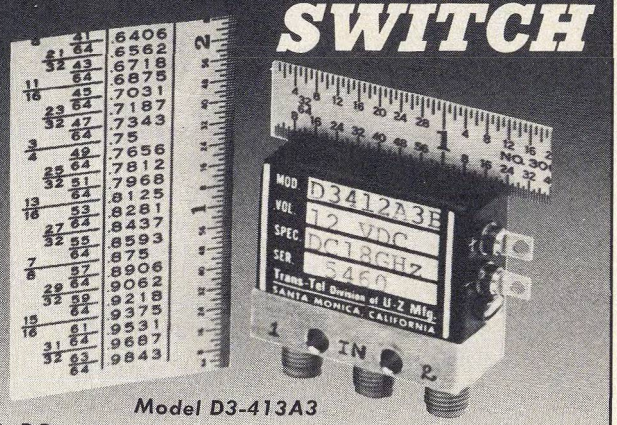

Model D3-413A3

- DC — 18 GHz
- VSWR: 1.5:1
- Isolation: 65dB min.
- Insertion loss: 0.3dB max.
- Life: 2 million cycles
- Built to military specs
- Fail safe or latching
- Also available in commercial versions for price savings

We have 326 switches designed—single, double throw, multiple position, failsafe or latching, transfer switches with logic, etc.

Write for new catalog

UZ Manufacturing Inc.

Transtel Products
1101 Colorado Avenue, Santa Monica, CA 90404
(213) 393-0567

READER SERVICE NUMBER 69

receiver".[5,7,8] It gets its name from the fact that, unlike the conventional receiver consisting of a wide i-f, a somewhat narrower doppler amplifier, and finally a narrow speedgate—an ever-narrowing funnel—it performs the narrow banding or speedgating at i-f, thus inverting the "funnel" of the conventional receiver.

The critical components necessary for the inverse receiver are high selective crystal filters at i-f frequencies and low-noise tunable solid-state microwave sources. The simplicity of the inverse receiver coupled with a fully solid-state seeker produces the high reliability needed while giving improved performance.

The simplified block diagram of an inverse receiver is shown in Fig. 8. Whereas in the conventional receiver, the target signal must compete with feedthrough, clutter and jamming signals until the final stages with the dynamic range requirements of the receiver and its agc loops dictated by these large undesired signals, the inverse receiver excludes them virtually at the input. The narrow crystal filter, constituting the speedgate bandwidth, is placed in the i-f, after only a nominal amount of fixed preamplifier gain, sufficient to maintain noise figure, has been added. One additional conversion is used in the receiver to avoid the problem of too much gain at one frequency. In the resulting two-conversion system, complexity is significantly reduced and unwanted signals are eliminated very early in the signal path, thus reducing dynamic range requirements and avoiding any possible source of distortion.

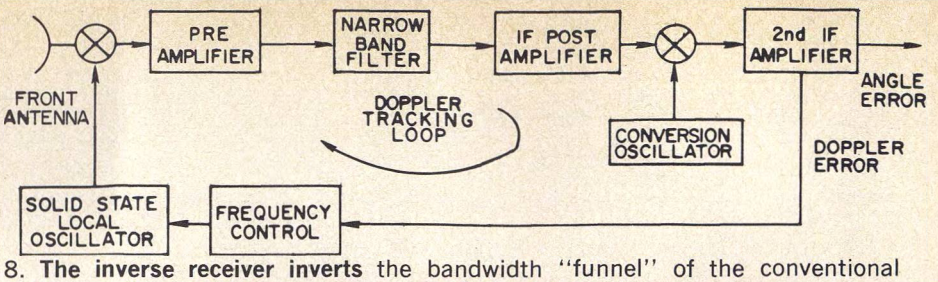

8. **The inverse receiver inverts** the bandwidth "funnel" of the conventional receiver to exclude interference very early in the seeker.

The doppler tracking loop is closed through the microwave LO, which must, therefore, be tunable over the doppler frequency range of interest. The microwave LO, thus essentially fulfills the role of the speedgate LO in the conventional receiver of Fig. 7. The inverse receiver, can be thought of as a double-conversion speedgate with the speedgate afc loop closed around the microwave LO and the input to the speed gate being the microwave output of the seeker antenna.

The i-f spectrum at the mixer output will have the same form as Fig. 6. Sweeping the LO moves the spectrum past the narrow crystal filter to accomplish acquisition as in the conventional speedgate. Doppler tracking is similarly done by controlling the LO frequency to keep the target in the narrow filter. The angle error signals required for guidance are extracted after the second i-f amplifier. A single agc loop, required to cope with only the target-signal variations, is used to normalize the angle error signals.

The inverse-receiver concept can be adapted to either a conical scan or monopulse angle-tracking system. For a conical-scan system, the scan sidebands must fall within the crystal-filter bandwidth, thus limiting the maximum scan frequency.

VARI-L DOUBLY BALANCED MIXERS GIVE "ECONOMICAL RELIABILITY"

LOW COST
HIGH RELIABILITY
IN THE SAME
PACKAGE

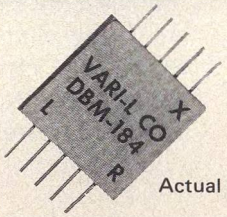

Actual Size

- 2-3000 MHz range
- 20 dB isolation
- Low conversion loss - 6.5 dB typical
- +20 dBm Typical 3rd order intercept
- Only .635" x .635" x 0.125" high
- Low cost - $145.00

This Vari-L doubly balanced mixer offers a combination of performance, size and price not found in any other DBM!

Send for Application Bulletins

VARI-L
3883 Monaco Pkwy., Denver, CO 80207
Ph: (303) 321-1511/TWX:910-931-0590
A-6

READER SERVICE NUMBER 70

NEW $5.00 EACH IN 100 QUANTITIES

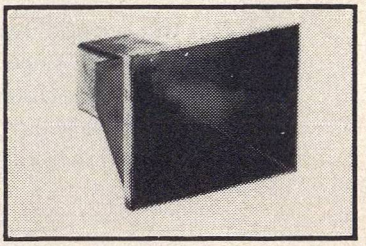

18db X-BAND HORN
PRECISION DIE CAST

FOR DETAILS ON THIS AND OTHER HIGH PERFORMANCE X-BAND FILTERS, DETECTORS AND SOURCES CALL TOLL FREE [800] 426-5966

OR WRITE

RACON INC
BOEING FIELD INTERNATIONAL
8490 PERIMETER RD., S.
SEATTLE, WASHINGTON 98108
(206) 762-6011

READER SERVICE NUMBER 71

HIGH PERFORMANCE/LOW PRICE

type 'N' terminations

• DC to 12.4 GHz
• DC to 18.0 GHz

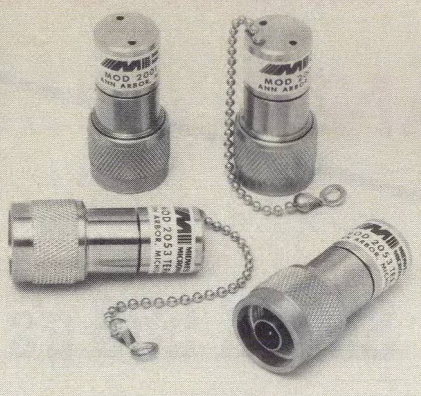

SPECIFICATIONS	
MODEL	**2001**
Frequency Range	DC to 18.0 GHz
Maximum VSWR	1.025 + 0.004f (GHz)
Connector	Stainless Steel
Price	$64.00 each

MODEL	**2053**
Frequency Range	DC to 12.4 GHz
Maximum VSWR	DC to 4.0 GHz 1.05:1 4.0 to 12.4 GHz 1.10:1
Connector	Stainless Steel
Price	$43.00 each

MIDWEST MICROWAVE 3800 Packard Road, Ann Arbor, Michigan 48104 • (313) 971-1992 • TWX 810-223-6031
FRANCE: S.C.I.E.-D.I.M.E.S. 928-38-65

READER SERVCE NUMBER 72

Use of a high-frequency scan would require wider bandwidth or separate processing channels for the directional information.

Use of a conventional monopulse angle tracking scheme normally requires three complete channels which must track in gain and phase to maintain the proper relative amplitude of the sum and difference channels. The well-known advantage of monopulse over conical scan,[9,10] however, is significant, since it eliminates externally-generated amplitude fluctuations (such as propeller modulation, fading noise or amplitude-modulated jammers) from the guidance signal. The monopulse system extracts all the angular information simultaneously rather than requiring a period of time to determine the position of a source of signals, as a conical-scan system does. The agc can, therefore, be made instantaneous and the amplitude variations since they affect sum and difference channels by the same relative amount, are never detected as erroneous guidance signals.

The inverse receiver permits the inherent capability of the monopulse and the basic simplicity of the conical-scan systems to be combined into one. Three identical mixers, preamps and crystal filters, first process the three monopulse signals. Immediately after the narrow-band filters, however, the difference channels are modulated to form sidebands at a multiplexing frequency higher than the filter bandwidth. Interference at the multiplexing frequency is, therefore, prevented from passing through the filters. The modulated-difference channels are combined with the sum signal and the composite signal is processed in a single channel, just as a conical-scan signal. The normalized monopulse error signals are then demultiplexed and used for closing the guidance loops.

Improved performance is inherent in such a seeker, while hardware is significantly less complex than for a conventional receiver.

PD sampled data and TVM

Either the conventional or inverse receiver can be configured to work with other than the simple cw waveforms.[5,7] The inverse receiver would retain its performance advantages over the conventional for these approaches.

For high-duty cycle and high prf pd, no fundamental receiver hardware changes are needed. The receiver only sees the central line of the spectrum and operates as in cw. Care must be taken to insure that the rear afc loop (if one is used) locks onto the central line. If range gating is used (a necessity for low-duty cycle pd), the range gates must, of course, precede the narrow speed-gate filter. Similarly, for pulse-compression waveforms, the pulse-compression lines would also have to precede the range gates and narrow-band filters. For all of these systems, the combination of i-f frequency and transmitter pulse spectrum must be chosen to avoid problems at the image frequency. A spectral line of the feedthrough or clutter occurring at the image may limit the SFV or SCV, sometimes necessitating use of image-rejection mixers or rf preselection.

For sampled data operation, the primary difference is in the doppler acquisition scheme. Since target illumination occurs only in short bursts, the use of a sweeping gate for acquisition would result in excessively long acquisition times. The doppler uncertainty region must, therefore, be examined in parallel by a bank of doppler filters. The illumination burst must be shaped or the received signal time gated to prevent the spreading of clutter through the target doppler spectrum due to the pulsed nature of the transmission. Finally, sample holds must be added in afc, agc and angle- track loops.

In the TVM mechanization, the block diagram is functionally the same as for the missile-borne seeker, except that the signal amplification and processing blocks are on the ground and a missile-to-ground data link and a ground to-missile command link replace the signal lines of the on-board seeker. ••

References

1. D. K. Barton, "Real World Radar Technology," *IEEE 1975 International Radar Conferences*, pp. 1-22, (April, 1975).
2. A. S. Locke, et al, *Guidance*, Van Nostrand Co., Princeton, NJ, (1955).
3. T. L. Phillips, "Anti-Aircraft Missile Guidance," *Raytheon Electronic Progress*, Vol. II, No. 5, pp. 1-5, (March-April, 1958).
4. F. A. Gross, W. M. Hall, D. K. Barton, "Detection and Tracking Systems: An Historical Overview," *Raytheon Electronic Progress*, Vol. XVI, No. 3, pp. 2-11, (Fall, 1974).
5. J. J Long, A. Ivanov, "Radar Guidance of Missiles," *Raytheon Electronic Progress*, Vol. XVI, No. 3, pp. 26-28, (Fall, 1974)
6. M. W. Fossier, B. A. Hall, "Fundamentals of Homing Guidance," (unpublished Raytheon seminar presentation), (1962).
7. A. Ivanov, "Radar Guidance of Missiles," *IEEE 1975 International Radar Conference*, pp. 331-335, (April, 1975).
8. R. M. Jaffe, "Monopulse Radar Receiver," U. S. Patent 3,713,155, (Jan. 23, 1973).
9. M. I. Skolnik, *Introduction To Radar Systems*, McGraw-Hill, New York, (1970).
10. M. I. Skolnik, et al, *Radar Handbook*, McGraw-Hill, New York, (1970).

Design A Ka-Band Polar Frequency Discriminator

A look at the requirements of this 26.5 to 40 GHz design shows how common MIC components, such as hybrids and couplers, must be modified to assure wideband, millimeter-wave performance.

UPWARD trends in frequency utilization have brought about a need for high-quality surveillance receivers to cover frequency bands above 18 GHz. The relatively low-density signal environment which prevails in upper frequency regions is particularly well suited to the capabilities of the instantaneous frequency measuring (IFM) type of surveillance receiver.

An IFM system instantaneously detects and identifies any signal within the system's band of coverage. Instantaneous bandwidth may encompass a full 3:2 waveguide band or greater. Intercept probability thus approaches 100% for any signal above detection threshold; moreover, an intercepted signal's frequency and relative strength are easily interpreted.

The key to this unique capability is the wideband polar frequency discriminator (PFD). The PFD's properties, in fact, provide the basis for the IFM receiver's fundamental concept. The inherent simplicity of the basic IFM receiver is illustrated in Fig. 1(a). A wideband preamplifier applies all signals within its passband to the PFD. The discriminator responds to an intercepted signal by activating a visual polar display, usually a CRT. The PFD's four detectors are connected to a pair of differential amplifiers which drive the CRT's horizontal and vertical inputs. An intercepted signal appears on the CRT as a radial strobe emanating from the center of the display screen. The strobe's length is proportional to the signal's power level, while its angular orientation provides an indication of frequency (see Fig. 1(b)).

Polar frequency discriminators have been available for applications below 18 GHz for more than a decade. Although stripline is usually the preferred method of construction at lower frequencies, technical problems have slowed development of stripline units above 18 GHz. At least one manufacturer has employed stripline at Ka-band, but not without encountering considerable difficulty. In this case, waveguide-mounted detectors were externally mounted on the stripline package, requiring multiple transitions from stripline to waveguide and resulting in a unit of relatively large volume. Guidelines for PFD development at the Naval Electronics Laboratory Center in San Diego, call for microwave integrated circuit (MIC) technology throughout.

David L. Saul, Electronic Engineer, Surveillance and Countermeasures Division, Naval Electronics Laboratory Center, 271 Catalina Blvd., San Diego, CA 92152.

Coupled-line elements eliminated

A number of circuits can be devised which are able, at least in theory, to perform the functions of a polar frequency discriminator. For the particular Ka-band PFD developed at NELC, a circuit had to be selected which incorporated components that could be fabricated in microstrip, yet operate at wavelengths in the millimeter region. One of the more formidable challenges facing the designers of millimeter MICs deals with coupled-line structures. Circuit elements based on coupled lines are widely used at frequencies below 18 GHz and, in theory, there is nothing to prevent extension of these techniques to millimeter wavelengths. Practical factors, however, impose severe constraints; circuits are phyically small, and uniform, closely spaced gaps are usually required.

Coupled-line devices are, by nature, particularly susceptible to behavior anomalies arising from relatively small circuit fabrication inaccuracies. A pragmatic approach suggests the use of circuits without coupled-line devices wherever possible. This possibility was considered in terms of PFD requirements, and a circuit, which is

(continued on p. 76)

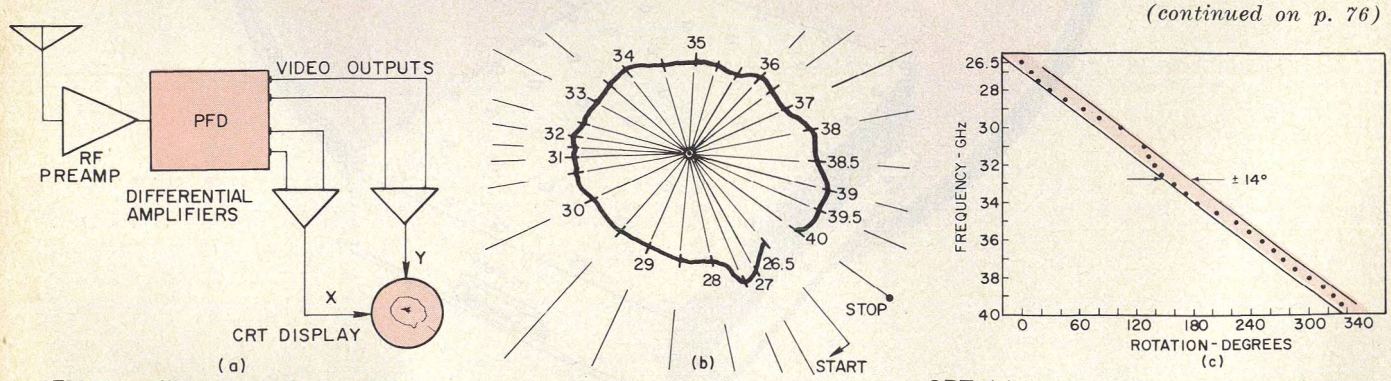

1. IFM surveillance receivers rely on polar frequency discriminators to drive a CRT (a). Sweeping a cw signal through the band at a constant rf power level produces the polar plot shown in (b). This data can be plotted linearly (c).

The "Inside Story" on NELC's Ka-Band Discriminator

The PFD circuit's operation is most conveniently described in mathematical terms, although no attempt is made here to treat the subject rigorously. For the sake of convenience and simplicity, a convention is adopted such that phase delays along pairs of signal paths of equal electrical lengths are omitted from the various expressions. These are arbitrary, and can be dropped without loss of generality. For similar reasons, figures of merit of the detectors are also omitted. Numbered and lettered references apply to Fig. 2.

The input signal V_i at point 1 can be expressed as

$$V_i = E_o(t) \cos \omega t$$

in which $E_o(t)$ is an arbitrary amplitude modulating function, ω is the radian frequency of the rf input signal, and t is time. P_1 and P_2 are power dividers of the Wilkinson type. Lines L_1 and L_2 are of unequal electrical lengths so that

$$L_2 - L_1 = \Delta L \neq 0$$

The signals applied to P_2 and P_3 following the power split of P_1 can thus be represented as

$$\frac{E_o(t)}{2} \cos(\omega t - \beta L_1) \text{ and } \frac{E_o(t)}{2} \cos(\omega t - \beta L_2)$$

respectively, with phase constant β defined as the rate of change of phase with respect to distance along a transmission line for fixed values of time. The value of β is given by

$$B = \frac{2\pi}{\lambda}$$

where λ is wavelength.

Further power splits are performed by P_2 and P_3. Lines L_4 and L_5 form an equal pair, as also do lines L_3 and L_6. The outputs of P_2 and P_3 at the indicated reference points can thus be expressed as follows:

$$\text{At } P_2 \text{ outputs: } \frac{E_o(t)}{2} \cos(\omega t - \beta L_1)$$

$$\text{At } P_3 \text{ outputs: } \frac{E_o(t)}{2} \cos(\omega t - \beta L_2)$$

The purpose of hybrid H_1 is to recombine signals which arrive via lines L_4 and L_5. Since H_1 is a 180 degree hybrid, signals at points 2 and 3 can be represented by the following:

$$\text{At point 2: } \frac{E_o(t)}{2\sqrt{2}} \cos(\omega t - \beta L_1) + \cos(\omega t - \beta L_2)$$

$$\text{At point 3: } \frac{E_o(t)}{2\sqrt{2}} \cos(\omega t - \beta L_1) - \cos(\omega t - \beta L_2)$$

Using the trigonometric indentity,

$$\cos X + \cos Y = 2 \cos \tfrac{1}{2}(X + Y) \cos \tfrac{1}{2}(X - Y)$$

the signal at point 2 can be expressed as

$$\frac{E_o(t)}{\sqrt{2}} \left\{ \cos[\omega t - \tfrac{1}{2}\beta (L_1 + L_2)] \right\} \left\{ \cos \tfrac{1}{2}\beta \Delta L. \right.$$

Assuming square law detection, the signal at point 6 is found to be

$$\frac{E_o^2(t)}{2} \cos^2 \tfrac{1}{2}(\beta \Delta L).$$

Using the trigonometric identity

$$\cos X - \cos Y = -2 \sin \tfrac{1}{2}(X + Y) \sin \tfrac{1}{2}(X - Y)$$

the signal at point 2 can be expressed as

$$\frac{-E_o(t)}{\sqrt{2}} \left\{ \sin[\omega t - \tfrac{1}{2}\beta(L_1 + L_2)] \right\} \left\{ \sin \tfrac{1}{2}(\beta \Delta L) \right.$$

which after square law detection yields

$$\frac{E_o^2(t)}{2} \sin^2 \tfrac{1}{2}(\beta \Delta L)$$

at point 7. Taking the difference of the detected signals at points 6 and 7 by means of A_1 and applying trigonometric identity

$$\cos^2 X - \sin^2 X = \cos 2X$$

the signal at output A is found to be

$$\frac{E_o^2(t)}{2} \cos \beta \Delta L.$$

Since β has an approximately linear rf frequency dependence, output A undergoes a cosine variation as the discriminator's input signal is varied in frequency. Note that the output varies as the square of modulation amplitude and hence as the power level of the input signal.

Hybrid H_2 serves to recombine signals passing along lines L_3 and L_6. By a mathematical process similar to the foregoing, output B can be shown to be equal to

$$\frac{E_o^2(t)}{2} \sin \beta \Delta L,$$

thus providing the remaining member of a pair of quadrature outputs needed for the polar display.

The angle (θ) of the polar strobe is given by

$$\theta = \beta \Delta L.$$

It is generally desirable to limit the angular variations of θ to a maximum 360 degrees to avoid ambiguity. For a frequency range of ω_1 to ω_2, this requires that

$$\frac{\Delta L}{V_o}(\omega_2 - \omega_1) \leq 2\pi$$

in which V_o is the propagation velocity in the transmission lines. ●●

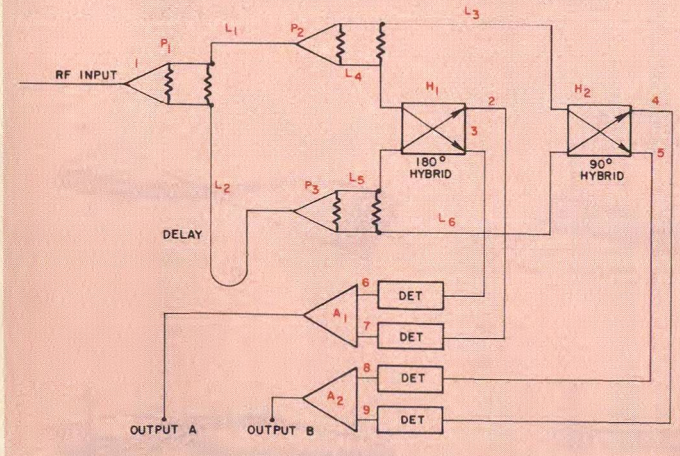

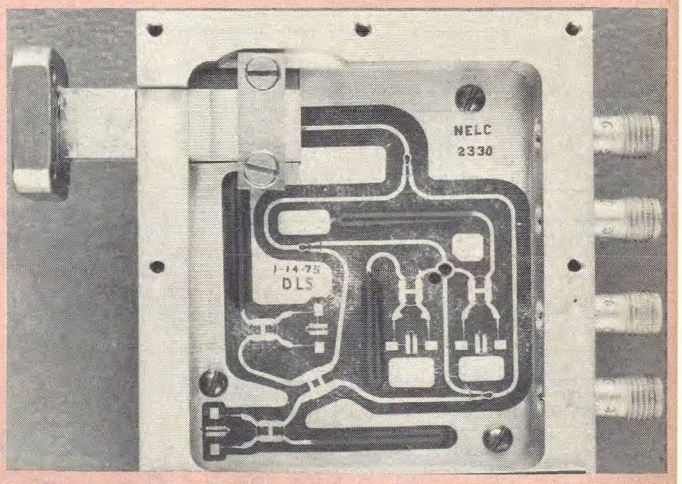

2. Built without a single coupled-line structure, this PFD is designed to cover 26.5 to 40 GHz. Detectors are connected to SMA press-fit connectors via semi-rigid coaxial cables routed through channels beneath the substrate. Differential amplifiers A1 and A2 are not part of the PFD package.

POLAR DISCRIMINATOR

shown in Fig. 2, was devised which requires no coupled-line elements. Operation of this PFD circuit is explained in the accompanying section, "The Inside Story on NELC's Ka-Band Discriminator." It is also noteworthy that this particular topology does not require a frequency-independent phase shifter, as many PFD circuits designed for lower frequency bands do.

Overall performance of the PFD circuit depends heavily on the quality of the individual components—the reverse phase hybrid ring, Wilkinson power splitters, branch-line couplers and balanced detectors. Performance of each key component is summarized in Table 1, but it is informative to look deeper into the thinking behind each element's design.

Table 1: Summary of Component Performance

Component	Power split (dB)		Isolation (dB)		VSWR	
*	A	B.	A.	B.	A.	B.
Reverse-phase hybrid ring	1.6	1.0	18.5	25	1.5	1.25
Wilkinson power splitter	0.3	0.1	22	26	1.4	1.2
Three-branch coupler	1.5	1.0	16.5	19	1.25	1.15
Four-branch coupler	2.0	1.0	16	22	1.3	1.2
Balanced detector					1.7	1.3

*A—Worst point in band B—Average over full band

Adding a twist to the "rat race"

The reverse-phase hybrid ring is a close relative of the conventional "rat race" ring. The ordinary rat race, or 6 $\lambda/4$ hybrid ring, is generally known to be a relatively narrow-band device. However, wideband capabilities of such a circuit were first reported more than two decades ago, although at frequencies far below the millimeter region.[1] To extend its performance to a full waveguide bandwidth, the ring structure must be modified by replacing the conventional ring's 3 $\lambda/4$ arm with a $\lambda/4$ arm and introducing a frequency insensitive reversal of phase. This reduces the ring's dimensions and also provides inherent symmetry not found in the 6 $\lambda/4$ ring.

Practical techniques were developed at NELC for fabricating reverse-phase rings in microstrip.[2] The microstrip reverse-phase ring incorporates a "twist" in one of its $\lambda/4$ arms for phase inversion. A section of line in parallel plate form is physically twisted to invert the polarity of the conductors, as shown in Fig. 3. This simple inversion effectively provides a 180-degree reversal of phase which is independent of frequency.

The Wilkinson power divider behaves as a hybrid junction with its isolated port internally terminated in a matched load. Connected as an in-phase power splitter, it provides very uniformly balanced output signal levels. Phase linearity is also excellent, and it is generally safe to say that the device's characteristics are among the most ideal to be found among microstrip components.

To obtain wideband operation with minimum VSWR, a two-stage divider based on design data published by S. Cohn was developed for the Ka-band PFD.[3] Each unit requires two terminating resistors, and some difficulties were experienced in obtaining resistors which would perform well at frequencies approaching 40 GHz. Special techniques were developed at NELC to fabricate "low-profile" resistors from metalized plastic film.

The polar frequency discriminator's quadrature hybrid requirements were met through development of branch-line couplers. Theory suggests that practically any bandwidth can be obtained by employing a sufficiently large number of shunt branches. Unfortunately, an increasingly wide range of line impedances are required as the number of branches grows. In microstrip, practical factors limit the number of branches to perhaps three or four, although experimental units have been fabricated with as many as five branches, using extremely fine gold wire for the higher impedance lines. A simple two-branch coupler was initially used to verify the Ka-band PFD circuit's operation. A three-branch design was subsequently incorporated, resulting in considerable performance improvement near the band edges. Some difficulties were still being considered, however, with ambiguities in the PFD's response. Eventually, a four-branch design was decided upon, based on the Chebyshev four-branch coupler described by Levy and Lind.[4]

Balanced detector cuts VSWR

Wideband MIC detector performance has historically been difficult to obtain in the 26.5 to 40 GHz range. Much of the problem stems from the fact that a diode in a package suitable for MIC mounting exhibits reactances which are difficult to deal with

(continued on p. 78)

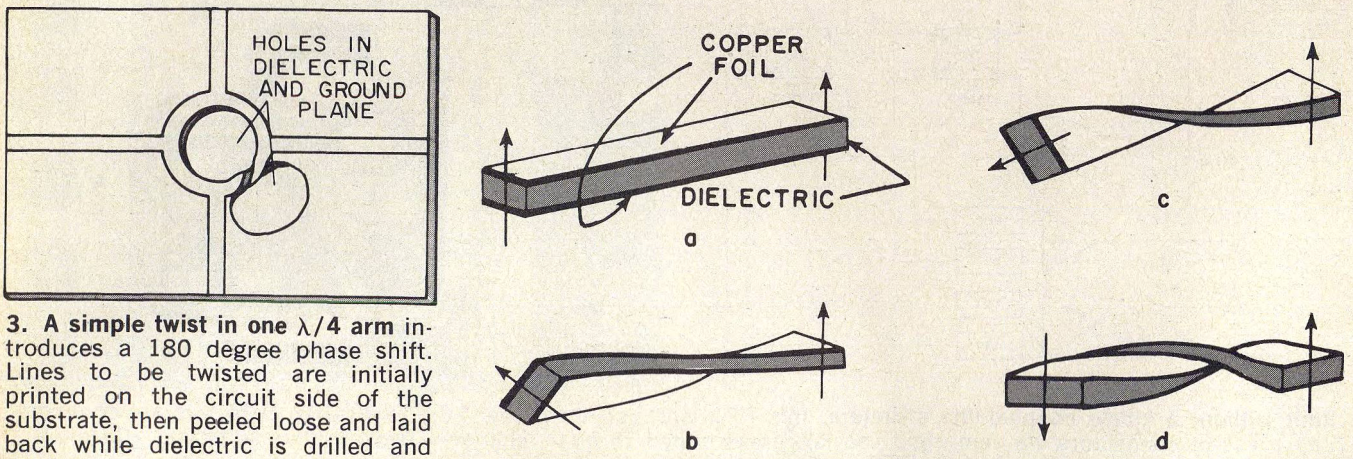

3. A simple twist in one $\lambda/4$ arm introduces a 180 degree phase shift. Lines to be twisted are initially printed on the circuit side of the substrate, then peeled loose and laid back while dielectric is drilled and cut to shape. After dielectric is formed to approximate twist shape, line ends are wrapped around and connected on ground plane side.

effectively over large bandwidths. If single frequency operation is desired, these reactances can be tuned out through use of stubs or other matching elements. Some degree of mismatch must be accepted, however, if wideband operation is to be achieved.

The effects of mismatch manifest themselves in reduced sensitivity, irregular response and large power reflections. The latter are particularly devastating to the operation of a polar discriminator, and must be kept to a minimum in all components. Detectors are among the worst potential offenders with regard to power reflections. Experimental results have confirmed that detectors with VSWR levels of 2:1 or greater are likely to cause serious discrepancies in performance of PFDs.

Power reflections can be minimized by using the balanced detector scheme illustrated in Fig. 4. This type of detector is more complex than a single-ended unit, but can, nevertheless, be implemented in a compact, useful form in MIC. The circuit consists of a quadrature hybrid with its isolated port terminated in a resistive load, as shown. A detector diode is connected to each of the hybrid's output ports. The chief advantage of the balanced detector stems from its ability to terminate power reflections from the diode pair. Examination of the circuit reveals that reflections of equal phase and amplitude from the two diodes will add in phase at the terminated port, while being isolated from the rf input port. In practice, it is never possible to eliminate power reflections totally; the behavior of a realizable hybrid will not remain ideal over a wide band, and members of a diode pair may not produce identical power reflections. Such anomalies, however, do not necessarily lead to unacceptable circuit performance. In practice, considerable VSWR improvement can be realized over a single-ended, wideband design.

Each of the PFD's four balanced detectors relies on a three-branch coupler as a quadrature

THE SPECTRUM ANALYSI

Select normal or variable persistence display, choose economy or high-resolution IF module.
Then pick or change your frequency range by simply plugging in the appropriate tuning module.

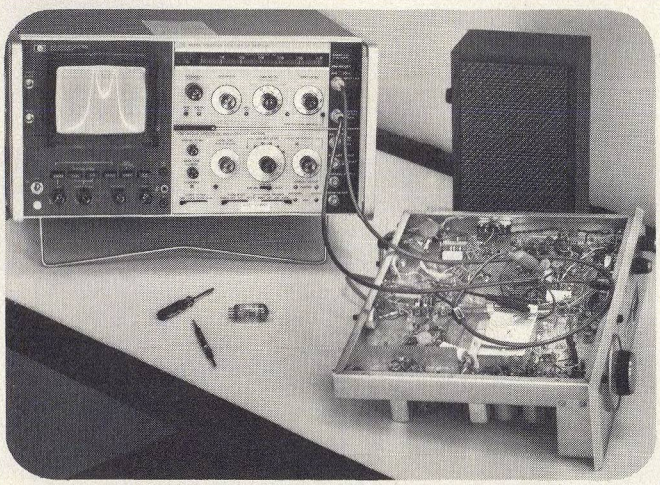

20 Hz to 300 kHz

The 8556A tuner covers 20 Hz to 300 kHz and comes with a built-in tracking generator. It's calibrated for measurements in both 50 and 600 ohm systems, with accuracies better than ±1 dB.

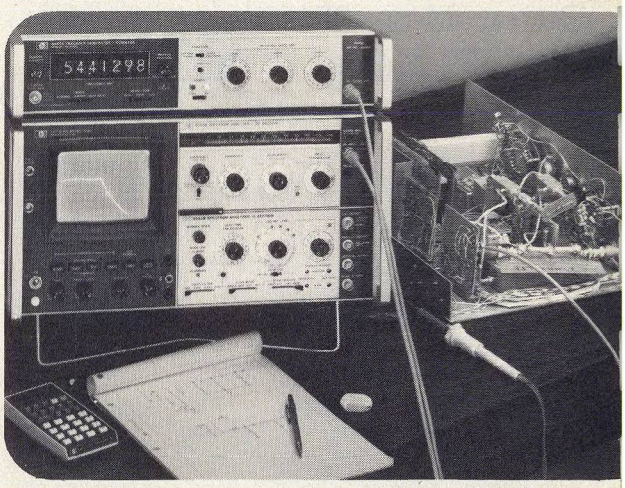

1 kHz to 110 MHz

The 8553B takes you from 1 kHz to 110 MHz with −140 dBm sensitivity. Signals can be measured with ±1¼ dB accuracy. Choose the companion tracking generator/counter for wide dynamic range swept frequency measurements and precise frequency counting.

No matter what range you're working in, you need reliable unambiguous answers.
HP's spectrum analyzers give you accurate measurements over wide, distortion-free dynamic ranges, time after time. Easy operation too, with front panel markings that really help reduce the possibility of operator error.

But there's much more. Call your nearby HP field engineer or write for the full story on HP's spectrum analyzer spectrum.

hybrid element. The matched termination is a tapered microstrip line folded back on itself, with a resistive element of metalized film attached. Diodes are beam-lead Schottky types manufactured by Hewlett-Packard.

Duroid chosen for substrate

Low-permittivity microstrip was chosen as a circuit medium for all components, chiefly on the basis of successful R&D work performed earlier at NELC. Initial component development utilized a planar dielectric substrate of irradiated polyolefin, a material noted for its extremely low dissipation loss at elevated frequencies. While polyolefin's electrical properties were found to be excellent for ehf MIC applications, recurring mechanical problems prompted a change to a more physically stable material. Duroid, a material whose dielectric consists of teflon reinforced with randomly oriented glass microfibers, was finally chosen due to its relatively low dissipation loss at frequencies well into the millimeter region.

A 10-mil (0.254 mm) dielectric thickness was adopted, yielding a reasonable compromise of line width to line wavelength ratio. The 10-mil value falls within a useful range of dielectric thickness bounded by moding cutoff at one extreme and excessive losses at the other. A standard line width of 0.023 inch (0.58 mm) was selected to yield a line impedance of 60 ohms. The substrate material was purchased with 0.5-ounce copper clad on both sides. Conductor thickness of 0.5 ounce copper is about 0.0007 inch (0.018 mm). A conventional photolithographic technique was employed for circuit fabrication,

(continued on p. 80)

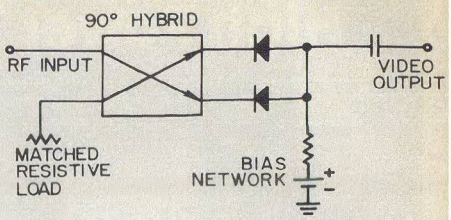

4. A balanced detector circuit minimizes power reflections.

SPECTRUM

The HP 140 family covers it.
Precisely. Conveniently.
Completely.
From 20 Hz to 40 GHz.

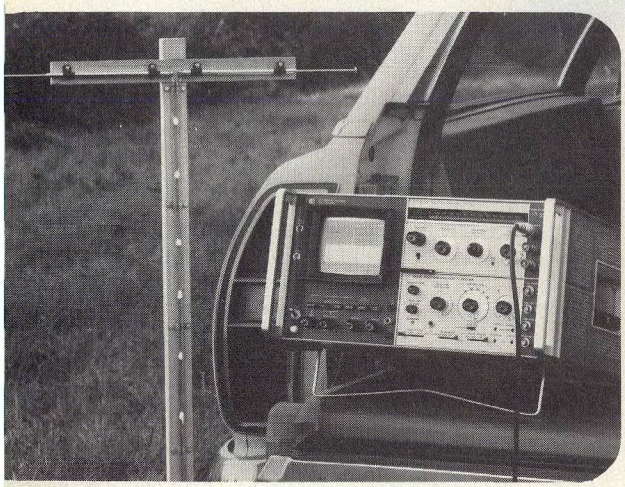

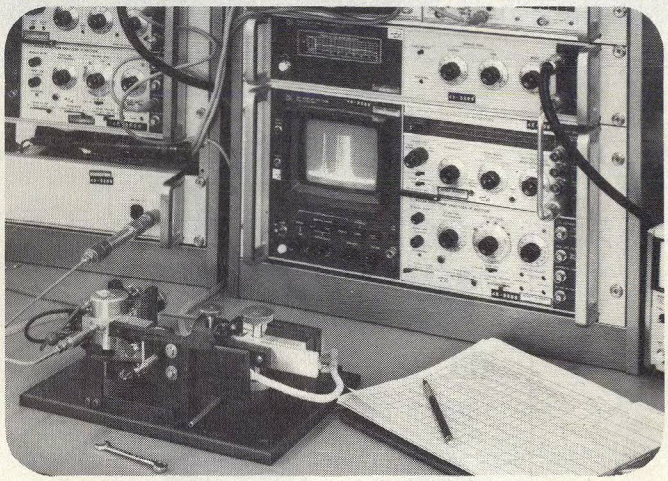

100 kHz to 1250 MHz

Use the 8554B tuning section to cover the 100 kHz to 1250 MHz range. Measure with ±1¾ dB accuracy. Its companion tracking generator (500 kHz to 1300 MHz) also works with the 8555A tuning section.

10 MHz to 40 GHz

For 10 MHz to 40 GHz, choose the 8555A. Its internal mixer covers to 18 GHz, accessory mixer for 18-40 GHz. Maximum resolution is 100 Hz. Measure with ±1¾ dB accuracy to 6 GHz, ±2¾ dB to 18 GHz. For wide scans free from unwanted response between 10 MHz and 18 GHz, add the automatic preselector.

HEWLETT hp PACKARD

Sales and service from 172 offices in 65 countries.
1501 Page Mill Road, Palo Alto, California 94304

45509

READER SERVCE NUMBER 79

High Power TWT Amplifiers

Operating range is 0.5 to 18 GHz with CW power outputs to 600 watts and peak pulse power to 2kW. Remote monitoring, readout, and logic control are standard for remote operation using simple switch logic with remote metering. A standard input jack allows remote sensing of excessive SWR with positive or negative detector sense to cut out the TWT when exceeding a pre-settable level. Complete internal SWR sensing is optional.

The TWT's are internally protected by helix current and voltage sensors, filament surge limiting, solid state delay circuitry and thermal overload sensors. LogiMetrics high power TWT amplifiers are available or can be modified for special military and commercial use. Standard communication band units and systems can be used as HPA's in single or automatic redundant configurations. Write or call for details.

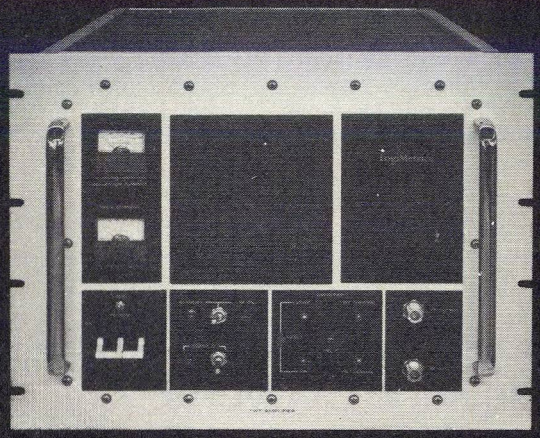

LogiMetrics

121-03 Dupont Street, Plainview, New York, 11803, (516) 681-4700/TWX: 510-221-1833
RF Signal Generators, Frequency Synthesizers, Traveling Wave Tube Amplifiers

READER SERVICE NUMBER 80

CRYSTAL CONTROLLED MW SOURCES

ALL TYPES
.1GHz to 10GHz

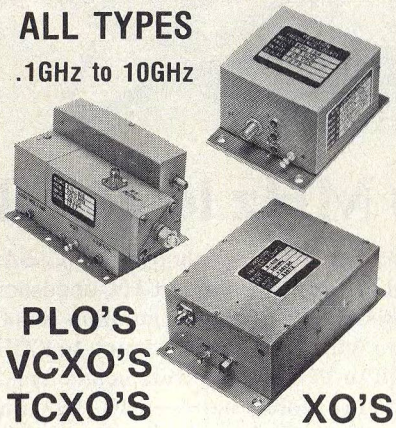

PLO'S
VCXO'S
TCXO'S
XO'S

μλ GRI MICROWAVE TECHNOLOGY

A division of Greenray Industries, Inc.

840 West Church Rd.
Mechanicsburg, PA 17055
Phone 717-697-4681

READER SERVICE NUMBER 81

utilizing positive-acting resist followed by Ferric Chloride etching.

It should also be mentioned that a rather novel waveguide to microstrip transition was devised for the WR-28 input to the PFD. An approach using a length of waveguide with a ridgeline transformer section initially appeared to be most desirable for wideband operation, but a smoothly-tapered, cosine-shaped ridgeline section was found to be more convenient. Back-to-back transitions of this sort exhibit a VSWR of less than 1.2:1 over the entire band; each transition introduces an insertion loss of about 0.35 dB. The gold-plated, brass component measures about 1.4 inches (3.56 cm) long, and can be reproduced quickly and inexpensively using a high-quality tracer equipped milling machine. In fact, in small quantities, this type of transition can be manufactured at a fraction of the cost of machining the discriminator package.

The discriminator circuit is housed in an aluminum enclosure designed to protect the contents in accordance with environmental requirements of the MIL-E-16400 specification. Since the interior dimensions of the enclosure represent multiple free space wavelengths at Ka-band, the potential for spurious-cavity resonance must be reduced. This is easily accomplished by gluing a slab of foam based rf absorber to the inside of the enclosure's cover. This effectively spoils the Q of the "cavity," while having practically no noticeable effect on circuit operation. Overall performance of the Ka-band can be judged from the frequency plots shown in Fig 1(b) and 1(c).

The success achieved with low permittivity microstrip in this and other related programs has prompted additional work at higher frequencies. Components and circuits are now being developed in this medium for application in the 40-60 GHz band, and yet higher frequency work is planned. ••

References

1. W. V. Tyminski and A. E. Hylas, "A Wide-Band Hybrid Ring For UHF," *Proc. IRE*, pp. 81-87, (January, 1953).
2. J. Reindel, "Wideband Ring Couplers and Some Microcircuit Applications," NELC Technical Report 1906, (Jan. 22, 1974).
3. S. B. Cohn, "A Class of Broadband Three-Port TEM-Mode Hybrids," *IEEE Trans. MTT*, Vol. MTT-16, No. 2, pp. 110-116, (February, 1968).
4. R. Levy and L. Lind, "Synthesis of Symmetrical Branchguide Directional Couplers," *IEEE Trans. MTT*, Vol. MTT-16, No. 2, pp. 80-89, (February, 1968).

15/7/76

AY
76

F.O.M. INSTITUUT voor
ATOOM- en MOLECUULFYSICA
Kruislaan 405-407
AMSTERDAM-O.

MICROWAVES

laser technology

PASSIVE COMPONENTS

Master the challenge of offset stripline ☐ Design more accurate interdigitated couplers
Transform impedance with branch-line couplers
ALSO: Buy a complete swept measurement system for under $4000.
BASIC program speeds corrugated horn design

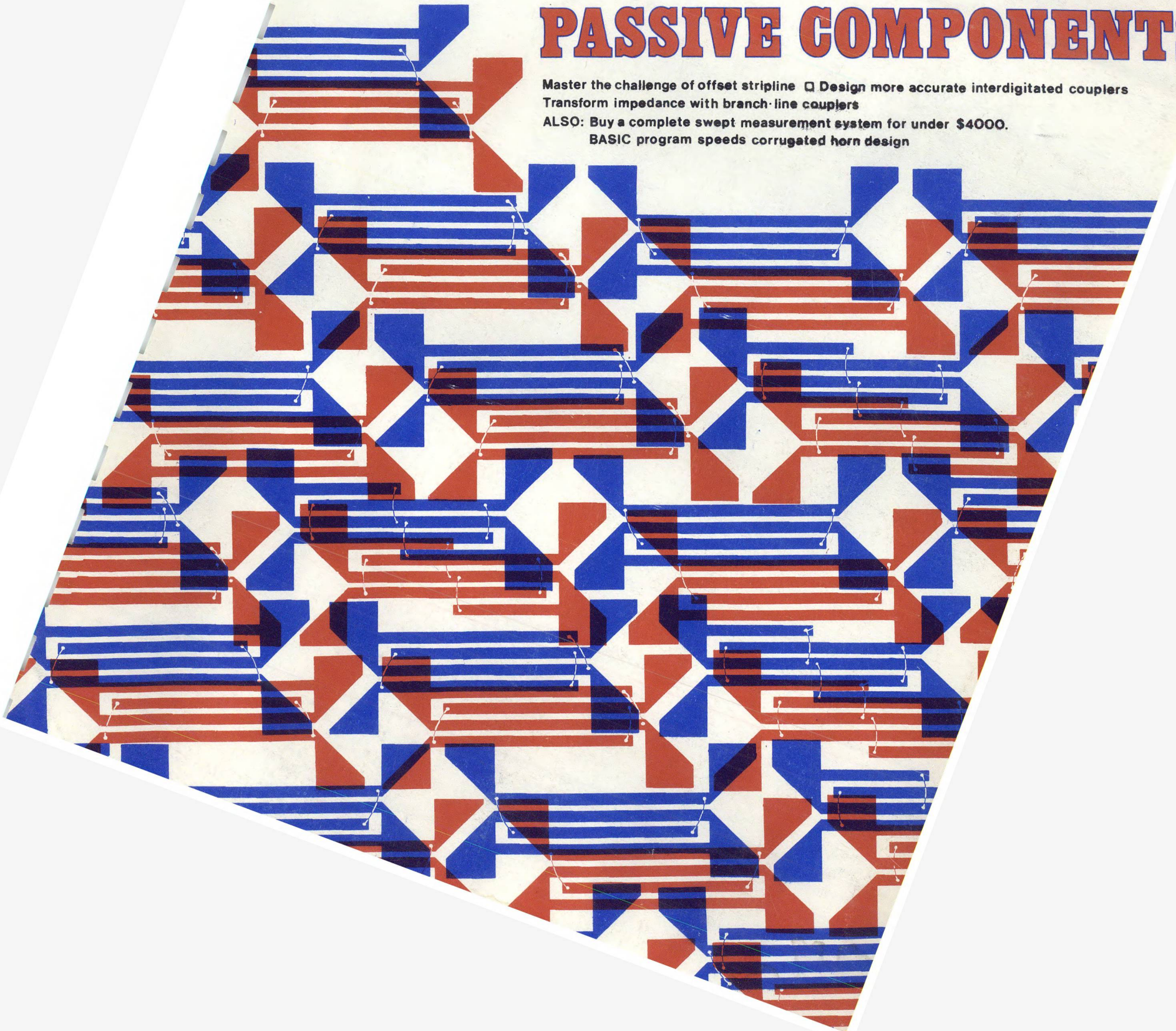

MICROWAVES

May 1976
Vol. 15, No. 5

news

9 Alternatives Weighed For MOS Capacitors
10 Accurate Measurements Key To Forecasting Earthquakes
14 Phase Shifters Evaluated For Economical EAR
16 R & D
18 Industry
20 Washington
24 International
28 For Your Personal Interest . . .
32 Meetings

editorial

30 Welcome To Our Feedback Circuit

technical section

Passive Components

34 **Design More Accurate Interdigitated Couplers.** Donald D. Paolino of the Naval Weapons Center presents design curves for interdigitated couplers built on alumina or fused silica substrates.

40 **Master The Challenge Of Offset Stripline Design.** Sachs Rimmon of the Israeli Ministry of Defense analyzes the impedance of stripline conductors which are sandwiched unequal distances from two groundplanes.

47 **Transform Impedance With A Branch-Line Coupler.** Dr. Chen Y. Ho of the Collins Radio Group shows how to eliminate interstage impedance transformers in hybrid-coupled amps by designing branch-line couplers with unequal input and output impedances.

55 **Specifying Isolation To Limit Frequency Pulling.** Arthur W. Vemis of Block Engineering explains how to calculate the minimum isolation necessary to keep an oscillator's pulling specification within limits under changing load VSWR and phase.

58 **Computer Analysis Speeds Corrugated Horn Design.** G. R. Loefer, J. M. Newton, J. M. Schuchardt and J. W. Dees of Georgia Institute of Technology provide a computer program, written in the BASIC language, which calculates the radiation pattern of a corrugated horn, given its flare angle, length and diameter.

products and departments

66 Product Feature: $4000 Buys A Complete Swept Measurement System.
67 New Products
84 New Literature
88 Application Notes
89 Bookshelf
90 Feedback
91 Advertisers' Index
92 Product Index

About the cover: Look closely and you will discover three versions of the popular Lange microstrip coupler in this design by Art Director Robert Meehan.

coming next month: Test and Measurements

How Accurate Is Your Spectrum Analyzer? Peter Linden of Hewlett-Packard examines the factors which influence the accuracy of a spectrum analyzer. Four basic measurement techniques are evaluated in terms of their accuracies: i-f substitution, linear display, rf substitution and relative measurement. Finally, the author suggests ways in which ancillary equipment such as an accurate signal source, power meter, attenuator, comb generator and frequency counter can be used to improve accuracy.

Measure Group Delay Fast And Accurately. M. J. Ahmed, A. Froese and G. Schmiing, of GTE Lenkurt Electric in British Columbia introduce a swept-frequency technique for the measuring group delay of filters and equalizers. The method relies on a standard CRT for display, yet achieves an accuracy of 0.2 ns.

Use Electrical Tests To Measure Thermal Parameters. Bernard Siegal of Sage Enterprises explains how the thermal resistance of a semiconductor device can be accurately measured by monitoring a temperature sensitive electrical parameter. Measurement methods must be carefully tailored to match the device.

Win A Scientific Pocket Calculator!
Return The Passive Component Survey Card On Page 64.

Publisher/Editor
Howard Bierman

Managing Editor
Stacy V. Bearse

Associate Editor
Joseph Ligori

Contributing Editor
Harvey J. Hindin

Washington Editor
Paul Harris
Snyder Associates
1050 Potomac St., NW
Washington, DC 20007
(202) 965-3700

Editorial Assistant
Gail Murphy

Production Editor
Sherry Lynne Karpen

Art Director
Robert Meehan

Production
Dollie S. Viebig, Mgr.
Dan Coakley

Circulation
Barbara Freundlich, Dir.
Trish Edelmann
Gene M. Corrado
Sherry Karpen,
Reader Service

Promotion Production Manager
Albert B. Stempel

Directory Coordinator
Janice Tapp

Editorial Office
50 Essex St.,
Rochelle Park, NJ 07662
Phone (201) 843-0550
TWX 710-990-5071

A Hayden Publication
James S. Mulholland, Jr., President

MICROWAVES is sent free to individuals actively engaged in microwave work. Subscription prices for non-qualified copies:

	1 Yr.	2 Yr.	3 Yr.	Single Copy
U.S.	$15	$25	$35	$2.50
FOREIGN	$20	$35	$50	$2.50

Additional Product Data Directory reference issue, $10.00 each (U.S.), $18.00 (Foreign). POSTMASTER, please send Form 3579 to Fulfillment Manager, MicroWaves, P.O. Box 13801, Philadelphia, PA. 19101.

Back Issues of MicroWaves are available on microfilm, microfiche, 16mm or 35mm roll film. They can be ordered from Xerox University Microfilms, 300 North Zeeb Road, Ann Arbor, MI 48106. For immediate information, call (313) 761-4700.

Hayden Publishing Co., Inc., James S. Mulholland, President, printed at Brown Printing Co., Inc., Waseca, MN.

Copyright © 1976 Hayden Publishing Co., Inc., all rights reserved.

news/meetings

September

14-17. 6th European Microwave Conference. Palazzo dei Congressi, Rome, Italy. Contact: Microwave Exhibitions & Publishers Ltd., Temple House, 36 High Street, Sevenoaks, Kent, TN13 1 JG, England (Tel) Sevenoaks 59533.

14-17. WESCON (Western Electronic Show and Convention). Los Angeles Convention Center, Los Angeles, CA. Contact: William C. Weber, Jr., WESCON General Manager, 999 No. Sepulveda Blvd., El Segundo, CA 90245 (213) 772-2965.

26-29. North American Symposium on Gallium Arsenide and Related Compounds. Stouffer's Waterfront Towers, St. Louis, Missouri. Contact: J. V. DiLorenzo, Secretary, North American GaAs Symposium, Room MH 7B-402, Bell Labs, Murray Hill, NJ 07974 (201) 582-3452.

29-October 1. Ultrasonics Symposium. Annapolis Hilton Ann, Annapolis, MD. Contact: Dr. L. R. Whicker, General Chairman, 1976 Ultrasonics Symposium, Naval Research Labs (Code 5250), Washington, DC 20375 (202) 767-3312.

Call For Papers

Deadline: July 1. Int'l IEEE/AP-S Symposium and USNC/URSI Meeting. University of Massachusetts, Amherst, MA. Areas of interest: multibeam and limited scan antennas, adaptive antennas, wave propagation, remote sensing and probing, etc. Contact: R. L. Fante, AFCRL (LZ), Hanscom AFB, MA 01731 (617) 861-3683. The meeting will be held on October 10-15.

Short Courses

June 1-3. Lasers and Applications. Pentagon City Quality Inn, Arlington, VA. Course is designed to provide a basic understanding of lasers leading to a discussion of state-of-the-art and potential applications. Fee: $395. Contact: Continuing Education Courses, PO Box 3278, Falls Church, VA 22403.

June 7-11. Digital and Optical Processing. University of Rochester, Rochester, NY. Course is designed to provide the basic concepts and methods of image processing from both digital and optical points of view: Fee: $380. Contact: The Institute of Optics, University of Rochester, Rochester, NY 14627.

If you work in volume, these can mean less work for you.

If you use miniature coaxial connectors in quantity, you'll be interested in the latest additions to the Johnson JCM family: Crimp-type straight cable plugs, and crimp-type straight cable jacks.

You use a standard crimping tool, so they're quicker to assemble. And when you're a volume user, the savings in labor can really mount up.

Like all other Johnson JCM's, these feature gold or nickel plating, brass body, Teflon® insulator, and beryllium copper center contact. There are five or fewer parts to assemble.

They are fully compatible with SMA types, yet cost less than SMA equivalents. Designed for frequencies into the microwave range.

New Johnson crimp-style connectors. We've put a lot of work into them.

To make less work for you.

E. F. Johnson Company
3005 Tenth Avenue S.W., Waseca, MN 56093

☐ Please send me technical information on JCM miniature coaxial connectors.

☐ Please send me samples. You can call me at

(____)_____

NAME_____

TITLE_____

FIRM_____

ADDRESS_____

CITY_____ STATE_____ ZIP_____

E. F. Johnson Company

READER SERVICE NUMBER 33

Design More Accurate Interdigitated Couplers

A TEM analysis leads to design curves for interdigitated couplers built on alumina or fused silica substrate. Numerical electromagnetic techniques account for the inhomogeneous dielectric.

THE interdigitated microstrip coupler introduced by Lange[1] cannot be designed by traditional coupled-line methods, such as the popular computer program of Bryant and Weiss[2], since the charge distribution for the four-strip coupler is completely different from that of two coupled lines.

Microstrip dimensions in the Bryant and Weiss program are used to determine even and odd mode impedances and propagation velocities for a given substrate material. Although some attempt has been made to derive "equivalent" even and odd modes for Lange's coupler design in order to apply the Bryant and Weiss data[3], the approach assumes equal mode velocities, when in fact, they are unequal.

The design curves reproduced on the opposite page overcome many of the difficulties associated with modifying a two-strip analysis, since they were derived specifically for four-strip interdigitated couplers. The curves are based on a computer-aided TEM analysis, rigorously checked by comparison with experimental data.

To use the curves, the voltage coupling coefficient K and characteristic impedance Z_0 (usually 50 ohms) must be known. The odd-mode impedance is given by:

$$Z_{oo} = Z_0 [(1 - K)/(1 + K)]^{1/2}$$

The even-mode impedance is:

$$Z_{oe} = Z_0^2/Z_{oo}$$

The point defined by a (Z_{oe}, Z_{oo}) pair will intersect a curve of constant W/H and another curve of constant S/H. These are the required cross-sectional microstrip parameters.

A line of constant 50-ohm characteristic impedance is plotted on the design curves. Thus, it is only necessary to find either Z_{oe} or Z_{oo} and locate the intersection of the impedance with the constant Z_0 line to obtain the physical dimensions. The range of coupling coefficients spanned by the curves is approximately −2 to −6 dB for a characteristic coupler impedance of 50 ohms.

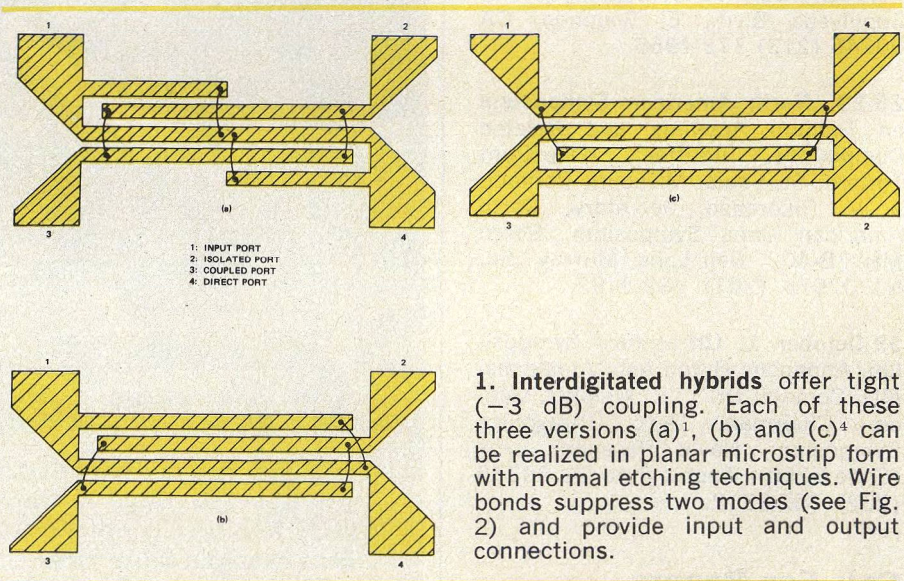

1. Interdigitated hybrids offer tight (−3 dB) coupling. Each of these three versions (a)[1], (b) and (c)[4] can be realized in planar microstrip form with normal etching techniques. Wire bonds suppress two modes (see Fig. 2) and provide input and output connections.

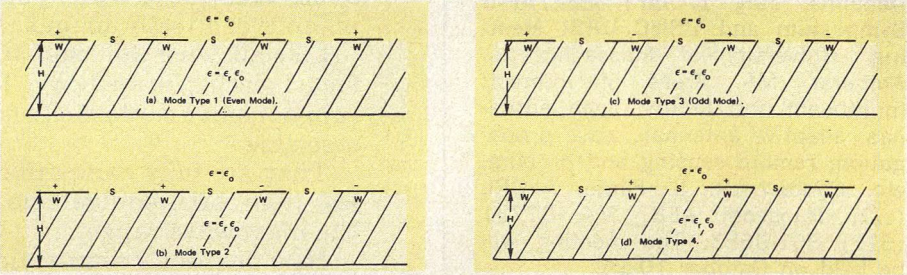

2. Four non-degenerate modes can exist with the four-strip Lange coupler. Note that modes two and four are virtually eliminated because potentials on those strips are equated by wire bonds.

Analyzing the Lange coupler

The interdigitated directional coupler shown in Fig. 1 may be viewed as a multiconductor transmission line of N (N must be even) elements, not including the ground plane. All transmission lines can be assumed lossless.

On any TEM, N-wire transmission line, N orthogonal modes can exist. In the case of the directional coupler, only two modes are of interest—the even and the odd. Even-mode excitation occurs when all conductors are at the same potential; the odd-mode case is where succeeding adjacent conductors are

Donald D. Paolino, Electronic Engineer, Naval Weapons Center, Code 3522, China Lake, CA 93555.

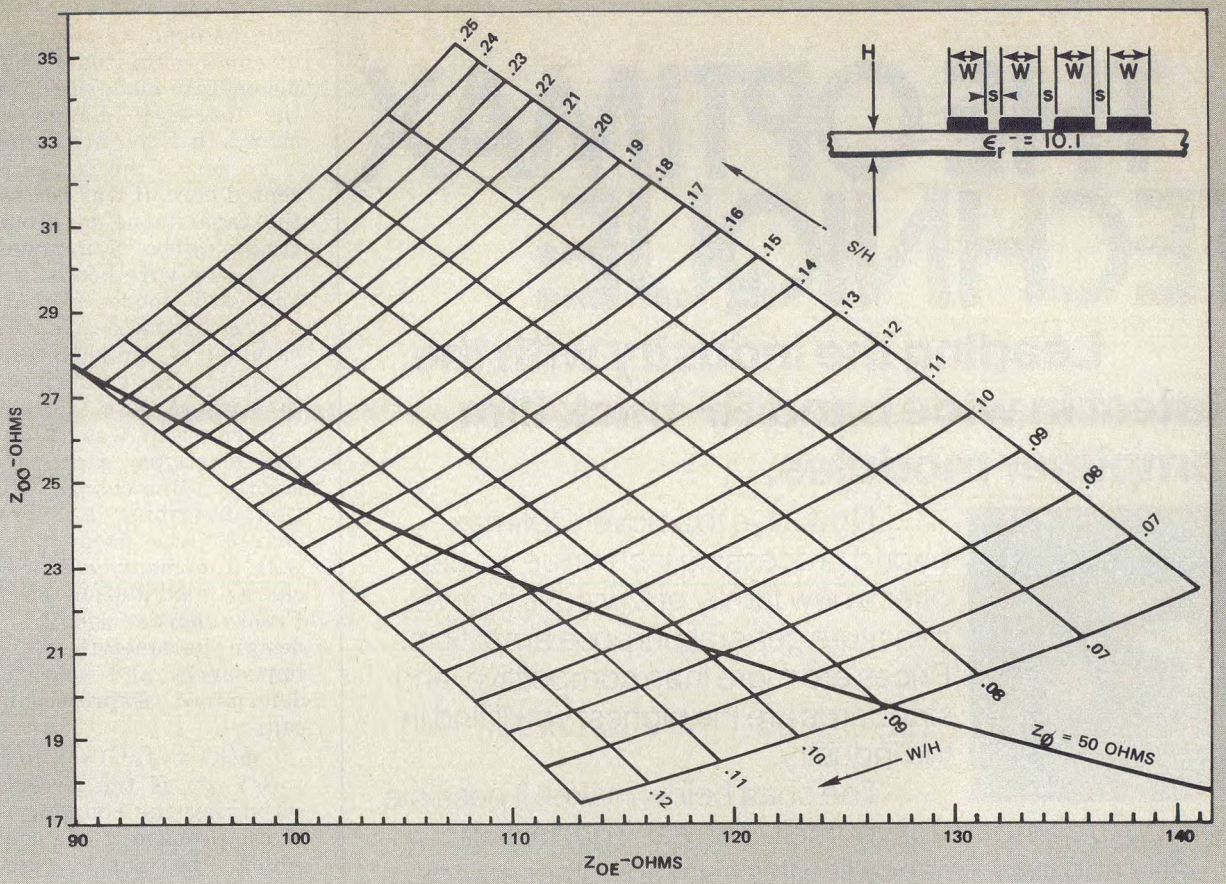

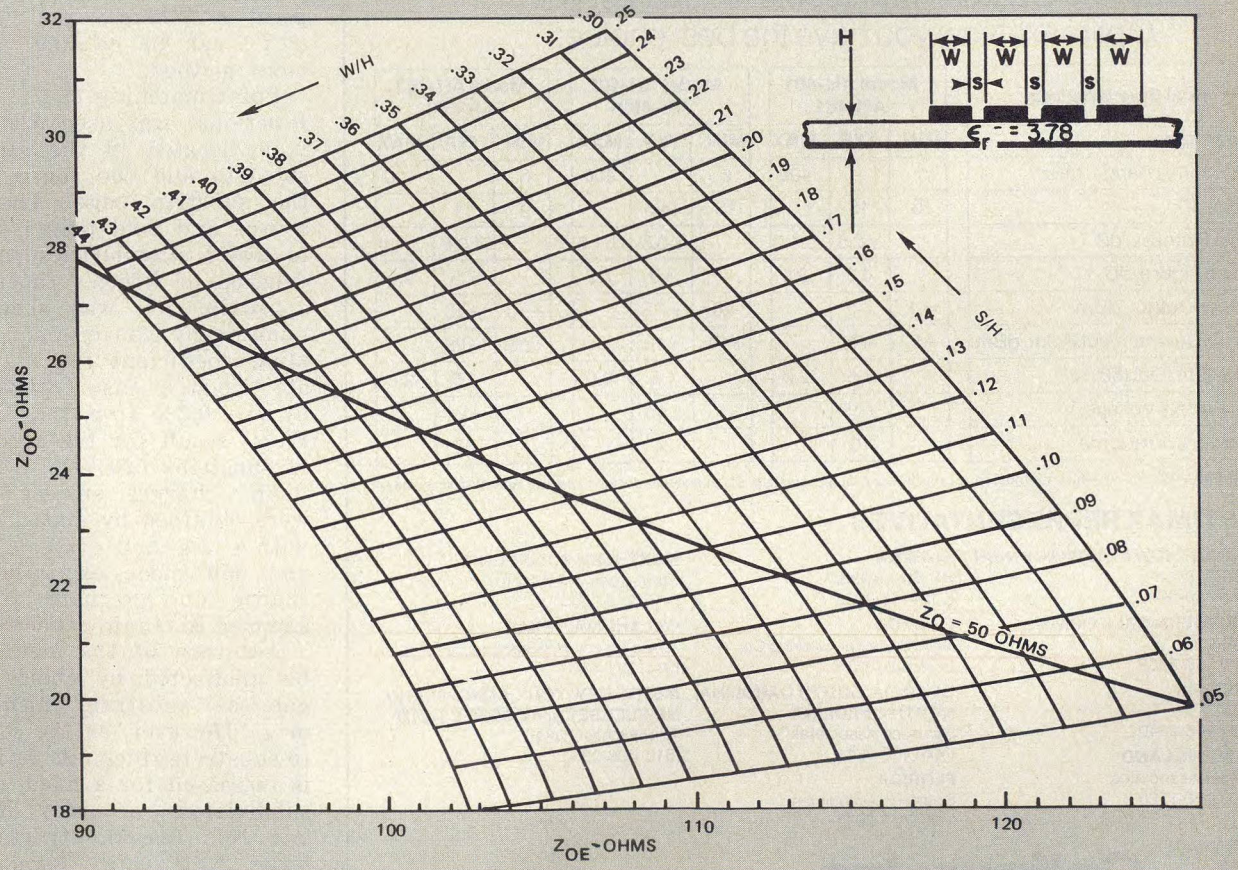

Design curves are valid for alumina (top) and fused silica (bottom) substrates.

(continued on p. 36)

THE OPTIMAX TECHNIQUE:

Leading the industry with the latest in wide band RF thick film amplifier modules.

Now, due to a novel Optimax hybrid processing technique we can offer a new family of low cost, high rel, miniature general purpose amplifiers. Prices are more than competitive, and standards are the highest you'll find in the industry.

The chart below makes it possible for you to compare for yourself. You can't get thick film quality and performance like this from any other source.

For a data sheet or further information, write us, or contact the Optimax representative nearest you.

Optimax. Now you have the best choice.

Electrical Specifications	Model AH-401 AH-461			Model AH-402 AH-462			Model AH-403 AH-463		
Parameter	MIN	TYP	MAX	MIN	TYP	MAX	MIN	TYP	MAX
Frequency Range, MHz*	5	–	400	5		400	5		400
Gain, dB	13	15		13	14.5		9	11	
Gain Flatness, dB		±0.5	±1.0		±0.5	±1.0		±0.5	±1.0
Noise Figure, dB		4.0	5.0		5.0	7.5		7.5	9.0
Power Output, dBm	–3	–2		+6	+7.5		+13	+15	
3rd Order Intercept Point, dBm	+6	+8		+14	+18		+23	+26	
VSWR In/Out (50Ω)		1.5	2.0		1.5	2.0		1.5	2.0
DC Supply Voltage, V		+15			+15			+24	
Supply Current, mA		10			24			65	

The AH-461, 462 and AH-463 units must have external input, output and bypass capacitors selected to establish low frequency roll-off.

OPTIMAX REPRESENTATIVES

ILLINOIS, IOWA and WISCONSIN
Sieger Assoc.
(312) 956-0963

SOUTHERN CALIFORNIA
DARCO
(213) 398-6239

ARIZONA
DARCi
(602) 948-2240

NEW ENGLAND
Lancer Associates
(617) 861-1720

INDIANA
RF Specialists
(219) 485-8982

CANADA
Solid State Engineering Co.
(514) 481-3313

GEORGIA, SOUTH CAROLINA, NORTH CAROLINA
Spartech Associates
(404) 432-3644

FLORIDA
Spartech Associates
(305) 727-8045

NORTHERN CALIFORNIA
Stout-Loeswick Assoc.
(415) 948-3265

OKLAHOMA, TEXAS
Texas Microwave Electronics
(214) 321-5381

METRO NEW YORK, LONG ISLAND, NEW JERSEY and CONNECTICUT
Trionics Associates
(516) 466-2300

Optimax, Inc.
a subsidiary of Alpha Industries, Inc.
P.O. Box 105, Advance Lane, Colmar, Pennsylvania 18915
(215) 822-1311 • Twx: 510-661-7370

READER SERVICE NUMBER 36

held at opposite-polarity potentials of equal magnitude. The four non-degenerate mode configurations for the four-strip Lange coupler are shown in Figs. 2(a) through (d).

To derive the design curves presented here, it was necessary to find the capacitance to ground of N/2 strips (since N/2 strips are connected by wire bonds) for the even and odd mode excitations with $\epsilon = \epsilon_r \epsilon_0$ and $\epsilon = \epsilon_0$. All coupling parameters, impedances and mode velocities can be derived from this capacitance data.

Each strip was subdivided into ten substrips, each substrip considered a line charge. Green's function describing a microstrip line charge[5] was used in conjunction with a moment method to calculate charge distribution on the strips. From charge density, important design parameters such as mode impedances and velocities can be determined. Expressed mathematically:

$$\phi(x) = \int_s G(x, x')\sigma(x')dx'$$

$G(x, x')$ is the Green's function satisfying the boundary conditions of the problem, s is a contour along which the charge density lies, $\sigma(x')$ is the charge density at point x' and $\phi(x)$ is the known potential on the strip conductor at point x. When $G(x, x')$ is known, $\sigma(x')$ can be obtained by a moment method.

Point matching (pulse expansion functions) was used with the field point located in the center of a substrip and the source point on the substrip edge. The disjoint source and field points were used to avoid singularities in the calculation of Green's function. This approximation was shown to be numerically convergent: The coupling coefficient for the degenerate two-strip case typically differs by only 0.2% from the Bryant and Weiss result for the same number of substrips (20).

The charges on each substrip were obtained by matrix inversion with $\epsilon = \epsilon_0$ and $\epsilon = \epsilon_r \epsilon_0$ for even and odd mode excitations. Total charge on alternate strips was summed to obtain capacitance data.

Accuracy of the method should be unaffected by choice of strip gap (s), substrate thickness (H) or ϵ_r. However, as the strip width to substrate thickness ratio (W/H) is increased for a fixed number of subdivisions, accuracy diminishes. For this reason, structures with large W/H ratios should not be analyzed by this technique. This is not a practical limitation, since for the range of useful coupling coefficients and characteristic imped-

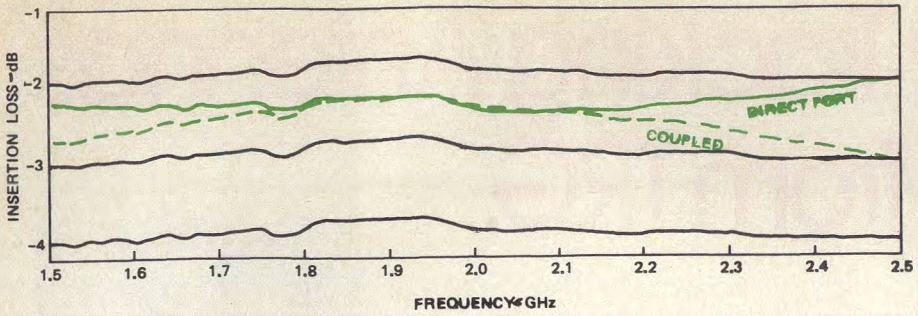

3. **Test data** on a 3 dB coupler built to dimensions provided by the computer program corresponds to predicted performance.

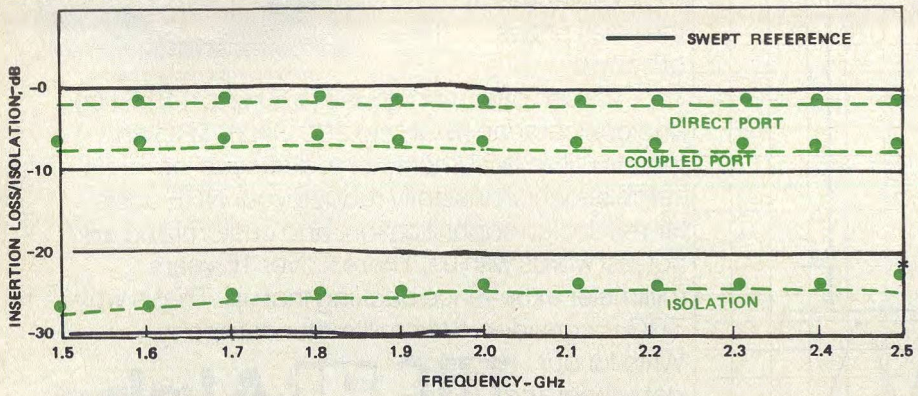

W/H=. 142000 S/H=. 302640

ZOE (OHMS.)	ZOO (OHMS)	COUPLING COEFF DB	CHARACTERISTIC IMPEDANCE(OHMS)
84. 410446	28. 488892	-6. 1022434	49. 038361

EFFE	EFFO	COUPLING COEFF	VEVEN M/SEC	VODD M/SEC
6. 9710675	5. 5720835	.49532223	.11420205E+09	.12700136E+09

****

DIRECT PORT

FGHZ	RTLSS	VSWR	INSLSS	OUTPHS	ISO
1. 50	-31. 599	1. 05	-1. 096	-71. 94	-26. 30
1. 60	-30. 770	1. 06	-1. 150	-76. 07	-25. 78
1. 70	-29. 993	1. 07	-1. 192	-80. 16	-25. 25
1. 80	-29. 261	1. 07	-1. 221	-84. 22	-24. 73
1. 90	-28. 566	1. 08	-1. 236	-88. 26	-24. 19
2. 00	-27. 905	1. 08	-1. 238	-92. 30	-23. 65
2. 10	-27. 274	1. 09	-1. 227	-96. 35	-23. 10
2. 20	-26. 668	1. 10	-1. 203	-100. 42	-22. 53
2. 30	-26. 088	1. 10	-1. 166	-104. 52	-21. 96
2. 40	-25. 530	1. 11	-1. 117	-108. 67	-21. 38
2. 50	-24. 995	1. 12	-1. 058	-112. 88	-20. 80

COUPLED PORT

FGHZ	RTLSS	VSWR	INSLSS	OUTPHS	ISO
1. 50	-31. 599	1. 05	-6. 575	18. 10	-26. 30
1. 60	-30. 770	1. 06	-6. 398	13. 99	-25. 78
1. 70	-29. 993	1. 07	-6. 270	9. 93	-25. 25
1. 80	-29. 261	1. 07	-6. 189	5. 89	-24. 73
1. 90	-28. 566	1. 08	-6. 153	1. 88	-24. 19
2. 00	-27. 905	1. 08	-6. 159	-2. 12	-23. 65
2. 10	-27. 273	1. 09	-6. 210	-6. 12	-23. 10
2. 20	-26. 668	1. 10	-6. 305	-10. 13	-22. 53
2. 30	-26. 088	1. 10	-6. 447	-14. 17	-21. 96
2. 40	-25. 530	1. 11	-6. 640	-18. 24	-21. 38
2. 50	-24. 995	1. 12	-6. 887	-22. 35	-20. 80

4. **Predicted performance** of a loosely coupled (−6 dB) hybrid is plotted next to measured performance of a coupler built to computer-derived dimensions below. Slight difference is due to measurement losses.

(continued on p. 38)

SAWS

Surface Acoustic Wave devices.

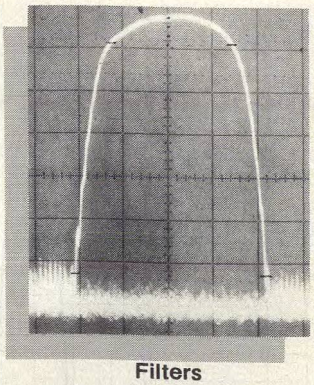

Filters

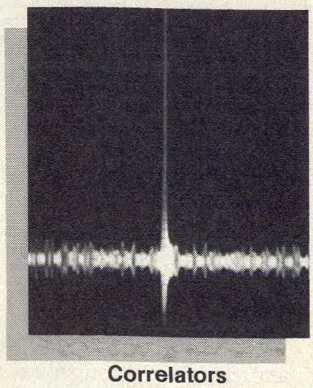

Correlators

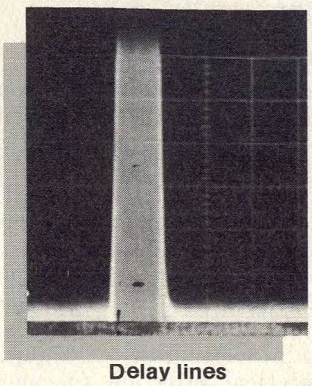

Delay lines

Our team will be glad to help you, from quotation through production. Teledyne MEC, 3165 Porter Drive, Palo Alto, CA 94304. Phone (415) 493-1770. TWX: 910-373-1746.

Regional Offices: Dayton, OH (513) 253-8144; Stamford, CT (203) 325-2535; Bethesda, MD (301) 530-2220. Belgium (02) 673.99.88. Telex: 25881 TDYBEL B. Other field offices around the world.

TELEDYNE MEC

Master The Challenge Of Offset Stripline Design

Wideband components may require stripline conductors located unequal distances from two ground planes. Here are curves that present strip width based on impedance and offset.

THE design of stripline conductors is done cookbook style when the line is sandwiched midway between a pair of ground planes. But what if it's off center?

When a center conductor is closer to one of the ground planes than the other (Fig. 1), impedance levels are not as easily calculated as with the more common center-line configuration. For the symmetrical geometry, Fig. 2, the line characteristic impedance, Z_o, is determined solely by the strip width to ground plane spacing ratio, W/B, and the dielectric constant of the medium, ϵ_r. The calculation of Z_o for the offset case, on the other hand, also depends on the offset (S/B) ratio. It turns out that it's possible to decrease W/B by increasing S/B for a given impedance level. This is particularly useful when space for conductor width is limited.

These characteristics are brought out in the three design graphs, Figs. 3, 4 and 5, which may be used for determining the transmission line characteristic impedances and spacing for offset lines. The symmetrical case, (S/B = 0.5) is also included as a limiting value. The curves are, of course, directly useful in analyzing the three-layer configuration (Fig. 6), which is the dominant stripline construction technique for volume production. The center conductor is offset by half the thickness of the central layer when this method is used. This causes an unbalance in both parallel plate capacities and fringe field capacities, which can result in an error of several ohms in a 50-

Sachs Rimmon, Research Engineer, State of Israel, Ministry of Defense, P.O. Box 7063, Tel Aviv, Israel.

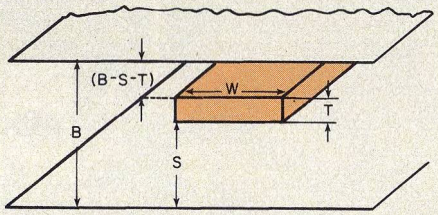

(a)

1. The impedance of the offset strip transmission line is a function of W/B, T/B and S/B.

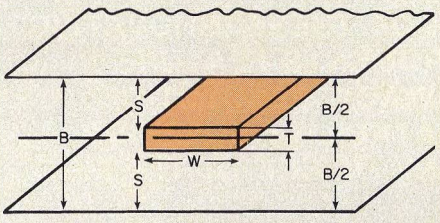

(b)

2. When the center strip is symmetrically placed, S/B = 0.5, and impedance is determined by W/B.

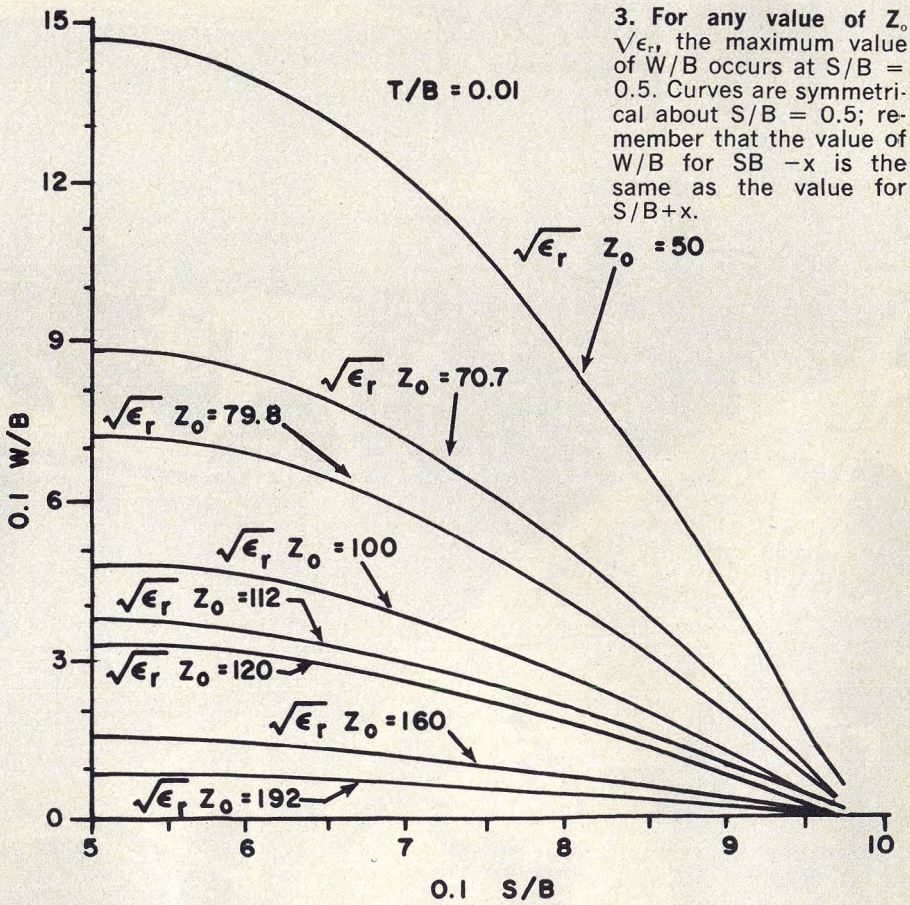

3. For any value of $Z_o\sqrt{\epsilon_r}$, the maximum value of W/B occurs at S/B = 0.5. Curves are symmetrical about S/B = 0.5; remember that the value of W/B for SB −x is the same as the value for S/B+x.

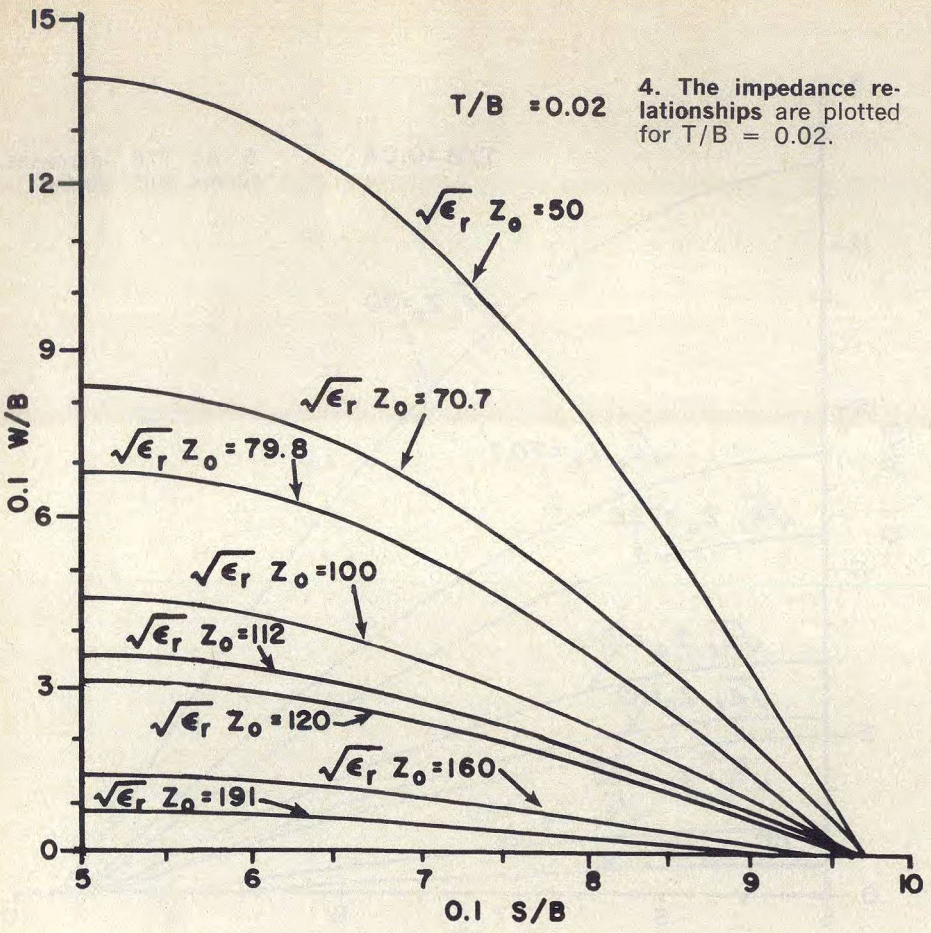

4. The impedance relationships are plotted for T/B = 0.02.

ohm line. This inaccuracy can be a disaster in the new multi-octave and greater bandwidth devices.

Each curve in Figs. 3, 4 and 5 plots the variation of W/B vs. S/B with $Z_0 \sqrt{\epsilon_r}$ as a fixed parameter. In order to have the highest accuracy, the thickness of the conductor (T) is taken into account. Three typical values of T/B, 0.01, 0.02 and 0.03, are considered.

It can be shown that W/B is a symmetric function of S/B about S/B = 0.5. This means, for example, W/B is the same for a given $Z_0 \sqrt{\epsilon_r}$, whether S/B equals 0.4 or 0.6. Hence, to save space, the curves are drawn for S/B $\geq$ 0.5 only. When calculating S/B, S should be taken as the distance from the strip to the farthest ground plane.

For non-offset or symmetrical lines, S/B = 0.5 always and the graphs are used to directly determine W/B for a desired $Z_0 \sqrt{\epsilon_r}$. The data for this limiting case has, of course, been available for many years.

Applying the curves

A significant advantage of the offset line is, as mentioned, that it is possible to decrease W/B for a given impedance level by in-

(continued on p. 42)

ENGELMANN MAKES IT!

TERMINATION/LOADS STANDARD OR CUSTOM

Over 30 Standard Types In Stock Including:
- **DC to 8 GHz — 10, 25, and 50 Watts.**
- **DC to 12 GHz — 2, 5 and 10 Watts.**
- **DC to 18 GHz — 1 Watt.**

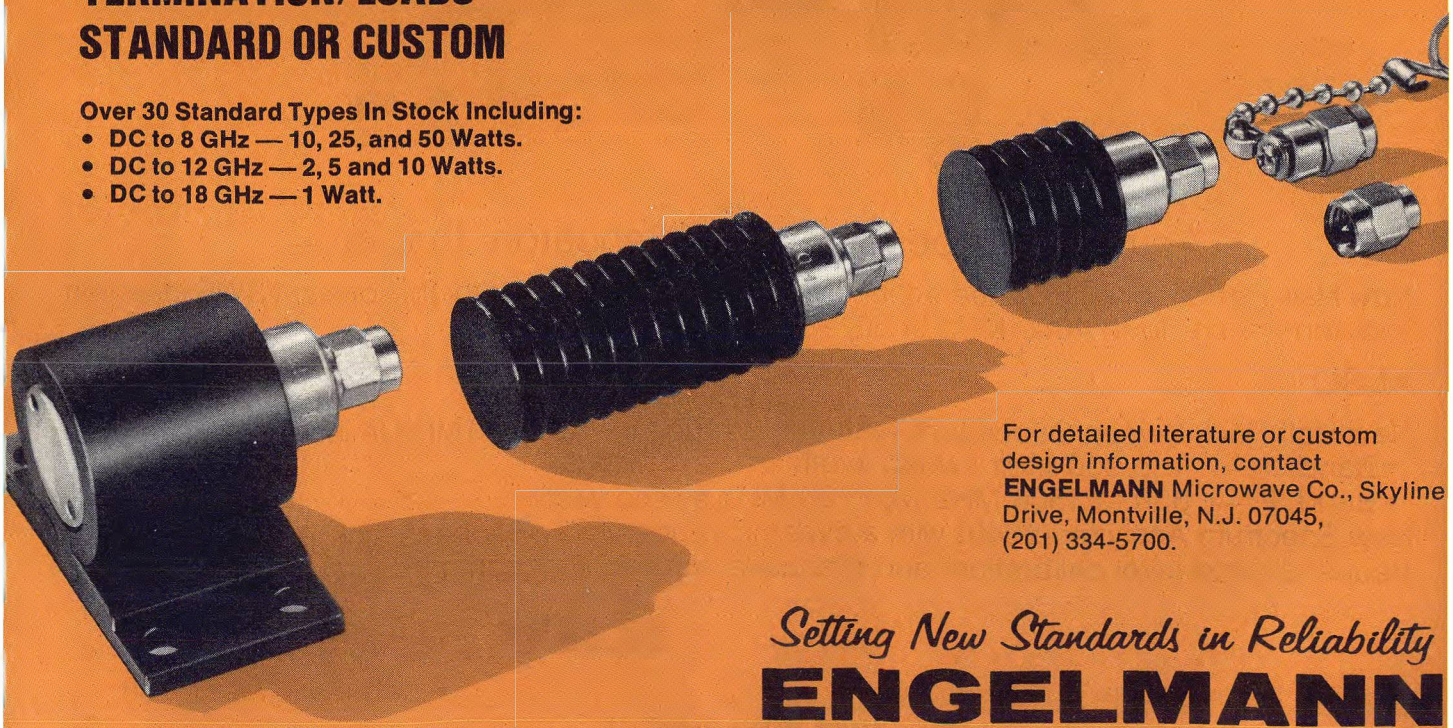

For detailed literature or custom design information, contact **ENGELMANN** Microwave Co., Skyline Drive, Montville, N.J. 07045, (201) 334-5700.

Setting New Standards in Reliability

ENGELMANN

Engelmann Microwave Co. — Subsidiary of Pyrofilm Corporation

READER SERVICE NUMBER 41

806

creasing S/B. This can be put to use in the design of stripline circulators. Consider the 8 GHz, three-port device shown in Fig. 7; all ports are terminated by 50 ohms. Three impedance transformers are used to match the 20-ohm ferrite with the output ports.

Simple trigonometry proves that the geometry of the puck restricts the width of the impedance transforming lines to a maximum of $\sqrt{3}R$, where R is the ferrite puck radius. Due to the low impedance level of the ferrite, it is very possible that a standard design with symmetrically-placed striplines will require that this width be greater than $\sqrt{3}R$. The solution, provided by the design graphs furnished in this article, is to use the offset line. B is already defined by the puck thickness, which in turn is set by frequency. Increasing S/B from 0.5 allows a lower value of W/B and hence, a narrower line to meet the $\sqrt{3}R$ limitation.

Another important application of the design curves for offset lines is in coupler design. For loose coupling values (greater than 10 dB), the narrow side coupling configuration shown in Fig. 8 is generally used. If a tightly coupled section (less than 10 dB or so) is required such as in a multi-octave

(continued on p. 44)

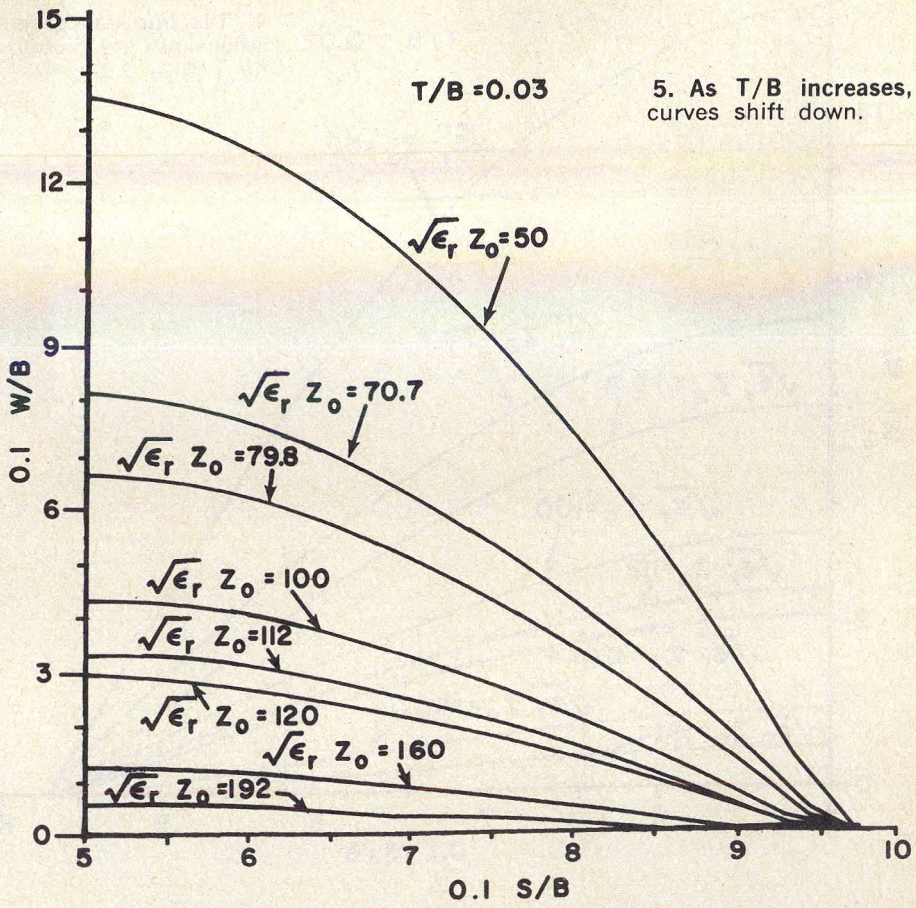

5. As T/B increases, curves shift down.

Just A Step Above The Rest

Actually the best step — Attenuators that is —

Now New Performance Engineered in-line and rotary attenuators for the lowest VSWR insertion loss, operating up to 4000 MHz in 50, 75, and 90 ohms.

ALSO

New Half Rack Sweep Generators featuring a range of 1 to 1500 MHz in just **TWO** bands:

- Band 1 — 1 to 900 MHz sweep width
- Band 2 — 800 to 1500 MHz with 700 MHz sweep width

New Spectrum Analyzer (9040) with a dynamic range of 72 dB, phase lock, 1 KHz resolution, frequency and level calibration, and manual/automatic filter control.

KAY Elemetrics Corp.
Pinebrook, N.J. 07058

See Us at Booths 2517 and 2519 Electro '76

READER SERVICE NUMBER 42

CONFORMAL ANTENNAS

Transco designed coplanar stripline antennas is transmitting biological information to the NIMBUS F satellite from the **backs of polar bears** in the Artic. Our unique design is only 6″ square at 400 MHz, yet it gives 2 dBi gain and circular polarization. The antenna forms the upper cover of the telemetry package attached to the back of the bear. It is designed for extremely rugged service conditions.

We are currently under contract to supply wrap-around, conformal antennas for **missile applications.** Our design is based on cavity-backed slot radiators, but with an important difference: the slots, cavities, and associated feed lines are built from a single printed circuit board with no rivets or mechanical fasteners required.

The result is superior electrical performance, compared to Microstrip designs with the low cost and reliability of single layered board.

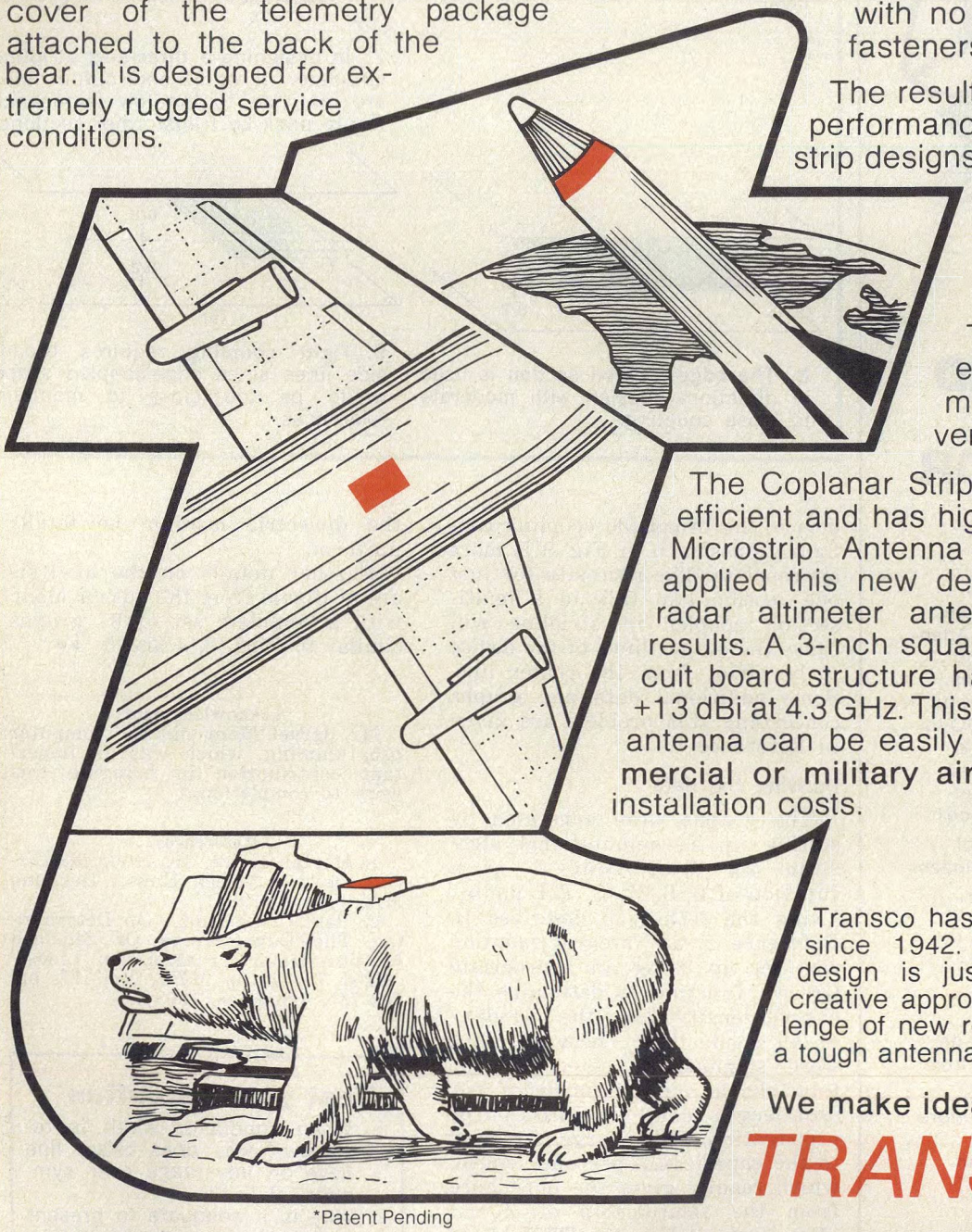

This new family of electrical thin, conformal antennas was invented at Transco.

The Coplanar Stripline Antenna is more efficient and has higher gain than similar Microstrip Antenna designs. We have applied this new design to conventional radar altimeter antennas with excellent results. A 3-inch square, 0.060″ printed circuit board structure has measured gain of +13 dBi at 4.3 GHz. This inexpensive altimeter antenna can be easily "pasted on" to **commercial or military aircraft** with minimal installation costs.

Transco has been building antennas since 1942. The Coplanar Stripline design is just one example of our creative approach in meeting the challenge of new requirements. If you have a tough antenna problem, call us!

We make ideas work!

TRANSCO

*Patent Pending

TRANSCO®

TRANSCO PRODUCTS, INC., 4241 GLENCOE AVENUE, VENICE, CALIFORNIA 90291
TELEPHONE: Area Code 213 / 821-7911 • TELEX 65 - 2448 • TWX 910 - 343 - 6569
Coaxial & Waveguide Switches • Antennas • Microwave Components
Quality Products Since 1942, Equal Opportunity Employer.

READER SERVICE NUMBER 43

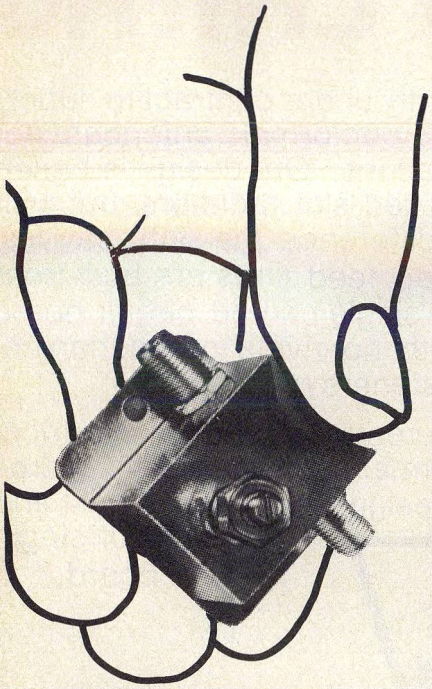

BROADBAND MINIATURE ATTENUATOR

DC-UHF

Merrimac's Model ARM-1 Continuously Variable Miniature Attenuator is ideal for level set and signal processing applications from DC through 400 MHz. In its optimum frequency range (DC-to-50 MHz), attenuation range is 0-to-20 db, with less than 1 db insertion loss and 0.2 db resetability. It weighs only 1.4 ounce!

Merrimac's versatile family of variable attenuators also includes:

Model ARS-1, a subminiature attenuator weighing only 0.7 ounce, ideal for mounting on PC boards; operates from DC to 400 MHz.

Model ARE-1, an electronic attenuator providing 0-to-20 db attenuation for applications from 2-to-200 MHz.

Contact Merrimac today for more details on these and other attenuators, including custom models.

MERRIMAC INDUSTRIES INCORPORATED
41 FAIRFIELD PLACE, WEST CALDWELL, N. J. 07006
(201) 228-3890 • TWX 710-734-4314

READER SERVICE NUMBER 44

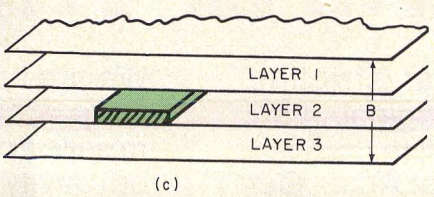

6. Three layer is the dominant stripline technique for volume production. The center conductor is offset by half the thickness of the central layer.

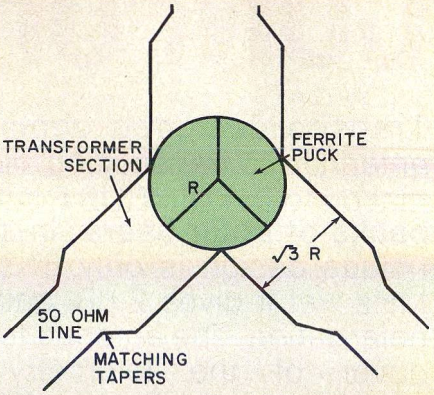

7. In designing a three-port stripline circulator, three 50-ohm output lines are matched to the low impedance ferrite puck by transformer sections.

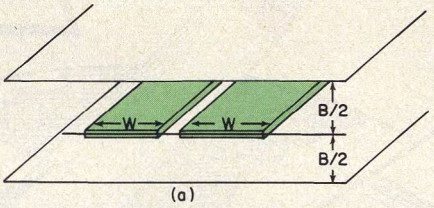

8. The edge-coupled section is used in directional design with moderate to loose coupling.

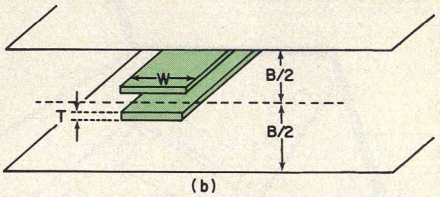

9. Tight coupling requires broadside lines since edge-coupled strips would be too close to maintain tolerances.

device, the broadside coupling configuration shown in Fig. 9 is more appropriate. The necessity for just one section like this in a multisection coupler in stripline will cause the output lines of the device to be offset from the center line. Some additional data and graphs concerning this problem are given in Reference 1.

Deriving the data

The graphs were generated by setting up a computational algorithm for determining Z_0 as a function of S/B, W/B, T/B and ϵ_r. Using the technique described in Reference 2, an integral equation was set up using an appropriate Green's function to determine the charge density along the boundary of all conductors. These densities were summed to determine the total charge on the conductor per unit length along the direction of propagation. This charge is related to the capacitance per unit length, which readily gives the impedance from the relationship of $Z_0 = (VC)^{-1}$ where V is the TEM phase velocity of propagation and C is the capacitance. The only limitations in the computer program used for calculation were that the conductors be perfect rectangles parallel to the ground planes and the dielectric medium be totally uniform.

Further details on the analysis are available from the author along with a complete set of 84 graphs similar to Figs. 3, 4 and 5. ••

Acknowledgment

Mr. Israel Maor did the computer programming, which was an important contribution in bringing this work to completion.

References

1. Harlan Howe, Jr., *Stripline Circuit Design*, Artech House, Dedham, MA, p. 37, (1974).
2. Paul C. Chesnut, "On Determining The Capacitances Of Shielded Multiconductor Transmission Lines," *IEEE Trans. on MTT*, Vol. 17, pp. 734-735, (October, 1969).

Test your retention

1. When conductor width is restricted, why does offset line have an advantage over symmetrical line?
2. Why is it adequate to present design curves only for values of S/B greater than or equal to 0.5?
3. In the commonly-used three-layer sandwich construction technique, what is the offset?

Transform Impedance With A Branch-Line Coupler

Eliminate interstage impedance transformers in hybrid-coupled amps by designing branch-line couplers with unequal input and output impedances and reduce circuit size by up to 50%.

CAREFULLY designed branch-line couplers can eliminate interstage impedance-matching transformers in the typical hybrid-combined transistor amplifier (Fig. 1), reclaiming several tenths of a dB in circuit losses, and cutting substrate area by up to 50%.

Branch-line couplers are traditionally designed with four, 50-ohm ports to match system impedance. However, most L and S-band power transistors present impedances of 5 to 50 ohms, in spite of internal matching circuitry. Interstage impedance transformers have been the classical solution.

A more practical approach incorporates the function of impedance transformation into the hybrid coupler. This article presents guidelines for designing branch-line couplers with unequal input and output port impedances, and equal or unequal power split. The analysis is based on well-established design formulas for branch-line couplers with an arbitrary power splitting ratio and equal impedances at all four ports.[1,2,3] Reference 3, in particular, provides specific design data for power splitting ratios of 10, 100 and 1,000 for three, four, five and six branch designs over a limited range of input-to-output impedances.

Deriving design formulas

A generalized branch-line coupler is shown in Fig. 2. All transmission lines are a quarter-wavelength long at the center design frequency. The admittances of the four lines normalized to the admittance of the input ports are Y_A, Y_B and Y_C. Y_D represents the admittance of each output port normalized to the input port admittance. Even and odd-mode coupler excitation ($M\pm$) can be described by 2 × 2 matrices.

$$M\pm = \begin{bmatrix} \mp Y_C/Y_B & j\,Y_B^{-1} \\ j(Y_B - Y_A \cdot Y_C/Y_B) & \mp Y_A/Y_B \end{bmatrix} \quad (1)$$

The even mode reflection coefficient (Γ_+) and the odd mode reflection coefficient (Γ_-), when set to zero, describe the conditions necessary for perfect match and infinite directivity, which are:

$$Y_A \cdot Y_D = Y_C \quad (2)$$

$$Y^2_B - Y_A \cdot Y_C = Y_D \quad (3)$$

The even mode transmission coefficient (T_+) and the odd mode transmission coefficient (T_-) can then be calculated from Eq. (1):

$$T\pm = Y_B/(jY_D \mp Y_C) \quad (4)$$

Dr. Chen Y. Ho, Engineer, Commercial Telecommunications Division, Collins Radio Group, Rockwell International Corporation, 1200 N. Alma Rd., Richardson, TX 75080.

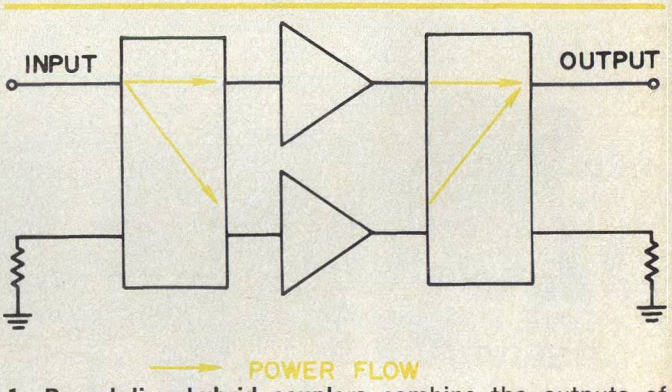

1. Branch-line hybrid couplers combine the outputs of parallel amplifiers.

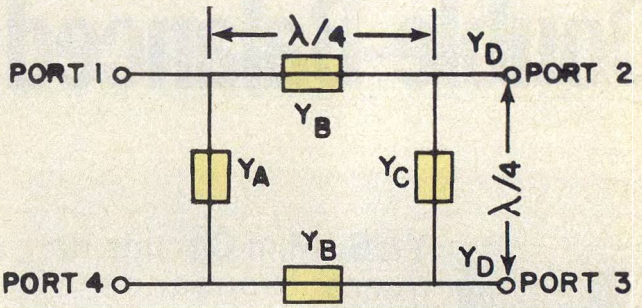

2. Each arm of a two-branch hybrid is a quarter-wavelength long.

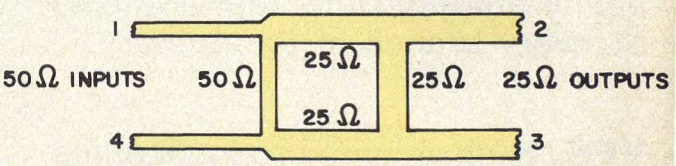

3. Fifty-ohm inputs are matched to 25-ohm outputs by this design.

The voltage appearing at port 2 is equal to:

$$V_2 = (T_+ + T_-)/2 = jY_B\,Y_D/(Y^2_C + Y^2_D) \quad (5)$$

and the voltage appearing at port 3 is

$$V_3 = (T_+ - T_-)/2 = -Y_B\,Y_C/(Y^2_C + Y^2_D) \quad (6)$$

Note that the phase of V_2 leads that of V_3 by 90 degrees.

To derive a design formula for the normalized admittance of each arm, assume that the conditions for perfect match and infinite directivity are satisfied,

(continued on p. 50)

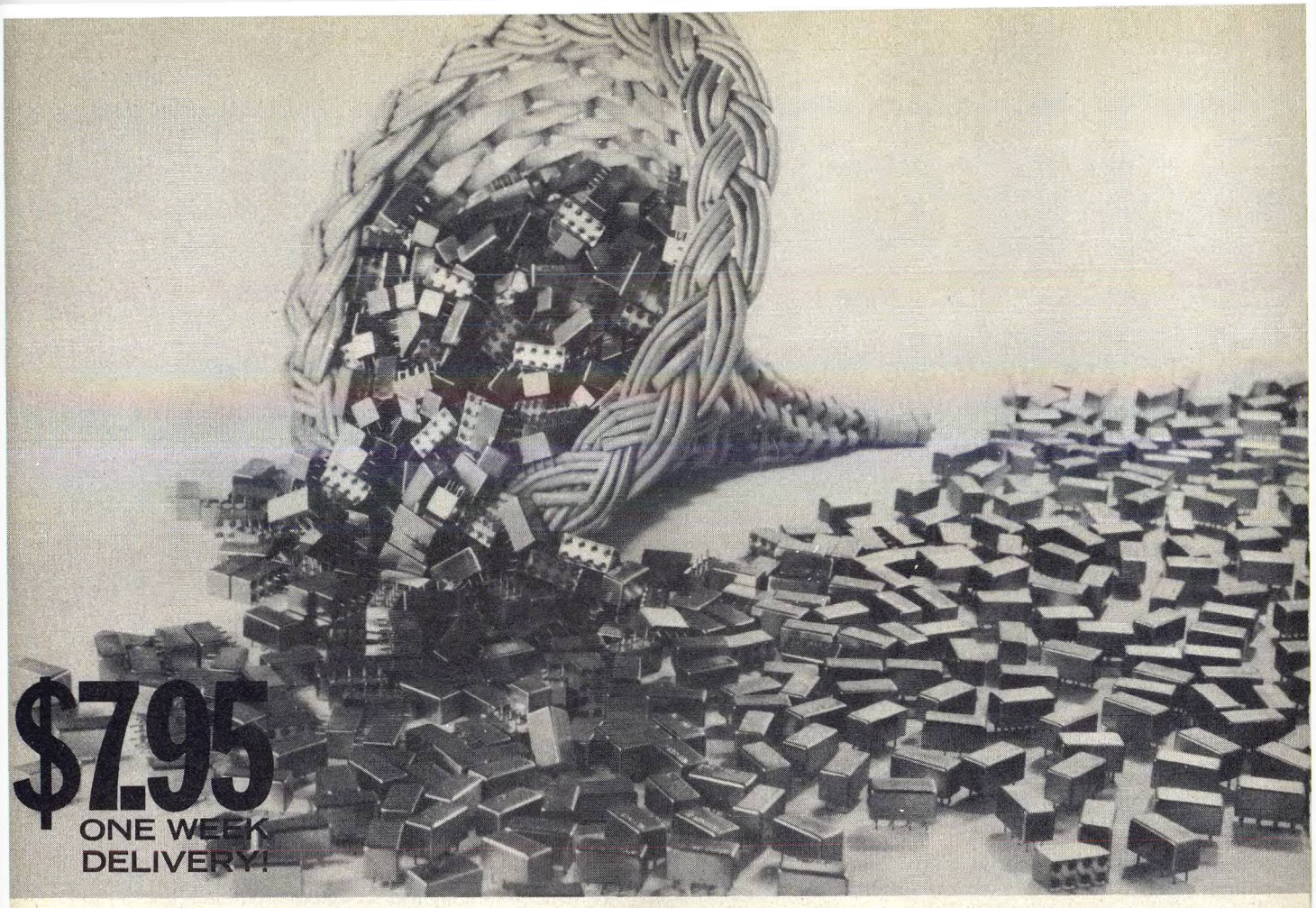

Double-Balanced Mixers, Directional

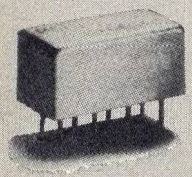

YES. Mini-Circuits delivers thousands of these units a week!

All with high-quality performance and reliability built-in. Units that are used by every branch of the military.

YES. High volume production like this brings lowest prices.

YES. We are the largest volume producers of double-balanced mixers satisfying the needs of almost every major communications company in the world.

☐ **Check these reliability features:**

☐ Exclusive use of hot-carrier diodes.

☐ Every diode is tested and matched.

☐ Every unit is tested 3 times

☐ Every solder connection is inspected.

☐ Bonding and encapsulation in 4 separate steps, for rugged moisture-proof units.

☐ A 1 year unconditional guarantee on every unit.

From Mini-Circuits...In One Week

Couplers, Power Splitter/Combiners

☐ Check these Specs SRA-1

Double-Balanced Mixers

$7.95 (500 quantity)

☐ **Frequency Range**	IF	DC to 500 MHz
	LO, RF	.5 to 500 MHz
☐ **Isolation**		40 dB
☐ **Conversion Loss**		6 dB
☐ **Size**		.4 x .8 x .4 in.
☐ **Metal Case**		RFI shielded Hermetically Sealed
☐ **Temperature Range**		−55°C to +100°C
☐ **Low Price**		$9.95 (1 thru 49 units)

☐ Check These Specs PDC 10-1B

Bi-Directional Coupler

$7.95 (500 Quantity)

☐ **Frequency Range**	1-400 MHz
☐ **Coupling**	11.5 dB ±0.5
☐ **VSWR**	1.2:1 typ.
☐ **Directivity**	25 dB typ.
☐ **Main Line Loss** — including theoretical 0.32 dB power split loss	0.6 dB typ.
☐ **Input Power**	4 Watts
☐ **Temperature Range**	−55°C to +100°C
☐ **Low Price**	$9.95 (6-49)

☐ Check these Specs PSC-2-1

Power Splitter/Combiner

$7.95 (500 quantity)

☐ **Size**	.4 x .8 x .4 in.
☐ **50 OHM Impedance**	all ports
☐ **Bandwidth**	0.1 to 400 MHz
☐ **Amplitude Balance**	0.1 dB
☐ **Phase Balance**	1°
☐ **Isolation**	40 dB
☐ **VSWR**	1.2
☐ **Metal Case**	RFI shielded Hermetically Sealed
☐ **Temperature Range**	−55°C to +100°C
☐ **Low Price**	$9.95 (6 thru 49 units)

DESIGNERS KIT AVAILABLE: 2 models of each type, SRA-1, PDC-10-1B, PSC-2-1
Kit # CMK-1 . . . **$49.95**

WE'VE GROWN

Customer acceptance of our products has been so overwhelming, we've been forced to move to larger facilities — THANKS.

World's largest supplier of double balanced mixers

Mini-Circuits Laboratory MCL
A Division Scientific Components Corp

837-843 Utica Avenue, Brooklyn, NY 11203
(212) 342-2500 Int'l Telex 620156 Domestic Telex 125460

International Representatives: ☐ **AUSTRALIA** General Electronic Services, 99 Alexander Street, New South Wales, Australia 2065; ☐ **ENGLAND** Dale Electronics, Dale House, Wharf Road, Frimley Green, Camberley Surrey; ☐ **FRANCE** S. C. I. E. - D. I. M. E. S., 31 Rue George - Sand, 91120 Palaiseau, France; ☐ **GERMANY, AUSTRIA, SWITZERLAND** Industrial Electronics GMBH, Kluberstrasse 14, 6000 Frankfurt/Main, Germany; ☐ **ISRAEl** Vectronics, Ltd., 69 Gordon Street, Tel-Aviv, Israel; ☐ **JAPAN** Densho Kaisha, Ltd., Eguchi Building, 8-1 1 Chome Hamamatsucho Minato-ku, Tokyo; ☐ **EASTERN CANADA** B. D. Hummel, 2224 Maynard Avenue, Utica, NY 13502 (315) 736-7821; ☐ **NETHERLANDS, BELGIUM, LUXEMBOURG:** Coimex, Veldweg II, Hattem, Holland.

US Distributors: ☐ **NORTHERN CALIFORNIA** Cain-White & Co., Foothill Office Center, 105 Fremont Avenue, Los Altos, CA 94022 (415) 948-6533; ☐ **SOUTHERN CALIFORNIA, ARIZONA** Crown Electronics, 11440 Collins Street, No. Hollywood, CA 91601 (213) 877-3550

For other Mini-Circuits Lab. Products see ads on Pgs. 3, 5

4. Calculated frequency response suggests a 10% operational bandwidth. Curves A, B, C and D represent couplers with output impedances of 50, 25, 16.66 and 12.5 ohms, respectively.

K = 2	Curve A	Curve B	Curve C	Curve D
Y_A	0.7071	0.7071	0.7071	0.7071
Y_B	1.225	1.732	2.121	2.449
Y_C	0.7071	1.414	2.121	2.828
Y_D	1.000	2.000	3.000	4.000

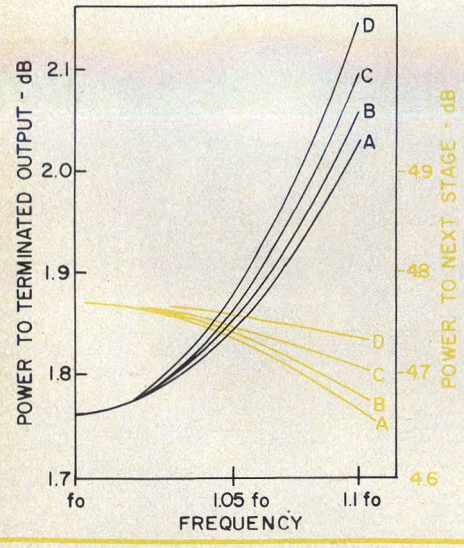

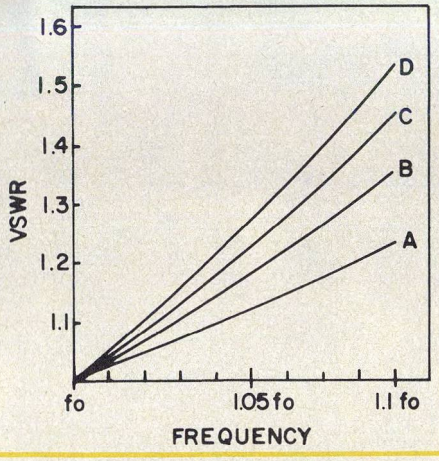

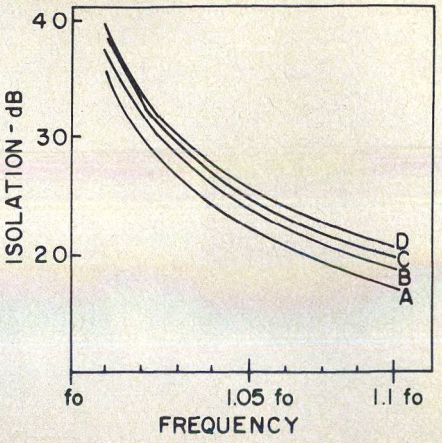

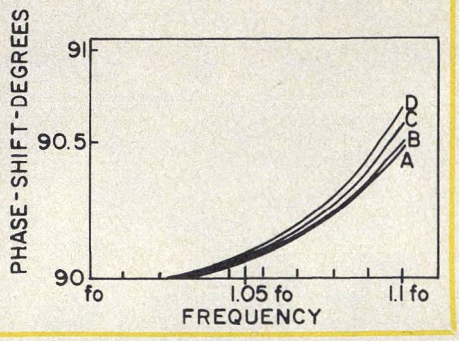

which implies that the input power is transmitted to port 2 and port 3 only. Therefore:

$$|V_2|^2 + |V_3|^2 = 1/Y_D \quad (7)$$

or equivalently,

$$Y_B^2 \cdot Y_D = Y_C^2 + Y_D^2 \quad (8)$$

Let K represent a power splitting ratio between ports 2 and 3. Then:

$$K = |V_2|^2/|V_3|^2,$$

and

$$Y_C^2 = Y_D^2/K \quad (9)$$

Substituting Eq. (9) into Eq. (8) yields:

$$Y_B = ((K + 1)\, Y_D/K)^{1/2} \quad (10)$$

and

$$Y_C = Y_D/(K)^{1/2} \quad (11)$$

Substituting Eq. (10) and Eq. (11) into either Eq. (2) or Eq. (3), for the conditions of perfect match and infinite directivity, yields:

$$Y_A = 1/(K)^{1/2} \quad (12)$$

Thus, the normalized admittances of the coupler arms are given by Eqs. (10), (11) and (12).

For example, consider a branch-line coupler with an equal output power split (K = 1), an input impedance of 50 ohms and an output impedance of 25 ohms. The normalized output admittance for this component would be $Y_D = 2$, and the normalized arm admittances are calculated as $Y_A = 1$, $Y_B = 2$ and $Y_C = 2$. Figure 3 shows the proper impedance conversions.

Ten percent bandwidth realized

The theoretical frequency response of the impedance matching, branch-line coupler can be calculated based on an approach described by Reed and Wheeler.[1] Predicted performance of four such hybrids, each

(continued on p. 52)

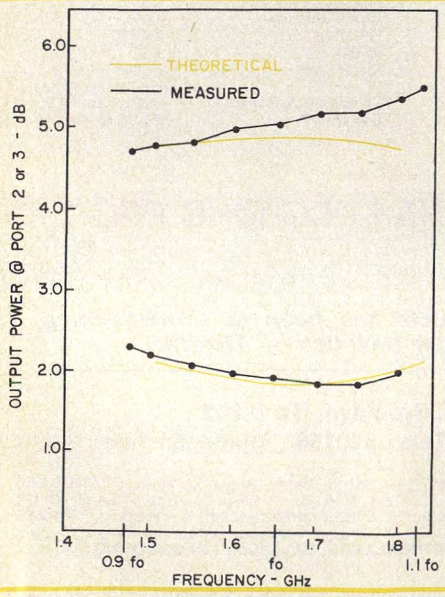

5. Experimental results follow theoretical curves closely over a 10% bandwidth.

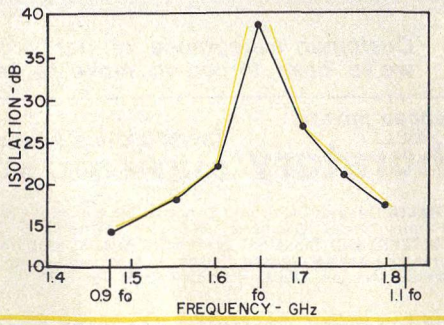

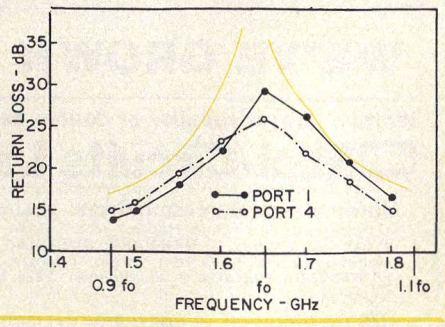

High in Power
low in Cost

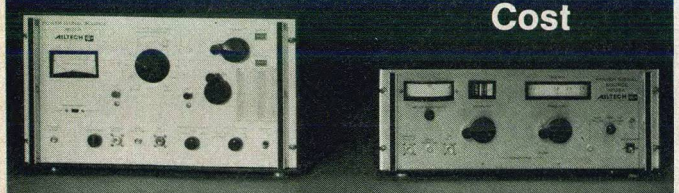

AILTECH'S
Models 125A/126A RF Power Signal Sources cover the entire spectrum — 0.2 to 8GHz with power outputs up to 100 watts CW and 1KW peak — just part of a complete line extending down to 10KHz.
Universally used for EMC testing, wattmeter calibration, component evaluation, and high-power solid-state amplifier design, and offering the "most MHz coverage per power source dollar," they are a favorite choice for research in areas ranging from biological to plasma studies. Their performance is matched by their value and versatility, with multi-watt outputs and long-term stabilities of the order of ±0.002% in frequency and ±0.1db in amplitude.

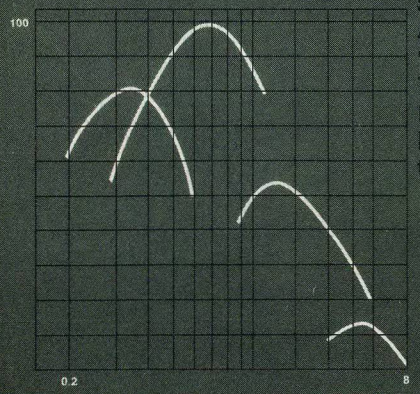

POWER CURVES

Save dollars with AILTECH'S "Economy Pair." They're the bargain in RF power today.

We've Got The Power

plus a complete line of Noise Figure Instrumentation, Spectrum Analyzers, System Noise Monitors and Frequency Synthesizers.

AILTECH
A CUTLER-HAMMER COMPANY
CONTROL

WEST COAST • CITY OF INDUSTRY, CA. 91748 • (213) 963-4811
EAST COAST • FARMINGDALE, NEW YORK 11735 • (516) 595-8471
FRANCE • LA GARENNE-COLOMBES • TELEPHONE (01) 780-73-73
UNITED KINGDOM • CROWTHORNE • TELEPHONE 5777
GERMANY • MUNICH • TELEPHONE (089) 5233029
JAPAN • TOKYO • TELEPHONE (404) 870

FOR DATA CIRCLE READER 50
FOR DEMO CIRCLE READER 52

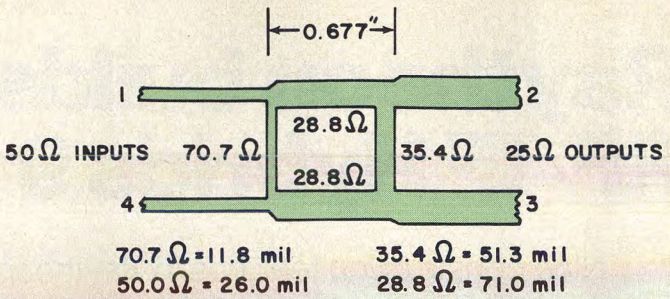

6. An experimental model was built to transform 50-ohm inputs to 25-ohm outputs and provide a 2:1 power splitting ratio between ports 2 and 3. For test purposes, two quarter wavelength, 35.4-ohm lines replaced the 25-ohm outputs so the coupler could be evaluated with 50-ohm equipment.

with a 50-ohm input, but outputs of 50, 25, 16.66 and 12.5 and a power split of 2:1 (K = 2), reveals that useful bandwidth should be about 10% (Fig. 4).

To test the theory, a two-branch coupler with a 50-ohm input, 25-ohm output and 2:1 power split was built in MIC form on 27 mil thick alumina substrate (See Fig. 5 for performance). Impedances of the quarter-wavelength (at 1.656 GHz), Ta-Pt-Au transmission lines are shown in Fig. 6 (note that these correspond to the normalized admittances of column B, Table 1, Fig. 4). Line widths corresponding to these impedances were calculated using the MSTRIP[4] computer-aided design routine.

Measured frequency response compares closely with theory, over a 10% bandwidth, as shown in Fig. 5. ••

Acknowledgement

The author wishes to thank R. E. Shipley of Collins Radio Group for his assistance.

References

1. J. Reed and G. J. Wheeler, "A Method of Analysis of Symmetrical Four-Port Networks," *IRE Trans. On MTT*, Vol. 4, pp. 246-252, (October, 1956).
2. G. L. Mathaei, L. Young and E. Jones, *Microwave Filters, Impedance Matching Networks and Coupling Structures*, McGraw-Hill, New York, p. 814, (1964).
3. L. F. Lind, "Synthesis of Asymmetrical Branch Guide Directional Coupler-Impedance Transformers," *IEEE Trans. on MTT*, Vol. 17, pp. 45-48, (January, 1969).
4. H. Sobol and L. Young, *Advances In Microwaves*, Vol. 8, Academic Press, (1974).

Technical Editor

Looking for new opportunities to meet people, travel, attend conferences, and write about the latest in microwave technology? MicroWaves is seeking a graduate engineer to add to its editorial staff. If interested and have good writing ability, send resume to:

Stacy V. Bearse
Hayden Publishing Co./MicroWaves
50 Essex Street
Rochelle Park, N.J. 07662
(201) 843-0550

Specifying Isolation To Limit Frequency Pulling

Here's a short note that explains how to calculate the minimum isolation necessary to keep an oscillator's pulling specification within limits under changing load VSWR and phase.

CHANGES in the VSWR or phase of a circuit loading the output of an oscillator can deviate, or "pull" the source's steady-state operating frequency. The effect is commonly observed when an oscillator circuit is loaded by an rf switch or duplexer. Frequency pulling is usually an undesirable trait, but it can be held within limits by introducing isolation between a source and its load.

To simultaneously guarantee good electrical performance at a reasonable cost, isolation should be provided in just the right amount: Too little will jeopardize the source's frequency stability, while too much is unnecessarily expensive and introduces extra loss. Given the maximum allowable source frequency deviation and load VSWR, the minimum amount of isolation required may be calculated by measuring the effect of a standard mismatch on the oscillator in question.

First, consider "built-in" isolation

In most instances, the load VSWR presented to the source is controlled to a reasonable upper limit. Thus, the designer can assume that output VSWR will afford some degree of built-in "effective source isolation." Referring to Fig. 1, the ratio of the power transmitted towards the load to the power reflected towards the source may be expressed as:

$$\frac{P_r}{P_t} = \left[\frac{VSWR_L - 1}{VSWR_L + 1}\right]^2 \qquad (1)$$

where: P_r is the power reflected from the load,
P_t is the power transmitted to the load, and
$VSWR_L$ is the mismatch presented by the load.

Return loss is defined as the reciprocal of Eq. (1):

$$\text{Return loss} = \frac{P_t}{P_r} = \left[\frac{VSWR_L + 1}{VSWR_L - 1}\right]^2 \qquad (2)$$

or in log form:

$$\text{Return loss} = 20 \log \left[\frac{VSWR_L + 1}{VSWR_L - 1}\right] \text{dB} \qquad (3)$$

Return loss of a load may be simulated by an attenuator, equal to one-half the value of the return loss, located between the source and a short circuit. The value of this pad represents the effective load isolation, which is described by:

$$\text{Effective Load Isolation} = \frac{\text{Return Loss}}{2}$$

$$= 10 \text{ Log} \left[\frac{VSWR_L + 1}{VSWR_L - 1}\right] \text{dB} \qquad (4)$$

Arthur W. Vemis, Design Engineer, Block Engineering, 19 Blackstone, Cambridge, MA 02139.

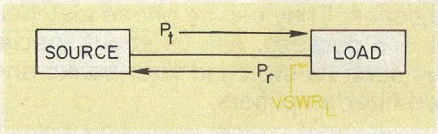

1. The portion of power reflected back to the source causes frequency pulling.

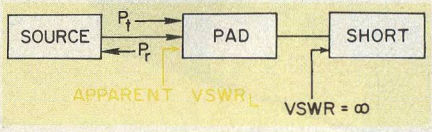

2. Return loss of a load may be simulated by a pad and a short circuit.

The pad represents the isolation that **need not** be supplied by buffer amplifiers, isolators or circualtors. This isolation may be subtracted directly from the minimum isolation requirement of the source, which is derived in the next section.

Measure a deviation factor

Frequency pulling is best explained by drawing an analogy with the theory of injection-locked oscillators.[1,2] If a low-level external locking signal (P_g), is injected into the output port of a source, the oscillators frequency (f_o) will experience a change (ΔF) given by:

$$\Delta F = \frac{f_o}{Q_L}\sqrt{\frac{P_g}{P_t}} \quad P_t >> P_g \qquad (5)$$

where: Q_L is the loaded Q of the oscillator, and P_t is the output power of the source.

The reflected power (P_r) in Fig. 1 corresponds to the external generator power in Eq. (5), and acts to pull the source's operating frequency. Using Eq. (1), this frequency change may be expressed as:

$$\Delta F = \frac{f_o}{Q_L}\sqrt{\left(\frac{VSWR_L - 1}{VSWR_L + 1}\right)^2}$$

$$= \frac{f_o}{Q_L}\left(\frac{VSWR_L - 1}{VSWR_L + 1}\right) \qquad (6)$$

Frequency pulling is characteristic of the specific oscillator circuit under evaluation. As seen in Eq. (6), it depends on loaded Q, which is difficult to measure

(continued on p. 57)

high performance type 'N' fixed attenuators

FEATURES

- DC to 12.4 GHz and DC to 18.0 GHz
- available in 1dB increments
- VSWR less than 1.07+ 0.015 f (GHz)
- 2 watts input power
- less than 2.0 inches overall length
- calibration supplied at 4.0, 8.0, 12.4 and 18.0 GHz

MIDWEST MICROWAVE 3800 Packard Road, Ann Arbor, Michigan 48104 • (313) 971-1992 • TWX 810-223-6031
FRANCE: S.C.I.E.-D.I.M.E.S. 928-38-65

READER SERVICE NUMBER 57

SPECIFYING ISOLATION

accurately. However, a figure of merit called deviation factor (K) can be obtained experimentally and used to cancel the Q term from Eq. (6). Deviation factor is defined as the frequency deviation, in Hz, that an oscillator experiences when subjected to a standard mismatch ($VSWR_s$) rotated through all phases.

Measuring K is relatively straightforward. Assume a standard load VSWR of 2:1 for convenience. Using Eq. (4), it can be seen that a 10 dB pad, terminated by a sliding short circuit, will simulate this load VSWR. By changing the position of the sliding short, the oscillator can be checked for frequency deviation through all phases of reflection.

Once this measurement is made, a ratio of deviation factor to maximum allowable deviation can be formulated. Let ΔF_{max} represent the maximum frequency deviation that can be tolerated in a specific application. Then, the maximum VSWR ($VSWR_{max}$) that the oscillator can tolerate is given by:

$$\frac{K}{\Delta F_{max}} = \frac{f_o/Q_L \left(\frac{VSWR_s - 1}{VSWR_s + 1}\right)}{f_o/Q_L \left(\frac{VSWR_{max} - 1}{VSWR_{max} + 1}\right)} \qquad (7)$$

Square both sides:

$$\left(\frac{K}{\Delta F_{max}}\right)^2 = \frac{\left(\frac{VSWR_s - 1}{VSWR_s + 1}\right)^2}{\left(\frac{VSWR_{max} - 1}{VSWR_{max} + 1}\right)^2} \qquad (8)$$

Then rearrange the equation and express in dB:

$$20 \log \left[\frac{VSWR_{max} - 1}{VSWR_{max} + 1}\right] = 20 \log \left[\frac{VSWR_s - 1}{VSWR_s + 1}\right] - 20 \log \left[\frac{K}{\Delta F_{max}}\right] dB \qquad (9)$$

Equation (9) is in the same form as Eq. (1), therefore, by taking one-half the reciprocal of Eq. (10), we obtain isolation:

$$10 \log \left[\frac{VSWR_{max} + 1}{VSWR_{max} - 1}\right] = 10 \log \left[\frac{VSWR_s + 1}{VSWR_s - 1}\right] - 10 \log \left[\frac{\Delta F_{max}}{K}\right] \qquad (10)$$

Substituting $VSWR_s = 2$, Eq. (10) simplifies to:

$$\text{Isolation} = 10 \log \left[\frac{VSWR_{max} + 1}{VSWR_{max} - 1}\right] = 10 \log \left[\frac{3K}{\Delta F_{max}}\right] dB \qquad (11)$$

If the load is either a short or an open ($VSWR = \infty$), the required source isolation is given by Eq. (11). In most cases, however, the load VSWR is less than infinity and thus offers an effective load isolation as expressed by Eq. (4). This is directly subtractive from the isolation equation to give:

$$\text{Actual Required Isolation} = 10 \log \left[\frac{3K}{\Delta F_{max}}\right] - 10 \log \left[\frac{VSWR_L + 1}{VSWR_L - 1}\right]$$

$$= 10 \log \left[\frac{3K}{\Delta F_{max}} \frac{VSWR_L - 1}{VSWR_L + 1}\right]$$

$$\text{for } \left[\frac{3K}{\Delta F_{max}} \cdot \frac{VSWR_L - 1}{VSWR_L + 1}\right] > 1$$

$$= 0 \quad \text{for } \left[\frac{3K}{\Delta F_{max}} \cdot \frac{VSWR_L - 1}{VSWR_L + 1}\right] \leq 1$$

Example: Let $VSWR_L$ = Maximum expected load VSWR of 1.50

K = 1 MHz measured with a standard VSWR of 2:00 and rotated through all phases.

ΔF_{max} = 10 kHz, maximum allowable source deviation.

Substituting these values into Eq. (13):

Required Isolation $= 10 \log \left[\frac{(3)\ 10^6}{(10)\ 10^3} \cdot \frac{1.50 - 1.00}{1.50 + 1.00}\right] = 17.8$ dB

This isolation can conveniently be satisfied by the use of a single circulator. ••

References

1. Robert Adler, "A Study Of Locking Phenomena In Oscillators," *IRE Proc.*, Vol. 34, pp. 351-357, (June, 1946).
2. L. J. Paciorek, "Injection Locking Of Oscillators," *IEEE Proc.*, Vol. 53, No. 11, pp. 1723-1727, (November, 1965).

Computer Analysis Speeds Corrugated Horn Design

Given the flare angle, length and diameter of a corrugated horn antenna, a radiation pattern can be quickly predicted using a computer program written in the BASIC language.

CORRUGATED horn antennas provide circularly symmetric, low side-lobe patterns for illuminating lenses and reflectors.[1,2,3] Horn design requires selection of an appropriate flare angle and often calls for as many as ten grooves per wavelength to be cut into the inside wall of the horn. (See Fig. 1). The BASIC program described herein permits selection of the optimum flare angle and horn length before any machining is done.

For narrow-band applications, the calculated antenna pattern is quite accurate, and may be used as a basis for other system calculations. For wideband applications, calculated results tend to be the average between the E and H planes. The complete program is presented in the accompanying section. "Equations programmed and BASIC program listing."

Applying the BASIC program

The analytical work of Narasimhan and Rao[4] using spherical hybrid mode expansion techniques is the basis for the BASIC program used. Certain difficult functions are integrated numerically rather than expanded in an infinite series of Bessel functions for simplification.

The program permits calculations of radiation patterns for horns having half-flare angles (α) of less than 30 degrees. Horns intended for use as lens illuminators and Cassegrain antenna feeds often require flare angles in this range. The calculations are very accurate for corrugations that are nearly $\lambda/4$ in depth, and useful results are obtained for depths approaching $\lambda/2$. Reference 1 provides equations that are valid for half-flare angles beyond 30 degrees.

The BASIC language is used because of its wide applicability and familiarity. The program listing presented should be directly useable, with elementary modifications, on most BASIC machines.

A sample printout of the program during the interactive program phase is shown in Fig. 2. One specifies the horn parameters as requested: aperture radius (in inches), horn axial length (in inches), the starting computational spatial angle (in degrees) and the number of angular dimension points between the starting and final angle—usually selected to provide 1, 2 or 5 degree increments. The final parameter to be entered is the integration conversion limit (or relative error in percent ÷ 100), as shown in Fig. 2; a value of 0.01 (1%) is normally used.

G. R. Loefer, Assistant Research Engineer, **J. M. Newton,** Research Engineer, **J. M. Schuchardt,** Senior Research Engineer and **J. W. Dees,** Principal Research Engineer, Georgia Institute of Technology, Engineering Experiment Station, Electromagnetics Laboratory, Atlanta, GA 30332.

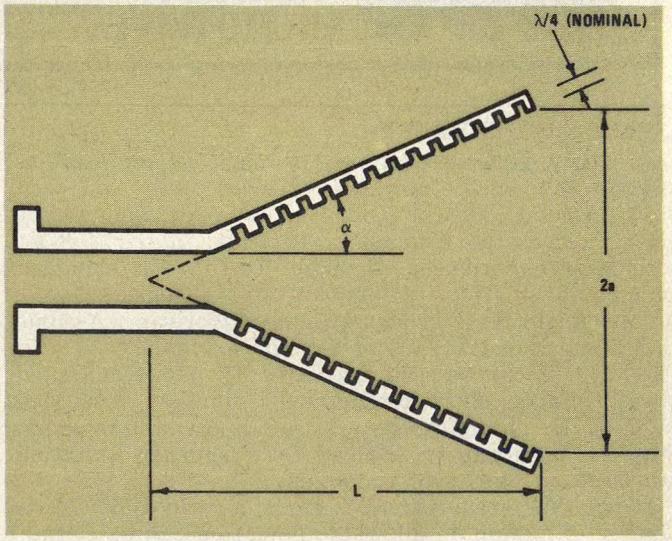

1. Corrugations in the horn wall result in low side and backlobes and a stable phase center. Typical depth ranges from $\lambda/4$ to $\lambda/2$. Thin corrugations are preferred, with ten per wavelength common.

Design examples illustrate results

Example 1: A Cassegrain antenna feed must be designed to illuminate a subreflector with a subtended angle of ±15 degrees. The following corrugated horn parameters are used: Aperture radius = 1.24 inches and horn axial length = 11.7978 inches, corresponding to an α of 6 degrees. The wavelength is equal to 0.59015 inches at 20 GHz and 0.3934 inches at 30 GHz. The computer results shown in Fig. 2 are plotted and compared with measured data[3] in Fig. 3.

This data shows excellent agreement at 20 GHz, where the actual corrugation slot depth was 0.288 λ, which is close to the greater-wave depth assumed in the computations. Also, at 20 GHz the measured E and H-plane patterns are nearly equal. At 30 GHz where the actual corrugation slot depth is 0.430 λ—significantly different than the assumed 0.250 λ depth—difference between E and H-plane patterns were measured, as shown in Fig. 3. Here the calculated results lie between the measured E and H-plane data—somewhat closer to the H-plane than the E-plane.

Example 2: A Cassegrain antenna feed is desired to illuminate a subreflector having a subtended angle of ±8.7 degrees. This is an extremely narrow angle

(continued on p. 60)

```
**********************************

APERTURE RADIUS =? 1.24
HORN AXIAL LENGTH =? 11.7978
WAVELENGTH =? .59015
START ANGLE =? 0
FINAL ANGLE =? 35
NUMBER OF DIVISIONS =? 7
INTEGRATION CONVERGENCE LIMIT =? .01
**********************************
```

THETA	MO (REAL)	M1 (IMAG.)	E AMP (DB)
0	.208046	4.50387E-2	0
5	.188278	3.83405E-2	-.906179
10	.137943	2.19291E-2	-3.72592
15	.07809	4.24166E-3	-8.84664
20	2.91913E-2	-7.32239E-3	-17.258
25	1.06425E-3	-1.0377E-2	-26.6119
30	-8.14577E-3	-7.35749E-3	-26.355
35	-6.46581E-3	-2.50574E-3	-30.5652

(a) 20 GHz, 5° STEPS

```
**********************************

APERTURE RADIUS =? 1.24
HORN AXIAL LENGTH =? 11.7978
WAVELENGTH =? .59015
START ANGLE =? 0
FINAL ANGLE =? 20
NUMBER OF DIVISIONS =? 10
INTEGRATION CONVERGENCE LIMIT =? .01
**********************************
```

THETA	MO (REAL)	M1 (IMAG.)	E AMP (DB)
0	.208046	4.50387E-2	0
2	.204773	4.39209E-2	-.143943
4	.195208	4.06739E-2	-.578145
6	.180084	3.56028E-2	-1.30992
8	.160529	2.91726E-2	-2.35228
10	.137943	2.19291E-2	-3.72592
12	.113847	1.45363E-2	-5.46088
14	8.97313E-2	7.47061E-3	-7.60319
16	6.69215E-2	1.26837E-3	-10.2191
18	4.64744E-2	-3.71653E-3	-13.4053
20	2.91913E-2	-7.32239E-3	-17.258

(b) 20 GHz, 2° STEPS

```
**********************************

APERTURE RADIUS =? 1.24
HORN AXIAL LENGTH =? 11.7978
WAVELENGTH =? .3934
START ANGLE =? 0
FINAL ANGLE =? 35
NUMBER OF DIVISIONS =? 7
INTEGRATION CONVERGENCE LIMIT =? .01
**********************************
```

THETA	MO (REAL)	M1 (IMAG.)	E AMP (DB)
0	.199013	6.57265E-2	0
5	.160013	4.51943E-2	-2.02734
10	.0773992	6.15053E-3	-8.69137
15	.0132362	-1.44265E-2	-20.7408
20	-7.50258E-3	-9.74758E-3	-24.8946
25	-3.32441E-3	8.05692E-4	-36.1618
30	1.80562E-3	3.37275E-3	-35.3753
35	1.33807E-3	3.84124E-4	-44.3769

(c) 30 GHz, 5° STEPS

```
**********************************

APERTURE RADIUS =? 1.24
HORN AXIAL LENGTH =? 11.7978
WAVELENGTH =? .3934
START ANGLE =? 0
FINAL ANGLE =? 20
NUMBER OF D VISIONS =? 10
INTEGRATION CONVERGENCE LIMIT =? .01
**********************************
```

THETA	MO (REAL)	M1 (IMAG.)	E AMP (DB)
0	.199013	6.57265E-2	0
2	.192309	6.21274E-2	-.318738
4	.173277	5.20625E-2	-1.28763
6	.144905	3.7449E-2	-2.94858
8	.111423	2.13034E-2	-5.37416
10	.0773992	6.15053E-3	-8.69137
12	4.68384E-2	-5.58786E-3	-13.0492
14	2.26064E-2	-1.26669E-2	-18.2867
16	5.79363E-3	-1.50665E-2	-22.4379
18	-3.80688E-3	-1.36357E-2	-23.6229
20	-7.50258E-3	-9.74759E-3	-24.8946

(d) 30 GHz, 2° STEPS

2. This sample printout of the BASIC program was taken during the interactive program phase.

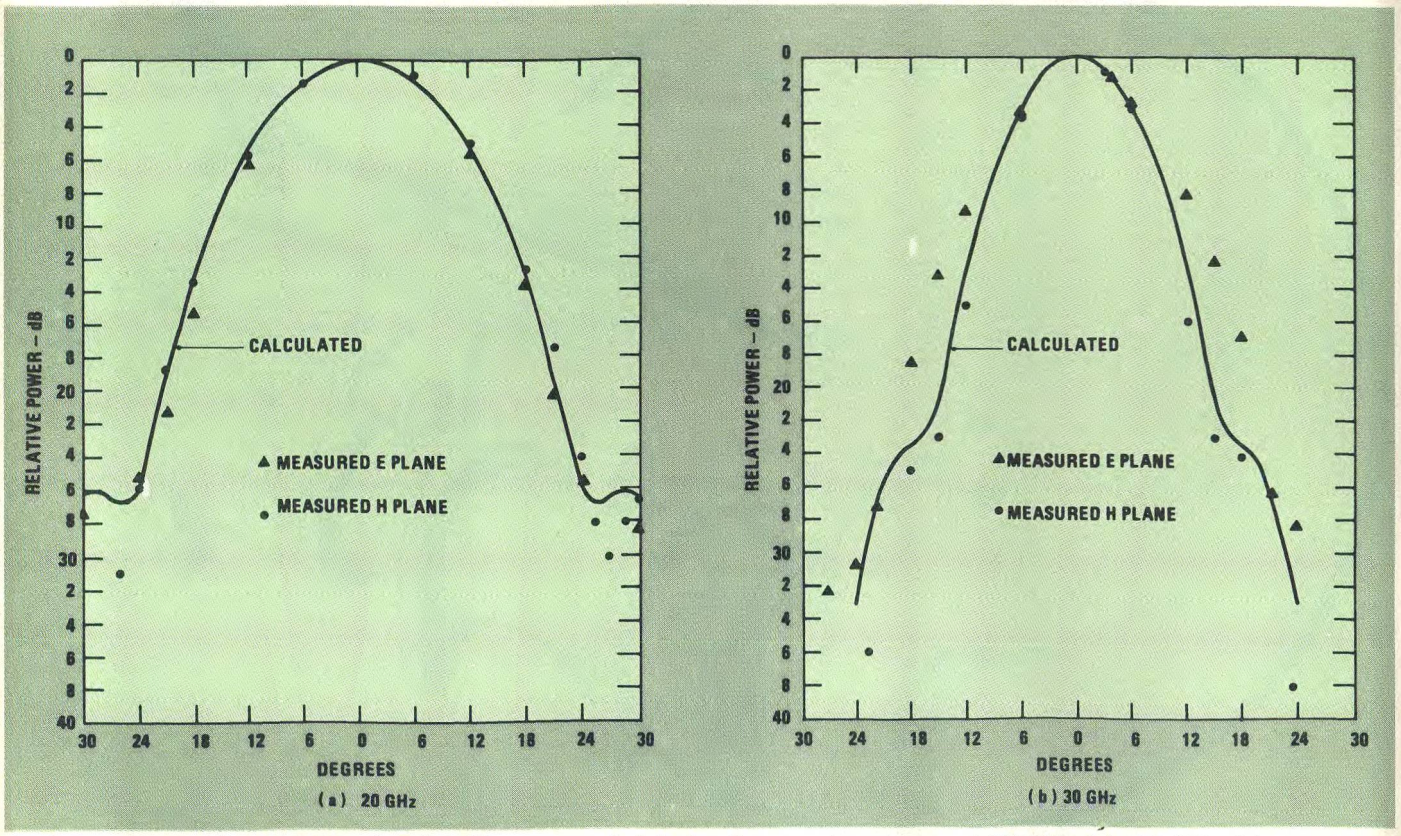

3. Computer results compare closely with measured data for Cassegrain antenna at 20 GHz (a), 30 GHz (b).

(continued on p. 62)

```
************************************

APERTURE RADIUS =? .323
HØRN AXIAL LENGTH =? 3.23
WAVELENGTH =? .06557
START ANGLE =? 0
FINAL ANGLE =? 35
NUMBER ØF DIVISIØNS =? 7
INTEGRATIØN CØNVERGENCE LIMIT =? .01
************************************
```

THETA	MO (REAL)	M1 (IMAG.)	E AMP (DB)
0	.18048	9.20291E-2	0
5	.11009	3.29527E-2	-4.9413
10	1.2888E-2	-2.05915E-2	-18.4892
15	-6.33891E-3	-2.50775E-3	-29.6098
20	1.34542E-3	3.25123E-3	-35.4708
25	4.40757E-5	-1.93209E-3	-40.8262
30	-3.52648E-4	7.05186E-4	-48.7991
35	3.50234E-4	5.39618E-4	-50.787

(a) 180 GHz, 5° STEPS

```
************************************

APERTURE RADIUS =? .323
HØRN AXIAL LENGTH =? 3.23
WAVELENGTH =? .06557
START ANGLE =? 0
FINAL ANGLE =? 20
NUMBER ØF DIVISIØNS =? 10
INTEGRATIØN CØNVERGENCE LIMIT =? .01
************************************
```

THETA	MO (REAL)	M1 (IMAG.)	E AMP (DB)
0	.18048	9.20291E-2	0
2	.167334	8.02887E-2	-.763453
4	.132364	5.04444E-2	-3.11852
6	8.68677E-2	1.58316E-2	-7.23706
8	4.38603E-2	-1.02093E-2	-13.1041
10	1.2888E-2	-2.05915E-2	-18.4892
12	-3.20694E-3	-1.72128E-2	-21.3625
14	-7.16627E-3	-7.31282E-3	-26.0573
16	-4.62543E-3	1.25152E-3	-32.6923
18	-8.21606E-4	4.58474E-3	-32.9839
20	1.34549E-3	3.25169E-3	-35.4697

(b) 180 GHz, 2° STEPS

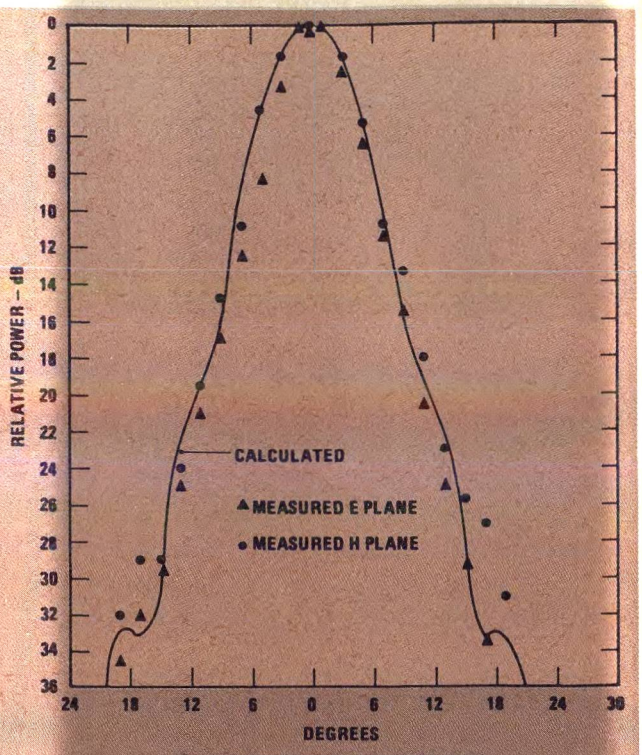

(c) PATTERN PLOT FOR COMPARISON

4. Calculated and measured results for a narrow angle (±8.7°) Cassegrain antenna feed agree.

```
************************************

APERTURE RADIUS =? .395
HØRN AXIAL LENGTH =? .68
WAVELENGTH =? .13114
START ANGLE =? 0
FINAL ANGLE =? 70
NUMBER ØF DIVISIØNS =? 14
INTEGRATIØN CØNVERGENCE LIMIT =? .01
************************************
```

THETA	MO (REAL)	M1 (IMAG.)	E AMP (DB)
0	1.78016E-2	9.64674E-2	0
5	3.22849E-2	.0860792	-.580015
10	5.77658E-2	5.44609E-2	-1.90387
15	6.26413E-2	1.09205E-2	-3.91503
20	3.85565E-2	-2.30739E-2	-7.04761
25	5.49387E-3	-3.06293E-2	-10.3895
30	-1.36643E-2	-1.64439E-2	-13.835
35	-1.38503E-2	9.56268E-4	-17.8064
40	-4.9091E-3	8.55135E-3	-21.0358
45	2.49208E-3	6.4743E-3	-24.3845
50	4.60951E-3	1.25074E-3	-27.9603
54.9999	3.10248E-3	-2.2969E-3	-30.1837
59.9999	7.37503E-4	-3.09065E-3	-32.2903
64.9999	-9.63888E-4	-2.30063E-3	-34.8526
69.9999	-1.72941E-3	-1.15051E-3	-36.9491

(a) 90GHz, 5° STEPS

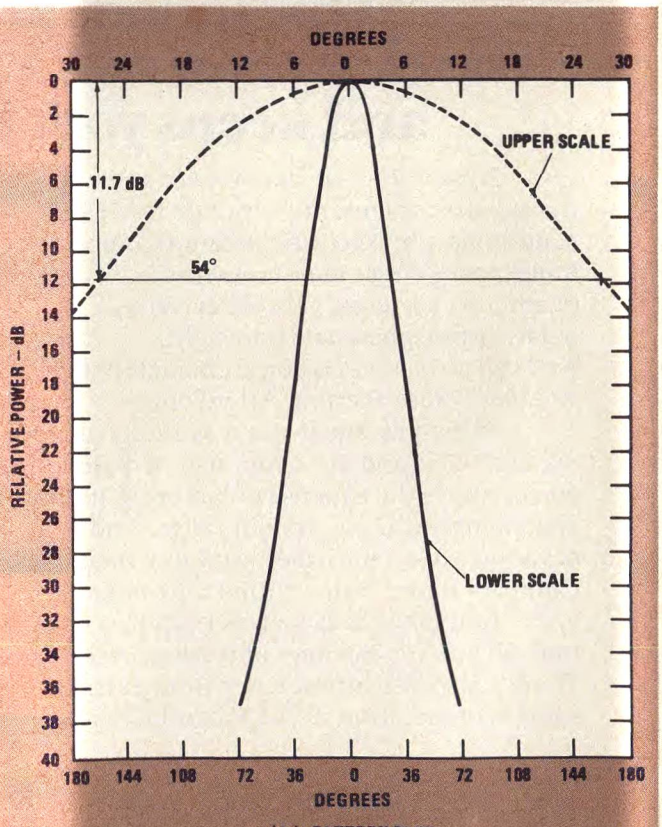

(b) PATTERN PLOT

5. Calculated antenna pattern illustrates a 90 GHz lens antenna feed application.

(continued on p. 64)

and the feed is actually located behind the reflector. The following parameters are used: aperture radius = 0.323 inches and horn axial length = 3.23 inches, corresponding to an α of 5.7 degrees. The wavelength is 0.0656 inches at 180 GHz. Figure 4 compares measured and calculated results.

Example 3: A horn feed must illuminate a lens having subtended angles of ±27 degrees. This is a lens with F/D = 1. The following parameters are used: aperture radius = 0.395 inches and horn axial length = 0.680 inches, corresponding to an α of 30.0 degrees. The wavelength equals 0.1311 inches at 90 GHz. Figure 5 presents the calculated data although no experimental data was taken for this example. ••

References

1. S. K. Buchmeyer, "Corrugations Lock Horns With Poor Beam Shapes," *MicroWaves*, Vol. 12, No. 1, pp. 44-49, (January, 1973).
2. I. Ohtera and H. Ujiie, "Nomographs For Phase Centers of Conical Corrugated and TE_{11} Mode Horns," *IEEE Transactions on Antennas and Propagation*, pp. 858-859, (November, 1975).
3. J. M. Schuchardt, "20 and 30 GHz Feed System For the ATS-F Millimeter Ground Antenna," 21st Annual USAF Symposium on Antenna R & D, Monticello, IL, (October, 1971).
4. M. S. Narasimhan and B. V. Rao, "Diffraction By Wide-Flare-Angle Corrugated Conical Horns," *Electronics Letters*, Vol. 6, No. 15, pp. 469-471, (July 23, 1970).

Acknowledgement

Text data for 180 GHz antenna were obtained by Mr. M. J. Sinclair from work on NASA Grant NSG-5012 (J. L. King, NASA/GSFC Technical Officer).

Equations programmed and BASIC program listing

The complex far-field antenna pattern amplitude is given by Eq. (1).

$$E(\theta) = [1 + \cos(\theta)] \cdot [M_0^2 + M_1^2]^{1/2} \quad (1)$$

(line 850 in program listing)

where, $M(\theta) = \int_0^1 J_0(\alpha_1 r) J_0(p_{01} r) \exp(-jvr^2) r dr = M_0 + jM_1$

$$\alpha_1 = \frac{2\pi a \sin\theta}{\lambda} \quad \text{(line 1000)}$$

$$v = \frac{\pi a^2}{\lambda L} \quad \text{(line 450)}$$

$P_{01} = 2.405$
a = horn radius
L = horn axial length
λ = wavelength
J_0 = Bessell function of first kind, order zero (lines 1200-1300)
$j = \sqrt{-1}$

```
LIST
100  PRINT
110  PRINT
120  PRINT
130  PRINT "**************************************"
140  PRINT
150  PRINT "APERTURE RADIUS =";
160  INPUT A1
170  PRINT
180  PRINT "HORN AXIAL LENGTH =";
190  INPUT L
200  PRINT
210  PRINT "WAVELENGTH =";
220  INPUT L1
230  PRINT
240  PRINT "START ANGLE =";
250  INPUT T0
260  PRINT
270  PRINT "FINAL ANGLE =";
280  INPUT T1
290  PRINT
300  PRINT "NUMBER OF DIVISIONS =";
310  INPUT N
320  PRINT
330  PRINT "INTEGRATION CONVERGENCE LIMIT =";
340  INPUT E
350  PRINT
360  PRINT "**************************************"
370  PRINT
380  PRINT
390  PRINT
400  PRINT "THETA","M0 (REAL)","M1 (IMAG.)","E AMP (DB)"
410  PRINT
420  DIM M[1]
430  LET C5=1000
440  LET C4= 0
450  LET V=3.14159*A1*A1/(L1*L)
460  LET T0=T0/57.2958
470  LET T1=T1/57.2958
480  LET C7=(T1-T0)/N
490  FOR Y=T0 TO T1 STEP C7
500    LET A= 0
505    REM  A IS LOWER LIMIT OF INT.
510    LET B=1
515    REM  B IS UPPER LIMIT OF INT.
520    LET C3= 0
530    GOTO  550
540    LET C3=1
550    LET H=(B-A)/3
560    LET C0= 0
570    LET C1= 0
580    LET S= 0
590    GOTO  640
600    LET C0=1
610    LET C1=C1+1
620    LET P=S
630    LET H=H/2
640    LET S=S/2
650    LET C6=H+C0*H
660    FOR X=A+H TO B-H STEP C6
670      GOSUB  1000
680    NEXT X
690    IF C0=1 GOTO  770
700 LIST
700  LET S=2*S
710  LET X=A
720  GOSUB  1000
730  LET X=B
740  GOSUB  1000
750  LET S=S*H/2
760  GOTO  600
770  IF  ABS (S)<=1E-20 GOTO  830
780  IF  ABS ((P-S)/S)<=E GOTO  830
790  IF C1<C5 GOTO  600
800  PRINT
810  PRINT "MAX. # ITER. INTEGRATION",C1
820  PRINT
830  LET M[C3]=S
840  IF C3<>1 GOTO  540
850  LET C2=(1+ COS (Y))*( SQR (M[ 0]*M[ 0]+M[1]*M[1]))
860  LET C2=20* LOG (C2)/ LOG (10)
870  IF C4<> 0 GOTO  890
880  LET C4=C2
890  PRINT Y*57.2958,M[ 0],M[1],C2-C4
900  NEXT Y
910  PRINT
920  PRINT "END? 0=YES"
930  INPUT C3
940  IF C3= 0 GOTO  9999
950  GOTO  100
1000  LET F0=2*3.14159*A1* SIN (Y)/L1
1010  LET X0=X
1020  LET X=F0*X0
1030  GOSUB  1200
1040  LET F1=S1
1050  LET X=2.405*X0
1060  GOSUB  1200
1070  LET F0=F1*S1*X0
1080  LET X=X0
1110  IF C3= 0 GOTO  1140
1120  LET F=F0* SIN (X*X*V)
1130  GOTO  1150
1140  LET F=F0* COS (X*X*V)
1150  LET S=S+(1-C0)*F+C0*F*H
1160  RETURN
1200  LET X=X/2
1210  LET S0=1
1230  LET S1=S0
1240  FOR S3=1 TO 100
1250    LET S0=S0*X*X/(-S3*S3)
1260    LET S1=S1+S0
1270    IF  ABS (S1)<=1E-20 GOTO  1330
1280    IF  ABS (S0/S1)<=.000001 GOTO  1330
1300  NEXT S3
1310  PRINT
1320  PRINT "100 ITER. W/O CONV. -- J0"
1330  LET X=X*2
1340  RETURN
9999  END
```

ANNOUNCING A WINNER!

Marty Hykin
Honeywell
Clearwater, Florida

is the lucky winner of a Lloyd's Scientific calculator. We thank **ALL** of you for filling out February's Semiconductor Survey Card. Your detailed estimates were very helpful.

The facing page carries a card for Passive Component information. Please take a minute, fill it out and mail now to be eligible for the next drawing.

$r = \rho/a =$ normalized radius coordinate

$\theta =$ spherical coordinate angle, the beam peak is at $\theta = 0°$.

Equation (1) is valid for α(half-flare angle) less than 30°. Since $\alpha = \tan^{-1} a/L \,|_{Max} = 0.58$.

In the BASIC program, the Bessel function $J_0(x)$ is calculated as follows: The $J_0(x)$ is given exactly as

$$J_0(x) = \sum_{m=0}^{\infty} \frac{(-1)^m (x/2)^{2M}}{m!)^2} \qquad (2)$$

An approximation of this function to a relative error ϵ, occurs after a summation of M terms so that

$$\left| \frac{J_0(x)|_{M+1} - J_0(x)|_M}{J_0(x)|_{M+1}} \right| \leqq \epsilon \quad \text{(lines 1270 \& 1280)}$$

In the program a relative error of $\epsilon = 10^{-6}$ is used.

Equation (2) is computed by noting the recursion relationship between the term of the sum S.

$$S_{M+1} = S_M \cdot \left[\frac{-(x/2)^2}{m^2} \right] \qquad \text{(line 1250)}$$

where $S_0 = 1$.

which permits each term to be found from the previous term without calculating high order factorials.

The integral computation for Eq.(1) is performed using the trapezoidal rule.

$$I = \int_0^1 f(x)\, dx \approx \frac{h}{2} [f(0) + 2f(h) + 2f(2h) \cdots + 2f(1-h) + f(1)] \qquad (3)$$

A helpful recursion formula is used to simplify this calculation by first setting h (the increment of integration) to $h|_{initial} = 1/3$, then Eq. (3) becomes

$$I|_{initial} \approx \frac{1}{6} [f(0) + 2f(1/3) + 2f(2/3) + f(1)].$$

Next the value of h is halved so $h|_{second\ trial} = 1/6$, and

$$I|_{second\ trial} = \frac{I|_{initial}}{2} + 1/6\, [f(1/6) + f(1/2) + f(5/6)]$$

This process can be repeated with h being halved each time. Finally, when

$$\left| \frac{I|n_{th\ trial} - I|(n-1)_{th\ trial}}{|n_{th\ trial}} \right| \leqq \delta,$$

(lines 770 and 780)

a convergence within a relative error of δ occurs. In the program a relative error of δ is an input—most often a value for δ (the integration convergence limit) of 0.01 is used. ••

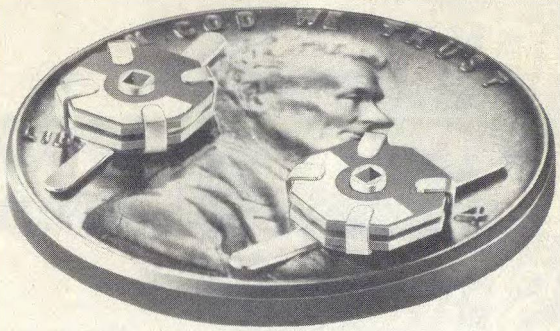

THIN-TRIM CAPACITORS FOR HYBRIDS AND MIC'S

Series 9410 Thin-Trims are sub-miniature variable capacitors for applications where size and performance are critical. Featured are high Q's for low circuit losses, high capacity values for broadband applications and low profile for "gap trimming" in tiny MIC's. Body size .200" x .200" x .060"T. Available in 5 capacitance ranges from 1.0 - 4.5 pf to 7.0 - 45.0 pf.

Johanson

MANUFACTURING CORPORATION
Rockaway Valley Road
Boonton, N.J. 07005
(201) 334-2676 TWX 710-987-8367

READER SERVICE NUMBER 65

now— microwave filters with ceramic performance!

actual size

Murata's new line of Gigafil-C® filters with ceramic dielectric resonators bring a new standard of performance to the microwave frequency spectrum. They are available for frequencies from 760 MHz to 14 GHz, with Q's over 5,000, and in a variety of bandwidths. Outstanding features also include diminutive size and amazing temperature stability. Put ceramic to work in your microwave system. Write for details.

muRata CORPORATION OF AMERICA
2 WESTCHESTER PLAZA, ELMSFORD, NEW YORK 10523
Phone: 914-592-9180 Telex: 13-7332

READER SERVICE NUMBER 66

PRECISION CABLE ASSEMBLIES

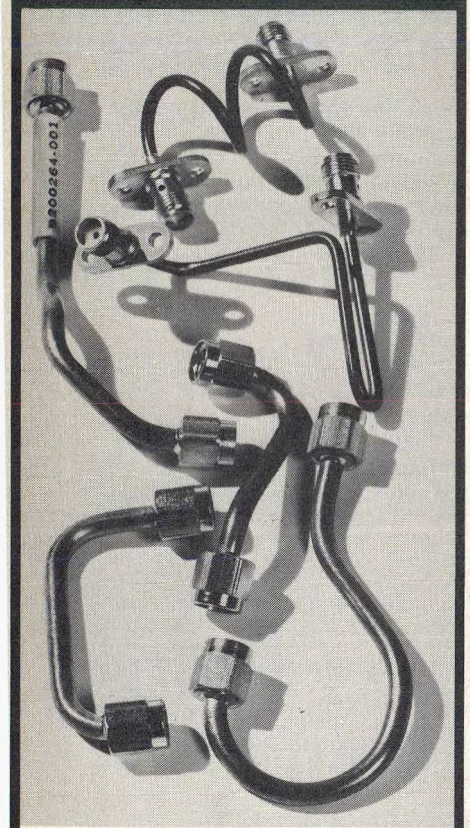

• Semi-rigid
• Flexible
• Patch cords

Send your drawings for our quotation.

cdi

CONNECTING DEVICES INC.

125 Lomita Ave.
El Segundo, Calif. 90245
(213) 322-6885
TWX (910) 348-6645

REPRESENATIVES INQUIRES INVITED

READER SERVICE NUMBER 64

product feature

$4000 buys a complete swept measurement system

Remember the slotted line with its calibration problems? How about that very special directional coupler that someone "borrowed" from your test station, and you haven't seen since? Well, here's a self-contained $4,000 network analyzer that will make you forget about both.

Wiltron's new model 640 swept measurement system is designed for simultaneous scalar measurements of the transmission (gain or loss) and reflection (return loss) properties of components from 1 to 1500 MHz (see photo). Ideally suited for production as well as laboratory use, the instrument requires no additional test components—bridges, detectors and calibration circuitry are all built in.

The new instrument consists of a mainframe incorporating a 4 × 5 inch CRT display and bays for three plug-in modules: A 1 to 1500 MHz rf sweep generator and two log amplifiers, one with a built-in flat-response rf detector for transmission measurements, and a second with an SWR autotester for reflection measurements. Each plug-in is available with either 50 or 75-ohm impedance.

The sweep generator plug-in, models 640G50 (50 ohms) and 640G75 (75 ohms), sweeps from 1 to 1500 MHz in one continuous band. Harmonics are 30 dB and spurious signals are 50 dB below the fundamental signal. A 10 dB step attenuator in conjunction with a 10 dB vernier control allows the output power to be adjusted from −70 to +10 dBm. Flatness is better than ±0.2 dB across the band at 10 dBm.

When sweeping the full band, the center frequency control becomes a variable frequency marker about which calibrated sweeps may be selected. In addition, comb markers of 100, 25, 5 or 1 MHz spacing are provided. Comb marker accuracy is 0.01 per cent and the various marker frequencies are graduated in height for frequency identification. The markers can be tilted ±45 degrees for ease of frequency identification on rapidly changing amplitudes such as filter skirts.

The log reflection plug-in is used to measure the return loss of the device-under-test. Return loss can be displayed at 10, 5, 2, 1 and 0.5 dB per division, with calibrated digital offset. Accuracy is assured by a built-in directional bridge with directivity that exceeds 40 dB from 100 to 1500 MHz, and 45 dB below 100 MHz.

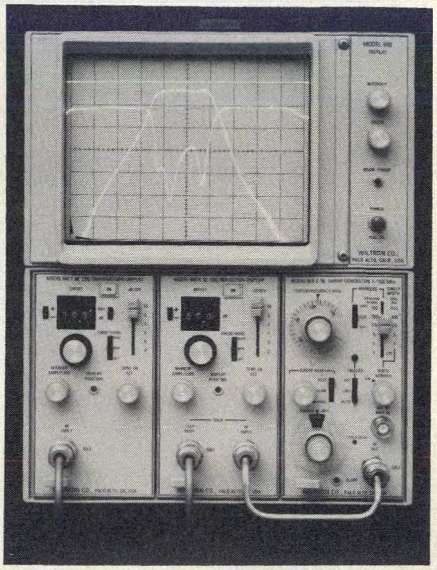

Transmission and reflection characteristics of a bandpass filter are simultaneously displayed.

The log transmission plug-in contains a flat response detector with log characteristic over a 70 dB dynamic range, with −55 dBm sensitivity. The display can be used at 10, 5, 2, 1, 0.5 or 0.2 dB per division. A precision digital offset permits calibrated expansion of the display. A typical noise level of −60 dBm aids in maintaining accurate calibration. In the dBm mode, the plug-in becomes a swept power meter for measurement of absolute power from below −55 dBm to +15 dBm.

Model 640 is housed in a 12 × 8.5 × 20.5 inch (30.5 × 21.6 × 52.1 cm) cabinet and weighs 30 lbs. (13.6 Kg). A model suitable for rack mounting is also offered. P&A: $3,985 (50-ohm system); 12 wks. **Wiltron Company, 930 East Meadow Drive, Palo Alto, CA 94303. (415) 494-6666.**

CIRCLE NO. 109

JUNE
1976

MICROWAVES

Just how accurate is your spectrum analyzer? More importantly, do you use the instrument in a way that takes full advantage of its potential?

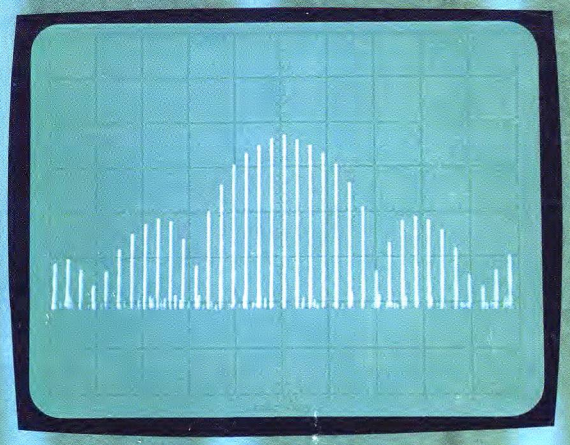

If you're not sure of the answers to either of these two questions, perhaps it's time to examine the three principal sources of instrument error . . . (continued on p. 36)

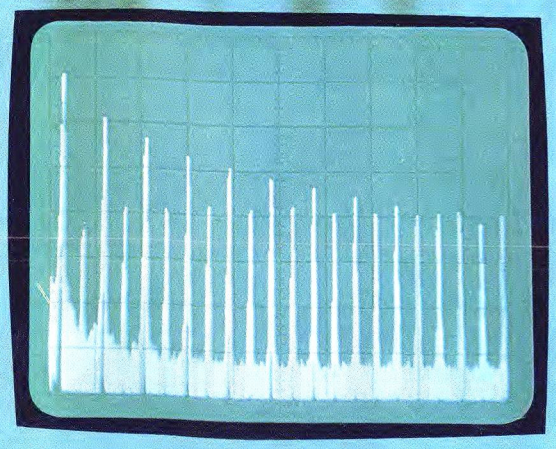

In this issue:

Test and Measurement

How Accurate Is Your Spectrum Analyzer? • Try DC Tests For Thermal Measurements • FM Speeds Group Delay Measurements

MICROWAVES

June 1976
Vol. 15, No. 6

news

9 Impatts And Trapatts Star In New Circuits
14 Microwave Monitor Keeps An Eye On The Road
16 2 GHz Repeater Built Without I-F
18 Industry
21 Washington
26 International
28 R & D
30 Meetings
33 For Your Personal Interest . . .

editorial

34 You And Truth In Advertising

technical

Test & Measurement

36 **How Accurate Is Your Spectrum Analyzer?** Peter Linden of Hewlett Packard demonstrates how the spectrum analyzer's basic accuracy can be improved through careful attention to technique and the use of other instruments.

48 **Use Electrical Tests For Thermal Measurements.** Bernard S. Siegal of Sage Enterprises describes ways in which the thermal resistance of a semiconductor device can be accurately measured by monitoring a temperature sensitive electrical parameter.

60 **Measure Group Delay Fast And Accurately.** M.J. Ahmed, A. Froese and G. Schmiing of GTE Lenkurt Electric, Ltd., introduce a simple swept-frequency technique that measures group delay to 0.2 ns.

62 **Try Impact Extrusion For Low-Cost MIC Packaging.** John E. Miley of Omni Spectra, Inc., and Gordon Simpson of Microwave Associates, Inc., report on rugged, hermetically-sealed MIC enclosures inexpensively fabricated by punching the housings out of slugs.

products and departments

70 New Products
82 New Literature
86 Application Notes
88 Feedback
90 Bookshelf
91 Advertisers' Index
92 Product Index

About the cover: The beauty of a spectrum analyzer display is explored by Art Director Robert Meehan in this composition. The accuracy of the display is investigated by HP engineer Peter Linden, beginning on page 36.

coming next month: Communications

Three Techniques For Measuring and Interpreting Short-Term Frequency Stability. Dr. John Payne, III, President of Communications Techniques, Inc., analyzes the theory and practice of measuring the short-term stability of microwave signal sources in communications systems.

Millimeter-Wave Doublers For Space Applications. Raymond L. Sicotte of Aiken Industries and Richard C. Mott of Comsat describe two exceptionally stable millimeter-wave sources designed for precise measurements of polarization isolation and attenuation. In both cases, the K-band signal is obtained by multiplying the output of a 132.222 MHz crystal-controlled reference by a chain of GaAs varactors.

Statistical Radiation Patterns Aid Spectrum Studies. Richard G. FitzGerrell and Leroy L. Haidle of the Institute For Telecommunication Sciences compare two formats for presenting antenna sidelobe characteristics.

Publisher/Editor
Howard Bierman

Managing Editor
Stacy V. Bearse

Associate Editor
Joseph Ligori

Contributing Editor
Harvey J. Hindin

Washington Editor
Paul Harris
Snyder Associates
1050 Potomac St., NW
Washington, DC 20007
(202) 965-3700

Editorial Assistant
Gail Murphy

Production Editor
Sherry Lynne Karpen

Art Director
Robert Meehan

Production
Dollie S. Viebig, Mgr.
Dan Coakley

Circulation
Barbara Freundlich, Dir.
Trish Edelmann
Gene M. Corrado
Sherry Karpen,
Reader Service

Directory Coordinator
Janice Tapp

Editorial Office
50 Essex St.,
Rochelle Park, NJ 07662
Phone (201) 843-0550
TWX 710-990-5071

A Hayden Publication
James S. Mulholland, Jr.
President

MICROWAVES is sent free to individuals actively engaged in microwave work. Subscription prices for non-qualified copies:

	1 Yr.	2 Yr.	3 Yr.	Single Copy
U.S.	$15	$25	$35	$2.50
FOREIGN	$20	$35	$50	$2.50

Additional Product Data Directory reference issue $10.00 each (U.S.), $18.00 (Foreign). POSTMASTER, please send Form 3579 to Fulfillment Manager, Microwaves, P.O. Box 13801 Philadelphia, PA. 19101.

Back Issues of MicroWaves are available on microfilm microfiche, 16mm or 35mm roll film. They can be ordered from Xerox University Microfilms, 300 North Zeeb Road Ann Arbor, MI 48106. For immediate information, call (313) 761-4700.

Hayden Publishing Co., Inc. James S. Mulholland, President, printed at Brown Printing Co., Inc., Waseca, MN
Copyright © 1976 Hayden Publishing Co., Inc., all rights reserved.

1976 International Microwave Symposium

Impatts and Trapatts star in new circuits

Stacy V. Bearse
Managing Editor

Circuit refinements aimed at furthering applications for first generation microwave semiconductors formed the core of this year's International Microwave Symposium, held earlier this month in Cherry Hill, NJ.

For example, an Impatt oscillator announced at the conference, that features a 1.6 watt output with 11.5 per cent efficiency at 55.5 GHz is claimed by its developers to offer the highest power-frequency (Pf^2) product reported thus far for any microwave solid-state device. A new coaxial-waveguide circuit designed to suppress circuit instabilities below 1 GHz is said to be the key to the oscillator's performance.

Researchers at Fujitsu Laboratories, Ltd., in Kawasaki, Japan, focused their greatest attention on the bias circuit of the new design. According to "A High Power 50 GHz Double-Drift Impatt Oscillator With Low Sideband Noise," presented by Y. Hirachi, Y. Toyama, Y. Fukukawa and Y. Tokumitsu, bias circuit impedance must be made much smaller than the negative impedance of the diode at all frequencies above the lowest unstable frequency, which is typically 80 MHz.

The new design employs a cap-type circuit (see Fig. 1) which, according to the authors, minimizes inductance in the vicinity of the diode, while adding a large amount of shunt capacitance, about 140 pF) to the low-pass bias filter. A cap-type circuit without the added capacitance delivers a maximum of 550 mW, the researchers report, while a conventional coaxial-waveguide circuit can deliver only about 250 mW. The silicon Impatts were fabricated by Fujitsu.

Another circuit advancement announced at the conference is the series interconnection of six Trapatt devices on a diamond substrate (Fig. 2). Researchers from the Georgia Institute of Technology claim nearly 100 per cent combining efficiency with an output of 35.5 watts cw at 7.5 GHz. "Researchers have experimented with series connected Trapatt diodes in the past, and have succeeded in stacking the devices vertically (thermally in series) from 1 to 9 GHz," notes Dr. N. Walter Cox, Chief of the Solid-State Sciences Div. at the Engineering Experiment Station of Georgia Tech. "However, efforts to mount such devices thermally in parallel (side by side), as required for high-power cw or long-pulse applications, have not previously been successful above 5 GHz."

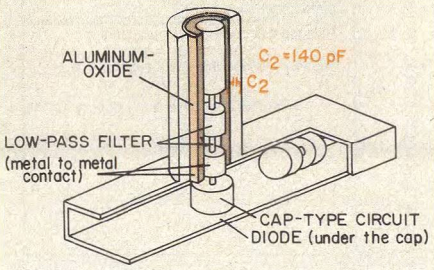

1. Quelling low-frequency instabilities is the key to this 1.6 W, 5.5 GHz Impatt oscillator.

Through computer simulation and experiments at 2 to 9 GHz, the researchers discovered that the location of the diode on the diamond metallization pad as well as the point of contact of the grounding strap had a significant effect on performance. In-depth experiments pointed to the fact that the metallization pads acted as transmission lines at high harmonic frequencies.

"The apparent significance of high harmonics on diode efficiency is certainly surprising and has been overlooked previously," claims Dr. Cox. "The harmonic shunt reactance tends to short the grounded diode. It should be stressed that these effects would be expected only at high harmonics, since the metallization pads are much less than one-tenth of a wavelength long at the fundamental frequency, and would certainly appear lumped for the first 'few' harmonics."

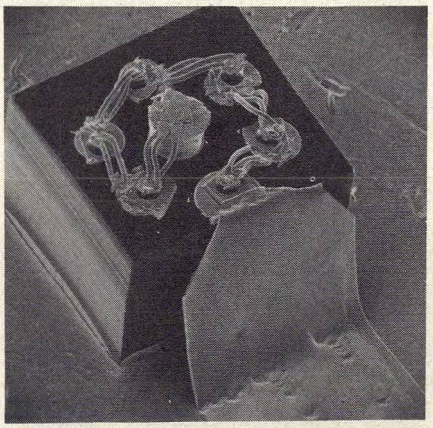

2. Six Trapatts are combined in series to produce more than 35.5 watts at 7.5 GHz.

Additional experiments assured the research team of Dr. Cox, G. N. Hill, J. W. Amoss and C. T. Rucker that minimizing both diamond metallization and package capacitance were necessary to achieve near-perfect combining efficiency. "Omission of either of these conditions results in a combining efficiency of approximately 50 per cent," Dr. Cox concludes.

Have Baritts found a place?

Which is the best type of diode for self-oscillating Doppler detector applications? There is little doubt in the minds of three researchers from the Electron Physics Laboratory of the University of Michigan that the most logical choice is the Baritt. "Operating in the self-mixed, Doppler mode, these devices are superior to both Impatt and Gunn devices in terms of minimum detectable signal, rf power required for operation, dc prime power required for operation and sensitivity to changes in bias point and rf tuning," report J. R. East, H. Nguyen Ba and G. I. Haddad.

Test results from the University indicate that the Baritt can detect signal levels 25 to 40 dB lower than commercially available versions of the other two competitors, depending upon the Doppler frequency used (see Fig. 3). "The −156 dBm minimum detectable signal from 5 to 20 kHz is the best measurement of any of the diodes tested," the researchers say in "Baritt Devices For Self-Mixed Doppler Radar Applications."

Rf power required for Doppler operation is reported to be 15 to 20 dB lower for the Baritt device. And, in spite of the poorer conversion efficiency of the Baritt, the

(continued on p. 10)

Impatts and Trapatts star in new circuits

dc power required is claimed to be much smaller. The X-band devices tested operated with biases of 10 to 50 volts.

For low noise, cool it

Three-terminal semiconductors are also drawing a great deal of attention these days, with many programs focused on the gallium arsenide field-effect transistor. Data from the AIL Division of Cutler-Hammer indicates that cryogenically cooled GaAs FET amplifiers are indeed competitive with uncooled S-band paramps in terms of noise, while offering more power and simpler circuitry.

John Pierro, an engineer in the Filter Technology and Applications Department of AIL in Melville, NY, reports the design of a 4.5 to 5.0 GHz GaAs FET amplifier that achieves a noise figure of 1.1 dB (80°K) and gain of 10 dB when cooled to 20°K. Room temperature noise figure and gain were measured at 3.3 dB and 8 dB, respectively. Power output is claimed to be greater than +7 dBm.

"By cooling the FET, a substantial reduction in the noise figure is realized since most of the noise generated by the device is thermal in nature," he told the conferees (see Fig. 4). "Unlike the bipolar transistor, whose gain drops with decreasing temperature, the FET gain increases producing the desirable effect of further increasing the output signal-to-noise (SNR) ratio for a fixed input SNR."

Pierro's design used NEC's model 24406, a device with a 1 μm gate length. "Using 0.5 μm GaAs FETs, it should be possible to realize noise temperatures of under 50°K in this frequency range," the researcher predicts.

FET mixers evaluated

Dr. Paul Bura of RCA, Ltd., Quebec, Canada, reports that when the FET is used as a mixer, significant improvement in noise figure results by injecting the LO signal into the drain, rather than driving the gate. Drain mixers rely on the non-linear $I_d - V_d$ characteristic for mixing, while gate-fed circuits use the non-linear $I_d - V_g$ response.

"It is interesting to note that the drain mixer has considerably lower noise figure than the gate circuit," comments Dr. Bura. "This is probably due to parametric upconversion of lower frequency noise in the FET to the output frequency in the gate mixer. With the Schottky-barrier gate remaining in reverse bias over the entire LO cycle, the variation of the depletion layer width results in the corresponding capacitance modulation. In the drain mixer, very little gate capacitance modulation takes place."

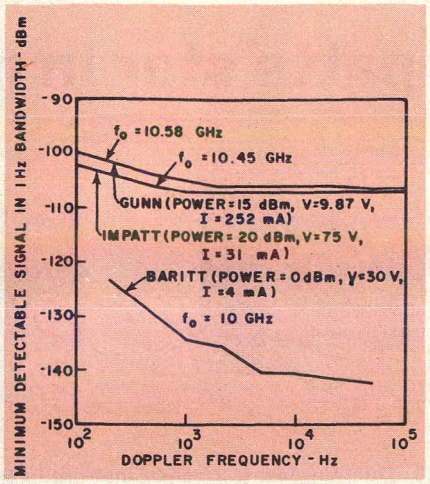

3. Baritts appear useful as Doppler detectors, although they are not competitive in terms of power output or efficiency with Gunns or Impatts.

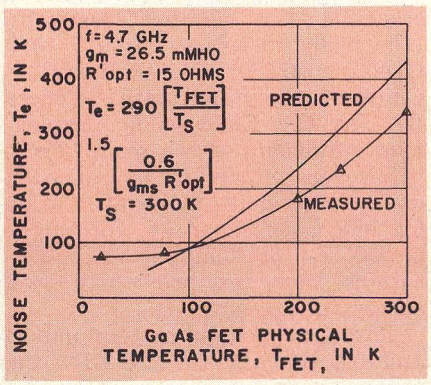

4. Effective noise temperature (T_e) decreases markedly as the actual temperature of the device (T_{FET}) is lowered.

Comparisons were made on two MIC mixer circuits developed for satellite transponder applications. Input frequencies ranged from 5.925 to 6.425 GHz, outputs varied from 3.7 to 4.2 GHz and the LO was set at 2.225 GHz. Both circuits yielded conversion gains up to 3 dB. Noise figures as low as 4 dB are reported for the drain mixer, while 5.7 dB is the minimum measured for the gate design, as shown in Fig. 5. "The minimum noise figure of the drain mixer is only 1.3 dB higher than the noise figure of the same FET in a 6 GHz amplifier circuit," Dr. Bura adds.

Other specifications reported by the Canadian research team of Dr. Bura and R. Dikshit in "FET Mixers For Communications Satellite Transponders" includes third-order intermodulation distortion intercept point of 16 dBm, group delay ripple of ±0.5 ns and in-band spurious suppression of 70 dB below carrier with a −40 dBm signal input to the mixer.

Diode noise source improved

The high output level of commercial solid-state noise sources combined with their ability to be

(continued on p. 13)

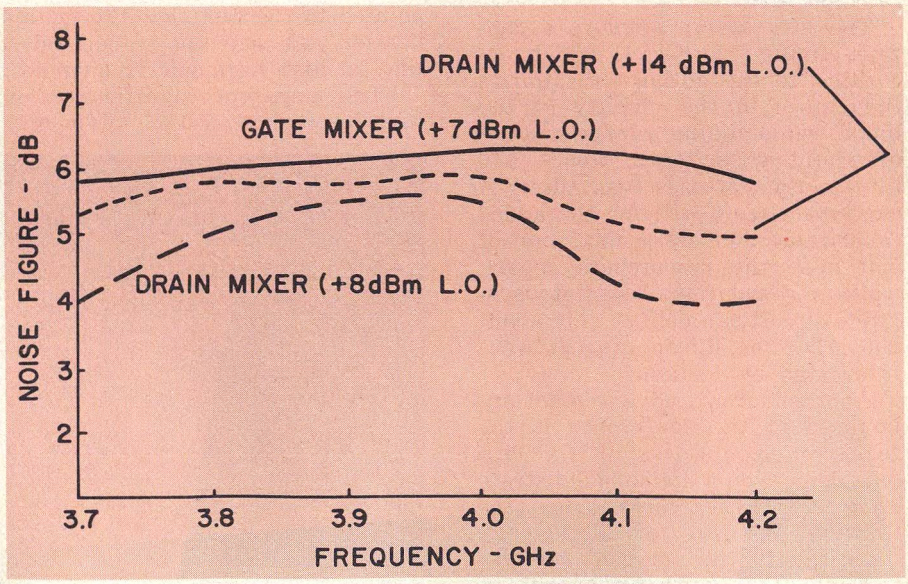

5. FETs make excellent mixing elements. Drain-driven mixers offer lower noise figure, but note higher LO power.

terminations

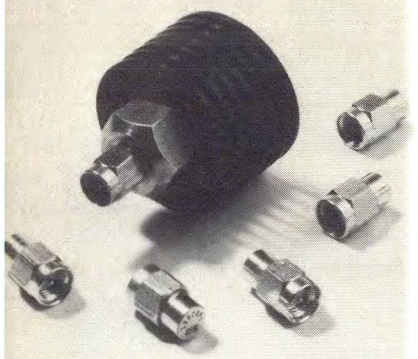

Largest variety available from a single source. Now includes miniature packaged units exhibiting low VSWR to 26 GHz.

READER SERVICE NUMBER 107

A **standard** OSM component is your best buy. That's why Omni Spectra maintains the broadest catalog line of miniature microwave components that you'll find. Off-the-shelf units that live up to Omni Spectra's reputation for quality, reliability, value and adherence to specifications.

When you need a **custom design** ...including integration of several functions in a single package... Omni Spectra has the in-depth engineering know-how and applications experience to provide you with a component that truly deserves the name OSM.

Standard or custom, every OSM component has the world's most desired mating launches... OSM quality connectors. OSM connectors include Omni Spectra's patented captivated center conductor construction that eliminates pin and socket travel.

Send for catalog... or call us for immediate action!

Continental Boulevard, Merrimack, N.H. 03054
(603) 424-4111, TWX 710-366-0674

Impatts and Trapatts star in new circuits

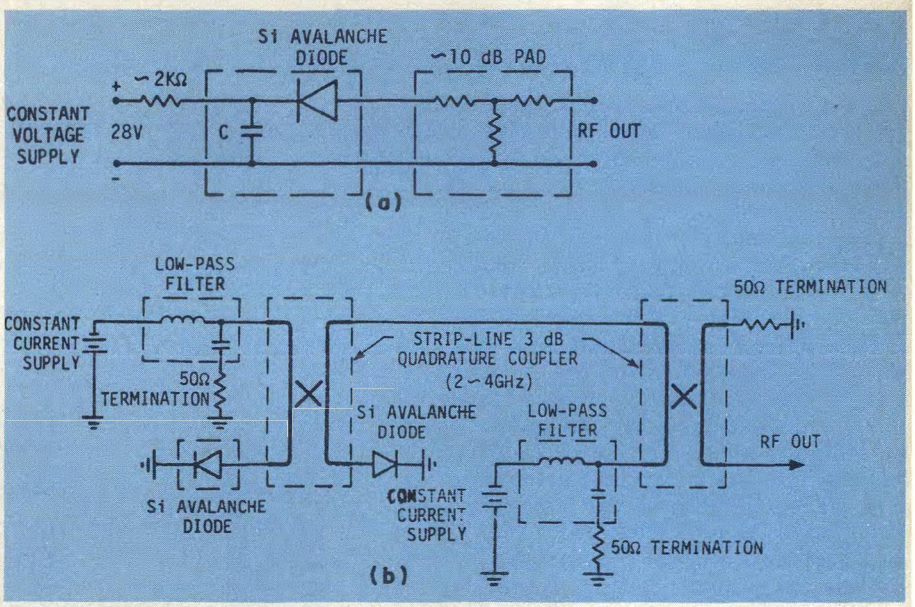

6. Conventional diode noise sources (a) tend to fluctuate. An improved version (b) includes heat sinking, dc/rf decoupling and impedance matching.

quickly switched make them ideal for system noise monitoring applications. However, as Motohisa Kanda of the Electromagnetics Division of the National Bureau of Standards point out, diode noise sources are easily influenced by their environment and tend to be unstable over long periods of time.

"A preliminary study of the stability of typical commercial solid-state noise sources indicates that the fluctuations in the output noise exhibit a random walk behavior which is divergent toward the lower frequencies," Kanda explains. "The square root of the variance of the average output noise power for a one day sampling time interval is typically 0.008 dB." The instability was attributed to three design flaws: poor diode heat sinking, ineffective dc/rf decoupling and impedance mismatches.

An alternate circuit suggested by Kanda requires more hardware, as shown in Fig. 6, but reportedly improves stability by a factor of four. The heat sink problem was attacked by attaching the diodes directly to the ground plane using conductive gold epoxy. Constant current bias was substituted for the constant voltage supply normally used, and bias current is passed through a low-pass circuit to isolate the power supply from the active device and to prevent any bias interaction. Interestingly, the circuit uses a stripline, 3 dB quadrature coupler to decouple dc and rf ports.

Stable operation also requires a precise impedance match between the diode and the 50-ohm stripline used in the design, Kanda stresses. Conventional matching devices, such as transformers or tuners, were rejected by the researcher due to bandwidth restrictions. The solution is to terminate the output of the hybrid with a second noise diode, carefully matched to the impedance of the first. This second device is biased in a similar way, through another hybrid, as shown in the figure. "Possibly one of the best, and perhaps the easiest way to achieve the proper impedance would be to fabricate one diode of the stripline 3 dB quadrature coupler with the same impedance as the diode at the operating bias," Kanda advises. "By selecting two diodes with nearly identical impedances (both amplitude and phase), an improvement in the basic VSWR of the circuit from 2.0 to 1.2 was readily achieved at 2 GHz." ••

Microwave monitor keeps an eye on the road

Joseph Ligori
Associate Editor

On a cold and dreary day, have you ever wondered why buses arrive in groups of two or three after waiting a dreadful period of time for just one? Or, did you ever think about how easy it is for a highjacker to simply drive off with a huge truck filled with valuable merchandise? And, when you need a policeman, doesn't it always seem that they are all on the other side of town?

These situations occur frequently, simply because it's so difficult to keep tabs on individual vehicles in a large fleet. But a new concept introduced by RCA Global Communications, Inc., in Piscataway, NJ, may help overcome the problem by using microwave technology and clever FSK modulation techniques to automatically pinpoint a vehicle's exact location.

RCA designers evaluated several approaches to vehicle location, including phase and pulse ranging, before finalizing on a proximity, or "signpost" system. The proximity system relies on a grid of semi-active reflectors, called signposts, mounted on light poles around a city. Vehicles are equipped with 100 mW cw X-band transmitters which illuminate signposts as they are passed. Each signpost imparts a unique FSK code to the signal reflected back to the vehicle. The mobile unit receives the reflection, decodes the phase information and stores the location in a memory. Upon command from a central processing station, the vehicle searches its memory and radios back its updated location code.

"A signpost system is almost certainly the simplest and least expensive for fixed route system," notes Gerald S. Kaplan, senior member of the technical staff at RCA Globecom. The narrow bursts of a pulse ranger require a large bandwidth and each vehicle would need an expensive, high-power pulse transmitter, he explains. While phase ranging equipment might cost less, Kaplan feels that its accuracy may not be adequate when severe multipath exists. Other types of signpost systems, which might use active signpost transmitters or passive signpost receivers linked directly to a central processor, were rejected due to cost.

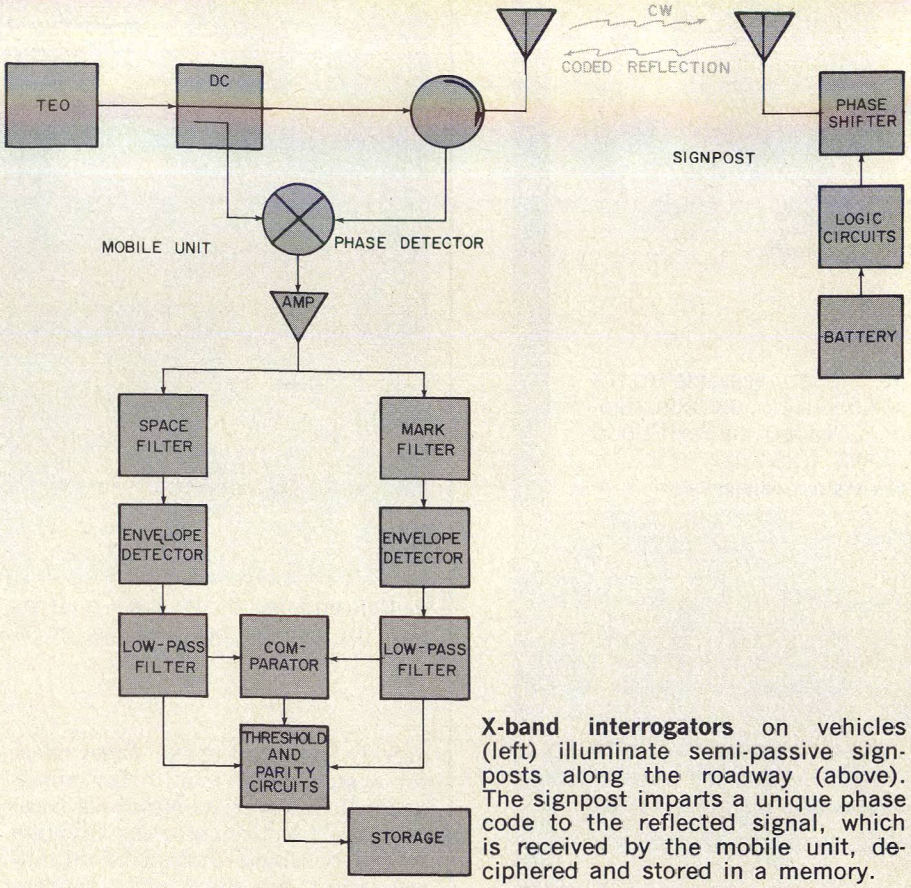

X-band interrogators on vehicles (left) illuminate semi-passive signposts along the roadway (above). The signpost imparts a unique phase code to the reflected signal, which is received by the mobile unit, deciphered and stored in a memory.

Each signpost in RCA's system consists of a flat, printed-circuit antenna array, a simple phase shifter incorporating a GaAs varactor and COS/MOS (complementary-symmetry MOS) logic circuitry powered by a lithium battery (see figure). "The COS/MOS circuit is similar to electronic watch circuits, consuming microwatts of power," notes Kaplan. Batteries are expected to last several years.

The designers chose X-band for the interrogation signal because they wanted a rapid decay over all paths other than line-of-sight, to reduce interference between signposts on adjacent streets. Also, the microwave frequency provides a bonus. "Use of antenna gain at the signpost, which is not practical at lower frequencies, is an additional factor in confining the reflected energy to the immediate vicinity of the signpost. This serves to reduce interference between signposts, and to define a narrow, ribbon-like beam across a street," Kaplan adds.

Phase diversity added to FSK

Each signpost encodes the illuminating signal with an n-bit code, each bit conveyed by phase modulating the X-band carrier at one of two-tone frequencies. When the mobile interrogator receives the modulated reflection, the phase information is stripped by the mixer, using a sample of the TEO output as a local oscillator. The mixer output is fed to an amplifier, then to a bandpass filter, envelope detector and comparator chain. Here, the signal is subjected to both strength and parity checks; messages which fail either are rejected in the receiver. "This insures that weak signals or noise alone will be ignored and only reliable messages based on strong signals will be received and accepted for storage," Kaplan comments.

(continued on p. 16)

2 GHz repeater built without i-f

Refinements in class A, solid-state rf amplifiers coupled with a better understanding of shrouded antenna performance has led designers at GTE Lenkurt to the development of a simplified low-cost repeater for the 2 GHz communications band. Installation costs included, the new repeater station reportedly offers a 5:1 cost advantage over a typical heterodyne site, and a 2:1 cost advantage over a passive, or "billboard" repeater.

In the past, active repeaters have been designed to shift the input signal down to an i-f for processing. After the i-f stage, the signal is typically upconverted to an output frequency that is offset from the repeater's input by 50 MHz to reduce antenna-to-antenna coupling. Lenkurt's alternative is simple—eliminate the i-f, use the same input and output frequencies and rely on shrouded antennas and cross polarization to reduce interference to an acceptable level. The result is a compact, all solid-state design that can rely exclusively on solar power.

Since input and output frequencies are not offset, extra care must be taken to achieve a 25 dB carrier-to-interference (C/I) ratio, especially when the angle between input and output paths is small, notes William R. Hampton, staff sales engineer at the San Carlos, CA firm and co-developer of the new repeater design. "By using cross polarization, horizontal on one path and vertical on the other, you pick up the 20 dB right off the bat," he notes. "But you still have to pick up at least 5 dB more, and that's where antenna separation and shrouds come in."

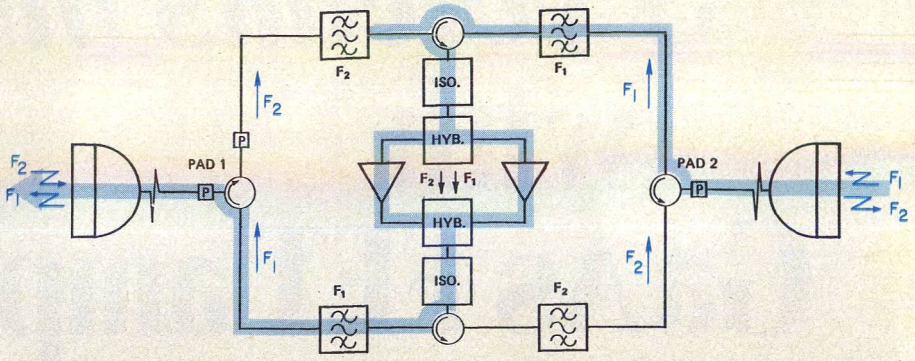

Transistor amplifiers are combined in parallel and provided with individual solar power supplies for added reliability. Note that it is not possible to add or drop channels at the repeater site.

The shrouded antennas offered with the system began as $2,500 "high-performance" models, says Hampton, but were stripped of accessories to sell for half as much. Specifications conform to FCC standard A, part 94, which is the commission's highest rating for 2 GHz communications antennas. "A 'plain-Jane' antenna can also be used with the system, but only if shielding such as a building is present between the dishes," Hampton notes.

Linear amps are critical

The availability of highly linear solid-state amplifiers was another key to the repeater design. "Amplifying devices available in the past, klystrons for example, were simply not linear enough for this application," says the Lenkurt engineer.

Two Varian VSL-7441JG transistor amplifiers are paralleled by hybrids in a patent-pending circuit designed by GTE Lenkurt that allows duplex operation. Consider a duplex system with frequencies F_1 and F_2. As shown in the figure, signal F_1 passes through an input circulator, through a bandpass filter tuned to F_1 and through a second circulator to another bandpass filter. This filter is tuned to F_2, however, and signal F_1 is reflected back through the circulator and an isolator to the hybrid-coupled amplifiers. F_2 follows a similar path from left to right. The gain of the repeater is 45 dB in both directions, which results in an overall site gain of 96 to 120 dB, depending on antenna size. ••

SVB

Microwave monitor keeps an eye on the road *(continued from page 14)*

"As in all homodyne systems, the exact rf phase is of great importance," the RCA engineer cautions. While in motion, he explains, slow fading due to a Doppler effect could be effectively superimposed on the signal at the output of the mixer. On the other hand, he adds, when the vehicle is stopped, there is a possibility that the LO and the reflected signal would be in phase quadrature, causing signal dropouts and unreliable messages.

These problems are attacked by switching additional phase shifts of about 90 degrees at the signpost reflectors. "This phase diversity has the effect of introducing fast-fading, compared with the data and Doppler rates, which dominates slower fading. It also insures that the reflected signal will not remain in phase quadrature with the LO for any significant length of time," Kaplan explains.

The RCA engineer predicts acceptable performance for threshold-to-noise ratios of 10 to 12 dB, and signal-to-noise ratios of 14 to 16 dB, when the vehicle is within reception range.

Field tests of the system verify the usefulness of phase diversity. Urban tests, conducted in Trenton, NJ, indicate that reflections from buildings or adjacent traffic have no degrading effect on the system's performance, according to RCA. Another test, conducted on a busy NJ freeway, proved the system operable at speeds up to and exceeding 60 miles per hour. Range is claimed to be sufficient for a ten-lane highway.

Although Kaplan says that RCA is not planning to market their automatic vehicle monitoring system, he notes that licensing agreements might be possible.

The system was introduced at the 1976 Vehicular Technology Conference, in a paper titled "An X-Band System for Automatic Location and Tracking of Vehicles Using Semi-Passive Signpost Reflectors," co-authored by Kaplan and Andrew D. Ritzie. ••

COVER FEATURE

How Accurate Is Your Spectrum Analyzer?

A comparison of amplitude and frequency measurement procedures reveals that the analyzer's basic accuracy can be improved through careful attention to techniques and by using other instruments.

JUST how accurate is your spectrum analyzer? More importantly, do you use the instrument in a way that takes full advantage of its potential?

If you're not sure of the answers to either of these two questions, perhaps it's time to examine the three major sources of instrument error: calibration, frequency response and comparison uncertainties. Recognizing the factors that influence each, is the first step to developing a rational set of measurement procedures.

Even with the most skilled user, however, there is a finite limit to a spectrum analyzer's accuracy. But in many cases, other instruments can be used to further reduce this uncertainty. It should be noted at the outset that all accuracies discussed here are worse-case and based on the instrument shown in Fig. 1; substantially better accuracy can be achieved in most situations.

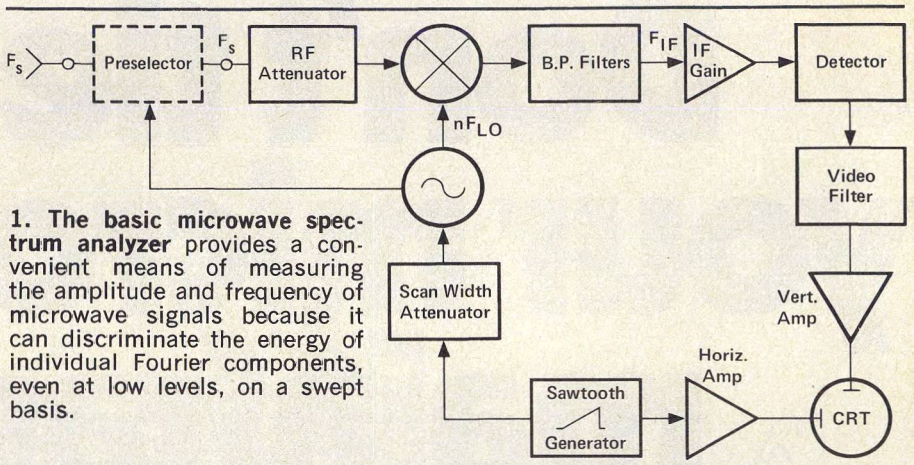

1. The basic microwave spectrum analyzer provides a convenient means of measuring the amplitude and frequency of microwave signals because it can discriminate the energy of individual Fourier components, even at low levels, on a swept basis.

Assessing amplitude accuracy

The first step in measuring amplitude is to establish a calibration reference level, as shown in Fig. 2(a). This is done by displaying a known signal on the CRT and noting the vertical position of the signal's peak. The calibration source is either built into the analyzer or supplied by the user. If the spectrum analyzer is not gain compensated band-to-band, the reference signal must be displayed on the same frequency band as the unknown signal.

Using the log display mode, signal levels may be measured in units of absolute power, such as dB referred to 1 mW (dBm), or in units of relative power, dB referred to a reference amplitude. In both cases, the unknown signal level can be compared to the reference level in one of three ways:

- **Relative measurement.** The number of vertical divisions between the unknown signal level and calibration level is multiplied by the vertical scaling per division, and this amount is either added to or subtracted from the calibration level (Fig. 2(b)). Comparison uncertainty inherent in this technique is a function of vertical scaling accuracy.
- **I-f substitution.** I-f gain within the analyzer is varied to match the position of the unknown signal peak with the calibrated reference level on the CRT, and the increase or decrease in i-f gain is subtracted from or added to the calibration level (Fig. 2(c)). Comparison uncertainty of i-f substitution is a function of the accuracy with which i-f gain can be set. Because of this, the technique requires a wide range of i-f gain calibrated in 1 dB increments.
- **Rf substitution.** Rf attenuation is changed to match the unknown signal level with the calibration level, and the increase or decrease in attenuation is added to or subtracted from the calibration level. Comparison uncertainty is a function of attenuator accuracy, thus a calibrated vernier is necessary.

If absolute amplitudes are measured, calibration reference accuracy is one source of measurement uncertainty. If the amplitude difference between two signals is measured, calibration uncertainty is not relevant.

Whenever signal amplitudes at one frequency are compared with signal amplitudes at other frequencies, system frequency response is a source of uncertainty. Errors can be traced to preselector flatness (assuming proper preselector tracking), spectrum analyzer frequency response and any band-to-band gain compensation uncertainties.

It should be noted that other potential sources of uncertainty become applicable whenever IF bandwidths and/or vertical scale factors are used for calibration and measurement. They may be disregarded,

Peter Linden, Product Marketing Engineer, Hewlett-Packard Company, 1400 Fountain Grove Parkway, Santa Rosa, CA 95404.

however, provided calibration and measurement are done with the same control settings.

The reader should also keep in mind the measurement uncertainty introduced by interconnection mismatches. While techniques do exist to reduce the effects of mismatch, a thorough treatment of the topic is beyond the scope of this article.

How large is the error?

The instrument uncertainty inherent in the three techniques described above varies considerably. For example, consider a microwave spectrum analyzer with the following specifications, which are applicable over its full tuning range:

Calibration uncertainty	±0.5 dB
Frequency response(including preselector flatness and gain compensation uncertainty)	±3.0 dB
Vertical display error	±2.0 dB
I-f gain error (including vernier)	±0.5 dB
Rf attenuator (including vernier)	±2.5 dB

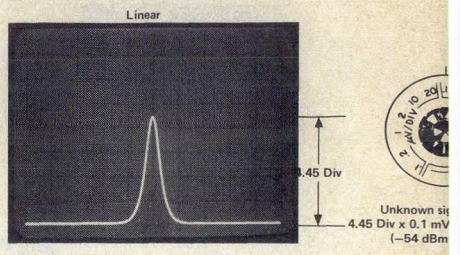

3. Linear measurements can be as accurate as i-f substitution log measurements.

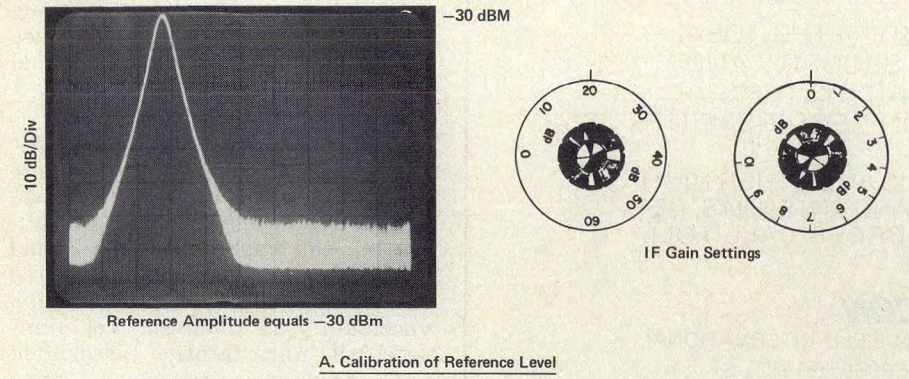

A. Calibration of Reference Level

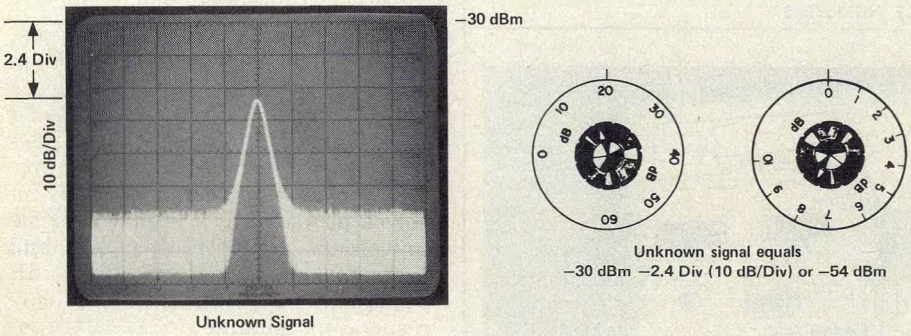

B. Relative Measurement Technique

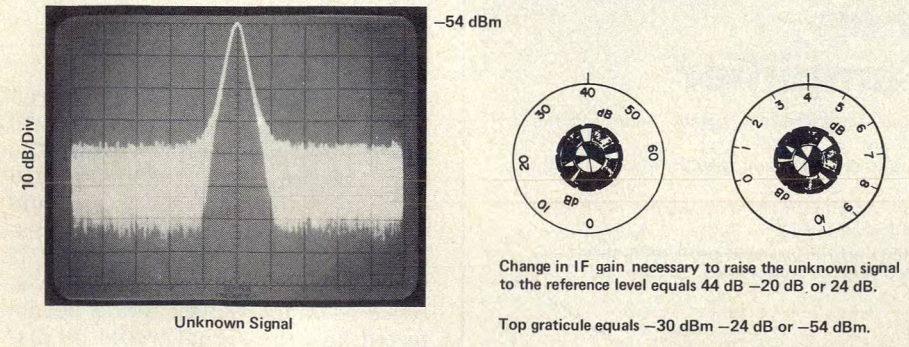

C. IF Substitution Technique

2. Reduce amplitude comparison uncertainty by calibrating the CRT with a reference level (a). Unknown signals may be compared to this level directly (b) or i-f gain can be adjusted to match the two levels (c).

The relative measurement technique would yield an instrument accuracy of ±(0.5 + 3.0 +2.0) or ±5.5 dB. Note that if i-f gain and rf attenuation were changed in the process of making the measurement, accuracy would be ±(0.5 + 3.0 + 2.0 + 0.5 + 2.5) or ±8.5 dB. The i-f substitution technique would yield an instrument accuracy of ±(0.5 + 3.0 + 0.5) or ±4.0 dB, while the rf substitution method would yield an instrument accuracy of ±(0.5 + 3.0 + 2.5) or ±6.0 dB.

Because rf attenuation accuracy gets worse as frequency increases, i-f substitution is typically the most accurate way to make amplitude measurments using a log display.

If the spectrum analyzer display can be calibrated linearly in voltage, signal amplitudes are measured by multiplying the number of divisions of signal deflection by the vertical voltage per division calibration, as shown in Fig. 3. The linear sensitivity of the analyzer may be calibrated directly or deduced by dividing a known voltage at some point on the display by the number of divisions between that point and the bottom of the CRT, in which case, linear sensitivity is a function of the size of the deflection.

The accuracy of this technique depends upon calibration and flatness uncertainties, as in the log mode of operation, as well as linear sensitivity accuracy and display linearity.

For instance, assume that the spectrum analyzer in the previous example was calibrated linearly in voltage, and had the following specifications:

Linear sensitivity uncertainty	±0.3 dB
Display linearity	±0.3 dB

Measurement accuracy would equal ±(0.5 + 3.0 + 0.3 + 0.3) or ±4.1 dB.

(continued on p. 38)

NEW $15.00
EACH IN 100 QUANTITIES

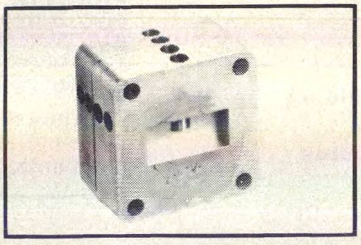

PASS BAND FILTER

DIE CAST X-BAND FILTER. IDEAL FOR MEETING SECURITY AND POLICE RADAR SYSTEMS FCC CERTIFICATION REQUIREMENTS

FOR DETAILS ON THIS AND OTHER HIGH PERFORMANCE X-BAND ANTENNAS, DETECTORS AND SOURCES CALL TOLL FREE (800) 426-5966

OR WRITE RACON INC.
BOEING FIELD INTERNATIONAL
8490 PERIMETER RD., S.
SEATTLE, WASHINGTON 98108
(206) 762-6011

READER SERVICE NUMBER 37

There's still nothing like vacuum tubes for an exceptional TWT amplifier

Sure our amplifier uses solid state components—everywhere, in fact, except in the high voltage regulator and the TWT itself.

Why a vacuum tube regulator? Because of the greater reliability with this inherently high voltage component.

It qualifies our TWT amplifier especially for antenna pattern measurement, EMI susceptibility testing and r-f power instrument calibration.

But we utilize contemporary concepts when they add to reliable performance. Our modular construction and plug-in boards will accommodate a variety of TWTs for example.

And we can and do add VSWR protection, harmonic filtering and variable output, where required.

Octave band width 10, 20, 100 and 200 watts TWTAs from 1 GHz to 18 GHz. For detailed specifications write MCL, Inc., 10 North Beach Avenue, La Grange, Illinois 60525. Or call (312) 354-4350.

MCL INC

READER SERVICE NUMBER 38

SPECTRUM ANALYZER

The uncertainty inherent in a linear measurement (assuming direct calibration) is typically very similar to that associated with a measurement made with i-f substitution on a log display. In those situations where limited i-f gain prevents a signal from being raised to the calibrated reference level, measurements in linear mode may be more accurate.

Improving basic accuracy

Special procedures and auxiliary instrumentation can often be employed to reduce calibration, frequency response and comparison uncertainties.

Obviously, calibration accuracy may be enhanced through the use of a very accurate reference signal with good spectral purity and a precision power meter.

By removing the preselector from the system (if separate), its contribution to flatness uncertainty can be eliminated. And, by calibrating the analyzer with a signal mixing on the same band as the unknown signal, gain compensation uncertainty is removed. To eliminate all uncertainties associated with frequency response, simply calibrate the analyzer at the same frequency as the signal of interest as described in Fig. 4.

Comparison uncertainty may possibly be reduced by using precision external attenuators to improve the calibration of the analyzer's i-f gain. The technique effectively substitutes rf attenuation uncertainty for i-f gain uncertainty and involves positioning a signal at some convenient point on the CRT, and then for every 10 dB or 1 dB change in i-f gain, noting the corresponding change in rf attenuation required to reposition the signal at the reference position as shown in Fig. 5. Perform the calibration below 1 GHz where the accuracy of most rf attenuators is highest.

Low-level signals pose problems

The uncertainties encountered when measuring signals within 10 dB of noise are complicated by the fact that the amplitude displayed on a spectrum analyzer is the sum of all signal and noise energy present in its passband. In theory, if the signal equaled the noise level, twice as much power would be detected and the signal would be displayed 3 dB above the noise. This 3 dB would have to be subtracted from the displayed level to deduce actual signal level. In reality, however, due to log amplification and the response of the detectors used

(continued on p. 40)

NEW

ULTRA WIDEBAND AMPLIFIER

Model 1W1000

1 to 1000 MHz 1 Watt Linear

Here's a unique, all-solid-state amplifier that delivers 1 watt of swept power output from 1 to 1000 MHz instantaneously. It's the Model 1W1000 from Amplifier Research. A reliable, unconditionally stable unit, the new Model 1W1000 provides 1 watt of linear power over three decades of bandwidth.

Its performance is matched only by its versatility. For example, Model 1W1000 can be used with high-level sweepers, VSWR measuring systems and network analyzers. It's also used to increase the sensitivity of spectrum analyzers, oscilloscopes and wideband detector systems. It has all the bandwidth you'll ever need. For complete information, write or call:

Amplifier Research
160 School House Road
Souderton, PA 18964
215-723-8181

AMPLIFIER RESEARCH

Your Best source for RF Power Amplifiers

READER SERVICE NUMBER 40

in general purpose spectrum analyzers, the noise level displayed is not true RMS noise[2], and the correction factors that must be applied to calculate actual signal level must be derived empirically.[3]

In the case of low-level signals or noise, i-f substitution may not be possible due to limited i-f gain, so measurements using a linear display may be more accurate. Best sensitivity for low-level signals is achieved at the minimum usable resolution bandwidth setting for

(continued on p. 43)

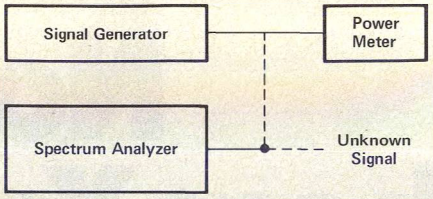

A. Make a rough measurement to determine the unknown signal's frequency.

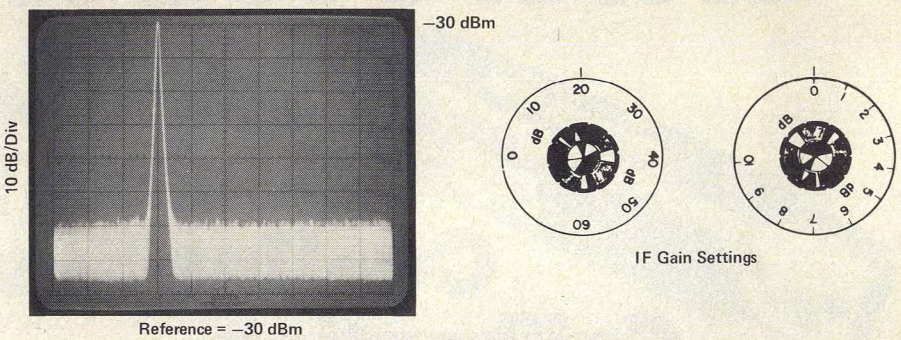

Reference = –30 dBm

B. Tune the Signal Generator/Power Meter to this frequency and use this known external reference to calibrate the reference level.

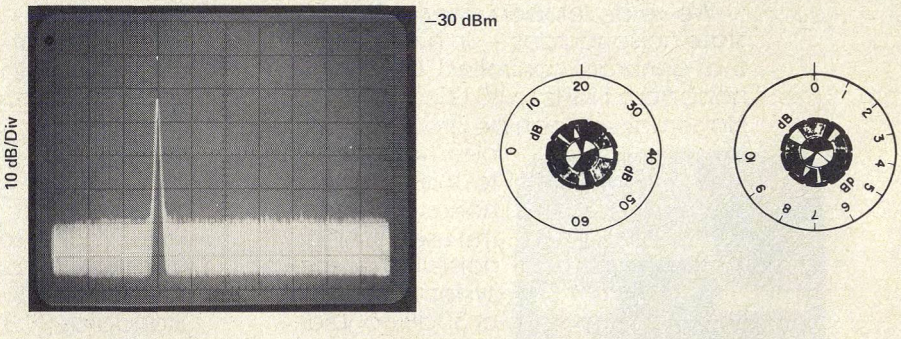

C. Input unknown signal.

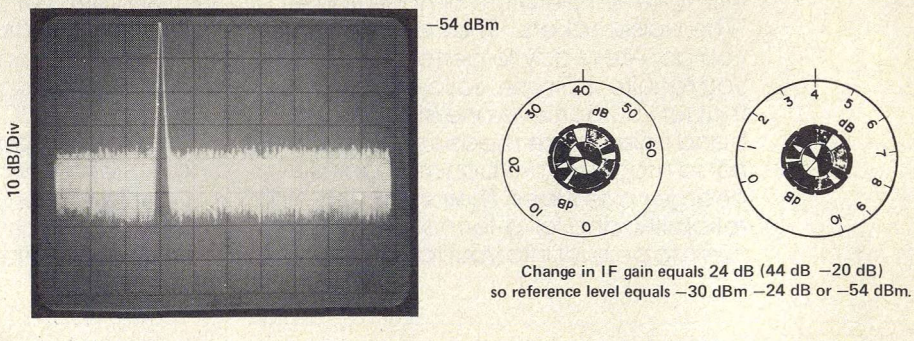

Change in IF gain equals 24 dB (44 dB –20 dB) so reference level equals –30 dBm –24 dB or –54 dBm.

D. Change IF gain to match the unknown signal's level to the reference level.

4. Minimize amplitude uncertainties due to frequency response by calibrating the instrument at a frequency near the unknown.

the frequency of interest (a function of residual fm), on the lowest mixing mode for that frequency (lowest noise figure and least gain compensation) and with sufficient video filtering so that the signal is adding with average noise. The preselector should also be removed to reduce systems insertion loss.

Pitfalls to avoid

In addition to calibration, frequency response and gain uncertainties, certain situations can occur which may degrade amplitude accuracy or otherwise invalidate amplitude measurements. For example, if the signal of interest is swept too fast through the i-f of the spectrum analyzer to accommodate the response time of the bandpass filter, the level displayed will be incorrect. In the absence of a warning light, sweep speed should be decreased until trace amplitude is maximized.

A signal level may also be displayed incorrectly if the signal level at the input mixer of the analyzer is so large that gain compression is occurring. To prevent this from happening, rf attenuation should be added until the decrease in displayed signal amplitude tracks the change in attenuation. This technique may also be used to insure that only external signals are measured rather than internally generated distortion products.

Finally, an error can result if an image or multiple response of the signal of interest is measured. While preselection substantially reduces the probability of this happening, the limited rejection (50 to 70 dB) of these false responses does not eliminate the problem. Such responses still should be identified prior to measurement.

Some notes on frequency accuracy

The frequency of an unknown signal can be measured if it is tuned to the center of the CRT and the analyzer's center frequency is read off its frequency scale or preselector's tune frequency. Accuracy is a function of the mechanical coupling of the frequency scale or tracking of the preselector, and is typically on the order of 1.0 to 0.2 per cent.

To improve frequency accuracy, a relative technique can be followed where an unknown signal is measured by comparison with an accurately known reference frequency. The number of divisions between the two signals is multi-

(continued on p. 45)

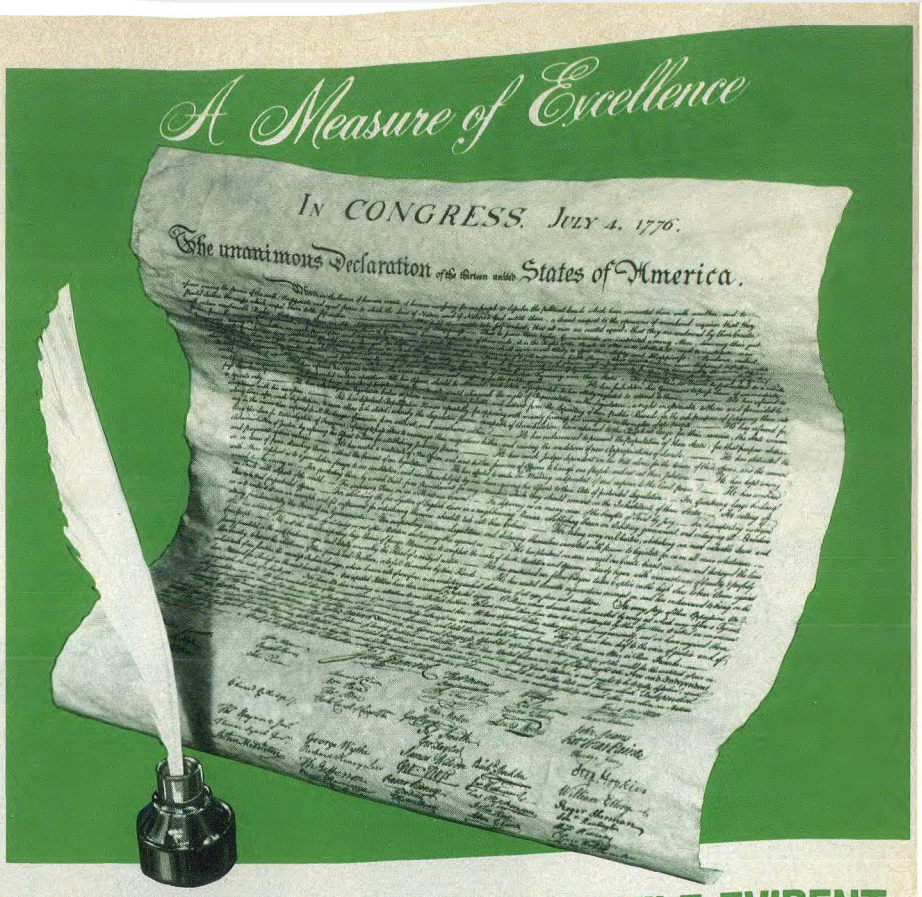

WE HOLD THESE TRUTHS TO BE SELF-EVIDENT...

- 10 KHz to 20 GHz Frequency
- 100 dB On-Screen Dynamic Range
- —125 dBm/KHz Sensitivity
- Built-in Preselection
- Automatic Phase-lock
- Digital Frequency Readout
- 1 KHz/Division Resolution
- 10 GHz Scan Widths
- All functions Built-in —No Plug-ins or ons

WITH AILTECH'S 727 SPECTRUM ANALYZER

Thanks to our forefathers, we enjoy the freedom of choice, and more and more systems designers around the world are recognizing the excellence of their choice, when they specify our 727 Spectrum Analyzer. A paradox in this world of complicated devices, the 727 is one of a kind, in that it combines sophistication with ease of use, and economy without sacrificing quality. We can't guarantee it will be around 200 years from today, but we can assure it will be your best independent source for Microwave signal analysis for many years to come.

Send us your John Hancock for a copy of our new "Notes on Spectrum Analysis" brochure.

AILTECH A CUTLER-HAMMER COMPANY CONTROL

EAST COAST OPERATION • 815 BROADHOLLOW ROAD • FARMINGDALE, NEW YORK 11735
Telephone (516) 595-6471 • TELEX 510-224-6558
WEST COAST OPERATION • 19535 EAST WALNUT DRIVE • CITY OF INDUSTRY, CA 91748
Telephone (213) 965-4911 • TELEX 910-584-1811
INTERNATIONAL OFFICES • FRANCE — La Garenne-Colombes • Telephone (01) 780-73-73 • Telex 62821
GERMANY — Munich • Telephone (089) 5233023 • Telex 529420
UNITED KINGDOM — Crowthorne • Telephone 5777 • Telex 847238
JAPAN — Tokyo • Telephone (404) 8701 • Telex 781-02423320 (Nippon Automatic)

INSTRUMENTS OF DISTINCTION

SPECTRUM ANALYZERS

FREQUENCY SYNTHESIZERS

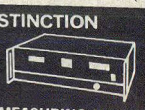
NOISE MEASURING INSTRUMENTS

RF POWER SOURCES

FOR DATA CIRCLE READER 43

FOR DEMO CIRCLE READER 45

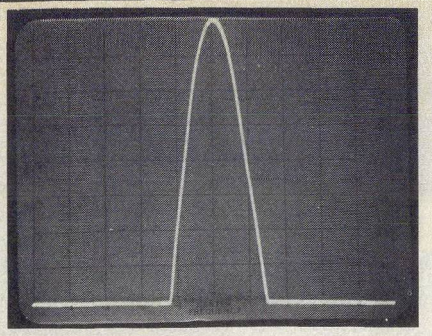

5. An external attenuator is useful for checking i-f gain calibration.

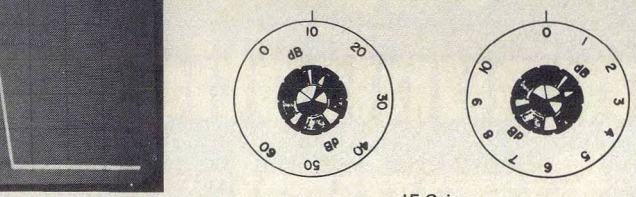

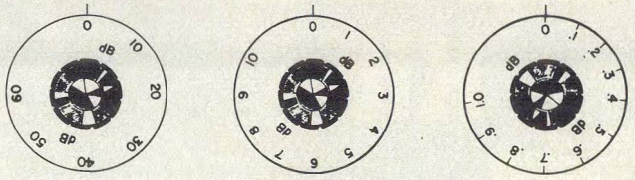

A. Position the signal at a convenient reference position.

Since RF attenuation changed by 9.5 dB, the change in IF gain between the 10 and 20 dB control settings is 9.5 dB.

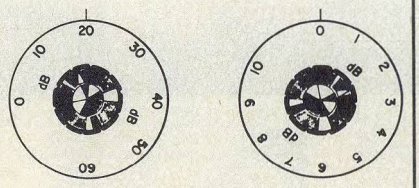

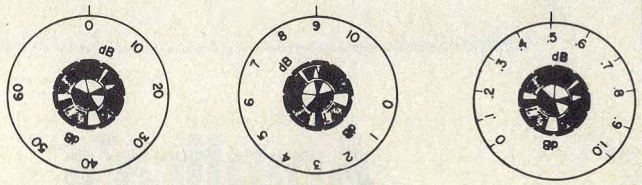

B. Change IF gain and note the change in RF attenuation required to keep the signal at the reference position.

plied by the frequency span per horizontal division and added to or subtracted from the reference frequency, as shown in Fig. 6. Measurement uncertainty is a function of reference accuracy and frequency span uncertainty, which is typically 5 to 10 per cent of the signal separation.

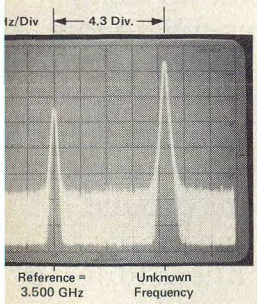

Frequency Span

Unknown frequency equals 3.500 GHz + 4.3 Div (10 MHz/Div) or 3.543 GHz.

6. Use a reference oscillator to more accurately determine the frequency of an unknown input.

To improve the accuracy of a relative measurement, the reference frequency should be as close to the unknown signal as possible. A precision comb generator (utilizing step recovery diodes) can be an effective standard because many reference signals (teeth) will be produced, some of which will be near the unknown signal. The source may also be modulated to produce interpolation sidebands of any desired spacing. Comb tooth accuracies on the order of 0.1 to 0.01 per cent are possible.

Alternately, a signal source and counter could serve as the precision frequency reference, where reference accuracy would equal source residual fm plus counter accuracy. If the signal source is tunable, a beat technique can be employed to eliminate any frequency span uncertainty from the measurement, as illustrated in Fig. 7. Measurement accuracies on the order of

(continued on p. 47)

NEW PRESENTATION DIELECTRIC MATERIALS CHART

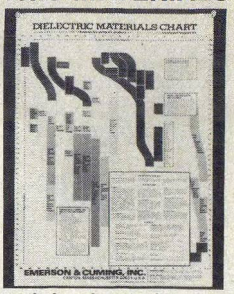

This colorful chart is a standard reference for electronic engineers. Shows Dielectric Constant (κ') and Loss Tangent (tan σ) for many E&C products and common materials plotted on 11″ x 16½″ graph. For notebook or wall mounting.

READER SERVICE NUMBER 12

ELECTRICALLY CONDUCTIVE ADHESIVES AND COATINGS

ECCOAMP products offer high performance and savings for bonding, coating, sealing electrical/electronic components with conductive plastic. They include "cold" solders, anti-static, reflective and absorbtive coatings. Some have electrical and thermal conductivity equivalent to metals.

READER SERVICE NUMBER 13

ECCOMAX HI-Q LOW-LOSS DIELECTRICS

18 low loss systems are described in new folder and chart. Casting resins, impregnants, coatings, adhesives, rod & sheet — some foams — some Hi K — all with dissipation factors below 0.001. For RF, UHF, VHF and microwaves — capacitors, coils, etc.

READER SERVICE NUMBER 14

Emerson & Cuming, Inc.

CANTON, MASS.
GARDENA, CALIF.
NORTHBROOK, ILL.
Sales Offices in Principal Cities
EMERSON & CUMING EUROPE N.V., Oevel, Belgium

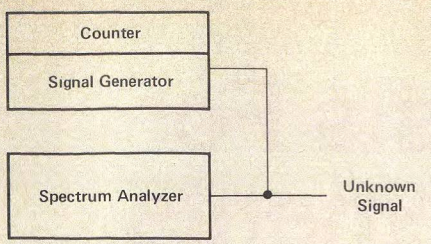

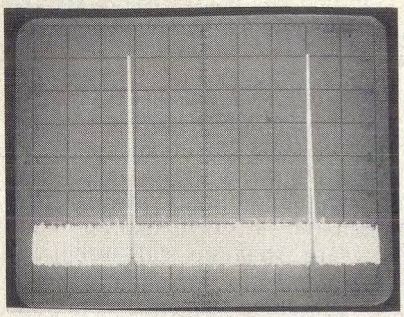

100 MHz/Div

A. Display the unknown signal with a generated signal of approximately the same amplitude.

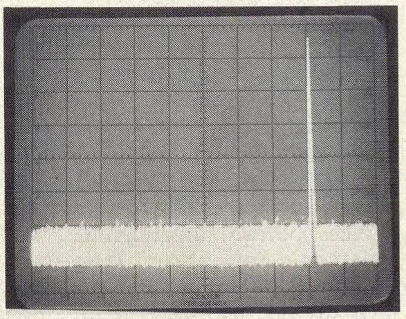

100 MHz/Div

B. Tune the generated signal to equal the unknown signal.

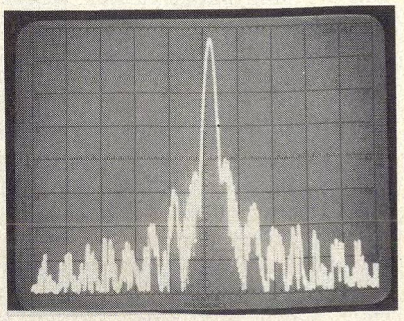

1 MHz/Div

C. Reduce frequency span to magnify the display and tune generated signal to exactly "beat" with unknown signal. Count generated signal.

7. A beat technique eliminates frequency span uncertainty.

0.001 per cent can be achieved.

At frequencies above the tuning range of preselectors, frequency meters may be used to measure unknown signals. The signal of interest is nulled and its frequency read off the meter. Accuracies of 0.2 to 0.4 per cent are typical.

Tracking generators, which closely follow the tuning of the instrument, are available to approximately 2 GHz, but achieving very close tracking at higher frequencies becomes extremely difficult.[5] By counting the output of such a source when the analyzer is manually scanned to the signal of interest, its frequency can be deduced. The uncertainty of this technique equals the tracking error and residual fm of the source, plus counter accuracy.

By counting the frequencies of the local oscillators of a spectrum analyzer when it is manually scanned to a signal of interest, that signal's frequency can be calculated. In greatly simplified form, the tuning expression for a microwave spectrum analyzer is as follows:

$$F_s = nF_{LO} \pm F_{i-f}$$

where

1) F_s is the unknown signal
2) n is the harmonic of the LO mixing with F_s.
3) F_{i-f} is the passband frequency of the instrument's filter.

Since F_{i-f} is known and F_{LO} counted, by multiplying by the proper value of n and using the correct sign, F_s can be calculated. In reality, the technique is more complicated,[6] but uncertainties on the order of 0.001 per cent or less are achievable. ••

A more extensive discussion of spectrum analyzer measurement accuracy, dealing primarily with Hewlett-Packard products, can be found in H-P Application Note 150-8, "Accuracy Improvement," which can be requested directly from Hewlett-Packard or by circling **reader service number 297.**

References

1. Hewlett-Packard, "Microwave Mismatch Error Analysis," No. AN-56.
2. Hewlett-Packard, "Noise Measurements," No. AN-150-4, pg. 8.
3. Hewlett-Packard, "Accuracy Improvement," No. AN-150-8, pg. 15.
4. Hewlett-Packard, "Spectrum Analyzer Basics," No. AN-150.
5. Hewlett-Packard, "Swept Frequency Measurements and Selective Frequency Counting with a Tracking Generator," No. AN-150-3, pg. 40.
6. Hewlett-Packard, "Accuracy Improvement," No. AN 150-8, pg. 20.

STRIPLINE Components or Assemblies

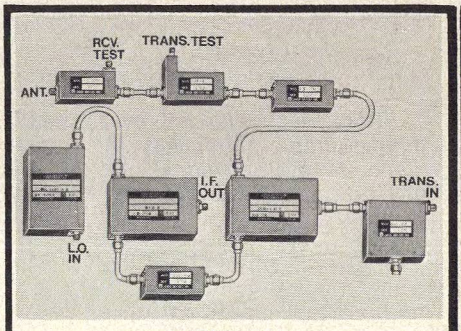

DISCRETE

- Maximum flexibility during experimental stage.
- Huge standard component selection from our catalog.
- Low cost for small quantities.
- Short lead-time.

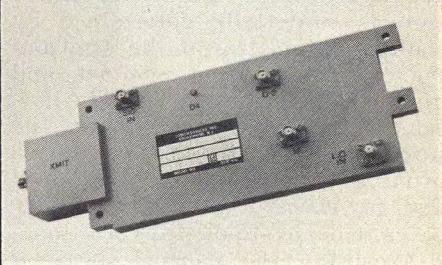

INTEGRATED

- Compact size.
- Enhanced reliability through elimination of connectors and interconnecting cables.
- Moderate and large production quantities at lower price.
- Optimum design to your exact requirements.

Lorch Devices specializes in the design and manufacture of highly reliable Stripline Discrete and Integrated Assemblies. All design factors receive careful attention, and our complete in-plant manufacturing capability, including environmental testing, permits the delivery of discrete components or sophisticated assemblies.

Our application engineering department is always available to assist you in arriving at the best solution for your specific problem.

A 64 page Catalog No. 749 which describes these products is available.

Send for your **free copy** today.

LORCH DEVICES INC.
105 CEDAR LANE, ENGLEWOOD, N.J. 07631
201-569-8282 • TWX: 710-991-9718

READER SERVICE NUMBER 47

Use Electrical Tests For Thermal Measurements

The thermal resistance of a semiconductor device can be accurately measured by monitoring a temperature sensitive electrical parameter. Measurement methods must be carefully tailored to match the device.

As new developments steadily increase semiconductor operating frequencies and power capabilities, chip and package sizes continue to shrink. This fact, coupled with efforts to reduce overall system size and weight in the face of increasingly severe environmental limitations, has imposed considerable stress on the thermal parameters of microwave semiconductor devices. Since the operating life of a semiconductor device is inversely related to its junction temperature, thermal considerations have become as important as electrical specifications.[1,2]

Data sheets usually describe at least two important thermal specifications: maximum junction or operating temperature (T_j or $T_{op\,max}$, respectively) and thermal resistance (θ_{jc}). The former specification is essentially determined by the characteristics of the semiconductor, metalization, contact and die attachment material. The latter, while also dependent on the same characteristics, is much more prone to manufacturing techniques and is, therefore, subject to significant device-to-device variation.

Accepting the thermal specs on the manufacturer's data sheet at face value, the circuit designer can compute the junction operating temperature as follows:

$$T_j = (P_{diss})(\theta_{jc}) + T_c$$

where T_j = junction temperature
T_c = case temperature
P_{diss} = device internal power dissipation
θ_{jc} = device thermal resistance from junction to case.

As the example of Fig. 1 shows, a diode with a maximum junction temperature specification of 200°C may be operating close to the safety limit at a case temperature of only 25°C! Increasing the case temperature to 61.4°C would cause the junction temperature to reach the maximum, assuming everything else remains constant.

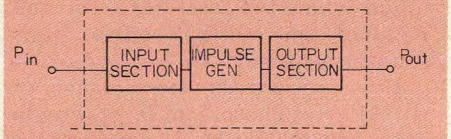

DESIGN SPECIFICATIONS

$T_j = 200°C$ (max)
$\theta_{jc} = 14°C/W$ (max)
$P_{IN} = 15$ W
$P_{OUT} = 2$ W (min)
$f_{IN} = 200$ MHz
$f_{OUT} = 2$ GHz
$T_A = T_c = 25°C$

THERMAL DESIGN EQUATIONS

$$P_{DISS} = P_{IN} - [P_{OUT} - P_{IS} - P_{IG} - P_{OS}] \quad (A)$$

$$\Delta T_j = \theta_{jc} P_{DISS} \quad (B)$$

$$T_j = \Delta T_j + T_c \quad (C)$$

Assume all circuit losses can be related to input and total 1 dB; ie:

$[P_{IS} + P_{IG} + P_{OS}] = 3.1$ W

Then,

$P_{DISS} = [15 - 2.0 - 3.1] = 9.9$ W
$\Delta T_j = 138.6°C$
$T_j = 138.6 + 25 = 163.6°C$

1. This step recovery diode multiplier example illustrates the importance of good thermal design. Diode specifications are for Hewlett-Packard's 5082-0300.

Test methods vary

The example illustrates the importance of careful thermal design, but is based on the assumption that the semiconductor manufacturer's thermal resistance specification is indeed correct. Unfortunately, this assumption is not necessarily valid for several reasons. Not all device manufacturers test θ_{jc} for 100 per cent of a production run. And lack of a standard measurement method results in θ_{jc} discrepancies even among manufacturers that do full production testing. Also, both manufacturer and customer thermal resistance specifications are usually not complete enough: they often fail to state the test method and/or test conditions. Thermal resistance is generally assumed to be a constant when, in fact, the measured value depends on operating conditions and temperature extremes, as well as the measurement method chosen. Further complicating matters is the lack of an absolute thermal resistance standard traceable to the National Bureau of Standards.

Thermal resistance is defined as the change in device junction temperature for a given change in device power dissipation, for a constant reference temperature. Power dissipation can be easily determined by monitoring device current and voltage. Junction temperature is not as easily measured, however, and has led to several different measurement techniques.

Four of the most common methods of monitoring device temperature are chemical, thermocouple, infrared and temperature sensitive parameter. Each method provides a fairly accurate measure of either junction or surface temperature that can be used to compute thermal resistance. Chemical and thermocouple methods require that direct physical contact be made to the semiconductor chip, thus risking device damage or contamination. Even the most skilled test operators find these measurement methods difficult and time consuming. Hence, both approaches are primarily suitable for research and development efforts.

The infrared (IR) method has found wide acceptance due to its versatility. Refinements in IR

(continued on p. 57)

Bernard S. Siegal, President, Sage Enterprises, P. O. Box 7189, Menlo Park, CA 94025.

Millimeter Test Components from TRG.

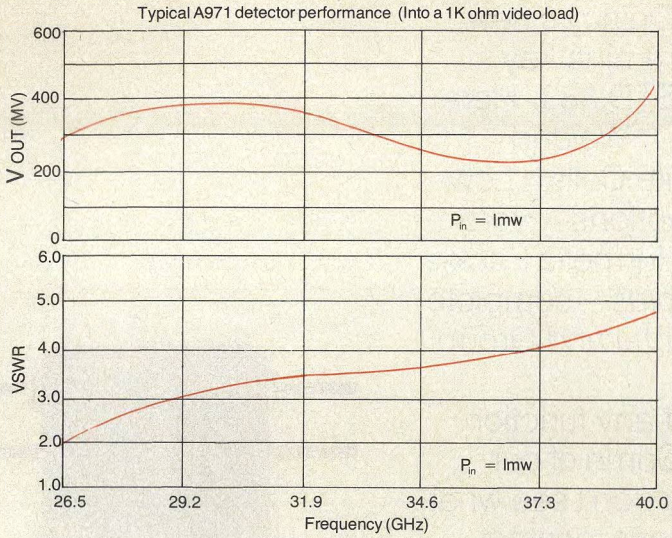

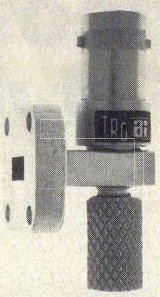
A971 broad band detector

Don't suffer a program delay because you lack a particular component . . . call TRG. For years we have been making the most complete line of waveguide test bench components available anywhere: precision direct reading frequency meters and rotary vane attenuators, directional couplers, phase shifters, hot & cold loads and calorimeters are just a few samples.

Compare the response curve of our wideband detector A971, for example . . . it stands alone.

That's why TRG is considered *the* millimeter company . . . we are already delivering 3rd generation millimeter components and sub systems.

Write for our data sheet and catalog.

TRG Alpha
DIVISION **Our limits are your imagination.**

ALPHA INDUSTRIES, INC. • 20 Sylvan Road, Woburn, Massachusetts 01801 • (617) 935-5150 • TWX: 710-393-1236 • TELEX 949436

READER SERVICE NUMBER 51

equipment enable device designers to prepare surface temperature profiles that quickly pinpoint hot spots. Since IR junction temperature measurements require no contact or interaction with the device under test, the method is particularly well suited for testing devices in operating hybrid circuits. Discrete, packaged units however, must be tested before encapsulation.

Every microwave semiconductor device has at least one parameter that varies with temperature in a consistent (from device to device) and well defined (linear, logarithmic, etc.) way. Using this temperature-sensitive parameter (TSP), it is possible to develop production-oriented, non-destructive test methods that provide accurate results for packaged devices and chips alike. An example of a temperature sensitive parameter of a junction diode is the device's forward voltage (V_F) under constant current conditions. For a current value large enough to insure operation above the I_F-V_F knee but low enough to avoid device heating, the forward voltage-temperature relationship is essentially a straight line of negative slope over a wide temperature range.

The TSP method has several advantages. Testing is fast, and analog or digital manipulation of the various voltages and currents used can provide a direct reading of thermal resistance in °C/W without too much difficulty, and to accuracies better than ±5 per cent. The total cost of a system to perform the tests and provide a direct reading output is about half that of the basic IR system. Finally, the TSP method is the only measurement alternative called out in MIL-STD-750B, which defines test methods for semiconductors.

Thermal resistance testing using the IR method is basically the same for all devices. Power is applied to the device in the normal manner with proper instrumentation to monitor all voltages and currents. The IR measured temperature rise is divided by a value corresponding to the dc power input less the rf power output, if any, to obtain the thermal resistance. Testing with the TSP method is not quite as simple, and must be tailored to each class of device.

Forward voltage tells the story

A very reliable temperature sensitive parameter for junction diodes is the device's forward voltage when measured at a "small" value of constant current. The actual value of constant current depends on the size and characteristics of the semiconductor junction, but the value must be low enough not to cause significant self-heating. Under this condition, the relationship between forward voltage and junction temperature can be considered a straight line of negative slope (K^{-1}), as shown in Fig. 2(a). Although the actual position of the V_F-T_j line may vary considerably for devices of the same type from different production runs, the slope of all the V_F-T_j plots will remain constant within a few per cent. Thus, a small sample of devices from several production runs, externally maintained at two or more values of T_j, can be monitored for changes in V_F. The resultant line slopes can be averaged to provide a meaningful calibration factor for converting ΔV_F to ΔT_j whenever devices of the same type are tested.

Although many TSP measurement techniques exist, the new MIL-STD-750B method recently proposed by the EIA Joint Electron Device Engineering Council Semiconductor Committee appears to be the most acceptable. In this method, the forward voltage (V_{F1}) for some small measuring current (I_M) is recorded for diode opera-

(continued on p. 53)

Attention!! ANA-ATE users

PRECISION
CALIBRATION KITS

COAXIAL
DC-18 GHz

WAVEGUIDE
1.7-40 GHz

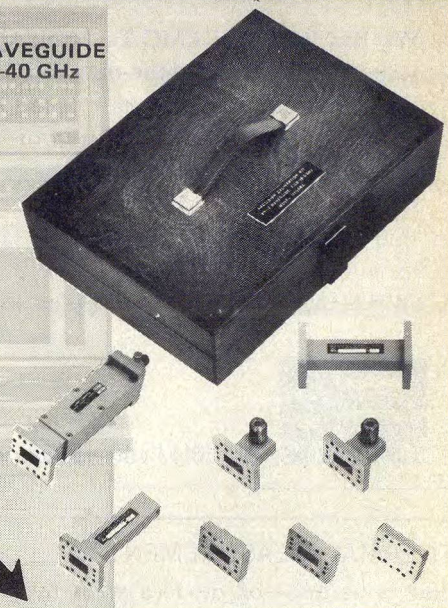

• ACCURATE
• CONVENIENT
• VERSATILE

MMC has developed a complete line of precision calibration kits to enable you to fully utilize your ANA, quickly and accurately. These kits contain all necessary adapters and calibration devices required. They are available in waveguide sizes from WR430 to WR28 and coaxial connector types APC7, N, SMA, TNC, SC, etc. You can buy complete kits or individual components, any way you like, many items as well as complete kits are carried in stock for immediate delivery. We can also tailor make kits to your specific requirements. Send for your complete MMC Cal Kit Catalog today.

NEW! EWN, EWTNC, EWSC, HN CONNECTOR CALIBRATION KITS.

NEW! DOUBLE RIDGED WAVEGUIDE KITS, WRD 750 ETC.

MAURY MICROWAVE CORPORATION
8610 HELMS AVE. • CUCAMONGA, CALIFORNIA 91730 • U.S.A. TELEPHONE 714-987-4715

CALL 714-987-4715 OR SEND FOR FULL DETAILS.. Today!

READER SERVICE NUMBER 53

tion at a specified reference temperature (usually taken as room temperature). Heating power (P_H) then is applied to the device-under-test to stabilize junction temperature. At the instant P_H is removed, a new value of forward voltage (V_{F2}) is measured with I_M applied. The various voltage and current levels are shown as a function of time in Fig. 2(b). The resultant difference in forward voltages is converted to a temperature rise, ΔT_j, which is divided by P_H to obtain thermal resistance.

Depending on the reference temperature, the resultant value of thermal resistance will be either θ_{jc} for junction-to-case or θ_{ja} for junction-to-ambient. Ambient is usually considered the air temperature surrounding the device when no heatsink is used.

As an example, consider the TSP measurement of a typical snap varactor, the Microwave Associates type 4B300. Referring to Fig. 2, measured parameters are:

$K = 0.516$ °C/W $I_M = 1$ mA
$I_H = 1.0$ A $V_H = 0.995$ V
$V_{F1} = 0.675$ V $V_{F2} = 0.655$ V

The calculation becomes:

$$\theta_{jc} = \frac{K(V_{F1} - V_{F2})}{I_H V_H}$$

$$= \frac{(0.516)(20)}{(1.0)(0.995)}$$

$$= 10.37 \text{ °C/W}$$

To obtain accurate thermal resistance measurements with this method, consideration must be given to the following:

- The heating time should be much longer than the device's thermal time constant to insure junction temperature stabilization.
- The second forward voltage reading should occur at the instant heating power is removed to avoid inaccuracies due to device cooling.
- Switching from the application of P_H to I_M must occur with minimal transients in the measuring-voltage waveform.
- Forward current through the device must quickly decay to I_M from I_H to insure that V_{F2} is read at the same current level as V_{F1}.

Current decay is particularly important when measuring ther-

(continued on p. 54)

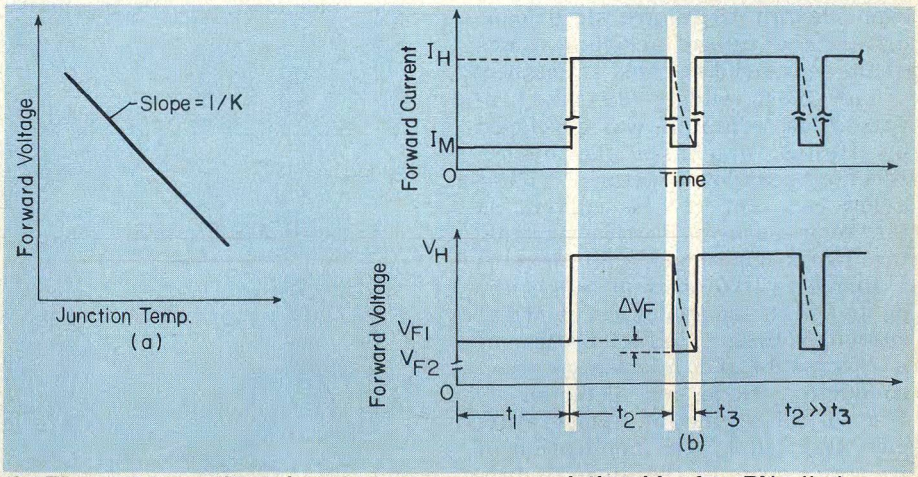

2. The forward voltage-junction temperature relationship for PN diodes remains linear over a wide range of temperatures. Current and voltage waveforms for TSP test are shown in (b). Broken lines indicate decay of a long lifetime device.

Dissipate up to 100 W cw with our new miniature STRIPLINE LOAD...$17.00

We did it again! EMC Technology offers you another state-of-the-art product. A conduction load. (which replaces the big air-cooled kludges you hang on the outside of your circuit housings) at less than 1/5 the cost of present loads. Useful for both strip-line and microstrip applications, this conduction load can also be used as an in-line resistor for such applications as power hybrid couplers. Write or phone for complete data and application information.

EMC TECHNOLOGY, INC. 1971 Old Cuthbert Road Cherry Hill, New Jersey 08034 Phone (609) 429-7800 TWX 710-896-0193

READER SERVICE NUMBER 54

THERMAL MEASUREMENTS

mal resistance of devices with minority carrier lifetimes in excess of several hundred nanoseconds. An accurate measurement of long lifetime diodes requires that the charge stored in the junction during the heating period be quickly removed before a measurement of V_{F2} is attempted. The dashed line in Fig. 2(b) shows the effects of slow current decay on V_{F2}.

Test Impatts under reverse bias

Certain devices, such as the tuning varactor and Impatt diode, are primarily intended for reverse bias operation. Hence, many designers feel that the forward bias technique is not a valid thermal resistance measurement method for these devices. However, analysis of forward and reverse bias thermal resistance test data reveals good correlation between the two test techniques for both devices, even though there are significant differences in the absolute values of the measured thermal resistance.

The most widely accepted reverse bias technique was developed by Haitz[3], and uses the diode's reverse breakdown voltage (V_B) at a low constant reverse current as the temperature-sensitive parameter. Haitz has shown that there is a distinct difference between the dc and high frequency ($\leq$ 1 MHz) current-voltage characteristics of a reverse biased microwave semiconductor diode, as depicted in Fig. 3. The junction temperature rise, induced by the application of heating power to the diode, is proportional to the difference between V_{B1} and V_{B2}. V_{B1} is easily measured before the application of heating

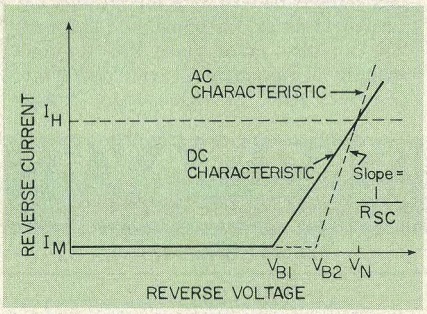

3. Junction temperature should not change more than 100°C for reliable Impatt diode tests.

power; V_{B2} is determined by subtracting the voltage across the space charge resistance (R_{sc}) from the total applied dc reverse voltage: "R_{sc} is the incremental resistance that would be measured in the absence of thermal effects, e. g., by a fast pulse or high frequency sine wave."[4] Since the thermal time constants of most microwave diodes operated in the reverse bias mode are in the multi-microsecond range, R_{sc} measurements require either submicrosecond pulses or sine waves of greater than 1 MHz to exceed the junction's thermal response capabilities.

The reverse breakdown voltage-junction temperature relationship is not as simple as that previously discussed for the forward bias technique. The constant relating the incremental change in breakdown voltage (ΔV_B) to ΔT_j depends on the initial value of breakdown voltage (V_{B1}).

Referring to Fig. 3, the complete equation for thermal resistance is:

$$\Theta_{jc} = \frac{\Delta T_j}{P_H} = \frac{(V_{B2} - V_{B1})}{(\beta V_{B1})(V_H I_H)}$$

A typical example might be Hewlett-Packard's type 5082-0400 Impatt. Measurements reveal the following parameters:

$V_{B1} = 76.1$ V $V_{B2} = 82.05$ V
$V_H = 83.6$ V $I_H = 50$ mA
$\beta = 1.17 \times 10^{-3}$

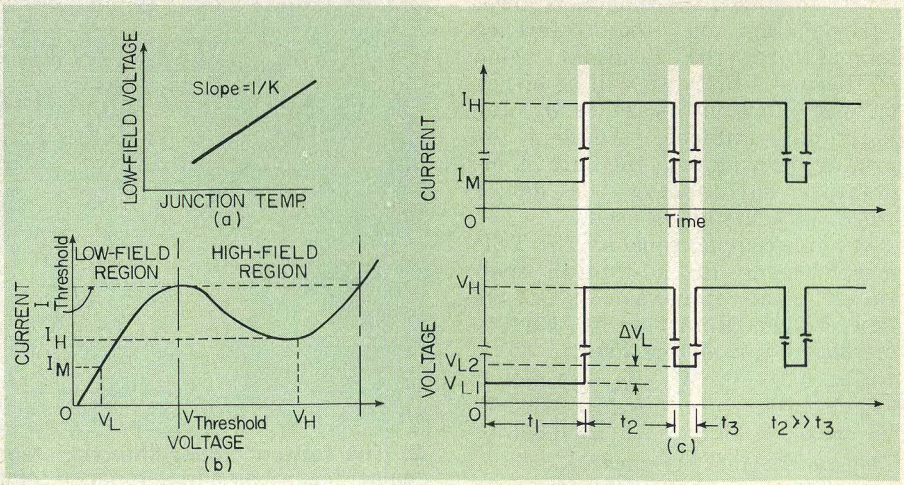

4. Bulk-effect devices should be measured in the low-field region (b). Relationship of measurement voltage and current is shown in (c).

Using the above equation, thermal resistance may be calculated as 15.99° C/W.

Several measurement precautions are required to assure reliable thermal resistance measurements of Impatts:

- The device should not be allowed to go into avalanche oscillation during the test cycle.
- The change in junction temperature must be within the linear ΔV_B—ΔT_j range, typically less than 100°C.
- The test cycle time must be long enough for the junction temperature to stabilize.

TED measurements more complex

Transferred electron devices, although often thought of as diodes, are not built around a semiconductor junction in the traditional sense.[5] Hence, neither of the two previously mentioned TSP techniques can be used directly.

The most practical method relies on the device's low-field (positive resistance region) electrical resistance as the TSP. Initial attempts at this technique[6] measured the device current for a specified value of pre-threshold voltage both before and after application of heating power. The ratio of these data points is exponentially related to the ratio of hot-to-cold temperatures, measured in degrees Kelvin. With this information, the previously determined value of exponent and the precise value of operating current and voltage, thermal resistance can be computed.

Recently, a modification of the initial approach has resulted in a technique that promises to be both simpler to use and more accurate.[7] Measurement of the low-field voltage (V_L) at a constant current value below the threshold level results in a TSP that is linearly related to operating temperature over wide temperature range—in excess of 100°C. The magnitude of the V_L — T_j slope depends on the value of constant current, but has a positive sign (see Fig. 4 (a)). Slope variations from device to device are similar to those for PN junction devices—on the order of a few per cent. The constant current, I_M, for V_L must be large enough to provide a slope value greater than 1 mV/°C, but still be below the threshold current as defined in Fig. 4(b).

Since Gunn diodes are actually constant voltage devices, a complex combination of voltage and current pulses must be applied to the device during the test cycle; waveforms are shown in Fig. 4(c).

(continued on p. 57)

Over 24 RF Amplifiers from Aydin Vector

Now You Have a Choice!

Get guaranteed specifications, low cost and MIL-STD-883A screening.

Model No.	Frequency MHz	Gain dB	Noise Figure dB	Power Out dBm	Voltage Vdc	Package
MHD-150A	5-500	25	2.5	+5	+12	DIP
MHD-150B	5-500	25	2.5	+5	−12	DIP
MHD-151	5-500	21	6.5	+11	+15	DIP
MHD-152	5-500	31	5.0	+11	+15	DIP
MHD-153	5-500	21	6.0	+15	+24	DIP
MHD-171	5-250	30	2.7	+9	+15	DIP
MHD-174	1-250	21	5.0	+11	+15	DIP
MHD-175	1-250	31	5.0	+11	+15	DIP
MHD-176	5-250	21	5.0	+11	+15	DIP
MHD-177	5-250	31	5.0	+11	+15	DIP
MHD-178	1-250	21	6.0	+20	+15	DIP
MHD-179	5-250	21	6.0	+20	+15	DIP
MHT-250	5-500	15	2.5	−2	+15	TO-8
MHT-251	5-500	14	3.5	−2	+15	TO-8
MHT-252	5-500	14	5.0	+7	+15	TO-8
MHT-253	5-500	10	7.0	+15	+24	TO-8
GHT-451	5-400	13	4.5	+5	+15	TO-8
GHT-452	5-400	13	5.0	+7	+15	TO-8
GHT-453	5-400	12	7.0	+15	+24	TO-8
GA-1	5-400	13	4.5	+5	+15	TO-12
GA-2	5-400	13	5.0	+7	+15	TO-12
GA-3	kHz-400	13	4.5	+5	+15	TO-12
GA-4	kHz-400	13	5.0	+7	+15	TO-12

VOLTAGE VARIABLE ATTENUATORS

Model	Frequency Range MHz	Insertion Loss dB	Attenuation Range dB	VSWR	Package
MHA-110	5-1000	2.5	17	2.0	TO-8
MHA-120	5-1000	4.5	30	2.0	DIP

Call, write or circle the reader service number for complete specifications...

AYDIN VECTOR division

Newtown Industrial Commons • P.O. Box 328, Newtown, Pa. 18940

Phone 215-968-4271 / TWX 510-667-2320

31

READER SERVICE NUMBER 55

HIGH PERFORMANCE/LOW PRICE

minipad attenuators

- DC to 18.0 GHz
- −55°c to +125°c
- 0.86 in. long
- VALUES 1 THRU 20dB

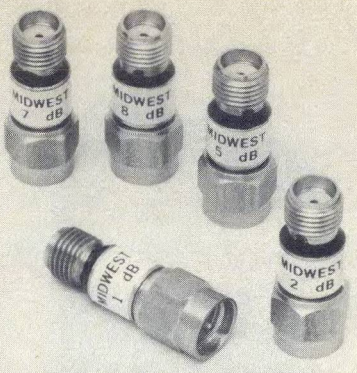

ATTENUATION VALUES OF:
1,2,4,5,7,8,9 & 11 thru 19dB

Available on short delivery.

All units handle 2 watts average power at +25°c derated linearly to 0.5 watts at +125°c.

All units are epoxy sealed for use in adverse environments (salt spray, humidity, sand, dust, etc.)

MIDWEST MICROWAVE

3800 Packard Road, Ann Arbor, Michigan 48104 • (313) 971-1992 • TWX 810-223-6031
FRANCE: S.C.I.E.-D.I.M.E.S. 928-38-65

READER SERVICE NUMBER 57

THERMAL MEASUREMENTS

During the application of heating power, the device under test must not be allowed to oscillate because of the detrimental effect on measurement accuracy. Oscillation can be avoided by inserting enough real resistance in series with the voltage supply to overcome the device's negative resistance. Care is also required to make sure that the TSP monitoring conditions always occur in the device's low field region, even under operating temperature extremes. This can be accomplished by keeping the I_M supply voltage compliance below the voltage threshold.

Referring to Fig. 4, the complete equation for thermal resistance is:

$$\Theta_{jc} = \frac{(K)(\Delta V_L)}{(V_H)(I_H)}$$

A typical example might be Varian's type VSX-9201S7/N23 Gunn diode. Measurements reveal the following parameters:

$V_{L1} = 162.0$ mV $\quad V_{L2} = 216.2$ mV
$V_H = 10$ V $\quad I_H = 465$ mV
$K = 1.45$ °C/W

Using the above equation, thermal resistance is 16.9 °C/W.

Treat transistors as PN diodes

Recent industry attempts to standardize thermal resistance tests for bipolar transistors has resulted in the deletion of several MIL-STD-750B test methods in favor of a single technique for both small-signal and power devices. The method, a revised version of Method 3131, uses the transistor's forward-biased emitter-base junction voltage as the TSP.

Calibration of the emitter-base forward voltage as the TSP requires the application of a measuring current large enough to guarantee a linear V_{BE} — T_j relationship, but small enough to cause negligible internal heating. In order to more closely duplicate the internal field distributions occurring during normal device operation, the same value of collector-emitter voltage (V_{CE}) applied during heating is maintained during the TSP calibration and measurement periods.

The thermal resistance test operation is very similar to that described for forward-biased diodes; voltage and current waveforms are shown in Fig. 5. The TSP reference value is measured during t_1. The heating power, defined as $V_{CE} \times I_H$ if emitter-base power is negligible, occurs in time t_2. Then, in t_3, the base current is returned to the measurement value for the new TSP reading. Times t_2 and t_3 are repeated often enough to insure temperature stabilization within the device; t_3 is made very small compared to t_2 to avoid junction cooling. The TSP reading must occur as quickly as practical after the t_2-to-t_3 transition.

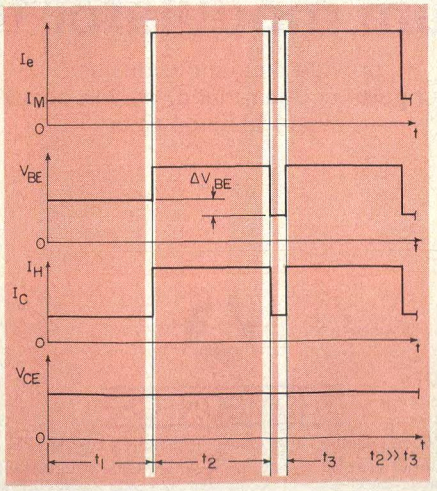

5. Base-to-emitter voltage is the temperature sensitive parameter for NPN bipolar transistor tests.

The measurement problems encountered in transistor testing are very similar to those for forward-biased diodes. If emitter-base power dissipation is negligible, the thermal resistance calculation becomes:

$$\Theta_{jc} = \frac{(\Delta V_{BE})(K)}{(I_H)(V_{CE})}$$

where K is the inverse V_{BE} temperture coefficient. Caution must be exercised when making the test to insure that the selected values of I_H and V_{CE} lie within the device's rated safe operating area specification.

For MESFETs, monitor V_{GS}

Advances in the power capability of microwave field-effect transistors (FETs) will eventually require the development of a suitable thermal resistance test method standard for these devices. Metal-semiconductor FETs (MESFETs) can be tested using the gate-source junction voltage (V_{GS}) under slight forward biased current conditions as the TSP.

Although no measurement standard presently exists, one possible approach to MESFET thermal resistance testing is to maintain a constant forward-biased gate current while applying heating power pulses via a drain-source circuit. In Fig. 6, the V_{DD} supply is shunted to ground during the TSP measurement times and connected to the drain during the heating period. Since forward-biased gate current is always present, the current from the V_{DD} supply will be

(continued on p. 59)

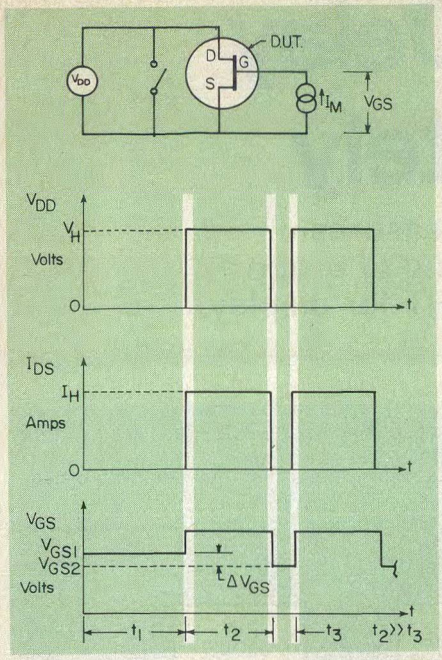

6. MESFETs can be tested with a constant forward gate bias. Heating power pulses are applied via a gate-source circuit.

slightly higher than the device's zero gate voltage saturation current (I_{DSS}). Assuming that the power dissipation in the gate junction can be neglected, the MESFET's thermal resistance is equal to

$$\Theta_{jc} = \frac{(\Delta V_{GS})(K)}{(V_{DD})(I_D)}$$

where K is the inverse $V_{GS} - T_j$ temperature coefficient. Even though this method does not duplicate the internal field distribution that would occur in actual device circuit operation, it does provide a useful result that is indicative of the device's thermal characteristics. ••

References

1. N. R. Galassi and B. S. Siegal, "A System For Measuring The Thermal Resistance Of Semiconductor Diodes," *Hewlett-Packard Journal*, Hewlett-Packard Company, Vol. 19-2, (October, 1967).

2. J. A. Walston, *Thermal Considerations In Transistor Circuit Design*, Texas Instruments, Inc., Application Note.

3. R. H. Haitz, et al, "A Method For Heat Flow Resistance Measurements In Avalanche Diodes," *IEEE Trans. Electron Devices*, ED-16, p. 438, (May, 1969).

4. *Microwave Power Generation and Amplification Using Impatt Diodes*, Hewlett-Packard Company, AN935, (June, 1971).

5. B. S. Siegal, "A Practical Guide To Microwave Semiconductors," *Microwave Systems News*, (June/July, August/September and October/November, 1972).

6. E. Hakim, et al, *Assessment Of A New Gunn Diode Thermal Resistance Measurement Using A Direct Infrared Measurement Technique*, Microwave Associates, Burlington, MA, (1973).

7. *THETA 110 Thermal Resistance Tester Data Sheet*, Sage Enterprises, Menlo Park, CA, (1975).

GX approved

DI-CLAD 527 laminates

offer consistent low loss at X Band.

Di-Clad 527 PTFE/glass/copper laminates have now received GX approval under MIL-P-13949 E. Produced under special "clean room" conditions, Di-Clad 527 offers reproducible dielectric constant control plus a maximum loss of .0022 at X Band.

Di-Clad 527 laminates less than 1/32-inch thick are also available. We make and test them by the same method that has earned GX approval. And we hold them to tight thickness tolerances—down to ± .0005 inch for a base thickness of .004 inch. All Di-Clad 527 laminates are engineered for plated-through-hole applications.

New free bulletins.

To help you meet your microwave design objectives, we've prepared detailed technical bulletins covering Di-Clad 527 laminate characteristics, plated-through-hole processing techniques, and computer-produced design parameters. To receive your copies, circle the reader service card. Keene Corporation, Chase-Foster Division, 199 Amaral St., East Providence, R.I. 02914.

KEENE CORPORATION

CHASE-FOSTER DIVISION

READER SERVICE NUMBER 59

Measure Group Delay Fast And Accurately

Here's a swept-frequency technique that measures group delay to 0.2 ns and allows rapid tuning of group delay equalizers. It relies on a standard CRT for display.

FOR many communication applications, it is essential to accurately measure the group delay of such microwave components as filters, group-delay equalizers and combinations of these. Using the test setup shown in Fig. 1, it's possible to measure group delay to an accuracy of 0.2 nsec. Also, group delay equalization may be carried out on a swept frequency basis, which is not possible using conventional systems because of their slow sweep rates.

Usually a group delay is determined by an amplitude-modulation method[1,2]. A cw signal is first amplitude modulated, then passed through the device-under-test to measure the phase shift of the envelope. Group delay is related to the envelope phase shift by:

$$t_d = \frac{\Theta_e}{f_m \times 360^\circ}$$

where Θ_e = envelope phase-shift in degrees

f_m = modulation frequency in Hz

t_d = group delay in seconds

For a modulation frequency, f_m = 277.8 kHz, the group delay is 10 nsec/degree of phase shift. The test setup, in Fig. 1, composed of standard microwave test equipment, includes a link analyzer, microwave sweep generator and a PIN diode modulator to generate an amplitude-modulated test signal. The PIN modulator is, however, also frequency modulated with a 16 Hz triangular waveform which gives this measurement system its main advantage. The dc component of the 16Hz signal is blocked by the 470 μF capacitor to prevent a shift in the microwave oscillator center frequency. The 277.8 kHz signal from the analyzer amplitude modulates the swept frequency test signal at the PIN diode modulator.

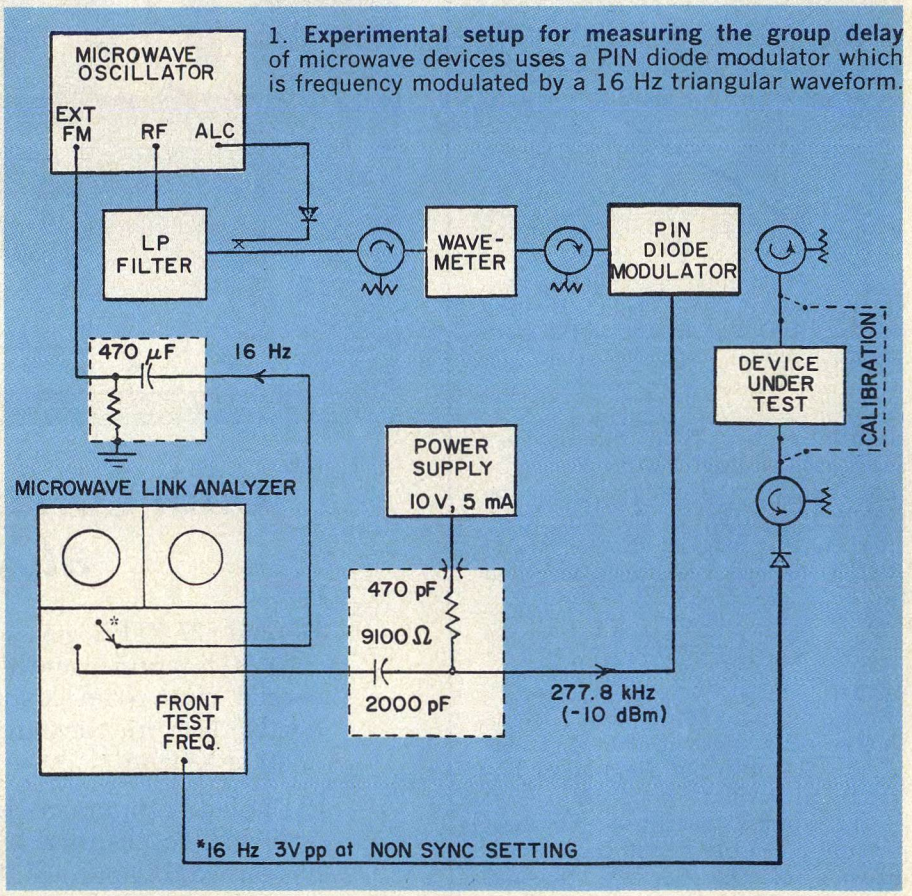

1. **Experimental setup for measuring the group delay** of microwave devices uses a PIN diode modulator which is frequency modulated by a 16 Hz triangular waveform.

The dc bias on the diode modulator is adjusted to obtain maximum depth of modulation. It's important to terminate the modulator at both input and output ports. The modulated signal is detected after passing through the device-under-test, then channeled to the receiver section of the analyzer. The link analyzer compares this recovered signal with a sample (obtained internally) of the original 277.8 kHz signal to obtain envelope delay, and displays it on a CRT as phase shift or group delay of the system. In order to measure the contribution of the test equipment to the group delay, the response of the system is calibrated with the device bypassed.

This test system has been used to measure group delay of 2 GHz filters and filter group delay equalizer combinations. Typical results, in Fig. 2, show the group delay of 2 GHz bandpass filter with and without equalization and illustrate that the delay can be measured to fractions of a nanosecond. This measurement technique, while simi-

M. J. Ahmed, Senior Engineer, **A. Froese,** Senior Systems Engineer, and **G. Schmiing,** Technologist, GTE Lenkurt Electric, Ltd., 7018 Lougheed Highway, Burnaby 2, British Columbia, Canada.

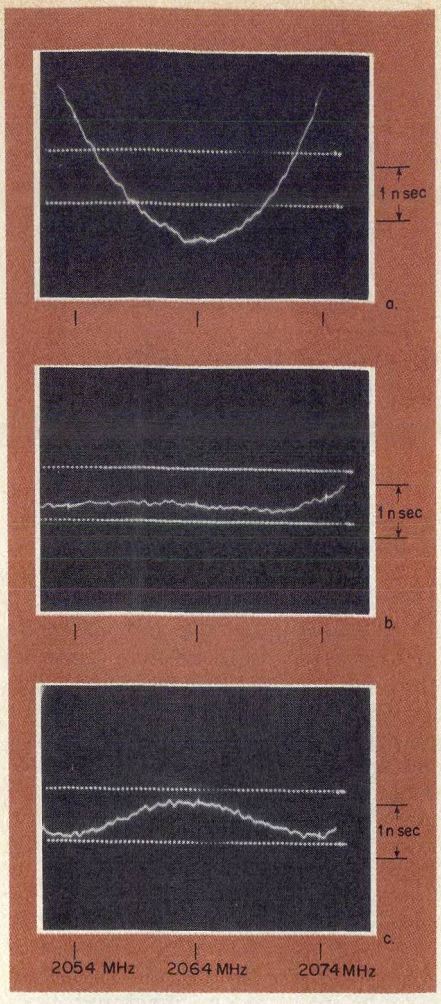

2. **Group delay of a 2 GHz bandpass filter** shows (a) unequalized, (b) equalized and (c) overequalized conditions. Delays can be measured to fractions of a nanosecond.

lar to that described in References 1 and 2, differs in that a vector voltmeter is not required to measure the envelope phase shift. As noted by Wardrop[2], if a vector voltmeter is used, the sweep rate must be very low to permit true reconstruction of the waveform from the signal samples. The slow sweep necessitates the use of an X-Y recorder or a storage oscilloscope and is, therefore, inconvenient, especially when group delay equalization has to be performed. The 16 Hz sweep rate employed in the measurement technique described here is fast enough to provide an adequate swept frequency display which facilitates rapid tuning of group delay equalizers. ••

References

1. "Swept Frequency Group Delay Measurements," Hewlett-Packard Application Note 77-4, (September, 1968).

2. B. Wardop, "The Measurement Of Group Delay," *The Marconi Review*, Vol. XXXV, No. 187, pp. 316-336, (Fourth Quarter, 1972).

THIN-TRIM CAPACITORS FOR HYBRIDS AND MIC'S

Series 9410 Thin-Trims are sub-miniature variable capacitors for applications where size and performance are critical. Featured are high Q's for low circuit losses, high capacity values for broadband applications and low profile for "gap trimming" in tiny MIC's. Body size .200" x .200" x .060"T. Available in 5 capacitance ranges from 1.0 - 4.5 pf to 7.0 - 45.0 pf.

Johanson

MANUFACTURING CORPORATION
Rockaway Valley Road
Boonton, N.J. 07005
(201) 334-2676 TWX 710-987-8367

READER SERVICE NUMBER 60

now—
microwave filters
with ceramic
performance!

actual size

Murata's new line of Gigafil-C® filters with ceramic dielectric resonators bring a new standard of performance to the microwave frequency spectrum. They are available for frequencies from 760 MHz to 14 GHz, with Q's over 5,000, and in a variety of bandwidths. Outstanding features also include diminutive size and amazing temperature stability. Put ceramic to work in your microwave system. Write for details.

muRata
CORPORATION OF AMERICA
2 WESTCHESTER PLAZA, ELMSFORD, NEW YORK 10523
Phone: 914-592-9180 Telex: 13-7332

READER SERVICE NUMBER 61

Try Impact Extrusion For Low-Cost MIC Packaging

Rugged, hermetically sealed MIC enclosures can be inexpensively fabricated by punching the housing and carrier out of aluminum slugs, then sealing the cover with a TIG weld.

A microwave integrated circuit (MIC) generally costs several hundred dollars to manufacture; in some instances, costs may exceed $1,000. Yet, it's interesting to consider that the ultimate performance of this sophisticated circuit design may very well be limited by a cheaper, non-electronic item—the package.

The truth is, the MIC package and its internal layout are integral factors in the circuit's electrical performance and reliability. Thus, the engineer faces both electrical and mechanical and design problems in packaging an MIC. And since the design has a high probability of containing uncased semiconductor devices, the engineer must also consider the hermetic seal necessary to provide high reliability.

A unique packaging method has been developed which avoids low quantity and high-cost constraints and also solves the hermetic sealing problems associated with solder or epoxy seals. The packages are formed using an impact extrusion process, and require only minimal machining to be suitable for an MIC. The tooling used for the extrusions is expected to have a minimum useful life of 50,000 pieces and has been designed to permit direct replacement of worn parts rather than replacement of the complete die set.

Compared to a machining processes, impact extrusion offers several subtle advantages in terms of package design, materials and electrical performance, but its prime benefit is in terms of cost. Table 1 presents a cost comparison of a 100-piece production run of a 1 x 2 inch MIC package. The estimate is based on a fully finished housing cover and simple flat carrier. The same rf connectors are used on both packages. Note that savings on a 1,000 piece run would total $17,410.

The package is hermetically sealed by a Tungsten Inert Gas (TIG) welding process as opposed to less reliable epoxy or soldered seals. TIG welding is capable of providing leak rates of less than 1×10^{-7} ATM-cc/sec. A special weld lip has been designed as part of the machined package to facilitate the welding process. The lip on the cover has a degree taper on all sides, including the corner radii, and is nominally 0.006 inch larger than the corresponding opening in the housing, insuring a slight interference fit of the cover over all tolerance conditions. The welded package has been designed so that it may be opened twice for repairability, and then resealed, if necessary.

Table 1
Manufacturing Cost Comparison

	Impact Extrusion	Machined
Housing	$10.13	$20.00
Cover	.50	2.96
Carrier	.81	2.22
Cost Per Package	**$11.44**	**$28.85**

The selection of an appropriate material is especially important, since it not only dictates the raw stock cost but also tends to dictate the manufacturing processes, finishing and plating, as well as the weight and structural characteristics of the finished item.

Thermal considerations important

All discussions of materials sooner or later will revolve around thermal compatability with the ceramic substrates from the viewpoints of substrate and interconnection failure. Materials initially considered for the substrate carriers were Kovar, Invar and other low expansion alloys. Although these materials closely match the expansion characteristics of the ceramic, this advantage must be weighed against their excessive cost, high weight (in the order of 0.3 lb/in^3), poor machinability, long lead delivery and magnetic properties. The series 300 stainless steels and cupro-nickel alloys, while having a higher expansion coefficient than the substrate, overcome several of these objections, but are still high density materials. Titanium, Beryllium and the exotic alloys were also considered but were rejected for price and availability problems.

Experiments conducted at Microwave Associates have shown that ceramic substrates are large as 2 × 2 inches could be successfully soldered to properly plated aluminum carriers. Extended temperature testing of this combination showed neither substrate cracking nor delamination, the primary concerns. Therefore, the decision was made to use 6061 aluminum for the substrate carriers.

The high thermal conductivity of aluminum has particular advantages over other materials when used as the substrate carrier. The most obvious advantage is its efficiency as a heat sink. But more important the aluminum housing reacts to changes in ambient temperature faster than the substrate material. Therefore, a low expansion alloy carrier having a low

(continued on p. 66)

John E. Miley*, Senior Engineer, Omni Spectra, Inc., 21 Continental Blvd., Merrimack, NH 03054 and **Gordon Simpson,** Staff Mechanical Engineer, Microwave Associates, Inc., South Ave., Burlington, MA 01803.
*formerly of Microwave Associates

odern Data mmunication: ncepts, nguage, d Media

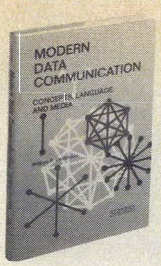

iam P. Davenport

on-the-job hand-ok mapping out e latest tech-ques, systems, d services for the most efficient data nsmission. Includes simplified cod- techniques; ways of dealing with stortion, distraction, interference; ef-iency and control techniques; modu-ing and multiplexing methods; and od advice on system costs. Hayden t price: $10.30

bscriber's club price: $9.25
der #S111

me aying th mputers, cond Edition

ald D. Spencer

w you can tch your wits ainst a digital mputer! Here over 70 games, puzzles, and math-atical recreations, along with more n 25 complete programs in FOR-AN or BASIC. Binary games, casino d board games, unusual gambling mes and many others. Hayden list ce: $14.95

bscriber's club price: $12.70
der #S112

icroprocessors: w Directions r signers

ard Torrero

re's two years of wealth of infor-tion on micro-ocessors from *ectronic Design.* s packed with ta and advice on selecting micros, d operating and improving them to ur best advantage. It's the "last rd" in micros. Hayden list price: .95

bscriber's club price: $7.95
der #S100

ndamentals d plications Digital gic rcuits

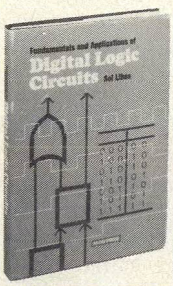

Libes

cludes every-ing from basic eory to the most advanced applica-ns—circuitry of calculators, voltme-s, frequency counters, and the latest mputer applications. Explores the ap-cations of RTL, DTL, TTL, and other ting circuits. Hayden list price: $8.98

bscriber's club price: $7.20
der #S121

". . . well-organized, extremely well written . . . highly recommended for practicing engineers . . ."
—IEEE Transactions

Digital Signal Analysis

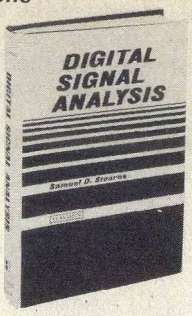

Samuel D. Stearns

Including a Foreword by Richard Hamming, this ideal master handbook on signal processing contains recent advances, new design material, and a comparison between continual and digital systems extremely helpful to newcomers to the field. Includes special sections on analog and digital filter design. Hayden list price: $18.95

Subscriber's club price: $15.20
Order #S120

Basic Electronic Switching for Telephone Systems

David Talley

Probably the most practical, complete coverage of today's telephone systems, particularly the operations of central offices and their switching networks. Discusses Bell's No. 1 and No. 2 ESS central offices, and the No. 1 EAX System from GTE labs. Great for engineers, technicians, and executives alike. Hayden list price: $6.95

Subscriber's club price: $5.90
Order #S115

Assembler Language Programming: The IBM/360 and 370 Second Edition

George W. Struble

This guide offers a double value, enabling you to gain command of the structure and operation of the System/360 and 370, as you master the system's versatile assembler language. This new edition contains additional problems and examples to strengthen your working knowledge. Addison-Wesley list price: $14.95

Subscriber's club price: $12.70
Order #S103

Mathematical Foundations of Systems Analysis

R. H. Kupperman and Harvey Smith

A high-powered refresher course for analysts who want to bolster their mathematical abilities and handle all their system work with more expertise. Filled with problems and examples to improve your problem-solving skills—particularly in the areas of optimization. Addison-Wesley list price: $13.95

Subscriber's club price: $10.50
Order #S110

MICROWAVES BOOK CLUB

50 Essex Street
Rochelle Park, New Jersey 07662

Order Form

Your new NO OBLIGATION book club is a great idea! Please send the following book(s) on 10-day examination. At the end of that time, I will send payment plus postage and handling (and state sales tax where applicable) or return the book(s) and owe nothing.

As a subscriber to *MicroWaves*, I understand that I am under no obligation to buy a specific number of books to continue to take advantage of your discounts.

FILL IN BOOK ORDER NO. AND TITLE BELOW:

Order #	Title	PRICE

Sales tax: N.J.—5%, Ca.—6%, Fla.—4% Sales Tax _____

Outside USA, add $2.00 shipping & handling. Total _____

SHIP TO:

Name _____

Firm/Institution _____

Address _____

City/State _____ Zip _____

To take advantage of our subscriber's club price, you must fill in your *MicroWaves* subscription number (the long number over your name at the top of your address label on the front of this issue).

_____
(Yes . . . We need all 29 numbers and letters)

CREDIT CARDS ACCEPTED—Customer pays postage and handling

CHECK ONE: ☐ Master Charge ☐ BankAmericard

Acct. No. _____

Expiration Date _____

InterBank No. _____ (Master Charge ONLY)

Signature _____

☐ **Payment (check or money order) enclosed.**

This order card good only until October 31, 1976. MW6/76

EXTRUDED PACKAGES

thermal conductivity exhibits a substantial temperature lag as the housing temperature changes, giving the same effect as materials having significantly different expansion characteristics. The net effect of the low expansion, low thermal conductivity carrier system is that the greater expansion of the housing over-stresses the carrier to connector bonds causing premature interconnection failures. This problem was alleviated by the use of aluminum carriers whose thermal characteristics match those of the housing, virtually eliminating the differential expansion problem. This was later substantiated by extensive high-low temperature testing.

The same general line of reasoning was applied to the material selection of the housing. In addition to thermal properties and cost factors, there was a greater emphasis placed on machinability, formability and structural characteristics. When the cost advantages of the impact extrusion process were clearly established, several alloys suitable for impact extruding were available, but only 6061 alloy had all of the following advantages:

- Good plastic flow
- Excellent structural characteristics
- Excellent machinability
- Capable of heat treatment
- Brazeable
- Excellent plating and finishing
- Good thermal characteristics
- Good welding characteristics

The cover material was, of course, selected primarily to be compatible with the housing for the hermetic welding operation and is 6061-T6 aluminum alloy. This is not a compromise, since the material also has good forming and coining characteristics necessary for low-cost fabrication.

The full environmental qualification of the several sizes of impact extruded packages has shown that the decision to use aluminum for substrate carriers and packages was technically sound and economically advantageous.

A major consideration in the design of the MIC package family was the housing itself. Machining the housings from aluminum bar stock was immediately rejected from a cost standpoint. A simple analysis shows that standard bar stock for machining a 2 × 4 inch housing would weigh 1.27 lbs and that the machined module would weigh 0.38 lbs, requiring that 0.89 lbs of aluminum be machined away. Therefore, the weight of the chips would be almost 2.5 times the weight of the finished item.

While castings would be far more economical in use of the metal, castings are not suitable for hermetic packages. Therefore, the effort was applied to forming techniques that would provide a continuous and homogeneous raw housing requiring a minimum of machining to create the final form.

The process selected as optimum for MIC hermetic enclosures was impact extrusion, which combines the best characteristics of both forging and extruding. The process is defined formally by "The Aluminum Association" as: "A part formed in confining die from metal slug, usually cold, by rapid single stroke application of a force through a punch causing the metal to flow around the punch and/or through an opening in the punch or die."

Impact extruding converts the kinetic energy of a high-speed impact into thermal energy raising the temperature of the metal slug to a plastic state sufficiently soft to permit a flow of the metal through the die and yet with sufficient strength retained to permit dimensional stability of the extruded portion. Figure 1 shows a new slug and the 1 × 2 housing formed from it. The slug is obtained by extruding a bar of impact alloy to the proper cross section, and slicing off slugs of the correct length. The tolerances of the slug is not critical except that the volume of a minimum thickness slug should equal the volume of a part having the minimum acceptable height. Thicker slugs will produce a slightly higher housing.

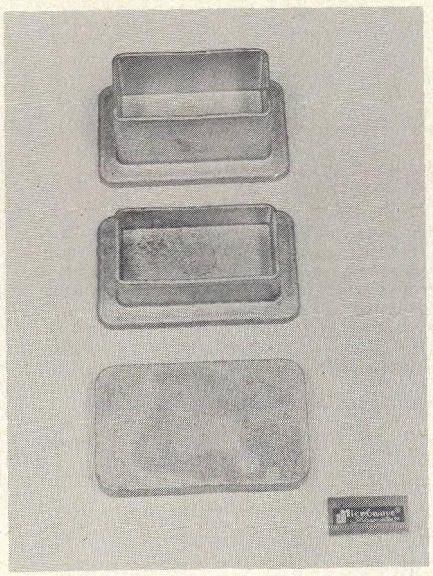

1. Housings are punched out of aluminum slugs. Taller housings require thicker slugs.

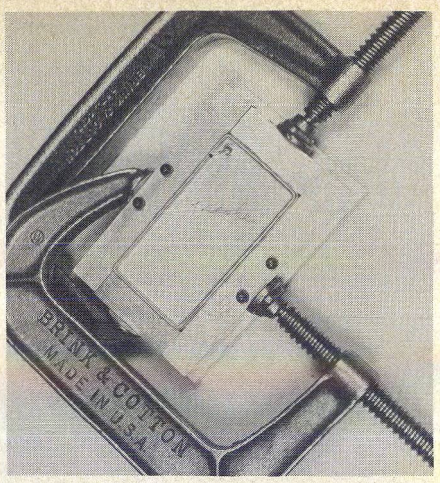

2. Tight clamping is a must to transfer heat from welding.

TIG welding preserves hermeticity

The process of welding the covers to the finished housing which provides the final closure is the "Tungsten Inert Gas" method utilizing fusion of the cover and housing material rather than the addition of filler material. From a production standpoint, the TIG welding procedure is readily adaptable to both low volume and high volume assembly. The primary difference in production rate will be a function of the type of heat sinking/holding fixtures required. For short run hermetic sealing, simple clamping bars have proven to be completely suitable. The bars must contact the housing faces equally and be relived as required for connectors and feedthroughs; allowance must be made for the 0.20 inch free projection of the weld lip. Clamping the heat sink bars with standard machine shop "C" clamps provides a good thermal path, as shown in Fig. 2. For this type of manual load, clamp and automatic weld, production rates for the 2 × 4 inch module will be in the order of 20 pieces per hour, including an occasional repair weld.

The manual load and clamp operation is the most time consuming element of the short-run approach. For large runs, pneumatic or hydraulic clamping can double the production rate. Hydraulic or pneumatic clamping is superior to mechanical clamping due to the ability to maintain a constant clamping pressure over the range of mechanical tolerances. Caution

(continued on p. 68)

Now noise load test your microwave radio in 60 seconds.

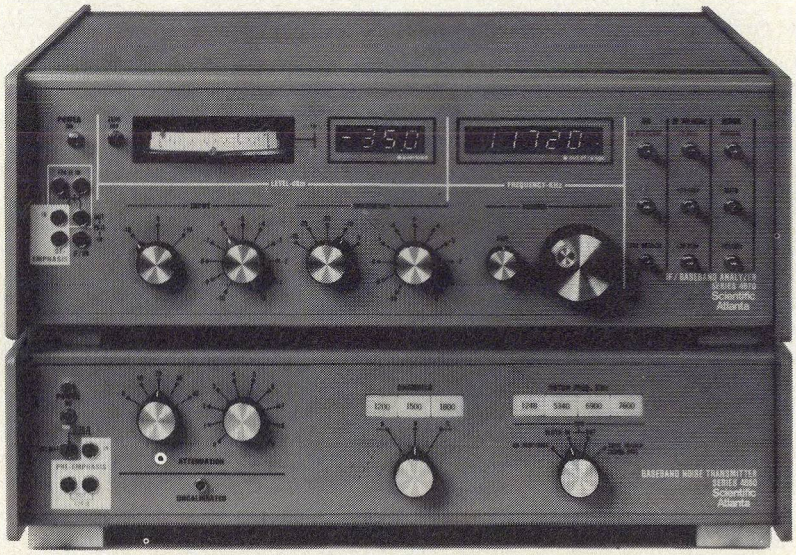

Or run a complete baseband routine including noise load, spurious tone search and baseband response in just 5 minutes. You do it with the new Scientific-Atlanta 4680 Radio Performance Analyzer.

We've combined an IF/baseband spectrum analyzer, white noise test set, and selective levelmeter into one inexpensive, lightweight test set. You make noise-load, baseband response, even spurious tone search measurements on a swept-frequency basis, this plus many other baseband and IF tests and all with one piece of equipment. At a fraction of the time previously required.

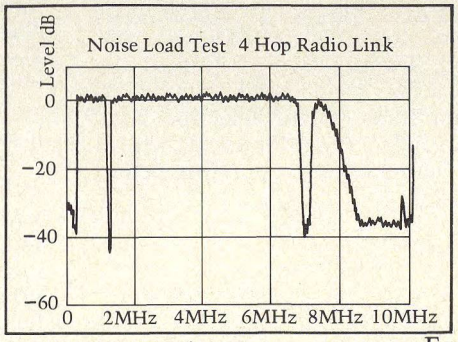

The Radio Performance Analyzer is designed for field use by telephone craftsmen. Every operator will get repeatable, dependable results the first time. Test oriented controls eliminate guesswork from parameter setups. Automatic recording makes testing that much simpler.

What's more, the Analyzer generates a permanent recording of the results. No more handwritten data or scope cameras.

The cost for all this? About 1/3 that of the instruments it replaces. You get a savings in money when you buy it. And a savings in money every time you use it.

For more information, please call or write Moti Shacham, 3845 Pleasantdale Road, Atlanta, Georgia 30340.

Scientific Atlanta
Instrumentation

United States: 3845 Pleasantdale Road, Atlanta, Ga. 30340, Telephone 404-449-2000, TWX 810-766-4912, Telex 054-2898
Europe: Hindle House, Poyle Road, Colnbrook, Slough, SL30AY, England, Telephone Colnbrook 5424/5, Telex 848561
Canada: 678 Belmont Avenue West, Suite 103, Kitchener, Ontario, Canada N2N-1N6, Telephone 519-745-9445

READER SERVICE NUMBER 67

should be exercised, however, that oil leakage or exhaust air does not contaminate the weld surfaces as any oil contamination will most certainly produce bad welds.

Examples of good, hermetic-quality welds are shown in Fig. 3. Note that the weld beads are quite small, and the width is comparable to the sum stock thickness. Also, note the smooth, uniform appearance of the weld. Any gross ripples or dips would indicate poor cleaning procedures. Apperance is a significant factor in weld quality; visual defects are usually hermetic failures.

Connectors, feedthroughs developed

At the inception of this program, hermetic SMA connectors for thin wall applications having suitable performance characteristics for 18 GHz operation were not available. Working in conjunction with connector manufacturers, a special, high performance connector was developed. This connector, shown in Fig. 4, features a separate dielectric for the female contact, which is inserted after the connector is furnace soldered to the housing. Note the airline transistion from the hermetic seal to the substrate carrier interface. VSWR is typically 1.1:1 (1.18 max) from 2 to 18 GHz.

Two types of inorganic isolation barrier feedthroughs have been designed for the impact extrusion package. One type, an end-to-end design, allows transmission through a barrier separating substrates in the same plane (i.e., on the same carrier). A second, back-to-back type, allows transmission between two substrates located on either surface of the carrier.

Both feedthroughs use glass as the inorganic insulating material: Corning Type 7070 with a 0.015 inch center conductor and 0.085 inch outer diameter on the Kovar

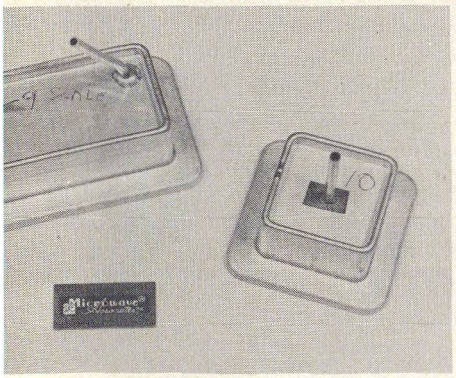

3. Clean, smooth welds usually indicate hermeticity. Units are ready for evaluation and pinch-off.

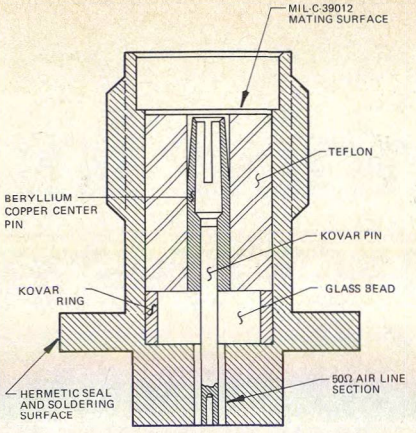

4. This SMA connector is designed to work up to 18 GHz.

steel. The bead length is 0.060 inch with a symmetrically located-center conductor. End-to-end feedthrough performance includes a 1.13:1 VSWR to 14.0 GHz.

To eliminate the inductive characteristics in the back-to-back design (Fig. 4), an endcap configuration was developed. The endcap provides a ground plane in the right angle transition area making a close approximation to 50 ohms possible. The back-to-back feedthrough is capable of a 1.13:1 VSWR to 16.0 GHz.

Whereas, the MIC packages are hermetically sealed and all exterior surfaces are painted or plated against humidity, the major environmental effects, in descending order, are temperature, vibration and mechanical shock.

To demonstrate the environmental effects on the impact-extruded housings, a run of 150 units with various rf circuits was conducted. Twenty-five of each of the four sizes used combinations of 50-ohm lines on carriers and fifty units of the type shown in Fig. 5 were submitted to environmental testing.

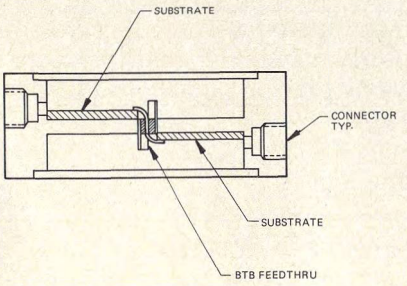

5. Back-to-back feedthrough provides high isolation by using part of the packages as a shield.

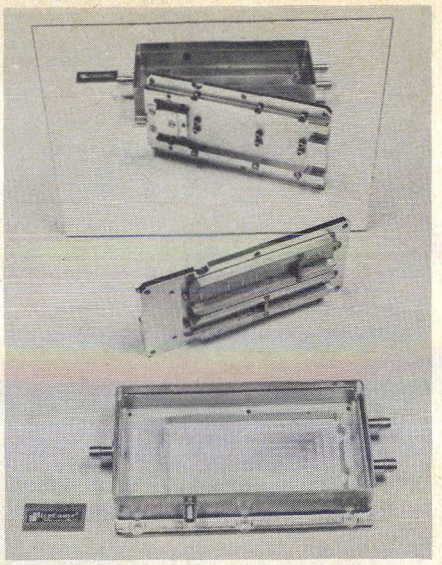

6. Complex packages formed by impact extrusion pass strict environmental tests.

The temperature testing included both thermal shock and temperature cycling. The temperature cycling was in accordance with MIL-STD 202, Method 102, Test Condition D, −55°C to +85°C for a total of 25 cycles. The thermal shock was in accordance with MIL-STD-883, Method 1011, Test Condition A, 0°C to 100°C, a dwell time of 15 minutes for 15 cycles. The greatest effect noted was the degradation of hermetic connectors from leak rates of 10^{-8} Atm-cc/sec to 10^{-6} Atm-cc/sec. This has been noted at Microwaves Associates prior to the impact extruded packaging program and is attributed to the oxide on the Kovar into which the glass bead is fired. This is evidently caused by a compromise to achieve low rf losses and obtain a hermetic seal.

The units were then subjected to vibration and mechanical shock with no noted degradations in electrical performance even with the use of substrate carriers. The vibration was conducted at 10, 15, 20 and 25 G's to 3000 Hz and at 35 and 40 G's to 1000 Hz. In addition, vibration was done in accordance with MIL-STD-202, Method 204B, Test Condition C. The mechanical shock was done in accordance with MIL-STD-202, Method 213, Test Condition D. Finally, the packages were subjected to Mechanical Shock in the Y_1 direction to five pulses at 500 G and 825 G for one millisecond. ••

Acknowledgement

This work was supported by the U. S. Army Electronics Command, Fort Monmouth, NJ, under Contract DAAB 05-72-C-5851.